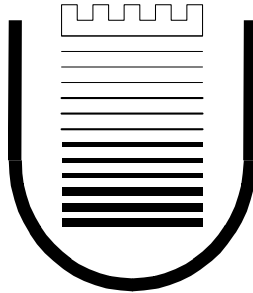


**Università degli studi di Roma**  
**“Tor Vergata”**



**Facoltà di Ingegneria**  
**Tesi di Dottorato in Ingegneria Ambientale**  
**XVII° CICLO**

**“Analysis and Application of Novel Method for Quantifying  
Infiltration and Exfiltration in Urban Sewer Systems”**

**Dott. Ing. Valentina Prigiobbe**



*Ad Alessandro, Luciana e Vincenzo*

# INDEX

<b>CHAPTER 1 THE PROBLEM.....</b>	<b>11</b>
<b>1.1 WHY SHOULD WE MEASURE THE INFILTRATIONS? .....</b>	<b>11</b>
<b>1.2 WHY SHOULD WE MEASURE THE EXFILTRATIONS? .....</b>	<b>12</b>
<b>1.3 SEWER PIPE DETERIORATION.....</b>	<b>15</b>
1.3.1 FACTORS AFFECTING THE STRUCTURAL STATE OF SEWER SYSTEM .....	16
1.3.2 SEWER DETERIORATION MODELLING.....	20
<b>1.4 DIAGNOSTIC TECHNIQUES .....</b>	<b>24</b>
<b>1.5 REFERENCES.....</b>	<b>31</b>
<b>CHAPTER 2 NOVEL METHODS FOR QUANTIFYING THE INFILTRATION AND THE EXFILTRATION IN URBAN SEWER SYSTEMS .....</b>	<b>35</b>
<b>2.1 INTRODUCTION.....</b>	<b>35</b>
<b>2.2 METHODS FOR QUANTIFYING THE EXFILTRATIONS.....</b>	<b>36</b>
2.2.1 QUEST .....	36
2.2.2 QUEST-C .....	38
2.2.3 HYDRODYNAMIC BACKGROUND OF QUEST AND QUEST-C .....	40
2.2.3.1 <i>Tracer Transport</i> .....	40
Near-Field and Vertical Mixing .....	45
Mid-Field and Transverse Mixing .....	50
Far-Field and Longitudinal Mixing.....	56
2.2.3.2 <i>Confluences</i> .....	63
2.2.4 APPLICATION ADVECTION-DISPERSION (AD) MODEL TO QUEST AND QUEST-C .....	68
2.2.5 SAMPLING AND MEASUREMENTS .....	70
2.2.5.1 <i>Choice of the tracer</i> .....	70
2.2.5.2 <i>Mass of tracer to be dosed</i> .....	70
<b>2.3 METHODS FOR QUANTIFYING THE INFILTRATIONS.....</b>	<b>72</b>
2.3.1 ISOTOPIC METHOD .....	72
2.3.2 POLLUTOGRAPH METHOD.....	73
2.3.2.1 <i>Isotopic method</i> .....	75
Environmental stable isotopes .....	75
Physical, chemical and biological fractionations .....	77
Hydrograph separation.....	87
<b>2.4 REFERENCE.....</b>	<b>90</b>
<b>CHAPTER 3 EXPERIMENTAL DESIGN AND FIELD APPLICATION .....</b>	<b>94</b>
<b>3.1 INTRODUCTION.....</b>	<b>94</b>

<b>3.2 EXPERIMENTAL DESIGN</b> .....	<b>94</b>
<b>3.3 QUEST</b> .....	<b>100</b>
3.3.1 DETAILED UNCERTAINTY ANALYSIS .....	103
3.3.1.1 Preparation .....	104
3.3.1.2 Field application .....	105
Dosage .....	105
Adsorption .....	105
Transport.....	105
Conductivity measurements .....	106
Data reduction.....	107
Error propagation for the detailed uncertainty analysis.....	107
3.3.2 RESULTS OF DETAILED UNCERTAINTY ANALYSIS.....	109
<b>3.4 QUEST-C</b> .....	<b>126</b>
<b>3.5 ISOTOPIC METHOD</b> .....	<b>127</b>
<b>3.6 POLLUTOGRAPH METHOD</b> .....	<b>128</b>
3.6.1 PRELIMINARY CAMPAIGNS .....	128
3.6.2 CALIBRATION AND INFILTRATION ASSESSMENT .....	130
<b>3.7 REFERENCES</b> .....	<b>133</b>
<b>ANNEX 1 - GIULIANELLI, M.; PRIGIOBBE, V. (2004). INFILTRAZIONE DI ACQUE DI FALDA NELLE FOGNATURE. L'ACQUA, 6, PP. 41-50. ....</b>	<b>134</b>
<b>ANNEX 2 - CARDOSO, A.; PRIGIOBBE, V.; GIULIANELLI, M.; BAER, E.; COELHO, S.T. (2005). ASSESSING THE IMPACT OF INFILTRATION AND EXFILTRATION IN SEWER SYSTEMS USING PERFORMANCE INDICATORS: CASE STUDIES OF THE APUSS PROJECT. 10<sup>TH</sup> INTERNATIONAL CONFERENCE ON URBAN DRAINAGE, COPENHAGEN, DENMARK, 21-26 AUGUST 2005.....</b>	<b>135</b>
<b>ANNEX 3 - GIULIANELLI, M.; MAZZA, M.; PRIGIOBBE, V.; RUSSO, F. (2003). ASSESSING EXFILTRATION IN A URBAN SEWER BY SLUG DOSING OF CHEMICAL TRACER (NACL). PROCEEDING OF A WORKSHOP ORGANIZED BY NATO ARW ON ENHANCING URBAN ENVIRONMENT, ROME, ITALY, NOV. 5-9, 2003.....</b>	<b>136</b>
<b>ANNEX 4 - PRIGIOBBE, V.; GIULIANELLI, M. (2004). EXPERIMENT DESIGN OF A NOVEL METHOD TO ASSESS EXFILTRATION IN SEWER. CONFERENCE ON URBAN DRAINAGE MODELLING, DRESDEN, 15TH-17TH SEPTEMBER 2004. ....</b>	<b>137</b>
<b>ANNEX 5 - RIECKERMANN, J.; BAREŠ, V.; BRAUN, D.; KRACHT, O.; PRIGIOBBE, V.; GUJER, W. (2004). ASSESSING EXFILTRATION FROM SEWERS WITH DYNAMIC ANALYSIS OF TRACER EXPERIMENTS. 19TH EUROPEAN JUNIOR SCIENTIST WORKSHOP “PROCESS DATA AND INTEGRATED URBAN WATER MODELLING” FRANCE 11-14 MARCH 2004. ....</b>	<b>138</b>



<b>ANNEX 6 - PRIGIOBBE, V.; GIULIANELLI, M. (2005). APPLICATION OF A NOVEL METHOD FOR ASSESSING THE INFILTRATION IN AN URBAN SEWER SYSTEM: CASE OF STUDY IN APUSS PROJECT. PROPOSED FOR WATER SCIENCE AND TECHNOLOGIES. ....</b>	<b>139</b>
<b>ANNEX 7 - FURTHER ENCLOSED ARTICLES .....</b>	<b>140</b>

# TABLE INDEX

TAB. 1.3-1: FACTORS AFFECTING THE STRUCTURAL STATE OF SEWER PIPE .....	17
TAB. 1.4-1: HOW TO USE DIAGNOSTIC TECHNIQUES BY (MAKAR, 1999).....	30
TAB. 2.2-1: ESTIMATES OF THE LENGTH OF THE ADVECTIVE ZONE (RUTHERFORD, 1994) .....	59
TAB. 2.3-1: ISOTOPIC ABUNDANCE OF HYDROGEN, OXYGEN AND WATER. ....	76
TAB. 3.2-1: UNCERTAINTY ANALYSIS IN EXPERIMENTATION (MODIFIED FROM COLEMAN AND STEELE, 1999) .....	98
TAB. 3.3-1: SOURCES OF UNCERTAINTY FOR EACH VARIABLE IN EQUATION EQ. 3.3-1. R: RANDOM ERROR; S: SYSTEMATIC ERROR.....	104
TAB. 3.3-2: VALUES OF THE ERRORS OCCURRING DURING THE QUEST METHOD APPLICATION.....	110
TAB. 3.3-3: CHARACTERISTIC OF THE QUEST EXPERIMENTS. ....	110
TAB. 3.6-1 INFILTRATION RATIO [-] AND RATE [L S-1] CALCULATED AFTER CALIBRATION OF THE MEASURED COD DATA WITH CALIBRATION CURVE 1. ....	132

# FIGURE INDEX

FIG. 1.3.1: PPIs FOR INFILTRATION (LNEC, 2003).....	23
FIG. 1.3.2: PPIs FOR INFILTRATION (LNEC, 2003).....	24
FIG. 1.4.1: IMAGE BY GRC THAT ALLOWED TO SEE AN ILLICIT CONNECTION ( <a href="http://www.nodig.it">HTTP://WWW.NODIG.IT</a> ). ....	26
FIG. 1.4.2: SCHEME OF OPERATION AND RESULTS BY FELL-41 ( <a href="http://www.metrotech.com">WWW.METROTECH.COM</a> ). ....	26
FIG. 1.4.3: IMAGES RECOVERED THAT HIGHLIGHT DAMAGES OR ILLICIT DISCHARGES THIS WAS CARRIED OUT BY A SONIC DISTANCE MEASUREMENT, IT IS EVIDENT THE REDUCTION OF WALL THICKNESS BECAUSE OF CORROSION (PRICE, 1995). ....	27
FIG. 1.4.4: THE IMAGE REPORTS A COLLAPSED SEWER (WRC, 1983). ....	28
FIG. 1.4.5: IMAGES RECOVERED THAT HIGHLIGHT DAMAGES OR ILLICIT DISCHARGES. C. THIS WAS CARRIED OUT BY SSET, THE INFILTRATION AT JOIN AND THE DAMAGES WERE DETECTED (ABRAHAM ET AL., 1997). ....	29
FIG. 2.2.1: CONCEPTUAL SCHEME OF THE QUEST METHOD (MODIFIED AFTER RIECKERMANN AND GUYER, 2002) ...	37
FIG. 2.2.2: GRAPH OF CONDUCTIVITY AND FLOW RATE VS. TIME. THE PEAKS NUMBER 1, 2, 4 AND 5 ARE THE REFERENCE SIGNALS; THE PEAKS NUMBER 3 AND 6 ARE THE INDICATOR SIGNALS. ....	37
FIG. 2.2.3: SCHEME OF TRACER DOSAGE AND SAMPLING OF QUEST-C METHOD (MODIFIED FROM RIECKERMANN ET AL., 2003B). ....	39
FIG. 2.2.4: CONCENTRATION PROFILE DOWNSTREAM FROM A STEADY POINT SOURCE (FROM RUTHERFORD, 1994). ..	48
FIG. 2.2.5: CONCENTRATION PROFILES DOWNSTREAM FROM A STEADY TRANSVERSE SOURCES (FROM RUTHERFORD, 1994).....	49
FIG. 2.2.6: CONCENTRATION PROFILES DOWNSTREAM FROM A STEADY TRANSVERSE SOURCES (FROM RUTHERFORD, 1994).....	54
FIG. 2.2.7: COMPARISON OF RATE OF MIXING FOR DIFFERENT VELOCITY AND DISCHARGE RATIO FOR: (A) CONCORDANT BED CONFLUENCE AND (B) DISCORDANT BED CONFLUENCE (FROM BIRON ET AL., 2004). ....	65
FIG. 2.2.8: RATE OF MIXING FOR CONCORDANT AND DISCORDANT BED CONFLUENCES FOR JUNCTION ANGLE OF 30, 60 AND 90° (FROM BIRON ET AL., 2004).....	65
FIG. 2.2.9: MIXING OF FLUID FROM EACH TRIBUTARY AT BAYONNE-BERTHIER CONFLUENCE INDICATED BY CONTOURS OF ELECTRICAL CONDUCTIVITY VALUES FOR: (A) LOW FLOW CONDITION AND (B) HIGH FLOW CONDITION; LETTERS CORRESPOND TO POSITION INDICATED IN INSET; VERTICAL EXAGGERATION 7.0 (FROM BIRON ET AL., 2004).....	66
FIG. 2.3.1: ABSORPTION SPECTRA IN THE RANGE UV-VIS OF WASTEWATER. ....	75
FIG. 2.3.2: SPECTROMETER USED DURING THE EXPERIMENTS IN ROME (TRADE: S::CAN). IT IS 506 MM HIGH AND ITS DIAMETER IS 44 MM.....	75
FIG. 2.3.3: RELAZIONE TRA L'ENERGIA POTENZIALE E LA DISTANZA INTER-ATOMICA PER ISOTOPI PESANTI E LEGGERI DI UNA MOLECOLA. L'ENERGIA DI DISSOCIAZIONE DIFFERISCE PER I DUE ISOTOPI, E INFLUISCE SULLE VELOCITÀ DI REAZIONE, QUINDI SUL FRAZIONAMENTO ISOTOPICO (FROM CLARK & FRITZ, 1997). ....	79
FIG. 2.3.4 FRACTIONATION FACTORS A VS. TEMPERATURE (FROM CLARK & FRITZ, 1997) .....	80
FIG. 2.3.5 (FROM KENDALL AND McDONNELL, 1998).....	83
FIG. 2.3.6 (FROM KENDALL AND McDONNELL, 1998).....	84
FIG. 2.3.7 SCHEME OF THE WATER CYCLE (FROM CLARK & FRITZ, 1997) .....	86

FIG. 2.3.8 SCHEMATIC ATTENUATION OF SEASONAL ISOTOPE VARIATIONS IN RECHARGE WATERS DURING INFILTRATION THROUGH THE UNSATURATED ZONE AND MOVEMENT WITHIN THE SATURATED ZONE AND THE CRITICAL DEPTH (FROM CLARK & FRITZ, 1997) .....	86
FIG. 3.3.1: CORRELATION BETWEEN THE MEASURED FLOW RATE AND THE AREA OF THE REFERENCE PEAKS.....	101
FIG. 3.3.2: CALIBRATION CURVE. THE CONDUCTIVITY VALUES WERE CORRECTED WITH THE INITIAL CONDUCTIVITY OF THE WASTEWATER SAMPLE. THE CALCULATED CALIBRATION COEFFICIENT IS $0.0006 [\text{GR NaCl} \cdot \text{L}^{-1} / \mu\text{S} \cdot \text{CM}^{-1}]$ .....	102
FIG. 3.3.3: SYSTEM USED FOR DOSING THE TRACER SOLUTION. ....	105
FIG. 3.3.4: RIGHT: EGG-SHAPED CROSS SECTION OF THE INVESTIGATED REACH. LEFT: MIXING LENGTH VS. WATER DEPTH.....	106
FIG. 3.3.5: LINEAR REGRESSION OF THE BASELINE FOR NON-OVERLAPPING PEAK QUEST METHOD (RED LINE) AND DEFINITION OF THE START AND END OF THE PEAK (PINK DOT LINE). ....	108
FIG. 3.3.6: ARCHITECTURE OF THE ROUTINES FOR ERROR PROPAGATION WRITTEN IN R-SCRIPT ENVIRONMENT. ....	108
FIG. 3.3.7: CONDUCTIVITY PEAKS IN GREEN LINE THE REFERENCE ONES AND THE INDICATOR ONE IN RED LINE. ....	110
FIG. 3.3.8: CONDUCTIVITY AND FLOW RATE DATA OF THE EXPERIMENT 030710T AND THE EXFILTRATION HISTOGRAM AFTER THE ERROR PROPAGATION. REFERENCE PEAKS (GREEN LINES), INDICATOR PEAKS (RED LINES), FLOWRATE (BLUE LINES); EXFILTRATION HISTOGRAM FOR A SAMPLE SIZE OF 10,000.....	111
FIG. 3.6.1: S::CAN COVERING.....	129
FIG. 3.6.2: PRELIMINARY COD MEASUREMENTS. ....	129
FIG. 3.6.3: COD MEASUREMENTS AFTER CHANGING SAMPLING MANHOLE AND CLEANING PROCEDURE.....	130
FIG. 3.6.4: COD TIME SERIES FOR CALIBRATION OF THE SPECTROMETER.....	131
FIG. 3.6.5: COD FROM LABORATORY VS. COD FROM SPECTROMETER AND CALIBRATION CURVES. ....	131
FIG. 3.6.6 HYDROGRAPH SEPARATION OF THE FLOWS IN INFERNETTO. IN RED THE WASTEWATER FLOW RATE AND IN GREEN THE INFILTRATION FLOW RATE.....	132

## MOTIVATION

This dissertation presents the results of an experimental research carried out in collaboration with the Water Research Institute of the National Research Council (IRSA-CNR) and the University of Rome “Tor Vergata”. That research has been developed within the framework of the European research project APUSS (Assessing Infiltration and Exfiltration on the Performance of Urban Sewer Systems) which partners were INSA de LYON (FR), EAWAG of Zurich (CH), Technological University of Dresden (DE), Faculty of Civil Engineering at University of Prague (CZ), DHI Hydroinform company in Prague (CZ), Hydroprojekt company in Prague (CZ), Middlesex University of London (UK), LNEC in Lisbon (PT), Emschergenossenschaft in Essen (DE) and IRSA-CNR in Rome (IT). That European project was supported by the European Commission under the 5th Framework Programme and it aimed at contributing to the implementation of the Key Action “Sustainable Management and Quality of Water” within the Energy, Environment and Sustainable Development Contract n° EVK1-CT-2000-00072.

APUSS project was also part of CityNet, a network of European research projects on integrated urban water management.

The scientific aim of the research project was to develop new methods for quantifying infiltration and exfiltration in urban sewer networks (i.e., pipes and house connections) and new models for forecasting the sewer reaches likely affected by infiltration and exfiltration. The infiltrations (parasitical waters infiltrated into a sewer) and the exfiltrations (wastewater leakages from a sewer) occur when the sewer pipes are not watertight anymore because of their structural damages. Both infiltration and exfiltration can seriously threat the surface and depth water bodies in an urban area. Although the problem is quite known and several methodologies already exist for quantifying I/E (Infiltration/Exfiltration), such methodologies are often time consuming, expensive and affected by high uncertainty. Thus, the motivation of the APUSS project was to develop speedy and more accurate methods as well as models for planning strategically the sewer rehabilitation. In particular, IRSA-CNR had to apply the methods developed by EAWAG in Rome in order to assess the applicability in urban areas and reliability of the results.

The entire study is summarized in this thesis. It started with a literature review about the causes of infiltration and exfiltration (I/E) in urban sewer systems, the several factors found out to be responsible of sewer deterioration could help in listing the criteria for individuating the urban areas where applying the new methods. Before applying the proposed methods, an experimental design has been done identifying the main sources of errors. Then application was

carried out in two urban areas in Rome and the collected data were analyzing with error propagation techniques.

Finally, considerations about the speediness and the uncertainty could be done.

## **Acknowledges**

Since the beginning of this research, several people and institutions have been collaborating and I want to thank them individually:

- Technicians of IRSA-CNR: Salvatore Tatti and Maurizio Ronda;
- Diploma students of University “Tor Vergata”: Umberto Cascetti, Michela Mazza, Giuseppe Di Giulio, Tiziano Cingolani, Silvia Grappone and Agnese Ricci;
- ACEAATO2 S.p.A;
- Municipality of Rome with Dipartimento alle Politiche della Programmazione e Pianificazione del Territorio, Ufficio Pianificazione e Progettazione Generale: dott. Claudio Succhiarelli;
- IGAC-CNR;
- Municipio V° of Rome.

# INTRODUCTION

The thesis is divided into three chapters.

The first one deals with the theoretical aspects of the subject: what the infiltration and exfiltration mean and, as they threaten the urban water environment; the causes of structural sewer deterioration and the traditional sewer diagnostic techniques.

The second chapter deals with the new methods developed in APUSS project and, an accurate analysis of the theoretical aspects behind them is presented. In particular, tracer transport models in surface water bodies are discussed for the exfiltration methods and, hydrograph separation approach in hydrology as well as water isotopes are discussed for the infiltration methods.

The third chapter introduces the methodology used for the uncertainty analysis applied for the experimental design of the methods. Finally, the results of the experiments are shown and discussed.

# **CHAPTER 1**

## **The Problem**

### **1.1 Why should we measure the infiltrations?**

The infiltration of parasitical water in a damaged sewer system can cause the inefficiency of the integrated system sewer-wastewater treatment plant. The impact upon the sewer is mainly due to transport of fine grains into the pipe that settling on the bottom reduce the cross area available as well as removing support around the pipe determine a less mechanical resistance of the backfilling. The impact upon urban surface water bodies is due to both the dilution of the pollutant concentrations into the wastewater stream causes serious problems at different stages within a WasteWater Treatment Plant (WWTP) if the infiltrations were unknown when that plant was build, and the rise of frequency of the combined/separated sewer overflows that can cause discharges of untreated wastewater into natural water bodies. Untreated wastewater can be deliver to the urban environment not only the known chemical and biological pollutants, but also numerous pharmaceutical and organic contaminants recently recognized as pollutants of increasing concern (Halling-Sorensen et al., 1998; Daughton and Ternes, 1999; Ayscough et al.,



2000; Jorgesen and halling-Sorensen, 2000; Dietrich et al., 2002; Heberer, 2002; Kolpin et al., 2004; Weigel et al., 2004).

Although the effect of the inefficiency of a damaged sewer characterized by high amount of infiltration can be checked at the wastewater treatment plants and at CSOs discharges, the individuation of the most damaged part of a network can be done only monitoring directly the system. Such an approach has been used by the European research project APUSS which principal aim has been to develop two methods for quantifying infiltration by measuring continuously the concentration of typical wastewater pollutants.

## **1.2 Why should we measure the exfiltrations?**

Exfiltration of wastewater from damaged sewer systems transport into the surrounding environment organic and inorganic pollutants dangerous for the human health.

Groundwater is the main source of potable water, nevertheless the use of urban groundwater is a serious challenge because of the severe anthropogenic pressure on it. As a matter of the fact, actually the principal groundwater sources are in the rural areas, but because of the increasing demand of water and the over-abstraction in the those areas, urban groundwater is getting an important potable water source. Consequently, worldwide a lot of researches are studying which pollutants are discharged from urban activities (industry, landfill, septic tank, sewer leakages, etc...) into the aquifers, which behaviour those pollutants have in the subsurface, how they can threat the human healthy, how they can be detected and then removed from groundwater or even from the aquifer itself. However, a natural protection of the groundwater quality is generally assumed, it is called “purification capacity” due to the unsaturated zone, but such capacity changes according to the sediment and hydrological characteristics of the aquifer (Rettinger et al., 1991).

The risk of contamination of soil and groundwater is especially high when wastewater, containing high concentrations of toxic chemicals, pathogenic bacteria for humans, and highly persist viruses, leaks from sewer (Dizer et al., 1985; Filip et al., 1986; Milde et al., 1987). When a pollutant does not vary its chemical and physical characteristics going through an aquifer, it could be considered an indicator of occurring exfiltration.

Since eighties, different approaches have been using for investigating the groundwater contamination by wastewater leakages, and the first studies were carried out in Germany, United

Kingdom and USA. The adopted methodology was the quality aquifer characterization and when such studies were approached one of the most important aspect to be defined was the sampling procedures. Generally, several monitoring-wells were built up and water samples were taken by suitable sampling system. The reliability of the collected data principally depended on the monitoring-well building criteria (e.g., deepness and extension of the abstraction section, location) and the sampling technique (e.g., by means of pump or multi layer sampler). (Ronen et al., 1986).

Rettinger et al. (1991) carried out an interesting study by building up a 10 m test pipe at 0.85 m below the ground and 5 m above the groundwater level and around the rig, which was parallel to groundwater flow, six monitoring wells were installed. The vertical spatial variation of:  $\text{Na}^+$ ,  $\text{NO}_3^-$ ,  $\text{HCO}_3^-$ ,  $\text{SO}_4^{2-}$ , Dissolved Organic Carbon, Dissolved Oxygen,  $\text{K}^+$  and  $\text{Zn}^{2+}$  was detected by means of multi-layer samplers based on the dialysis cell technique (Ronen et al., 1986). Only the first five parameters above showed high concentrations and high variability. Such a variability was only evident by multi-layer sampler which use, together with the ratio between the sewer leakage flow and the contaminated groundwater flow, and the dissolved oxygen in the contaminated groundwater, is important when the purification soil capacity has to be assessed.

Powell et al. (2003) studied the impact of sewer leakages on sandstone aquifers (confined and unconfined) detecting sewer-derived bacteria (*E.coli*, faecal streptococci and sulphide-reducing clostridia) and viruses (enteroviruses, Norwalk-like viruses, adenovirus, rotavirus, astrovirus). The aim of their study was to determine the deepness of the penetration of these sewer-derived microorganisms in Permo-Triassic sandstone aquifer underlying the city of Birmingham and Nottingham. The results proved that the microbiological contamination by sewer leakages in this kind of soil is not reduced by adsorption, filtration and inactivation. Indeed the aquifer thickness was entirely contaminated (90 m below the ground level) by the bacteria which concentration varied with the deepness; among these the sulphide-reducing clostridia bacteria were found to have a very long resistance in an aquifer and then to be indicator of sewer leakages in the past. The aquifer thickness was also contaminated by Virus, which presence could not be correlated to the bacteria. They hypothesized that the local aquifer features, which might affect the microorganism transport (averagely estimated 1 m/day) and survival, are: temperature, rain events and soil heterogeneities. Sometimes the component of groundwater flow responsible for long distance transport does not reflect the main hydraulic property, and beyond every expectation tens of meters far away from the leaking sewer the microorganisms could be found.

Concerning virus transport and survival, Bhattacharjee et al. (2002) developed a two dimensional models for virus transport in physically and geochemically heterogeneous subsurface porous media, considering the removal by attachment, release and inactivation by temperature. They estimated that: (i) in physical layered heterogeneous porous media the preferential transport is altered when geochemical heterogeneity is considered; (ii) under randomly heterogeneous hydraulic conductivity can provide preferential pathways; while high variation of heterogeneous geochemistry results in a slower transport; (iii) about the breakthrough behaviour the important parameters are: patches available for deposition; inactivation rate constant.

Dizer and Hagendorf (1991) analyzed the groundwater quality in an aquifer under leaking sewer, in particular they considered the physiological groups of microorganisms like: general aerobic bacteria, amylolytic bacteria, denitrifying bacteria, actinomycetes and fungi. Some of them are autochthonous microorganisms at different trophic levels which react rapidly as the substrate concentration changes and mostly of them (i.e., anaerobic bacteria as sulphate-reducing and denitrifying ones) are in the aquifers under urban areas where situation like low oxygen and high organic matter concentrations may occur. They found that denitrifying bacteria, actinomycetes and fungi were more abundant in wastewater contaminated samples than in uncontaminated ones, and the distributions of Total Organic Carbon, COD and total Nitrogen in the sewer leakages were similar to the denitrifying bacteria, actinomycetes and fungi thus the microbiological response seemed to be consistent with the substances aided to the soils from exfiltrations.

Barrett et al. (1999) applied a multi-component investigation in Nottingham (UK) in order to identify the different sources of recharges of groundwater (drinking water, wastewater and precipitation). The measured parameters were chosen among those defined as markers (i.e., easily analysed solute that is unique to one water source and pathway, at a constant concentration in the source and is non-reactive in all conditions, these kind of substances is rare and has to be identified carefully). In the shallow groundwater they found out a set of wastewater markers:  $^{15}\text{N}$ , total coliform, E.coli, faecal streptococci, d-limonene.  $^{15}\text{N}$  allowed them to distinguish the different recharges, and where the groundwater showed an enrichment of  $^{15}\text{N}$  they considered it due to wastewater contaminations. d-limonene ( $\text{C}_{10}\text{H}_{16}$ ) recently used as an aromatic scenting agent in domestic cleaning products as a speciality solvent. Nevertheless, none of the considered markers could be absolute indicators because of the die-off of microorganisms, the mixing and the fractionation (principally during denitrification) of  $^{15}\text{N}$  and the not constant presence of d-limonene in raw water.

As a conclusion of the results of the research presented above, since bacteria and viruses can penetrate into the groundwater and persist for a long period the microbiological approach for the exfiltration investigation should be an useful tool. Nevertheless uncertainty remains about:

- the real and actual source of contamination (e.g., septic tanks or sewer);
- the sewer reach damaged which wastewater comes from;
- the actual sewer state, because such a markers could mean an old contamination by exfiltration phenomena occurring in the past.

Thus it might be more accurate to use conservative tracers directly added into running sewer pipes in well known network part and time for quantifying directly the water losses (Ellis, 2001). Such an approach has been used by the European research project APUSS which principal aim has been to develop two methods for quantifying exfiltrations by dosage of chemical conservative and non-buoyant tracers into running sewer reaches.

### **1.3 Sewer pipe deterioration**

About this topic a literature review was done and published in an Italian journal:

Giulianelli, M.; Prigiobbe, V. (2004). Infiltrazione di acque di falda nelle fognature. L'ACQUA, 6, pp. 41-50.

In annex 1

The motivation of the study of the main factors affecting the sewer state arise from necessity to locate suitable urban sewer where carrying out the experimental activities. The initial questions were:

- which characteristics are to be considered as important ones for a sewer to be tested;
- which grade of spatial heterogeneity these characteristics can have;
- how we can suppose two sewer systems to have a different state of deterioration;
- which informations we are able to gathered from the authorities of Rome.

The urban characteristics taken into account were established on the basis of the factors that in an urban area can affected the state of sewer network as well as those that are actually used for predicting the sewer deterioration and planning the rehabilitation.

In the next chapter is presented a brief review about: the sewer deterioration factors, the approaches for the sewer deterioration forecasting and the sewer diagnostic techniques.

### ***1.3.1 Factors affecting the structural state of sewer system***

The deterioration of sewer system causes the pipes to be not watertight anymore; consequently, infiltrations of parasitical water (e.g., groundwater, leakage from water system, ...) and exfiltrations can occur.

The sewer damages can be divided in two groups (Gokhale and Graham, 2004):

- structural defects that include cracks, fractures, joint displacement, deformation and collapse;
- operational damages that include root intrusion, siltation and blockage. The roots can cause structural damage as well as the opening of joints, while siltation can lead to blockage which in turn can cause excessive pressure in the system, and producing leakages.

For an detailed knowledge of sewer deterioration, the sewer should be considered as a composite structure consisting of: the pipe itself (geometry, material, use, etc...), the ground in which it is buried, and the local environment.

The principal factors that affect the state of sewer pipes were studied by several researchers and a summary of such factors is shown in Tab. 1.3-1.

Davies et al. (2001A) provide an exhaustive review focused on the features that have been recognized as influencing the structural stability of rigid pipes. Davies et al. (2001B) carried out a statistical investigation using logistic regression analysis for the individuation of restricted data set of variables describing the sewer network state; they found out that there were some variables that can help determining the risk of collapse of sewer as:

- sewer pipe section length;
- sewer size;
- sewer use;
- backfilling soil properties;
- sewer location;
- local groundwater regime;
- sewer material;
- traffic load, mainly the bus load;
- sewer depth.

Moreover, the infiltration and the exfiltration (principally in hydraulic surcharge regime) are recognized as important causes of loss ground surrounding the pipes, reducing the backfilling soil mechanical resistance (WEF/ASCE,1994; Serpente, 1994; WRc, 2001), since the loss of ground into a defect of pipes can result in the formation of voids or zones of low density adjacent soil to the sewer, which permit progressive deformation of defective sewer (WRc, 2001).

**Tab. 1.3-1: Factors affecting the structural state of sewer pipe.**

FACTORS	COMMENTS
<b>Construction factors</b>	
Load transfer	From cars, buses, others
Standard workmanship	It is one of the principal cause of collapses for a lot of authors.
Sewer size	There are a lot of conflicting opinions about relationship between diameter and fractures. O'Reill et al. (1989) concluded that the incidences of cracks increases with diameter.
Sewer depth	The effect decreases up to a depth of 5.5 m, but beyond 5.5 m the defects begin increasing with depth (O'Reill <i>et al.</i> , 1989).
Sewer bedding	The bedding and surrounding material determine the

---

	distribution of the loads over a pipe. The rate of exfiltration (Rauch and Stegner, 1994) and infiltration (Fenner, 1991) are sensitive to this factor.
Sewer material	For example, clay sewer provides excellent corrosion protection in comparison with concrete ones.
Sewer joint type and material	The rubber seals used for flexible joints are more vulnerable to corrosion due to the soil than the pipe itself.
Sewer pipe section length	Fenner (1990) reported that a potential point for infiltration is the joint, and as longer individual sewer pipes, less joints per unit of sewer length, then less infiltration could go in the system.
Connections	The connections of houses represent one of the principal point of infiltration and exfiltration (Ellis, 2001)
<b>Local external factors</b>	
Surface loading and surface use	General static and dynamic loads, maintenance works of infrastructures, etc... For example the load of traffic that is not important itself, but the characteristic of the road pavement and bedding material have greater influence on the load transfer (O'Reill <i>et al.</i> , 1989). Furthermore the construction traffic is another important load contribution.
Water mains bursts and leakage	
Ground disturbance	For example differential settlements of soil during the first years and afterwards. Davies et al. (2001B) found that sewers laid in fracture potential soils (as clay) are at lower risk than sewer constructed in other soil. Anyway, it is to be considered that sewer are build in trenches that could reduce the ground disturbances.
Groundwater level	The water flows into or out the sewer, infiltration and exfiltration, respectively, promote the ground loss around the pipes (see below).
Ground condition	The shrinkage and/or swelling of the soil under different temperatures produce various stress on the pipes.
Soil-backfill type	For example, the defect rate was found higher on sewer laid in

---

---

	clay soil-backfill than in chalk and sand one (O'Reill <i>et al.</i> , 1989).
Root intrusion	The roots can break the sewer walls as well as open the joints.
<b>Other factors</b>	
Sewage characteristics	Wastewater can be corrosive, in particular if it is characterized by: pH<5.5, Sulphate>200 mg/L and CO <sub>2</sub> >0.23 mg/L*carbonate hardness for concrete and asbestos cement (WSA/FWR,1993). Davies <i>et al.</i> (2001B) estimated that separated sewer can more likely be damaged than combined one.
Inappropriate maintenance method	The cleaning by means of pump jetting can erode the inner sewer wall
Age of sewer	It is not the age itself, principally, but the period of construction according to the historical and technological development.
Sediment friction	

---

An interesting analysis is given by WRc (2001) which is based on a comparison among the effects of sewer defect size, hydraulic surcharge, groundwater level with water depth and soil type on ground loss. The worst situation is for a submerged sewer with severe defects, laid in a sandy fine sand or fine sand subjected to frequent high magnitude hydraulic surcharges; whereas one of the best picture is a non-submerged sewer with small defects, laid in a medium to high plasticity clays never subjected to hydraulic surcharges. The location of the experimental areas in Rome has been done on the basis of this analysis, and the investigated sewer systems (called Torraccia and Infernetto) were chosen because one was supposed to represent the best situation (Torraccia) and the worst situation (Infernetto).

Finally, Fenner (2000) identified some informations to be collected for completely characterizing an urban sewer systems, those information can support the decision for a strategic rehabilitation planning. They are divided in three groups: physical attributes, data by field visits and other. In particular:

1. the key physical attributes are: levels cover manhole, pipe sizes, invert levels of incoming and outgoing pipes and pipe material;



2. data by field visits: condition of manholes, overall integrity of the manhole structure, degree of tree roots, silt and evidence of surcharge levels;
3. other: pipe shape, function/location/condition of the upstream catchment, hydraulic load and frequency surcharge, drift/underlying geology, groundwater level, traffic and surface loadings, age and construction techniques, event history and frequency of CSO operation, years since last inspection as well as previous maintenance and rehabilitation history.

Even though all these informations are useful when multi-parametric models are used for assessing and forecasting the urban sewer state, gathering them is a very cost effective work, then the informations' collection should be only concentrated on those parts of the sewer asset that are at most risk from a likely future failure.

A brief description of some models developed so far for sewer deterioration assessment in order to plan a prioritizing interventions is given in the following paragraph.

### ***1.3.2 Sewer deterioration modelling***

The functionality of the sewer system includes hydraulic, environmental and structural aspects, and for a good performance of the system the operators should provide an efficient rehabilitation planning. The urgency of sewer rehabilitation reflects the criterion used for classifying the damaged reaches in a priority way for the renovation, tools for the optimization of sewer rehabilitation can be summarized in three points (Baur, 2003):

1. development of a rehabilitation strategy;
2. selection of cost-efficient rehabilitation projects;
3. choice of the most appropriate rehabilitation technology for the selected projects.

While for understanding how the researchers approached at pipe deterioration modelling, it is profitable to know how they have studied the water pipe deterioration. Although recently more efforts have been done on improving the quality of this infrastructure, there are several old sewer systems whose there are not historical data about the their deterioration, but only the collapse of sewer pipes have been recorded over the years. Nevertheless, some historical failure records for water pipes have been available, and on these cases researchers can develop models for forecasting pipe deterioration.

Kleiner and Rajani (2001A and 2001B) wrote a comprehensive review about the models used for quantifying the structural deterioration of water mains by analysing historical performance data. Such models are divided in two groups: physical and statistical.

The physical models are scientifically more robust because consider the real loads supported by the pipe and its mechanical resistance, but because they needed the huge amount of data, this approach is applied when the important consequences of pipe failures can justify the accumulation of such data.

The statistical models with various levels of input data may be useful for minor water mains for which there are few data available or for which the cost of failure does not justify the amount and the quality of the required data. The statistical models assume that the historical patters can continue in the future, and the prediction can be done by:

- deterministic models, that are either time-exponential models or time-linear models based on two or three parameters. They are applied on an homogeneous group of pipes that have to be selected carefully;
- probabilistic multi-variate models consider many covariates (defined with awareness by an expert), that influence the pipe breakage patterns, and the selection of homogeneous groups it is not necessary. This kind of model can be useful for define a priority for rehabilitation;
- probabilistic single-variate group-processing models, that include models that use probabilistic processes on grouped data to derive: probabilities of pipe life expectancy (useful for future financial needs), probability of breakage and probabilistic analysis of break clustering phenomenon (useful for short-term planning of water main rehabilitation and renewal).

For example, the EN 752-5 formulates: “the investigation of the construction may comprise either a complete examination of the drainage system or a selective method”. Mueller (2003) argued out the benefit of random selection because it is convenient in terms of time and costs. Then the sewer network has to be grouped in quite homogeneous set according to the relevant characteristics to be considered.

The number of the selected groups depend on heterogeneity of the urban area and the aim of the selective inspection is to infer from the distribution of the classes of condition resulting from a representative random sample the distribution of the classes of condition of specific groups of reaches (Mueller, 2003). These groups have to be small enough to be quite uniform but

to be large enough to provide significant results (Kleiner and Rajani, 2001). The steps for the selection could be:

1. grouping the reaches in samples according to the factors in Tab. 1.3-1;
2. randomly evaluating, inspecting and classifying the condition of each sample, and possibly the longest reaches in each one;
3. projection of the distribution of the condition of the samples taken;
4. localization of the inspection and rehabilitation priorities.

The methods developed within APUSS project for assessing the infiltration at sub-catchment scale allow to improve the sewer grouping. For example, an urban area defined potentially affected by infiltration in a certain period of the year can be investigated by isotopic or pollutograph method in order to confirm this statement quantifying the infiltration rate. While an urban area defined potentially affected by exfiltration in a certain period of the year can be investigated and some of the reaches of its sewer system could be chosen as sample (90% of the reaches (Mueller, 2003)) for quantifying the leakages. In this way, the novel method could be useful for quantifying the consequence of assumed structural damages.

Furthermore, Fenner (2000) described a number of different methods that can be used to optimise and to prioritise proactive maintenance analysing sewer performance. All of them tend to define criteria for classify the sewer pipes in critical or in non-critical <sup>1</sup>. This kind of models consist of performance assessment by parameters defined in agree with local characteristic, legal constraints, operational and management strategies (Fenner, 2000). Cardoso et al. (1999) developed a standardised performance assessments suggesting domains of performance indicators (PPIs) relied on hydraulic, environmental, structural, economic and social aspects. The PPIs may be used for immediate decision for technical management or design oriented just on some important performance aspects. A performance indicator list developed within the APUSS project is shown in Fig. 1.3.1 and Fig. 1.3.2 and they are used in a model for supporting decision making during planning rehabilitation allowing a hierarchy of the intervention estimate the performance assessment of the sewer systems by infiltration and exfiltration (LNEC, 2003).

---

<sup>1</sup> Critical sewers are defined as those for which the repair costs after a collapse are expected to be the highest (WRc, 1983).

Definition	Unit	Designation	Concept/Explanation
$Q_{inf}/Q_{full}$	(%)	Infiltration full capacity utilization	<i>The proportion of the sewer's full section flow capacity used up by the infiltration flow. This indicator makes no distinction between the possible origins of infiltration (such as joints, manholes, etc.). Its value may be assessed for a single sewer, for groups of sewers (subsystems) or for the entire system. The data needed is the full flow capacity of the sewer or group of sewers, which is normally available if the topology, geometry and material of the pipes is known. This indicator supplies information on the hydraulic performance of the analysed sewer(s), but gives no indication as to the net infiltration flow. For example, for a network branch with 3 consecutive sewers of growing capacity but with a constant infiltration flow, the indicator might be worth 60%, 30% and 10% (upstream to downstream) simply because the capacity was growing, while effectively the infiltration flow was of the same magnitude throughout.</i>
$Q_{inf}/Q_{avdwf}$	(%)	Infiltration proportion of dry weather flow	<i>The infiltration flow expressed as a percentage of the daily mean dry weather flow. This indicator does not take into account the different origins of infiltration. Its value may be assessed for a single sewer, for groups of sewers (subsystems) or for the entire system. It requires measurements or estimates of the dry weather flow. A drawback of this indicator is its dependency on the values of the dry weather flow. For example, a 1 km-long 1000 mm sewer with an infiltration flow of 50 m<sup>3</sup>/day would rate as a low-infiltration case in the light of the Portuguese regulation 23/95. The value of the indicator would be 0.5% in a system with a dry weather flow of 8640 m<sup>3</sup>/day, and 1.2% in another where the dry weather flow would be 4320 m<sup>3</sup>/day. When applied to the flow that reaches the WWTP, this indicator gives an estimate of the weight of infiltration flow on treatment costs. In this respect, it may be expressed either as a volume percentage or as a cost percentage.</i>
$Q_{inf}/n^{\circ}$ of manholes	(m <sup>3</sup> /s)	Infiltration flow per manhole	<i>Mean infiltration flow per manhole unit. Manholes are an important source of infiltration. This indicator gives an idea of the influence of the number of manholes on total infiltration. It should be evaluated in sewers or groups of sewers of equal length, for comparisons, in order to avoid a bias related to the infiltration along the pipes, which is ignored by this indicator. Infiltration taking place in service connections is equally disregarded. The data needed is the total number of manholes.</i>
$Q_{inf}/n^{\circ}$ of service connections	(m <sup>3</sup> /s)	Infiltration flow per service connection	<i>Mean infiltration flow per service connection. Service connections are an important source of infiltration. This indicator gives an idea of the influence of the number of service connections on total infiltration. The data needed is the total number of service connections.</i>
$Q_{inf}/\text{sewer length}$	(m <sup>3</sup> /s/km)	Infiltration flow per unit sewer length	<i>Mean infiltration flow per unit length of sewer. This indicator does not take into account the influence of infiltration taking place in manholes or service connections. Again, the indicator may be calculated for sewers, groups of sewers or entire systems. The data needed is the total length of sewers contributing to the section where it is being calculated. This indicator will give relevant results in systems where infiltration takes place predominantly along the sewers.</i>
$Q_{inf}/\text{sewer longitudinal area}$	(m <sup>3</sup> /day/(cm.km))	Infiltration flow per unit sewer wall area	<i>mean infiltration flow per unit area of sewer wall. This indicator does not take into account the influence of infiltration taking place in manholes or service connections. Again, the indicator may be calculated for sewers, groups of sewers or entire systems. The data needed is the total wall surface area of the sewers contributing to the evaluation point. This indicator will give relevant results in systems where infiltration takes place predominantly along the sewers.</i>

Fig. 1.3.1: PPIs for infiltration (LNEC, 2003).

Definition	Unit	Designation	Concept/Explanation
Qexf /n° of manholes	(m <sup>3</sup> /s)	Exfiltration flow per manhole	<i>Mean exfiltration flow per manhole unit. Manholes are an important source of exfiltration. This indicator gives an idea of the influence of the number of manholes on total exfiltration. It should be evaluated in sewers or groups of sewers of equal length, for comparisons, in order to avoid a bias related to the exfiltration along the pipes, which is ignored by this indicator. Exfiltration taking place in service connections is equally disregarded. The data needed is the exfiltration flow and the total number of manholes..</i>
Qexf /n° of service connections	(m <sup>3</sup> /s)	Exfiltration flow per service connection	<i>Mean exfiltration flow per service connection. Service connections are an important source of exfiltration. This indicator gives an idea of the influence of the number of service connections on total exfiltration. It should be evaluated in sewers or groups of sewers of equal length, for comparisons, in order to avoid a bias related to the exfiltration along the pipes, which is ignored by this indicator. The data needed is the exfiltration flow and the total number of service connections.</i>
Qexf /sewer length	(m <sup>3</sup> /s/km)	Exfiltration flow per unit sewer length	<i>Mean exfiltration flow per unit length of sewer. This indicator does not take into account the influence of exfiltration taking place in manholes or service connections. Again, the indicator may be calculated for sewers, groups of sewers or the entire systems. The data needed is the exfiltration flow and the total length of sewers contributing to the section where it is being calculated. This indicator will give relevant results in systems where exfiltration takes place predominantly along the sewers.</i>
Qexf /sewer longitudinal wet area	(m <sup>3</sup> /day/(cm.km))	Exfiltration flow per unit sewer wet wall area	<i>Mean exfiltration flow per unit area of wet sewer wall. This indicator does not take into account the influence of exfiltration taking place in manholes or service connections. Again, the indicator may be calculated for sewers, groups of sewers or the entire systems. The data needed is the exfiltration flow and the wet wall surface area of the sewers contributing to the evaluation point. This indicator will give relevant results in systems where exfiltration takes place predominantly along the sewers.</i>

**Fig. 1.3.2: PPIs for infiltration (LNEC, 2003).**

A scientific paper proposed for an international conference about the application of PPIs is:

Cardoso, A.; Prigiobbe, V.; Giulianelli, M.; Baer, E.; Coelho, S.T. (2005). Assessing the impact of infiltration and exfiltration in sewer systems using performance indicators: case studies of the APUSS project. 10<sup>th</sup> International Conference on Urban Drainage, Copenhagen, Denmark, 21-26 August 2005.

In annex 2.

## 1.4 Diagnostic techniques

Although the methods for assessing the infiltrations and the exfiltrations developed within APUSS project can help understanding which part of an urban sewer systems is likely more damaged than another, never they can substitute the direct diagnostic techniques. The infiltration or/and exfiltration estimated by these methods will never give punctual description of

a structural damage. Thus, after applying these methods and individuating which sewer reach could need to be repaired, the sewer direct detection should be carried out.

Different diagnostic techniques exist and they can be divided in three groups that examine (Wirahadikusumah et al., 1998):

1. the overall condition of the external part of the sewer;
2. the overall condition of the sewer wall and, in some cases, the soil around the pipe;
3. specific problems within or behind the sewer wall.

Below each group of the diagnostic techniques listed above is described.

The detection of the overall condition of the external part of a sewer (i.e., sewer wall and the soil surrounding) can be carried out by means of:

- infrared thermography (GRC) that is carried out by an airplane flying over the area or by specially-equipped vans traversing all over the ground. It allows individuating the WW leakage, GW infiltration and the erosion voids (Weil et al., 1994), but it is susceptible to environmental conditions and it is expensive (Fig. 1.4.1).
- ground penetrating radar (GPR) technique that allow gathering information about the structure condition of sewer pipes and surrounding environment (Foillard et al., 1995), but Makar (1999) showed by experimental tests that this system is inaccurate in detecting the voids near the pipes, in particular if the sewer is laid in clay soil.
- dye test by means of smoke or liquid tracers. For example, the first one can be carried out by blowing smoke into an investigated pipe under pressure and then observing where the smoke appears over the ground;
- water tests that are 100% accurate but it is time consuming and labour intensive;
- a new system developed in Germany called FELL-41 system and validated by Gokhale and Graham (2004) in USA. It measures the electrical current between a probe moving in the pipe and a surface electrode. The pipe to be tested can contain sewage or water. The points where water flows out or into cause electrical signal intensity to increase proportionally to damages (Fig. 1.4.2). Gokhale and Graham (2004) successfully tested the device on circular small pipes made by different non-conductive materials (clay, PVC and HDPE) ranging in diameter from 200 through 300 mm. The assessments were reproducible and repeatable as

well as cost-effective. Although it is applicable in larger pipes (up to 1500 mm), the flooding could be cost and time consuming. Finally, practical problems are: bends, jumps and roots that could be damaged the probe.

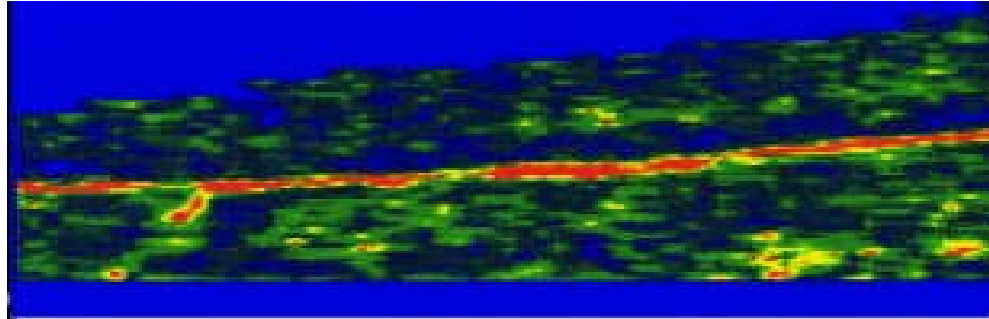


Fig. 1.4.1: Image by GRC that allowed to see an illicit connection (<http://www.nodig.it>).

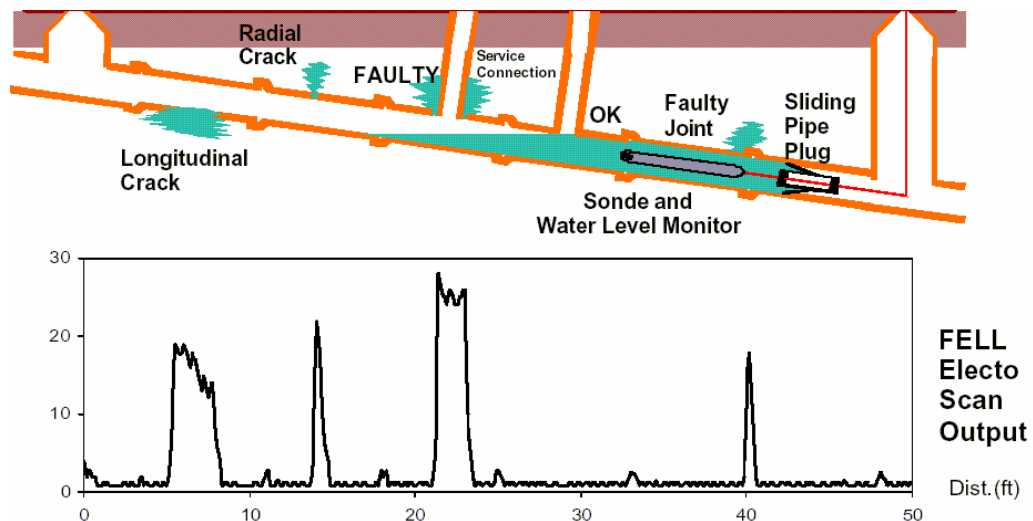


Fig. 1.4.2: Scheme of operation and results by FELL-41 ([www.metrotech.com](http://www.metrotech.com)).

Detection of the part within and behind the sewer wall can be done by means of:

- sonic distance measurement method that use the sound waves generated by a piezoelectric transducer that detects the corrosion loss (Fig. 1.4.3) and the volume of the debris on the invert of sewer as small as 0.5 m or as large as 4 m (Price, 1995; Browne et al., 1993). This system allows to detect the state of the sewer under the water, thus it is useful for detecting leakages;
- a system based on the micro-deflection of sewer pipe could be used in order to investigate the state of both sewer wall and the bedding soil. Applying pressure to the inside surface of the wall to very slightly deform it (Makar, 1998). The deflection pressure applied ratio allows to estimate the mechanical resistance of both sewer and soil bedding. Anyway just rigid pipes can be investigated and,

because of the pressure applied, new damages could be produced. At the state of the art of this method, it is not possible to separate these new damages from the those already presented before the pressure application;

- impact echo and spectral analysis of surface waves that consists of applying the natural vibration by means of hammers and detecting the vibration by microphones (Sack and Olson, 1994). Unfortunately, it is not possible either to distinguish the defects in sewer wall from those into the bedding soil either to locate the damages.

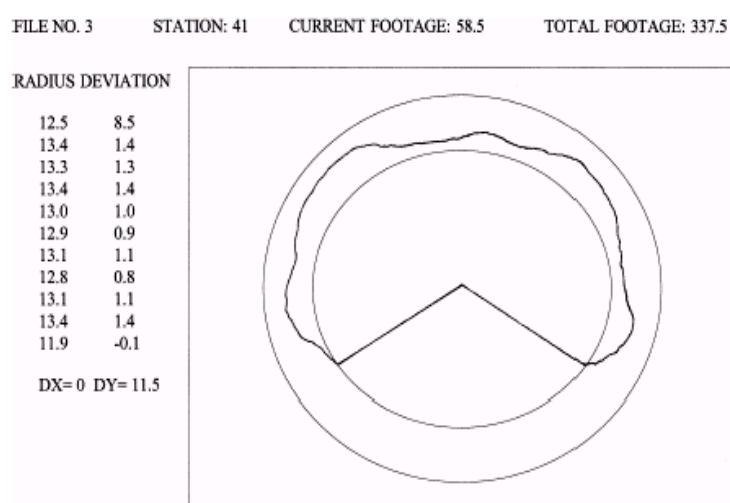


**Fig. 1.4.3: Images recovered that highlight damages or illicit discharges this was carried out by a sonic distance measurement, it is evident the reduction of wall thickness because of corrosion (Price, 1995).**

Detection of the overall part inside the pipe (i.e. joins, house connections, etc.) can be done by means of:

- Close-Circuit TeleVision (CCTV) the first system was a stationary CCTV (Fig. 1.4.4). The stationary CCTV is one of the cheapest method for sewer investigation but the principal disadvantages are: (i) long sewer could be believe without any defects, (ii) defects under water or behind obstructions could be missed, (iii) the images could be subjectively interpreted and a not reference image for the deformation assessment existed so far. The first was overcome disadvantage the mobile CCTV was developed; the second one by the multi-sensor system. The third disadvantage was overcome by computer aided CCTV that assists the analysis process and both qualifies and identifies the defects. Anyway recently a new European standard EN 13508 and in particular the EN 13508-2 (Condition of



drain and sewer system outside buildings-part 2 visual inspection coding system - final draft) codifies the pipe damages recorded by visual inspections (i.e. CCTV, photos, direct inspections, etc.). The damage is codified by three letters: the first one identifies the investigated structure (manhole, pipes ...); the second one defines the material, the use, etc...; and the third one the detected damages (cracks, collapse ...) and then there are other informations that describe how large is the cracks and where it is placed around the pipe wall.

- a method for assessing the exfiltration at pipe scale consisting of filling the investigated pipe with water and keeping it in this condition for 24 for hours. The level of water used to fill it has to marked at the upstream manhole. The exfiltration rate would be the amount of water that in 1 hour is required to maintain the level constant;
- a method for assessing the infiltration at pipe scale consisting of completely sealing the pipe upstream and measuring the infiltrated flow rate at downstream by an accurate system like as a weir



**Fig. 1.4.4: The image reports a collapsed sewer (WRc, 1983).**

For a more accurate inspection of sewer condition the Laser-Based Scanning system should be applied, furthermore it has substantially reduced operator errors (Gibert, 1997), and in order to detect both above and below the water line the ultrasonic inspection system can be adopted (Andrews, 1998). It allow to see pits, voids and crack, even if some small cracks are not detectable.

Nowadays, advanced multi-sensoric systems like as KARO (optical, ultrasonic and microwave) (Kuntze et al., 1995), PIRAT (CCTV, laser and sonar scanners) (Campbell et al., 1995) and SSET (CCTV, scanner and three axis mechanical gyroscope) (Abraham et al., 1997)

exist, which can optimize the sewer detection (Fig. 1.4.5). The advantages of these systems are: more reliable data, continuous profile of pipe walls, robot module, higher benefit/cost ratio than the rational methods (e.g., CCTV, Ultrasonic and GPR). The disadvantages of these systems are: they are in prototypical or testing stage that require further development for field implementation and high initial cost (Wirahadikusumah et al., 1998).

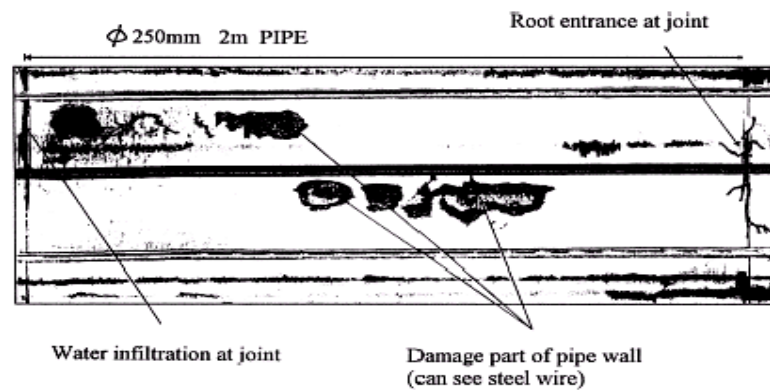


**Fig. 1.4.5: Images recovered that highlight damages or illicit discharges. C. this was carried out by SSET, the infiltration at join and the damages were detected (Abraham et al., 1997).**

The following Tab. 1.4-1 summarizes and compares the method for sewer investigation discusses above.

Tab. 1.4-1: how to use diagnostic techniques by (Makar, 1999).

Technique (1)	Where to use (2)	What will be found (3)
<i>(a) Inspection of inner pipe surface</i>		
Conventional CCTV	Empty pipes; partially filled pipes above the water surface	Surface cracks; visible deformation; missing bricks; some erosion; visual indications of exfiltration/infiltration
Stationary CCTV	Pipes with <50-m distance between manholes	As CCTV
Light line CCTV	Pipes where deformation is issue	Better deformation measurements + CCTV results
Computer-assisted CCTV	As CCTV, currently small diameter pipes only	As CCTV, but with quantitative measurements of damage
Laser scanning	Partially filled pipes; empty pipes	Surface cracks, deformations; missing bricks; erosion losses
Ultrasound	Flooded pipes; partially filled pipes; empty pipes	Deformation measurements; erosion losses; brick damage
<i>(b) Inspection of pipe structure and bedding condition</i>		
Microdeflections	Rigid sewer pipes	Overall mechanical strength
Natural vibrations	Empty sewer pipes	Combined pipe and soil condition; regions of cracking; regions of exfiltration
Impact echo	Larger diameter; rigid sewers	Combined pipe and soil condition; regions of wall cracking; regions of exfiltration
SASW	Larger diameter; rigid sewers	Regions of wall cracking; overall wall condition; variations in soil condition; regions of exfiltration
<i>(c) Inspection of bedding</i>		
Ground penetrating radar	Inside empty or partially filled pipes	Voids and objects behind pipe walls; wall delaminations; changes in water content in bedding material

The diagnostic techniques that: give informations about the structural sewer state comparable to those provided by the novel methods developed within APUSS project and allow to estimate the structural state of running sewer are:

- Stationary CCTV;
- Computer assisted CCTV;
- Laser scanning;
- Ultrasound;
- Micro-deflection;
- Impact echo;
- SASW.

## 1.5 References

EN 13508-2 (Condition of drain and sewer system outside buildings-part 2 visual inspection coding system - final draft).

D.M. 97/1999.

D.L. 152/1999 and D.M. 258/2000.

Abraham, A.D.; Iseley, T.; Prasanth, R.K.; Wirahadikusumah, R. (1997). Integrating Sensing Technologies for Underground Utility Assessment, ASCE Conference on Infrastructure Condition Assessment, Boston, MA, August 1997.

Andrews, M. E. (1998). Large diameter sewer condition assessment using combined sonar and CCTV equipment. Proc. APWA Int. Public Work Congr. National Research Council of Canada.

Ayscough, N. J.; Fawell, J.; Franklin, G.; Young, W. (2000). Review of human pharmaceuticals in the environment. Environment Agency, R&D Technical Report P 390.

Barrett, M. H.; Hiscock, K. M.; Pedley, S.; Lerner, D. N.; Tellam, J. H.; French, M. J. (1999). Marker species for identifying urban groundwater recharge sources: a review and case study in Nottingham, UK. *Water Research*, 33 (14) pp. 3083-3097.

Baur, R. (2003). Developing a decision framework for sewer network rehabilitation. Proceedings of the 17<sup>th</sup> European Junior Scientific Workshop on Rehabilitation

Bhattacharjee, S.; Ryan, J. N.; Elimelec, M. (2002) Virus transport in physically and geochemically heterogeneous subsurface porous media. *Journal of Contamination Hydrology*, 57, pp. 161-187.

Browne, R.; Knott, G. (1993). Television and Scanning Sonar in Seattle Metro's Siphons and Brick Sewers, ASCE International Conference on Pipeline Infrastructure II, San Antonio, p. 694–701.

Campbell, G.; Rogers, K.; Gilbert, J. (1995). PIRAT—A System for Quantitative Sewer Assessment, International No-Dig '95 Conference, Dresden, Germany, September 1995 pp. 455–462.

Cardoso, M. A., Coelho, S. T., Matos, J. S. and Matos, R. S. (1999). A new approach to the diagnosis and rehabilitation of sewerage systems through the development of performance indicators. In Proceedings of the eight international conference urban storm drainage, Sidney - Australia. pp. 610-617.

Dauthton, C. G.; Ternes, T. A. (1999). Pharmaceuticals and personal care products in the environment: agents of subtle change? *Environ Health Perspect*, 107(Suppl. 6), pp. 907-938.

Dietrich, D. R.; Webb, S.F.; Petry T. (2002). Hot spot pollutants: pharmaceuticals in the environment. *Toxicological Letter*, 131, pp. 1-3.

Davies, J.P.; Clarke, B.A.; Whiter, J.T.; Cunningham, R.J. (2001A). Factors influencing the structural state deterioration and collapse of rigid sewer pipes. *Urban Water* vol.3, pp. 73-89.

Davies, J.P.; Clarke, B.A.; Whiter, J.T.; Cunningham, R.J.; Leidi, A. (2001B). The structural condition of rigid sewer pipes: a statistical investigation. *Urban Water*, 3, pp. 145-154.

Dizer, H.; Filip, Z.; Lopez Pila, J.; Milde, G.; Nasser, A.; Seidel, K. (1985). Laborversuche zur persistenz unfid zum trasportverhalten von viren. *Materialen* 2, pp.20-26, umweltbundesamt. Schmidt, Berlin.

Dizer, H.; Hagendorf, U. (1991). Microbial contamination as an indicator of sewer leakage. *Water Research*, 25 (7), pp. 791-796.

Ellis, B. (2001). Sewer infiltration/exfiltration and interactions with sewer flows and groundwater quality. Conference Proceedings of the 2<sup>nd</sup> International Conference “Interactions between sewer, treatment plants and receiving waters in urban areas”. Interurba II°, Lisbon, 19<sup>th</sup>-22<sup>nd</sup> February 2001, pp. 311-320.

Fenner, R.A. (1990). Excluding groundwater infiltration into new sewers. *Journal of IWEM*, 4.

Fenner, R.A. (1991). The influence of sewer bedding arrangement on infiltration rates and soil migration. *Municipal Engineer*, vol. 8, pp. 105-117.

Fenner, R.A. (2000). Approaches to sewer maintenance: a review. *Urban Water*, vol. 2, pp. 343-356.

Filip, Z.; Dizer, H.; Kaddu-Mulindwa, D.; Kiper, M.; Lopez Pila, J. H.; Milde, G.; Nasser, A.; Seidel, K. (1986). Untersuchungen ueber das verlhaten pathogener und anderer mikroorganismen und viren im grundwasser im hinblick auf die bemessung von wasserschutzzonen. In *WaBoLu Hefte 3*: Bundesgesundheitsanmt, Berlin.

Foillard, R.; George, B.; Schwarze, C. (1995). New Applications of Ground Penetrating Radar for Construction and Rehabilitation in the Pipe Sector. International No-Dig '95 Conference, Dresden, Germany September 1995, pp. 147–159.

Gibert, J (1997). *Newsdesk. Insight* January 39 (1), 9.

Gokhale, S.; Graham, J. A. (2004). A new development in locating leaks in sanitary sewers. *Tunneling and Underground Space Technology* n.19, pp. 85-96.

Halling-Sorensen, B.; Nielson, S.N.; Lanzky, P.F.; Ingerslev, F.; Holten Luthoft, J.; Jorgensen, S.E. (1998). Occurrence, fate and effects of pharmaceutical substances in the environment – a review. *Chemosphere*, 35, pp. 357-393.

Heberer, T. (2002). Occurrence, fate, and removal of pharmaceutical residues in the aquatic environment: a review of recent research data. *Toxicological Letters*, 131, pp. 5-17.

Jorgensen, S.E.; Halling-Sorensen, B. (2000). Drugs in the environment. *Chemosphere*, 40, pp. 691-699.

Kleiner, Y.; Rajani, B. (2001). Comprehensive review of structural deterioration of water mains: statistical models. *Urban Water*, 3, pp. 157-176.

Kolpin, D.W.; Skopec, M.; Meyer, M.T.; Furlong, E.T.; Zaugg, S.D. (2004). Urban contribution of pharmaceutical and other organic wastewater contaminants to streams during differing flow conditions. *Science of the Total Environment*, 328, pp. 119-130.

Kreitler, C.W. (1975). Determining the source of nitrate in groundwater by nitrogen isotope studies: Austin, Texas, Univer. of Texas, Austin, Bureau of Econ. Geol. Rep. of Inves. #83, 57 p.

Kreitler, C.W., 1979. Nitrogen-isotope ratio studies of soils and groundwater nitrate from alluvial fan aquifers in Texas. *Journal of Hydrology*, 42, pp. 147-170.

Kuntze, H.B.; Schmidt, D.; Haffner, H.; Loh, M. (1995). KARO—A Flexible Robot for Smart Sensor-Based Sewer Inspection. International No-Dig '95 Conference, Dresden, Germany, September 1995, pp. 367–374.

LNEC (2003). Infiltration and exfiltration performance indicators- sewer system performance assessment methodology and formulation. Project APUSS delivery.

Management of Urban Infrastructure Networks, Dresden 2003.

Makar, J.M. (1999). Diagnostic Techniques for Sewer Systems. *Journal of Infrastructure Systems*, 5 (2), pp. 60-78.

Milde, G.; Filip, Z.; Leschber, R.; Hagendorf, U. (1987). Auswirkungen von Abwasser auf Boden und Untergrund. *Gewaässersch. Aest. Abwäss.* (100), pp. 351-370.

Mueller, K. (2003). Selective inspection of sewer system and connecting pipes. *Proceedings of the 17<sup>th</sup> European Junior Scientific Workshop on Rehabilitation*

O'Reilly, M. P.; Rosbrook, R. B.; Cox, G. C.; McCloskey, A. "Analysis of defects in 180 km of pipe sewers in southern water authority" TRRL Research Report, 1989.

Powell, K. L.; Taylor, R. G.; Cronin, A. A.; Barrett, M. H.; Pedley, S.; Sellwood, J.; Trowsdale, S.A.; Lerener, D. N. (2003). Microbial contamination of two urban sandstone aquifers in the UK. *Water Research* 37, 339-352.

Price, T. (1995). Inspecting Buried Plastic Pipe Using A Rotating Sonic Caliper. *Proceedings of the 2nd International Conference on Advances in Underground Pipeline Engineering*, pp. 126–137.

Rauch, W.; Stegner, Th. (1994). The colmation of leaks in sewer systems during dry weather flow. *Water Science and Technology*, 30 (1) pp. 205 - 210.

Rettinger, S.; Ronen, D.; Amiel, A.J.; Magaritz, M.; Bischopsberger, W. (1991). Tracing the influx of sewage from a leaky sewer into a very thin and fast-flowing aquifer. *Water Research* 25, 75-82.

Ronen, D.; Margaritz, M.; Levy, I. (1986). A multilayer sampler for the study of detailed hydrochemical profiles in groundwater. *Water Research* 20, pp. 311-315.

Sack, D.; Olson, L. (1994). In situ non-destructive testing of buried precast concrete pipe. *Proc. ASCE 1994 Mat. Engrg. Conf. ASCE Reston. Va.*

Sacher, F.; Lange, F. T.; Brauch, H.-J.; Blankenhorn, I. (2001). Pharmaceuticals in groundwaters Analytical methods and results of a monitoring program in Baden-Wuerttemberg, Germany. *Journal of Chromatography A*, 938, pp. 199-210.

Serpente, P.E. (1994). Understanding the modes of failure for sewers. In W. A. Macaitis (Ed.), *Urban drainage rehabilitation programs and techniques selected papers on urban drainage rehabilitation from 1988-1993*. New York, ASCE.

TU Dresden (2004). Conceptual model for the ex and infiltration of sewer. Project APUSS delivery.

WEF/ASCE (1994). Existing sewer evaluation and rehabilitation. 2nd edition. WEF manual of practice FD-6/ASCE manuals and reports on Engineering practice n. 62.

Weigel, S.; Beger, U.; Jensen, E.; Kallenborn, R.; Thoresen, H.; Huehnerfuss, H. (2004). Determination of selected pharmaceutical and caffeine in sewage and seawater from Tromso/Norway with emphasis on ibuprofen and its metabolites. *Chemosphere* 56, pp. 583-592.

Weil, G.J.; Graf, R.J.; Forister, L.M. (1994). Remote sensing pipeline rehabilitation methodologies based upon the utilization of infrared thermography. *Urban drainage rehabilitation programs and techniques*, ASCE.

Wirahadikusumah, R.; Abhaham, D. M.; Iseley, T.; Prasanth, R. K. (1998). Assessment technologies for sewer system rehabilitation. *Automation in Construction* 7, pp. 259-270.

WRc, (1983). *Sewerage Rehabilitation Manual*. 2<sup>nd</sup> edition. UK.

WRc, (2001). *Sewerage Rehabilitation Manual*. 4<sup>th</sup> edition. UK.

WSA/FWR (1993). *Manual of sewer condition classification*. 3<sup>rd</sup> edition.

# **CHAPTER 2**

## **Novel Methods for Quantifying the infiltration and the exfiltration in Urban Sewer Systems**

### **2.1 Introduction**

Within the project APUSS novel methods for quantifying the infiltrations and exfiltrations in urban sewer systems have been developed by EAWAG (CH) and they have been applied by IRSA-CNR (IT) in two sewer systems in Rome. Anyway, these methods do not intend to replace the use of direct diagnosis techniques (described into §[1.4]), but money can be saved by using them for selecting sewer parts to be carefully investigated. As a matter of the fact, an advantage into use these novel methods is that they allow to quantify the infiltration and the exfiltrations and then to prioritise sewer parts for the inspection, as well as they can be applied



for the calibration and/or validation of the models used for the strategic planning of sewer rehabilitation.

This chapter is divided into two principal parts:

1. in the first one, the methods for quantifying the exfiltrations are described and the physical phenomena is critically discussed;
2. in the second one, the methods for quantifying the infiltrations are described and the applicability of those methods on an urban sewer system is critically discussed, as well.

## **2.2 Methods for Quantifying the Exfiltrations**

In this paragraph, two methods developed for the quantification of the exfiltrations from the urban sewer networks are described. The methods are called QUEST (QUantification of Exfiltration from Sewer with artificial Tracer) and QUEST-C (QUantification of Exfiltration from Sewer with artificial Tracer Continuously dosed). They share a basic common idea, that is they consist of calculating a mass balance upon chemical a running urban sewer reach to be investigated of conservative tracer dosed into the wastewater stream. Nevertheless, they distinguish on the dosage system:

1. QUEST is based on the slug injection of a chemical tracer at two different points along the reach to be tested;
2. QUEST-C is based on a continuous dosage of two different chemical tracers at two different points along the reach to be tested.

The methods are described below, and subsequently there is a critical discussion of them, but for more details about them it suggests to read the protocol written by the partner of APUSS project that developed these methods and the literature by Rieckermann and Gujer, 2002, Rieckermann et al., 2003 and Rieckermann et al., 2004.

### ***2.2.1 QUEST***

The method QUEST applied has been developed within European Project APUSS. It essentially consists of a slug dosage of a tracer solution at known concentration in two different manholes of a sewer pipe and in the detection of tracer cloud plume<sup>2</sup> at downstream (Fig. 2.2.1).

At the first manhole upstream of the investigated pipe the amount of tracer affected by exfiltration is dosed and at measuring manhole (Fig. 2.2.1) the conductivity is recorded. When the cloud of tracer arrives at this section a peak is detected, as it allows evaluating the residual mass of tracer it is called indicator peak.

At the second manhole the tracer slug dosage aims at estimating the flow rate and the conductivity peak measured at downstream is called reference peak.

Between the second manhole and the measuring one the exfiltration ratio is not assessed, because it affects both the indicator and the reference signals.

In the following Fig. 2.2.2 reference and indicator conductivity signals are shown together with the hydrograph.

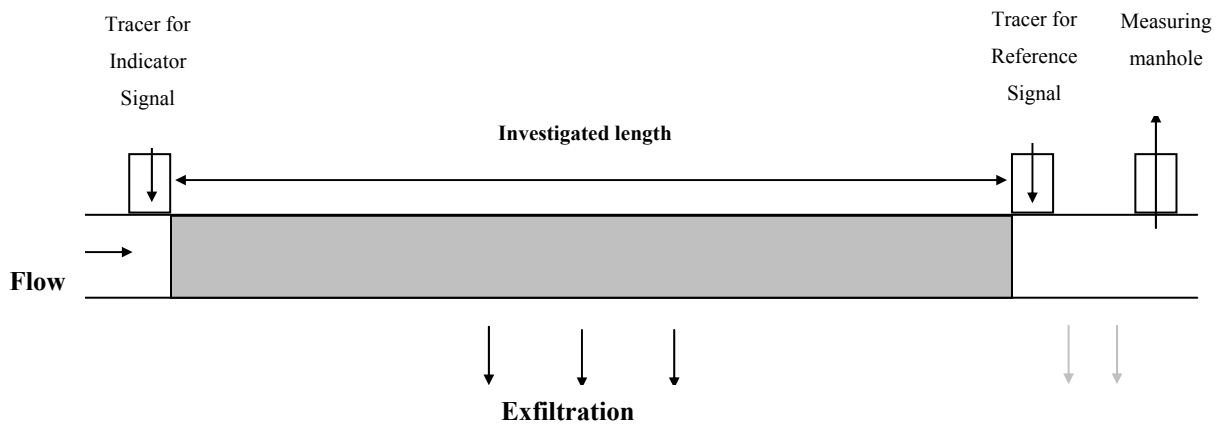


**Fig. 2.2.1: Conceptual scheme of the QUEST method (modified after Rieckermann and Guyer, 2002)**

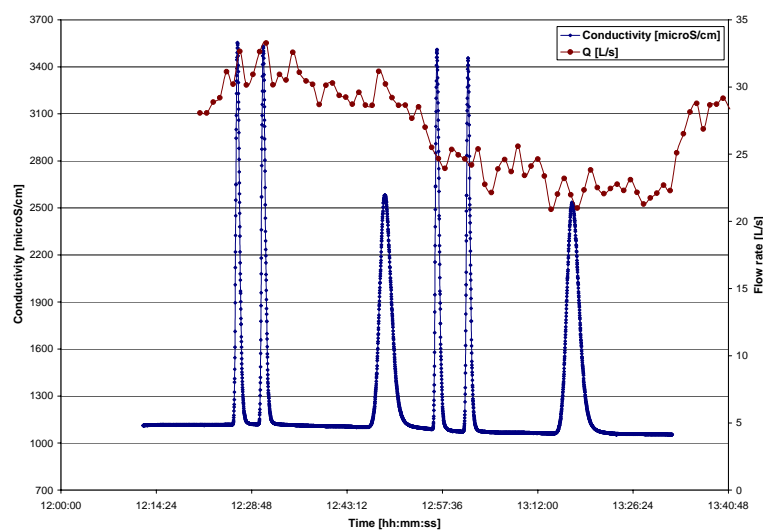


**Fig. 2.2.2: Graph of conductivity and flow rate vs. time. The peaks number 1, 2, 4 and 5 are the reference signals; the peaks number 3 and 6 are the indicator signals.**

If the complete mixing occurs the exfiltration rate of tracer mass is equal to wastewater one, so the equation used for the calculation of exfiltration ratio is:

$$exf = 1 - \frac{M_{meas}}{M_{dosage}}$$

Eq. 2.2-1

where  $M_{dosage}$  is the dosed NaCl amount [gr] and  $M_{meas}$  is evaluated by the following equation:

$$M_{meas} = \int_{span\_ind.} Q(t) * e * (C(t) - C_{baseline}(t)) dt$$

Eq. 2.2-2

in the Eq. 2.2-2 *span ind.* indicates the time during which the conductivity peak of indicator signal passes through the measuring manhole;  $Q(t)$  is the flow rate during the indicator peak passage [L/s];  $C(t)$  is the indicator signal conductivity measured [ $\mu\text{S}/\text{cm}$ ];  $e$  is the conversion coefficient evaluated in the laboratory ( $e = 0.0006 \text{ gr cm (L } \mu\text{S)}^{-1}$ ) and  $C_{baseline}(t)$  is the background conductivity of wastewater during the indicator peak passage [ $\mu\text{S cm}^{-1}$ ].

### 2.2.2 QUEST-C

The method QUEST-C allows quantifying the exfiltration in urban sewer pipes (Rieckermann et al., 2003 A and B; Rieckermann et al., 2004). It consists of a continuous dosing of two different tracer solutions (LiCl and NaBr) at two different locations along a tested sewer. The LiCl solution has to be dosed for measuring the discharge at the beginning of investigated reach ( $Q_1$  in Fig. 2.2.3), the NaBr solution has to be dosed for measuring the discharge at the end of investigated reach ( $Q_2$  in Fig. 2.2.3). The wastewater samples taken at Manhole 3 are to be analyzed by means of IC in order to determine the  $\text{Li}^+$  and  $\text{Br}^-$ . The background concentration of  $\text{Br}^-$  is determined by sampling at Manhole 2.

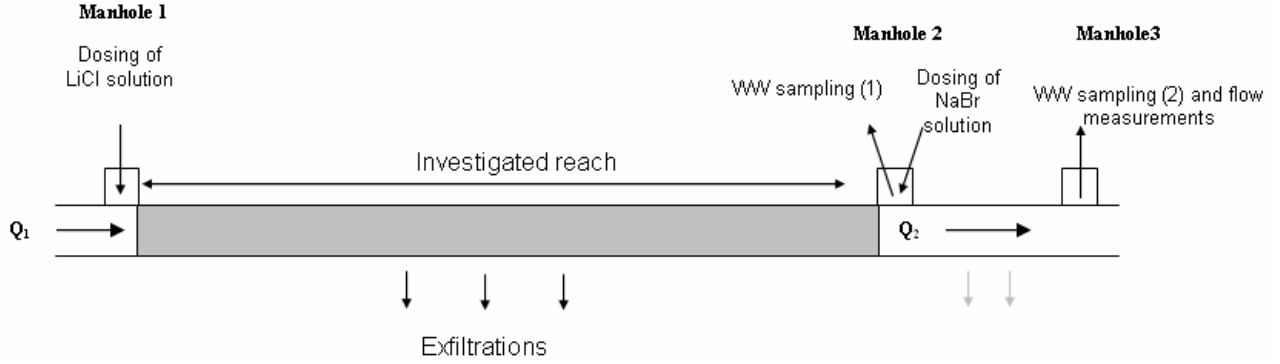


**Fig. 2.2.3: Scheme of tracer dosage and sampling of QUEST-C method (Modified from Rieckermann et al., 2003B).**

The exfiltration ratio percentage is calculated by the following equation:

$$exf. = \left( \frac{Q_1 - Q_2}{Q_1} \right) * 100$$

**Eq. 2.2-3**

In particular, considering a steady flow the latter equation becomes:

$$exf. = \left( 1 - \frac{\frac{c_{solBr} * q_{solBr}}{C_{wwBr}}}{\frac{c_{solLi} * q_{solLi}}{C_{wwLi}}} \right) * 100$$

**Eq. 2.2-4**

where:  $c_{solBr(Li)}$  [mg/L] is the  $Br^-$  ( $Li^+$ ) concentration in the dosed solution;  $q_{solBr(Li)}$  [L/s] is the flowrate of the peristaltic pump dosing NaBr (LiCl) solution;  $C_{wwBr(Li)}$  [mg/L] is the concentration of  $Br^-$  ( $Li^+$ ) in the wastewater samples. The  $q_{solBr(Li)}$  is checked during the experiment in order to control the stability of the dosed tracer masses.

The Eq. 2.2-3 is applicable when the flow is quite steady during the trials; in this case Rieckermann et al. (2003B) estimated that the standard deviation of exfiltration ratio changed between 2.4% - 2.6%, and Rieckermann et al. (2004) observed that it decreased at 0.5% as the flow rate variability was taken into account. Following the exfiltration ratio has been calculated by the Eq. 2.2-3, because all the experiments were carried out in a period of the day when the lowest variability of flowrate had been calculated.

### ***2.2.3 Hydrodynamic background of QUEST and QUEST-C***

QUEST and QUEST-C base on the dilution method (ISO 9555-1, 1994) and allow to estimate the flowrate more accurately than the flowmeter, because of the high accuracy of the equipments applied. Nevertheless, there can be some sources of uncertainty affecting the exfiltrations calculated with the equations Eq. 2.2-1 and Eq. 2.2-3, and they are generally due to:

1. dosage of tracers;
2. adsorption and precipitation of tracers;
3. tracers transport;
4. uncorrected sampling or uncorrected measurement of tracers;
5. data regression.

In this chapter the physical phenomena involved during the transport (point three above) of non-buoyant tracers in a channel is discussed in order to highlight the importance of some key points of the QUEST and QUEST-C methods (e.g., mixing, dilution, etc.). The other points are discussed in the next chapter, because in this chapter more emphasis is given to the hydraulic aspects of the tracer transport, while in the next chapter deals with the uncertainty sources.

Finally, the sampling and the measurement procedures for taking representative water samples are given.

#### **2.2.3.1 Tracer Transport**

The methods QUEST and QUEST-C consist of dosing a non-buoyant conservative tracer into a wastewater stream and calculate how much of this exfiltrates.

When a tracer is introduced into a stream, it is carried away from the point of discharge by the current and this phenomena is called advection and it spreads out because of the molecular diffusion or dispersion. Most of the considerations in this chapter are taken from (Rutherford, 1994).

In laminar flow we have the following situation. The advection causes the fluid parcels to move downstream without spreading, for a parcel that is carried in the direction  $x$ , the advective flux is modelled by:

$$I_x = u_x c$$

**Eq. 2.2-5**

where  $I_x$  is the advective flux in x direction [ $\text{g m}^{-2} \text{s}^{-1}$ ];  $u_x$  is the average longitudinal velocity [ $\text{m s}^{-1}$ ];  $c$  is the tracer concentration [ $\text{g m}^{-3}$ ]. The Lagrangian system, which lies at the centre of the tracer cloud (collection of fluid parcels whose dimension are comparable with the smallest length scale of interest and with velocity and concentration characteristics), is use for advection.

The molecular diffusion is modelled by the Fick's law:

$$J_x = -e_m \frac{\partial c}{\partial x}$$

**Eq. 2.2-6**

where  $J_x$  is the molecular diffusive flux in the x direction [ $\text{g m}^{-2} \text{s}^{-1}$ ];  $e_m$  is the molecular diffusion coefficient whose typical value in water changes between  $0.5 - 2.0 \times 10^{-9} [\text{m}^2 \text{s}^{-1}]$ ;  $\delta c/\delta x$  is the tracer concentration gradient in the x direction [ $\text{g m}^{-4}$ ]. The negative sign means that the molecular diffusion develops in the opposite direction of the concentration gradient. The molecular diffusion is defined in a fixed Eulerian coordinates.

The advection/diffusion three dimensional equation can be derived from a mass balance on a rectangular parcel fluid moving at mean velocity is in rectangular Cartesian coordinates<sup>2</sup>:

$$\frac{\partial c}{\partial t} + \sum_{i=1}^3 \left( u_i \frac{\partial c}{\partial x_i} \right) = e_m \left[ \sum_{i=1}^3 \left( \frac{\partial^2 c}{\partial x_i^2} \right) \right]$$

**Eq. 2.2-7**

where  $u_i$  is the average velocity along the three orthogonal directions defined by the rectangular Cartesian coordinates [ $\text{m s}^{-1}$ ] where 1="x", 2="y" and 3="z".

A solution of this system for:

- a. a conservative tracer;
- b. known initial conditions;
- c. stationary situation;
- d. unbounded channel;

allows us seeing that the variance of tracer cloud increase linearly with time.

If the Reynolds number is below 500 the flow is laminar, if it is above about 2000 the flow is turbulent which is generated by velocity shears where there are velocity gradients. In a turbulent flow the tracer spread more rapidly than in the first one.

---

<sup>2</sup> It is considered the right Cartesian coordinate system.

The three dimensional equation (Eq. 2.2-7) can be written under the turbulent condition, but considering as field of velocity and concentration, the velocity and the concentration of an ensemble average (that is the average concentration and velocity of tracer clouds measured over several identical experiments) plus the deviation from this state:

$$u_i = \langle u_i \rangle + u_i'$$

Eq. 2.2-8

$$c = \langle c \rangle + c'$$

Eq. 2.2-9

where  $\langle \rangle$  denotes an ensemble average;  $u_i'$  and  $c'$  indicate the deviation from the ensemble average which average values by definition are zero.

Consequently, the advection/diffusion three dimensional equation (Eq. 2.2-7) for a turbulent flow can be derived from a mass balance on a rectangular parcel fluid moving at mean velocity is in rectangular Cartesian coordinates:

$$\frac{\partial \bar{c}}{\partial t} + \sum_{i=1}^3 \left( \bar{u}_i \frac{\partial \bar{c}}{\partial x_i} \right) = e_m \left[ \sum_{i=1}^3 \left( \frac{\partial^2 \bar{c}}{\partial x_i^2} \right) \right] - \sum_{i=1}^3 \left( \frac{\partial \overline{u_i' c'}}{\partial x_i} \right)$$

Eq. 2.2-10

In the equation (Eq. 2.2-10) the additional terms  $\left( -\frac{\partial \langle u_i' c' \rangle}{\partial x_i} \right)$ , for  $i = 1 \div 3$ ) are called Eddy diffusion or turbulent diffusion that with molecular diffusion cause rapid tracer mixing in turbulent flow. The problem in solving this equation stems from the unknown fluctuations of concentration and velocity terms.

Taylor (1921) adopted a Lagrangian coordinates system and examined the longitudinal mixing in homogeneous and stationary turbulence, and an important result was the variance of tracer ensemble increases linearly with time at the rate of squared turbulent intensity ( $u_i'$ ) after a certain time since the tracer injection this time is called integral Lagrangian time-scale ( $T_i$ ). As this is in analogy with laminar flow modelled by Fickian diffusion, the following relationship, valid for  $t \gg T_i$ , can be written:

$$-\frac{\partial \langle u_i' c' \rangle}{\partial x_i} = e_t \frac{\partial^2 \langle c \rangle}{\partial x_i^2}$$

Eq. 2.2-11

where  $e_t$  is the turbulent diffusion coefficient (Eddy diffusivity, of the order  $10^{-3} \text{ m}^2 \text{ s}^{-1}$ ) that is higher than  $e_m$  which is of the order  $10^{-9} \text{ m}^2 \text{ s}^{-1}$ . Moreover,  $e_t$  depends on the flow, whereas  $e_m$  depends on the fluids.  $e_t$  is assumed to be isotropic and homogeneous.

The equation (Eq. 2.2-11) provides an economical and a tolerable accurate model for turbulent diffusion at the mid- and far-fields that are explained below.

The Reynolds analogy comes from the following consideration. In a turbulent flow the turbulent velocity fluctuations transfer momentum more rapidly than in laminar flow and the shear stresses between adjacent water layers are higher than in laminar flow. These stresses are called turbulent or Reynolds stresses:

$$\tau_t = \rho \langle u'_x u'_y \rangle$$

**Eq. 2.2-12**

$\tau_t$  is proportional to the correlation between the turbulent velocity fluctuations and remembering the equation (Eq. 2.2-11) where  $e_t$  is proportional to the correlation between the tracer concentration and the velocity fluctuation then because of the problem for estimating  $\tau_t$  into the momentum equation, Boussinesq in 1877 proposed the following relationship for turbulent stress:

$$\tau_t = \rho \nu_t \frac{\partial \langle u_x \rangle}{\partial y}$$

**Eq. 2.2-13**

Reynolds pointed out that the turbulent Eddies that transfer momentum transfer mass too and then it is possible to write by analogy:

$$J_y = -e_t \frac{\partial \langle c \rangle}{\partial y}$$

**Eq. 2.2-14**

As equation (Eq. 2.2-15),  $e_t$  and  $\nu_t$  have the same units [ $\text{m}^2/\text{s}$ ].

The equation Eq. 2.2-14 is equal to equation Eq. 2.2-11, but the first one is generally valid for turbulent flow, while the second one stems from the analogy between the laminar and homogeneous stationary turbulent flows where the variance of tracer cloud increases linearly with time.

Another approach is from Reynolds analogy for tracer mass the eddy diffusivity is equal to turbulent viscosity:



$$e_t = v_t$$

**Eq. 2.2-15**

but for buoyant tracer or high sediment concentration the following equation have to be considered:

$$e_t = S_c v_t$$

**Eq. 2.2-16**

where  $S_c$  is the turbulent Schmidt number (0.3-1.0) which needs to be determined experimentally.

From this analysis, it is straightforward to say that for improving and accelerating the mixing between the dosed tracer and the water stream the dosage should be done where the flow is turbulent or an artificial turbulence could be created, for instance, by means of a propeller.

The 3-D mixing equation, which is the basis for the river mixing problem, is:

$$\frac{\partial c}{\partial t} + \sum_{i=1}^3 \left( u_i \frac{\partial c}{\partial x_i} \right) = \left[ \sum_{i=1}^3 \left( e_i \frac{\partial^2 c}{\partial x_i^2} \right) \right]$$

**Eq. 2.2-17**

where  $e_i$  coefficients have to be estimated by fitting the solutions to measured data. The equation (Eq. 2.2-17) can be simplified on the basis of the following points:

1. state of the flow (i.e.: steady or unsteady, laminar or turbulent);
2. type of dosage spatially and temporally (i.e., vertical continuous dosage, punctual slug dosage, etc...);
3. distance from the tracer injection point where the mixing problem is to be solved.

The first point influences the first and the second terms of the equation (Eq. 2.2-17); the second point influences the first and the third terms of the equation (Eq. 2.2-17); the third point only influences the third term. When the tracer is released, it spreads out firstly vertically, secondly transversely and thirdly longitudinally; thus in the first case the gradient of tracer concentration is no zero along  $x$ ,  $y$  and  $z$  and it happens around a distance from the trace injection called near-field; in the second case it is no zero over  $x$  and  $z$  and it happens around a distance from the trace injection called mid-field; finally, it is no zero over  $x$  and it happens around a distance from the trace injection called far-field.

Below some the mixing problem within near-, mid- and far-fields is described.

### ***Near-Field and Vertical Mixing***

In this section the mixing phenomena near the dosage discharge point is explained. It is called Near-Field, and it is within a distance from the tracer dosage point of 50 times the channel width. In the near-field, the tracer is being mixing long x, y and z, if a damage is located within this part the exfiltrated tracer is not proportional to the exfiltrated water, and the QUEST and QUEST-C methods cannot be properly applied. If this length becomes negligible compared to the total investigated length the error due to this part could be neglected. For reducing the effect of this part either a propeller could be applied or a preliminary investigation of the sewer could be done by means of CCTV and the dosage point should be located where the sewer walls appear to be in good conditions.

The near field is the place where the vertical, transverse and longitudinal mixings occur. The time scale for vertical mixing is shorter than for transverse and longitudinal ones. The principal mechanism causing the vertical mixing is the turbulence due to velocity shear at the bed.

Along the vertical direction the velocity profile in turbulent open channel for a non-buoyant tracer is:

$$\frac{u_x(y)}{u^*} = \frac{1}{\chi} \log_e \left( \frac{y}{y_o} \right)$$

**Eq. 2.2-18**

where  $u_x$  is the assemble longitudinal mean velocity [ $\text{m s}^{-1}$ ];  $\chi$  is a constant of proportional (called Von Karman's contant);  $y_o$  is an arbitrary fixed depth;  $u^*$  is the velocity shear defined as:

$$u^* = \sqrt{\frac{\tau_o}{\rho}}$$

**Eq. 2.2-19**

where  $\tau_o$  is the bed shear stress [ $\text{N m}^{-2}$ ] at  $y_o$  and  $\rho$  is the water density [ $\text{g m}^{-3}$ ].

The shear stress profile is:

$$\tau_t = \tau_o \left( 1 - \frac{y}{h} \right)$$

**Eq. 2.2-20**

where  $y$  is the vertical axis [m] and  $h$  is the water depth [m].

The Eddy diffusivity from Eq. 2.2-15, Eq. 2.2-13, Eq. 2.2-20 and Eq. 2.2-18 is:

$$e_y = \chi u^* y \left(1 - \frac{y}{h}\right)$$

**Eq. 2.2-21**

Jobson & Sayre (1970) for practical problems found to be accurate the depth-averaged value:

$$e_y \approx 0.067 h u^*$$

**Eq. 2.2-22**

The Eddies, which cause vertical diffusion, cause the longitudinal diffusion, as well, thus  $e_x = e_y$ . While  $e_z$  variation with depth is not known, but for a channel it is assumed  $e_z = 2e_y$  (Webel & Schatzmann, 1984; Nokes & Wood, 1988).

The vertical mixing can be increased by means of: obstacles, disturbances close to the source and secondary currents at the sharp bends.

In the near-field the QUEST and QUEST-C methods can be mathematically described as follows. In particular, the QUEST method consisting of a slug injection of the tracer can be modelled as an unsteady tracer source in a steady uniform flow in a straight channel ( $u_y = u_z = 0$ ) for which the Eq. 2.2-17 is:

$$\frac{\partial c}{\partial t} + u_x \frac{\partial c}{\partial x} = \sum_{i=1}^3 \frac{\partial^2 e_i c}{\partial x_i^2}$$

**Eq. 2.2-23**

The solution of Eq. 2.2-23 describes the transport of a conservative tracer dosed during the application of QUEST method. The Eq. 2.2-23 has not been solved considering the variation along the  $y$ -axis because: if  $e_x$  and  $e_y$  vary parabolically with depth then  $v_x$  varies logarithmically and the behaviour of  $e_z$  is not known so far.

Considering these parameters constant the model is called constant-parameter model and the solution for a source dosing  $M$  mass of tracer, placed at  $x=0$ ,  $y=y^0$  and  $z=z^0$  and for no-flux boundary condition is:

$$c(x, y, z, t) = M \frac{\exp(-\frac{(x-u_x t)^2}{4e_x t})}{\sqrt{4\pi e_x t}} \sum_{n=0}^{\infty} \exp(-\frac{((2nh \pm y \pm y^0) - y^0)^2}{4e_y t}) \sum_{n=0}^{\infty} \exp(-\frac{((2nb \pm z \pm z^0) - z^0)^2}{4e_z t})$$

**Eq. 2.2-24**

where b and h are the width and the depth of the channel, respectively, varying with the flow.

The longitudinal velocity is not constant with depth because of the bed friction, but it varies parabolically with depth, that makes the tracer cloud to be distorted. The distortion increases the turbulent diffusion along y-axis, that profile increases the vertical diffusion. Increasing opportunely the  $e_x$  and the  $e_y$  the solution in Eq. 2.2-24 approximates the reality.

The Eq. 2.2-17 for a steady tracer source in a steady uniform flow in a straight channel ( $u_y=u_z=0$ ) is:

$$u_x \frac{\partial c}{\partial x} = \sum_{i=1}^3 \frac{\partial^2 e_i c}{\partial x_i^2}$$

**Eq. 2.2-25**

The solution of this equation describes the transport of a conservative tracer dosed during the application of QUEST-C method. The Eq. 2.2-25 can be solved as Eq. 2.2-23 considering the parameters  $e_x$ ,  $e_y$ ,  $v_x$  and  $e_z$  constant, then for a source of tracer mass M, placed at  $y=y^0$  and  $z=z^0$  and for no-flux boundary condition:

$$c(x, y, z) = \frac{M}{4\pi x \sqrt{e_y e_z}} \sum_{n=0}^{\infty} \exp(-\frac{(u_x(2nh \pm y \pm y^0) - y^0)^2}{4e_y x}) \sum_{n=0}^{\infty} \exp(-\frac{(ux(2nb \pm z \pm z^0) - z^0)^2}{4e_z x})$$

**Eq. 2.2-26**

For a source placed at the middle of the depth the concentration profiles are shown in the Fig. 2.2.4.

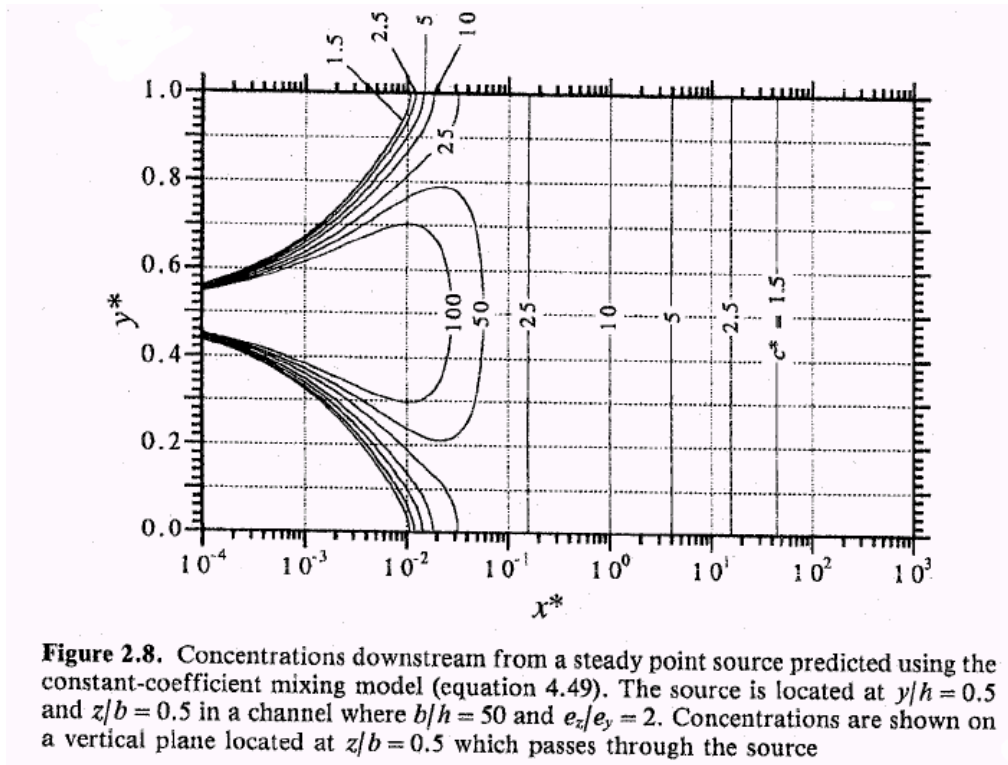


Fig. 2.2.4: Concentration profile downstream from a steady point source (from Rutherford, 1994).

It is important to note that when the concentration is fully mixed vertically, transversally the mixing is continuing.

The vertical mixing distance for a constant-parameter model if the source is at the middle of the water depth is:

$$L_y = 0.134 \frac{u_x h^2}{e_y}$$

Eq. 2.2-27

while if the source is at the bed:

$$L_y = 0.536 \frac{u_x h^2}{e_y}$$

Eq. 2.2-28

Anyway, a practical rule is that  $L_y = 50 h$ .

The mixing problem at the near-field was solved using both constant and variable parameters ( $e_x$ ,  $e_y$ ,  $v_x$  and  $e_z$ ) for a steady transverse dosage system, and the first model predicts longer distance for complete mixing than the second one then the constant parameter model is

more conservative, but for the rough bed channel the second one is more conservative for a factor about 2 - 3.

Rougher the bed, quicker the tracer concentration moves towards the bed and from the variable parameter model the best location for the dosage is slightly closer at the surface (Fig. 2.2.5).

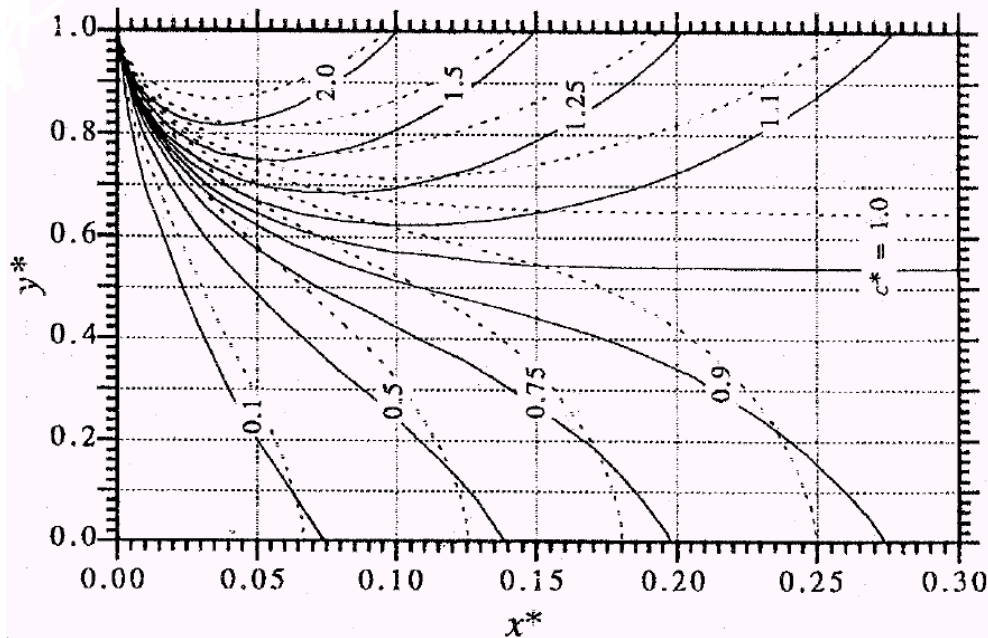


Fig. 2.2.5: Concentration profiles downstream from a steady transverse sources (from Rutherford, 1994).

The vertical diffusion can be estimated experimentally dosing continuously a conservative tracer with a transverse system and the mixing problem solution for an unbounded channel is:

$$\bar{c} = \frac{m}{b\sqrt{4\pi e_y x u_x}} \exp\left[-\frac{u_x(y - y_o)^2}{4e_y x}\right]$$

Eq. 2.2-29

where  $m$  is the tracer mass dosed [g];  $b$  is the water width [m] and  $y_o$  is the distance from the channel bottom location of the tracer source [m].

A plot of  $\frac{m}{b\sqrt{4\pi e_y x u_x}}$  vs.  $\frac{1}{\sqrt{x}}$  allows to estimate  $e_y$  for each  $x$  provide  $u_x$ ,  $b$  and  $m$ .  $e_y$

value estimated in this way is 10-20% higher then the true value, but if it is used in the constant mixing model this overestimation is cancelled out.

### ***Mid-Field and Transverse Mixing***

The mid-field is the distance from the tracer discharge point around which the tracer is completely mixed vertically, while the transverse mixing is being occurring. From the exfiltration method point of view, it is important to estimate where mid-field starts and stops because it is possible to know that over that cross-section the tracer is completely mixed. Gaudet and Roy (1995) defined complete mixing as deviation values of tracer concentration that were less than 10% when the tracer concentration be measured in several points over the cross section.

In an uniform and steady flow when a slug of tracer injection is used at the mid-field we can neglect the vertical tracer concentration and consider the transport of the depth-average concentration.

The theory of transverse mixing is far from complete, thus the develop of the mixing problem is not rigorous entirely.

The Eq. 2.2-17 becomes two-dimensional after an integration along the y-axis and the resulting equation in a turbulent flow using the Reynolds decomposition is:

$$h \frac{\partial s}{\partial t} + \frac{\partial(hv_x s)}{\partial x} + \frac{\partial(hv_z s)}{\partial z} = \frac{\partial}{\partial x}(-hu'_x c' + he_x \frac{\partial s}{\partial x}) + \frac{\partial}{\partial z}(-hu'_z c' + he_z \frac{\partial s}{\partial z})$$

**Eq. 2.2-30**

where  $s$  is the average tracer concentration calculated integrating over y-axis the tracer concentration [ $\text{g m}^{-3}$ ];  $v_x$  and  $v_y$  are the average tracer velocity calculated integrating over y-axis  $u_x$  and  $u_y$  [ $\text{m s}^{-1}$ ].

The terms  $-\overline{hu'_x c'}$  and  $-\overline{hu'_z c'}$  stem from the non-uniformity over the depth of velocity and concentration and determine additional transport which is called shear dispersion or dispersion. These terms quantify the transverse and longitudinal fluxes affected by the vertical shear stresses which spread the tracer longitudinally and transversely.

The Taylor's analysis of the turbulent shear flow for steady laminar and homogenous turbulent flows in channels (Ruthenford, 1994) allowed to estimate the terms  $-\overline{hu'_i c'}$  at asymptotical large time when an equilibrium becomes established between velocity shear and turbulent diffusion. After that time the variation of concentration fluctuations become independent of time ( $t$ ) and location ( $x_1$ ). From this analysis, longitudinal and transversal dispersive fluxes are proportional to the longitudinal and transversal gradient of the depth average concentration, respectively:

$$\begin{aligned} -\overline{u'_x c'} &= k_x \frac{\partial s}{\partial x} \\ -\overline{u'_z c'} &= k_z \frac{\partial s}{\partial z} \end{aligned}$$

**Eq. 2.2-31**

where  $k_x$  ( $k_z$ ) is the longitudinal (transverse) dispersion coefficient which accounts for the effects on the depth-averaged tracer concentration of depth variations in longitudinal (transverse) velocity.

Shear dispersion has been shown to be the dominant mixing process by several orders of magnitude (Smith, 1992) and it is the net effect of:

- velocity variations (velocity shear) over the depth and width which acts to spread the tracer cloud;
- turbulent mixing which counteracts the effect of velocity shear and is the random scattering of particles by turbulent motion, similar to the molecular diffusion but with a much larger value.

The dispersion is defined as the scattering of particles or clouds of tracers by the combined effects of shear and diffusion (Fischer et al., 1979), that is it is caused by the variation over the depth of the fluctuation of velocity and concentration due to the turbulence.

Incorporating the Eq. 2.2-31 in Eq. 2.2-30 and considering that  $k_x \gg e_x$  and  $k_z \gg e_z$  and for the continuity equation Eq. 2.2-48, the Eq. 2.2-30 becomes:

$$\frac{\partial s}{\partial t} + \frac{\partial(v_x s)}{\partial x} + \frac{\partial(v_{xz} s)}{\partial z} = \frac{1}{h} \frac{\partial}{\partial x} (h(e_x + k_x) \frac{\partial s}{\partial x}) + \frac{1}{h} \frac{\partial}{\partial z} (h(e_z + k_z) \frac{\partial s}{\partial z})$$

**Eq. 2.2-32**

The equation is used for mixing problem at the mid-field when the flow is an uniform steady laminar or a steady homogenous turbulent flow after a large time since the tracer is elapsed in the stream. If the channel geometry changes rapidly the equilibrium is not reached and the Eq. 2.2-31 cannot be applied, unless in some long part where the bathymetry is unchanged. In the Eq. 2.2-31 the transverse mixing is due to the turbulent diffusion ( $e_z$ ) and vertical variation of the transverse velocity (quantified by shear dispersion  $k_z$ ).

$e_z$  is mathematically formalized by the use of the Prandtl's length approach:

$$e_z = L_t u_t$$

**Eq. 2.2-33**



where  $u_t = \sqrt{\langle u_x'^2 \rangle} = u^*$  and  $L_t$  = water depth (h). From several studies collected by Rutherford (1994)  $e_z/uh^*$  ratio changes between 0.1-0.26 and it does not change with for different channel roughness or water width-depth ratio whereas  $e_z$ . Then, because of equation (2.18)  $e_z \approx 2e_y$ .

For a straight rectangular channel, the parameters affecting the transverse mixing coefficient ( $e_z (u^* h)^{-1}$ ) are: mean velocity, flow depth, width, bottom shear stress ( $u^*$ ), density and dynamic viscosity:

$$\text{for uniform flow } \frac{e_z}{u^* h} = f\left(\frac{u^*}{u}, \frac{w}{h}, \frac{\rho u h}{\mu}\right)$$

Eq. 2.2-34

$$\text{for highly turbulent flow } \frac{e_z}{u^* h} = f\left(f, \frac{w}{h}\right)$$

Eq. 2.2-35

where  $f = 8(u^* u^{-1})^2$  is the Darcy friction factor. Chau (2000) carried out laboratory experiments for assessing the transverse mixing in a rectangular channel at turbulent flow and with different bed roughness. He calculated  $e_z = 0.18uh^*$  with an uncertainty of  $\pm 30\%$ .  $e_z$  coefficient is affected by channel bathymetry, in particular by two dimensional meander currents and three dimensional secondary currents.

Meander currents due to depth variation over the cross section (e.g., in sewer where solid material settled) the transverse velocity profile that varies with the depth will promote the transport at the surface increasing the vertical concentration gradient and vertical mixing. The tracer will be transversally mixed faster.

El-Hadi et al. (1984) found out that  $k_z$  is positive in divergent regions (the channel is wider but shallower) and  $k_z$  is negative in convergent regions (the channel is narrow but deeper). Thus, along sewer pipes in the urban area when the flow is low and sediments accumulate on the pipe's bottom the sewer bathymetry is not uniform, the tracer plume width changes cyclically and does not increase monotonically as if the bathymetry were uniform. Holley et al. (1972) carried out several numerical experiments on rectangular and trapezoidal channels and they observed an accumulation of tracer near the banks, but in reality this effect could be reduce by the spreading that reduces the differences vertically.

Secondary currents occur where the transverse velocity is strongly non uniform, like as at the bend where the water moves towards outside at the surface and towards inside at the bed, this transverse velocity profile increases the transverse mixing affecting the transverse dispersion parameter ( $k_z$ ).

In the straight channel part with weak meanders  $k_z$  shows a longitudinal variations:

$$0.3 < \frac{k_z}{HU^*} < 0.9$$

**Eq. 2.2-36**

where  $H$  is the mean depth of an irregular channel [m];  $U^*$  is the average shear velocity ( $U^* = (g R s)^{1/2} \approx (g H s)^{1/2}$ ) where  $R$  is hydraulic radius [m] and  $s$  is the slope.

On the contrary, at the bend, Fisher (1969), Yotsukura and Sayre (1976) and Sayre (1979) developed three different equations for the hydrodynamic behaviour, whose the first one doesn't fit the data in natural channels and the other ones do not fit any laboratory data:

$$\frac{k_z}{HU^*} = \frac{0.25}{\chi^5} \left( \frac{V_x H}{U^* r_c} \right)^2$$

**Eq. 2.2-37**

$$\frac{k_z}{HU^*} = 0.4 \left( \frac{V_x b}{U^* r_c} \right)^2$$

**Eq. 2.2-38**

$$\frac{k_z}{HU^*} = 0.3 - 0.9 \left( \frac{V_x b}{U^* r_c} \right)^2$$

**Eq. 2.2-39**

where  $V^*$  is the cross-sectional averaged velocity [ $\text{m s}^{-1}$ ];  $\chi$  is von Karman's constant;  $r_c$  is radius of curvature.

For an channel irregular longitudinally, it is possible to divide it in  $N$  uniform parts each one  $\Delta x_i$  long and the average value of  $k_z$  can be calculated:

$$k_z = \frac{1}{L} \sum_{i=1}^N k_i \Delta x_i$$

**Eq. 2.2-40**

Finally, in straight channels  $k_z$  increases with the flow (Rutherford and Williams, 1992; Somlyódy, 1977); instead at the bends it is not clear the trend of  $k_z$  because the quantitative effect of secondary currents on  $k_z$  is not estimated yet.

The Eq. 2.2-30 can be entirely used for QUEST and QUEST-C mixing problems, even if for QUEST-C method the time derivative is zero.

The mixing distances are determined from the constant parameter model obtained from Eq. 2.2-32 solved for a straight, rectangular and uniform channel for both steady tracer sources and unsteady tracer sources:

$$L_z = 0.536 \frac{v_x b^2}{k_z} \text{ if dosed from the bank side}$$

Eq. 2.2-41

$$L_z = 0.134 \frac{v_x b^2}{k_z} \text{ if dosed in the mid}$$

Eq. 2.2-42

for a straight and meandering channel the  $L_z$  is about 100-300 channel width.

As if the dosage is done in the middle of the channel the distance is shorter, thus it is advisable to dose in the mid, while applying QUEST and QUEST-C methods.

In the next Fig. 2.2.6, the concentration profiles of the tracer concentration dosed by means of a vertical line system in the mid are shown.

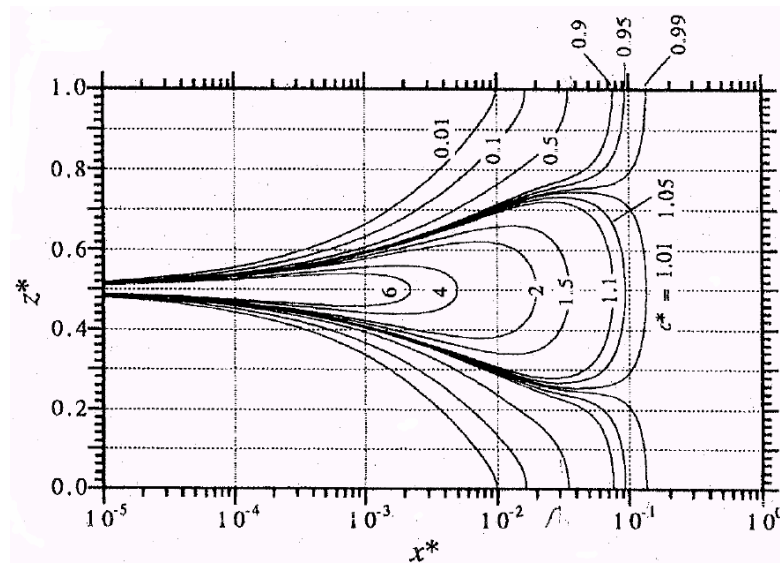


Fig. 2.2.6: Concentration profiles downstream from a steady transverse sources (from Rutherford, 1994).

The constant parameter model ignores the transverse variation of water depth, velocity and dispersion coefficient, and the most important differences between this model and the variable parameter model are the evaluation of mixing length, behaviour of the maximum concentration along the longitudinal direction and the optimum source location.

The constant model uses the averaged values of transverse velocity, depth and dispersion coefficient, consequently it has two limits due to:

1. the variation of these parameters as the plume size change;
2. the transverse variation of these parameters (i.e. both the velocity and the diffusivity are lower near the bank) that promote the tracer to be fully mixed rapidly because it tends to migrate towards the regions where the velocity and the diffusivity are lower. Taking both the velocity and the diffusivity constant the model could overestimate the mixing length, but Nokes (1986) pointed out that the variability of velocity along the vertical direction (logarithmic) and transversal one (parabolic) cannot help to predict the mixing length.

The Eq. 2.2-17 for a steady tracer source in a steady uniform flow in a straight channel ( $u_y=u_z=0$ ) is:

$$v_x \frac{\partial S}{\partial x} = k_z \frac{\partial^2 S}{\partial z^2}$$

**Eq. 2.2-43**

The solution of this equation describes the transport of a conservative tracer dosed during the application of QUEST-C method. The Eq. 2.2-43 can be solved considering the parameters  $v_x$  and  $k_z$  constant, then for a source of tracer mass  $M$ , placed at  $y=y^0$  and  $z=z^0$  and for no-flux boundary condition:

$$c(x, z) = \frac{M}{H \sqrt{4\pi v_x k_z}} \sum_{n=0}^{\infty} \exp\left(-\frac{(u_x(z-z^0))^2}{4k_z x}\right) \sum_{n=0}^{\infty} \exp\left(-\frac{(u_x(2nb \pm z \pm z^0) - z^0)^2}{4k_z x}\right)$$

**Eq. 2.2-44**

For an accurate estimation of mixing length field measurement should be carried out from which the transverse dispersion coefficient  $k_z$  can be estimated by Eq. 2.2-41 or Eq. 2.2-42. Otherwise the transverse dispersion can be estimated experimentally dosing continuously a conservative tracer and estimating the rate of change of spatial variance of the tracer profile.

$$k_z = \frac{1}{2} V_x \frac{\sigma_z^2(x_2) - \sigma_z^2(x_1)}{x_2 - x_1}$$

**Eq. 2.2-45**

$V_x$  is constant for uniform flow and thus plotting  $\sigma_z^2(x)$  vs.  $x$  and from the slope ( $2 k_z V_x^{-1}$ ) the  $k_z$  value can be calculated. It is 20% about higher than the true value, but this overestimation can be cancelled in the constant mixing model.

The methods used for measuring the coefficients of the constant mixing problem allow to carry out a preliminary planning of the experiment knowing that the constant mixing problem it is easy to apply even if it is more conservative.

### ***Far-Field and Longitudinal Mixing***

The far-field is the distance from the tracer discharge point around which the tracer is completely mixed vertically and transversely, while the longitudinal mixing is being occurring. Identifying where far-field starts it is important just for QUEST method because it consists in slug injection the travel the tracer peak downstream have to be modelled. Whereas for QUEST-C method that consists in continuous injection the tracer concentration along the longitudinal axis shows a steady concentration.

In a steady flow the mixing problem at the far field is only of interest for slug injection and when the tracer is released at first it is carried downstream by longitudinal velocity that changes across the channel area and the spatial tracer concentration is skewness when the equilibrium between the transverse (and vertical) velocity shear and transverse (and vertical) diffusion is establish the spatial distribution of concentration is Gaussian. The first part is called advective zone, the second one equilibrium zone. Taylor by theoretical and experimental works showed that in the latest zone the tracer cloud variance increase linearly with time then the concentration can be modelled by the Fickian law. As in the equilibrium zone he assumed the tracer concentration gradients zero over the z-axis and y-axis, thus the mixing problem, which concerns the longitudinal advection and the longitudinal dispersion of the cross-sectional averaged concentration  $S$ , is written by the following differential equation :

$$A \frac{\partial S}{\partial t} + \frac{\partial (AV_x S)}{\partial x} = \frac{\partial}{\partial x} \left( -A \overline{v'_x s'} + A k_x \frac{\partial S}{\partial x} \right)$$

**Eq. 2.2-46**

where  $S$  is the average along the z-axis of average-vertical concentration [ $\text{g L}^{-1}$ ];  $V_x$  is the average-vertical velocity [ $\text{m s}^{-1}$ ]; the first term on the right of the Eq. 2.2-46 is the longitudinal dispersion due to the variation of the longitudinal velocity over the cross section of the channel. From the Taylor's analysis that is for large time after the tracer release and when equilibrium becomes established between velocity shear and diffusion (e.g., homogeneous turbulent flow or steady flow) that term, called longitudinal dispersive flux, is proportional to the longitudinal gradient of the depth-averaged concentration. Then:

$$-\overline{v'_x s'} = K_x \frac{\partial c}{\partial x}$$

Eq. 2.2-47

$K_x$  is the longitudinal dispersion coefficient, that is larger than  $k_x$ . Longitudinal dispersion arises because vertical and transverse velocity shear carry the tracer downstream more slowly near the bed and the banks than in mid-channel.

Considering the continuity equation that describes the principle of conservation of mass, assuming that both velocity and mass are continuous functions of space and time:

$$\frac{\partial \rho}{\partial t} + u_j \frac{\partial \rho}{\partial x_j} + \rho \frac{\partial u_i}{\partial x_i} = 0$$

Eq. 2.2-48

where  $u_i$  are velocity components,  $x_i$  (and  $x_j$ ) are spatial coordinates (with  $i, j=1, 2, 3$ ) and  $\rho$  is the density of the fluid, and if  $\rho$  is constant, i.e., the fluid is incompressible, the conservation of mass can be reduced to the conservation of volume

$$\frac{\partial u_i}{\partial x_i} = 0$$

Eq. 2.2-49

and if  $V_x$  and  $K_x$  are constant, the Eq. 2.2-46 becomes:

$$\frac{\partial S}{\partial t} + V_x \frac{\partial S}{\partial x} = K_x \frac{\partial}{\partial x} \left( \frac{\partial S}{\partial x} \right)$$

Eq. 2.2-50

The Eq. 2.2-50 is used for mixing problem at the far-field and when the flow is uniform steady laminar or steady homogenous turbulent flow assuming constant both the mean velocity  $V_x$  and the longitudinal dispersion coefficient. It will be entirely used for the mixing problem in QUEST, while for QUEST-C the time derivative is zero

The solution of the Eq. 2.2-50 is:

$$S(x, t) = \frac{M}{A\sqrt{4K_x t\pi}} \exp \left[ -\frac{(x - V_x t)^2}{4K_x t} \right]$$

Eq. 2.2-51

This equation gives a Gaussian spatial tracer distribution, but a skewness temporal one. Anyway experimentally the Gaussian spatial distribution are seldom observed in natural channel and the skewness persists even far from the injection point.

For long distances when the slug injection is adopted the velocity shear distorts the tracer pulse, the longitudinal velocity gradient along the y-axis causes the peak to get flattening. Initially, the variance of the cloud increase as the square of time, for long time it decreases linearly with time because the vertical velocity shear determine a vertical concentration gradient that promote the vertical diffusion and the tracer concentration tend to be homogeneous. However, during the QUEST experiment the time is short and we can assume the variance to increase as square of time from the tracer injection.

Longer the time, flatter the tracer cloud and then the tracer concentration approaches the background natural concentration of the wastewater. Thus the measuring manhole should be located along the sewer pipe where the tracer-background concentration ratio is larger of the uncertainty of both the measuring probe and the regression data analysis.

Although the Taylor's analysis is valid only for steady or homogeneous turbulent flow that seldom happen in sewer, as we carried out previous flow measurements in order to determine the period in the day when the flow rate had the lowest variability it was possible to assume the flow rate to be steady during the experiment.

The vertical and transverse velocity shears play an important role because they act to spread the tracer along the channel determining concentration gradients across the channel area, whereas the transverse mixing tends to uniform the concentration across the channel area.

The concentration gradients persist across the channel because  $v_x$  is not constant along z-axis and y-axis and the velocity shear creates concentration gradients which are not completely removed by the turbulent diffusivity (Sayre, 1968a). Thus even at the far-field, or better called into the equilibrium zone, the concentration over the cross section is not uniform, although the gradients are of the order of 5-10%. That happens when the QUEST experiment is carried out, even in the so called equilibrium zone the tracer concentration is uniform across the channel. Nevertheless even if in a small sewer this problem could be overcome, in a main sewer the QUEST method can't be applicable because the water exfiltrated is proportional to the tracer concentration lost. Anyway, field measurements should be carried out to confirm that.

The Eq. 2.2-51 gives a Gaussian spatial profile of the concentration, but skewed temporally. The tail that gives a concentration peak a negative skew is evident in the advective zone and decays after 2.5-50  $L_x$  (that is the length of the advective zone), but it could persist

longer if a lot of dead zones are present. After an equilibrium becomes established between advection in the overlying water and exchange with the dead zones (Valentine and Wood, 1977). The length of the advective zone is:

$$L_x = \alpha \frac{V_x L_t^2}{k_z}$$

Eq. 2.2-52

where  $V_x$  is the cross-sectional averaged velocity;  $L_t$  is the transverse distance between the point where the velocity is maximum and the farthest bank and in our case that in sewer it is  $b/2$  where  $b$  is the channel width;  $\alpha$  is a constant increasing with the roughness of the channel bed (Tab. 2.2-1).

Tab. 2.2-1: estimates of the length of the advective zone (Rutherford, 1994).

Reference	$\alpha = L_x k_z / L_t^2 V_x$	Comments
<b>Smooth channels</b>		
Fischer (1973)	0.2	Review of numerical experiments
Fischer (1967)	0.3	Laboratory channel, transverse line source
Tsai and Holley (1978)	0.4–0.5	Numerical experiments
Sayre (1968)	0.5	Numerical experiments
Fischer (1968)	0.6	Bankside injection
Chatwin (1972)	1	Theoretical analysis
<b>Rough channels</b>		
Denton (1990)	1.4	Numerical experiments, 5% dead zones
Valentine (1978)	1.6	Laboratory channel, 4% dead zones
Valentine (1978)	2.8	Laboratory channel, 25% dead zones
Valentine and Wood (1979b)	>3	Irrigation canal, 8–12% dead zones
Valentine and Wood (1979b)	>10	Irrigation canal, 27–38% dead zones

$L_x$  = length of the advective zone;  $k_z$  = transverse dispersion coefficient;  $L_t$  = transverse length scale (normally 0.5–0.7b);  $b$  = channel width; and  $V_x$  = cross-sectional averaged velocity.

The longitudinal dispersion coefficient ( $K_x$ ) has been estimated during several experiments and it is given by a non-dimensional relationships:

$$2 < \frac{K_x}{bU^*} < 50$$

Eq. 2.2-53



where  $K_x$  is undimensionalized by  $b$  because the longitudinal dispersion depends on the transverse velocity gradient and higher it is, higher is the  $K_x$  value. In large channel we could expect a large value of  $K_x$  then. Considering the relation  $K_x (H U^*)^{-1}$ , it is inversely proportional to the radius of curvature. Finally, larger the number of the dead zones higher  $K_x$ .

The values of  $V_x$  and  $K_x$  in the Eq. 2.2-51 have to be estimated by field measurements applying one of the available methods:

1. Taylor's approach (1954);
2. Fischer's method (1968);
3. Modified routing method (Singh and Beck, 2003).

The first approach by Taylor assumes that the spatial concentration profiles are Gaussian and it is based on moments of concentration

$$K_x = \frac{1}{2} \frac{\partial \sigma_x^2}{\partial t}$$

**Eq. 2.2-54**

where  $\sigma_x$  is the spatial variance calculated from the tracer concentration measured at different point for each time  $t$ . A finite difference approximation is:

$$K_x = \frac{1}{2} \frac{\sigma_x^2(t_2) - \sigma_x^2(t_1)}{t_2 - t_1}$$

**Eq. 2.2-55**

As the measuring of the time profile is easier the Eq. 2.2-55 is changed into

$$K_x = \frac{1}{2} \left( \bar{v} \right)^2 \frac{\sigma_x^2(x_2) - \sigma_x^2(x_1)}{t_2 - t_1}$$

**Eq. 2.2-56**

where  $\sigma_t(x)$  is the temporal variance calculated from the tracer concentration measured at a fix point  $x$ ;  $\bar{t}_{1(2)}$  is the time corresponding to the centroids of the tracer cloud at the location  $x_{1(2)}$ ;  $\bar{v}$  is:

$$\bar{v} = \frac{x_2 - x_1}{t_2 - t_1}$$

**Eq. 2.2-57**

The second approach is by Fischer (1968) that use the frozen cloud approximation that assume that during the time of the passage of the tracer peak at the measuring point there is not longitudinal dispersion but only advection and the centroid position is:

$$x_1 = t_1 V_x$$

**Eq. 2.2-58**

where  $x_1$  is the location of measuring and  $t_1$  the time of centroid at  $x_1$  and  $V_x$  is the longitudinal cross-averaged velocity.

The concentration vs. time is:

$$S(x_1, t) = S(x_1 + V_x(t_1 - t), t)$$

**Eq. 2.2-59**

$$S(x, t_1) = S(x_1, t + \frac{x_1 - x}{V_x})$$

**Eq. 2.2-60**

For estimating the  $K_x$  value the convolution equation is then used.

The third approach developed by Singh and Beck (2003) is more accurate. The estimation of  $K_x$  has been done by a non-linear parameter estimation using the Gauss-Newton algorithm. The measured data have been fitted by a tracer concentration function obtained by solving completely the partial differential equation of the mixing problem with constant parameter (Eq. 2.2-51). The advantage of this method is:

1. there are not numerical error due to the approximation of the concentration function like as in the frozen cloud method;
2. the integration interval is limited on the concentration function

If the measurements for the mathematical estimation of  $K_x$  are not available, there are several formulae for  $K_x$ , and for sewer pipes. Rieckermann et al. (2004) analyzed 60 tracer experiments in 37 different sewer reaches in order to estimate the longitudinal dispersion ( $K_x$ ) under dry weather flow conditions and to determine the more suitable formula for it. They applying a routine procedure based on the method of Singh and Beck (2003) that doesn't involve the frozen-cloud approximation for estimating  $K_x$  from experimental tracer data, but they consider that the temporal variation of concentration at the downstream section,  $c(X, t)$ , due to a

time-varying concentration input at the upstream section  $c_u(\tau)$  can be expressed by the following convolution equation:

$$c(X, t) = \int_0^t c_u(\tau) u(X, t - \tau) d\tau$$

**Eq. 2.2-61**

where  $c_u(\tau)$  is the upstream concentration at time  $\tau$  and  $u(X, \tau)$  is the downstream response due to an instantaneous unit concentration upstream.

Rickermann et al. found out that  $K_x$  of all examined sewer the variation of the calculated values was very small. the distribution of the estimated values was skewed with average value of  $0.16 \text{ m}^2 \text{ s}^{-1}$  ( $K_x^{10} = 0.05 \text{ m}^2 \text{ s}^{-1}$ ;  $K_x^{50} = 0.10 \text{ m}^2 \text{ s}^{-1}$  and  $K_x^{90} = 0.36 \text{ m}^2 \text{ s}^{-1}$ ). The formulae in literature that they verified to be suitable for predicting  $K_x$  in sewer reaches are:

$$K_x = 2.0 \left( \frac{W}{H} \right)^{3/2} Hu^*$$

$$K_x = 0.6 \left( \frac{W}{H} \right)^2 Hu^*$$

$$K_x = 0.003 \frac{u^2 W^2}{Hu^*}$$

**Eq. 2.2-62**

the first equation is by Iwasa (1991), the second one by Koussis (1998) and the third one by Huisman (2000).

The stagnant or dead zones are the pockets of stagnant water or of very low velocities, which trap the injected tracer. These stagnant zones are distributed along a sewer reach due to collapsed, settled solid matter, chambers, irregularity etc... The dead zones tend to increase the average flow velocity accountable for solute-dispersion because they reduce the cross section available to the flow. At the same time the tracer is adsorbed on the solid trapped in those dead zones and the effect is the reduction of the average flow velocity. The result is that the velocity accountable for the tracer dispersion is an apparent average velocity and the tracer mass transported by the flow is different from the real mass injected. Singh (2003) suggested a method for the estimation of longitudinal dispersion coefficient, average apparent velocity and the effective injected mass. He modified the 1D transport model in

$$K_x \frac{\partial^2 c}{\partial x^2} - u \frac{\partial c}{\partial x} = (1 - \eta + k) \frac{\partial c}{\partial t}$$

**Eq. 2.2-63**

$$c_{\eta} = \eta c$$

$$c_k = kc$$

where  $\eta$  is the average dead zone fraction as a fraction of average cross-sectional area;  $k$  is the coefficient of adsorption;  $c_{\eta}$  the concentration released from the dead zones;  $c_k$  the adsorbed concentration. The solution for this model in unsteady condition is

$$c = \frac{u_a}{\sqrt{4\pi K_{xa}t}} \left( \frac{M}{Q} \right)_a \exp \left( -\frac{(x - u_a t)^2}{4K_{xa}t} \right)$$

**Eq. 2.2-64**

$$u_a = \frac{V_x}{1 - \eta + k}$$

$$K_{xa} = \frac{K_x}{1 - \eta + k}$$

where the subscript “a” indicates the apparent value of the subscripted parameters. He found the parameters  $K_{xa}$ ,  $(M/Q)_a$  and  $u_a$  by the Marquardt (1963) algorithm minimizing the integral squared error of experimental concentration and simulated concentration. That algorithm assures the convergence even with very poor initial values of the parameters.

### 2.2.3.2 Confluences

In this paragraph the hydrodynamic phenomena occurring at a confluence is described. The interest in this phenomena derives from the structure of an urban sewer system that is a network with several nodes and in which it is difficult to investigate a reach without any nodes along it.

As QUEST and QUEST-C methods consist essentially on the mass balance of non-buoyant and conservative chemical tracers into wastewater streams on an investigated reach, the tracer dilution occurring at the dosing point is proportional to the flow at that point and has to be constant and homogeneously mixed along the whole reach.

Nevertheless, if confluences or infiltrations exist along the investigated reach the tracer is diluted and the concentration at the final point where the samples are taken is not representative of the flow rate at the beginning of the investigated reach anymore.

Furthermore, at the confluences the tracer concentration becomes not uniform over the cross section both transversally and vertically. Then the methods should be modified when applied in an sewer network, that is the flow rate from each confluences must be estimated and the distance for the mixing after each junction must be calculated, as well. Anyway, another aspect cannot be neglected, that is the accumulation of the tracer on one side of the cross section

at the confluence, because if exfiltration occurs the tracer mass lost isn't proportional to the exfiltration rate at all.

Following a brief description of recent results about the phenomena at a confluences is given.

Some authors (Best and Roy, 1991; Gaudet and Roy, 1995; Biron et al., 1996a, b; Bradbrook et al., 1998, 2000, 2001; De Serres et al., 1999) have recently demonstrated that at the river confluences the transverse mixing can be improve when the tributary is shallower than the main stream. As secondary currents due to the meanders cause the tracer to move from the deep stream (main river) towards the shallow one (tributary).

The effect of the confluence over the mixing process has been studied by Biron et al. (2004). They applied a steady-state 3-D model (PHOENICS, version 3.4) for studying the mixing rate both immediately after a confluence and further downstream in the mainstream. The aim of their study was to understand the effect of the confluence's bathymetry on the mixing of a non-buoyant tracer at the near field. They studied the mixing in laboratory and in a natural site.

The mixing rate downstream confluence in the mainstream was estimated using the standard deviation of concentration which is calculated using the value of concentration at each cell for a given cross section. They applied the 3-D model to concordant bed confluence and to discordant bed confluence and they observed that:

- a. within five times the mainstream width, the standard deviation decreases more quickly (30%) for discordant bed confluence than for concordant bed confluence (10%);
- b. this disparity doesn't change with the flow ratio at the confluence. That is if the flow ratio between the mainstream and the tributary increases or decreases the discordant bed confluence always presents a smaller standard deviation that decreases quicker, as well (Fig. 2.2.7);

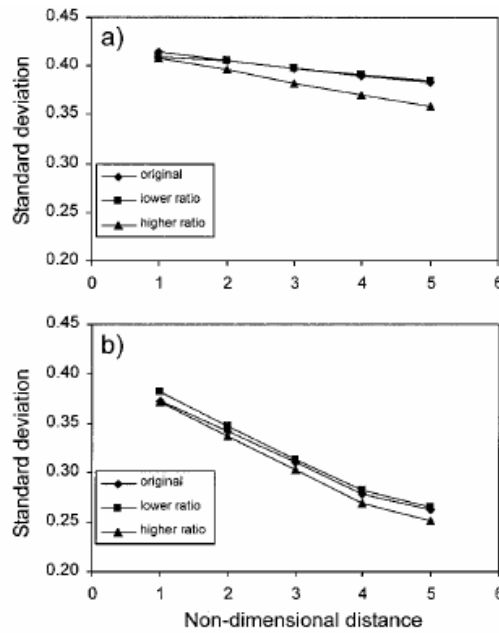


**Fig. 2.2.7: Comparison of rate of mixing for different velocity and discharge ratio for: (a) concordant bed confluence and (b) discordant bed confluence (from Biron et al., 2004).**

- c. after ten times the mainstream width the standard deviation gradient decrease slower in the both cases and it is approximately the same;
- d. the junction angle affects the mixing rate, too. Higher the angle, more rapid for concordant beds is the mixing, but the discordant bed confluence shows a higher mixing rate (Fig. 2.2.8);

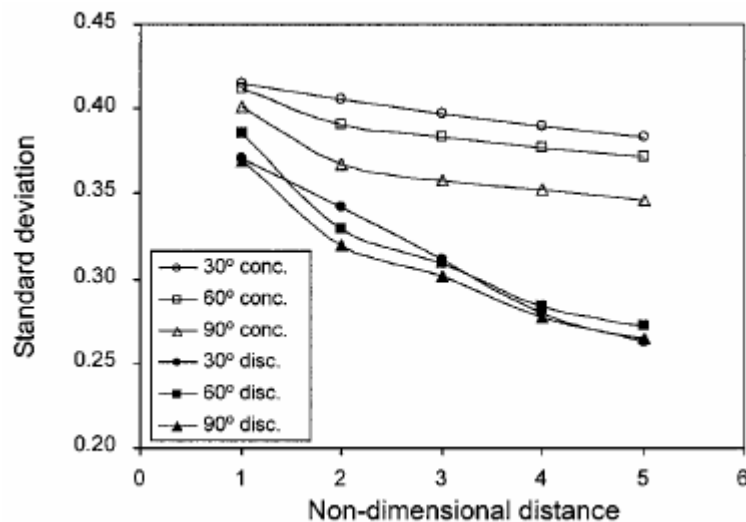


**Fig. 2.2.8: Rate of mixing for concordant and discordant bed confluences for junction angle of 30, 60 and 90° (from Biron et al., 2004).**

- e. at the natural site the discordant bed confluence at the laboratory scale had the same effect at low flow. At low flow the depth ratio between the two stream is more evident and affects the secondary currents strongly;
- f. at the natural site and at the high flow the bend more efficiently effects the mixing rate;
- g. for discordant bed confluences the effect of a bed height differential is more important than the role of width-to-depth ratio to determine the mixing rate.

The simulated concentration using the state 3-D model are shown in the Fig. 2.2.9.

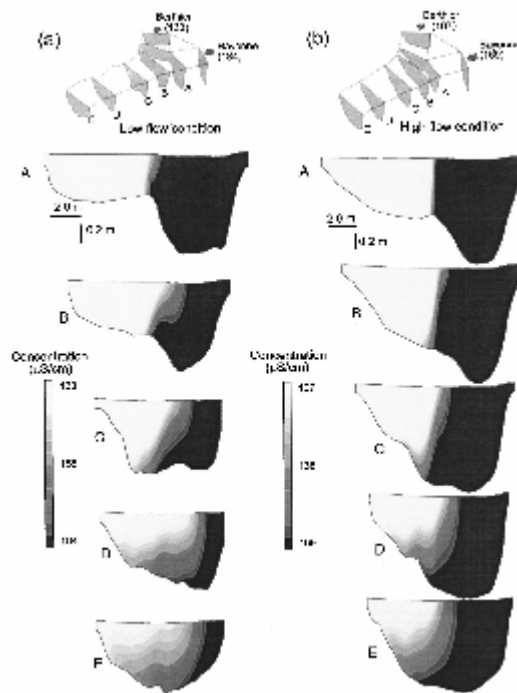


**Fig. 2.2.9: Mixing of fluid from each tributary at Bayonne-Berthier confluence indicated by contours of electrical conductivity values for: (a) low flow condition and (b) high flow condition; letters correspond to position indicated in inset; vertical exaggeration 7.0 (from Biron et al., 2004).**

Gaudet & Roy (1995) carried out measurements over three river confluences of small size (i.e. width 5-15 m ) and they noted that the bed discordant at the channel confluences can markedly increase the mixing rate. They found out that the mixing always completed before a downstream distance of 25 channel width. When the water levels of mainstream and tributary are high and bed discordance is less important flows from each confluent channel tend to be segregate along their respective side of the receiving channel. Mixing length is longer and the observed deviation from the complete mixing:

$$Dev = \frac{(C_o - C_p)}{C_p} \times 100$$

**Eq. 2.2-65**

is high. Where  $C_o$  is observed electrical conductivity value [ $\text{mS cm}^{-1}$ ];  $C_p$  predicted conductivity value [ $\text{mS cm}^{-1}$ ] that is:

$$C_p = \frac{(C_1 Q_1 + C_2 Q_2)}{Q_3}$$

**Eq. 2.2-66**

where  $C_{1(2)}$  is the conductivity into the river 1(2) before confluence;  $Q_{1(2)}$  is the flow rate into the river 1(2) before confluence;  $C_3$  is the conductivity after confluence;  $Q_3$  is the flow rate after confluence.

Whereas when the water levels of mainstream and tributary are low and bed discordance is more important flows, water from the shallower tributary tends to flow above the water from the mainstream that is deeper spreading laterally the tracer from the tributary over the cross section of the receiving channel. The transverse mixing completes before the vertical one.

The conclusion was when the confluent stream are of almost similar depth and relative bed discordance is low the mixing complete slowly; whereas the water from the shallower channel flows over the deeper channel due to the deep differential the mixing complete quickly.

From the QUEST and QUEST-C point of view when the investigated pipe includes some nodes along the route as typically happens in an urban sewer network, the investigated reach and the other one must be discordant. This means the two sewer convey different flows and/or the sewers' bottoms lay at two different levels.



### 2.2.4 Application Advection-Dispersion (AD) model to QUEST and QUEST-C

Near-, mid- and far-field problems have to be solved, and the hydraulic conditions taken into account were steady laminar flow for both injections: punctual (QUEST) and continuous (QUEST-C). Despite of the unsteadiness of the flow in a sewer system, the mixing problem has been solved under steady condition because the experiment was carried out in a period of the day when the flow was quite steady. A statistical analysis of several flow measurement data has been applied for individuating a 1h period with low variability (around 5 L s<sup>-1</sup>). Although during the night the flow is quite steady, the exfiltration rate is not meaningful during that period because the damaged area involved in the exfiltration phenomena is very small.

In a straight sewer channel, the solutions of the AD models for QUEST and QUEST-C are:

For QUEST

at the near-field:

$$c(x, y, z, t) = M \frac{\exp\left(-\frac{(x-u_x t)^2}{4e_x t}\right)}{\sqrt{4\pi e_x t}} \sum_{n=0}^{\infty} \exp\left(-\frac{((2nh \pm y \pm y^0) - y^0)^2}{4e_y t}\right) \sum_{n=0}^{\infty} \exp\left(-\frac{((2nb \pm z \pm z^0) - z^0)^2}{4e_z t}\right)$$

Eq. 2.2-67

at the far-field:

$$S(x, t) = \frac{M}{A\sqrt{4K_x t\pi}} \exp\left[-\frac{(x-V_x t)^2}{4K_x t}\right]$$

Eq. 2.2-68

For QUEST-C

at the near-field:

$$c(x, y, z) = \frac{M}{4\pi x \sqrt{e_y e_z}} \sum_{n=0}^{\infty} \exp\left(-\frac{(u_x(2nh \pm y \pm y^0) - y^0)^2}{4e_y x}\right) \sum_{n=0}^{\infty} \exp\left(-\frac{(ux(2nb \pm z \pm z^0) - z^0)^2}{4e_z x}\right)$$

Eq. 2.2-69

at the mid-field:

$$c(x, z) = \frac{M}{H \sqrt{4\pi v_x k_z}} \sum_{n=0}^{\infty} \exp\left(-\frac{(u_x(z - z^0))^2}{4k_z x}\right) \sum_{n=0}^{\infty} \exp\left(-\frac{(u_x(2nb \pm z \pm z^0) - z^0)^2}{4k_z x}\right)$$

**Eq. 2.2-70**

The previous equations describe the concentration in the space and over the time, they are useful at the first stage of an experimental planning in order to:

- estimate the amount of the tracer to be dosed, taking in account the tracer solubility;
- calculate the maximum distance detectable;
- locate the sampling point;
- estimate the mixing distance.

The length of the near- and the mid-fields have to be estimated in order to know where the hypothesis of the homogeneous concentration over the cross section starts to be valid<sup>3</sup>. The estimation of this length allows us defining the investigated sewer part as well as locating the sampling point. Whether along the investigated reach there are confluences the tracer becomes unmixed again, and a mixing length should be estimated. The mixing length could be considered zero if propellers were used and located properly, but the energy supply to each one could make that prohibitive; because the number of propellers we needed is equal to number of the unmixed zones. Consequently, QUEST and QUEST-C could successfully be used for investigating the tightness of a main sewer where there are long reaches without any confluences, but due to of the high flowrate the near- and mid-fields could be very long and an artificial turbulence should be determined anyway.

In practice, we applied AQUASIM software (Reichert, 1994) for simulating virtual multi-tracer experiment where QUEST and QUEST-C methods were applied simultaneously. AQUASIM assumes the tracer to be in the equilibrium zone at the far-field.

---

<sup>3</sup> As we need an homogeneous concentration of tracer over the cross-section in order to applied the Eq. 2.2-1 and Eq. 2.2-3, we need to individuate the parts of the sewer where the concentration of tracer is fully mixed.

### ***2.2.5 Sampling and Measurements***

In this paragraph, the criteria for sampling and measuring the concentration of the tracers dosed into the investigated sewer and for measuring the flow rate during the application of the QUEST and QUEST-C methods are described. The paragraph develops into the following parts:

1. choice of the useful tracer;
2. sampling location.

#### **2.2.5.1 Choice of the tracer**

A chemical substance can be used as a tracer for assessing exfiltration using QUEST and QUEST-C methods if:

- characterized by a rapid dissolution into water at ordinary temperatures;
- absence or has a very low natural concentration into wastewater;
- can to be monitored at low concentration;
- is conservative, that is low adsorption onto solid material in sewer and reacts into water;
- no toxic for the environment and humans at the applied concentrations.

Thus, the tracers that can be used are: fluorescent dyes, Rhodamine WT, chemical salt, and radioactive substances like as Tritium.

#### **2.2.5.2 Mass of tracer to be dosed**

The mass of tracer to be dosed depends on:

- wastewater flowrate and background concentration;
- length of the reach to be investigated;
- solubility of tracer.

For example, the amount of tracer to be dosed for the QUEST method when NaCl is used as tracer can be calculated following the next steps:

1. to calculate the average discharge and the average conductivity during the 1h period of the day chosen for the experiment;
2. to define the part of the network to be investigated;

3. to estimate the tracer solubility (300 gr L<sup>-1</sup> for NaCl @ 20°C).

Fixing the maximum tracer concentration that is the maximum peak height, the dosed tracer mass can be estimated using:

$$M = CV$$

**Eq. 2.2-71**

where C is the tracer concentration in solution [gr L<sup>-1</sup>], and V is the solution volume [L].

The amount of tracer to be dosed for the QUEST-C method when NaBr and LiCl are used as tracers can be calculated following the next steps:

1. to calculate the average discharge and the average concentrations of Br<sup>-</sup> and Li<sup>+</sup> during the 1h period of the day chosen for the experiment. Usually, Br<sup>-</sup> and Li<sup>+</sup> concentrations are negligible;
2. to define the part of the network to be investigated;
3. to estimate the tracers' solubility (900 gr L<sup>-1</sup> for NaBr @ 20°C and 769 gr L<sup>-1</sup> for LiCl @ 20°C).

Fixing the maximum tracers' concentrations, the dosed tracer mass rate can be estimated using:

$$\dot{M} = Cq$$

where C is the tracer concentration in solution [gr L<sup>-1</sup>], and q is the dosage flowrate [L s<sup>-1</sup>].

## 2.3 Methods for Quantifying the Infiltrations

In this paragraph, the two methods developed within the APUSS project by Kracht et al. (2003A and B) for the quantification of the infiltrations in urban sewer networks are described. They base on the hydrograph separation method (Clark and Fritz, 1997). One, called isotopic method, distinguishes the mixed flows into a sewer using isotopic characterization of stable isotope  $^{18}\text{O}$  in water (Kracht et al., 2003A); while the other one, called pollutograph method, using concentration of typical wastewater pollutants (e.g., COD) (Kracht et al., 2003B).

Infiltration can be estimated at urban catchment scale and includes parasitical water due to groundwater, spring, and drinking water network leakages in the dry weather period.

The methods are described below, but for more detailed understanding of them, the reading of protocol by Kracht et al., 2004 is suggested.

### 2.3.1 Isotopic method

The isotopic method allows separating the wastewater hydrograph into two components using stable isotopes. The principle of this method is based on the contrast in the isotopic composition between the infiltration contributes and those of a given aqueduct. Assuming the total flow as:

$$Q_{\text{wastewater}}(t) = Q_{\text{foulwater}}(t) + Q_{\text{infiltration}}(t)$$

Eq. 2.3-1

where  $Q_{\text{wastewater}}(t)$  is the total flow measured at the end of an investigated urban catchment [ $\text{m}^3 \text{s}^{-1}$ ];  $Q_{\text{foulwater}}(t)$  is the used drinking water [ $\text{m}^3 \text{s}^{-1}$ ];  $Q_{\text{infiltration}}(t)$  is the total contribute of infiltration [ $\text{m}^3 \text{s}^{-1}$ ].

Using as a tracer  $\delta^{18}\text{O}$ , a mass balance can be written:

$$\delta^{18}\text{O}_{\text{wastewater}}(t) \times Q_{\text{wastewater}}(t) = \delta^{18}\text{O}_{\text{foulwater}}(t) \times Q_{\text{foulwater}}(t) + \delta^{18}\text{O}_{\text{infiltration}}(t) \times Q_{\text{infiltration}}(t)$$

Eq. 2.3-2

where  $\delta^{18}\text{O}_{\text{wastewater}}(t)$  is the isotopic content of the wastewater after the mixing between the used drinking water and the infiltration vs. SMOW;  $\delta^{18}\text{O}_{\text{foulwater}}(t)$  is the isotopic content of the drinking water vs. SMOW;  $\delta^{18}\text{O}_{\text{infiltration}}(t)$  is the isotopic content of the infiltration contributes (e.g., groundwater, springs, etc.) vs. SMOW. It is naturally inferred that this method cannot

assess the infiltration due to the water network leakages, because the contribution from the direct discharges or from the infiltration are not isotopically distinguishable.

By substitution for  $Q_{\text{foulwater}} = Q_{\text{wastewater}} - Q_{\text{Infiltration}}$  and rearranging:

$$Q_{\text{inf iltration}}(t) = \left( \frac{\delta^{18}\text{O}_{\text{wastewater}}(t) - \delta^{18}\overline{\text{O}}_{\text{foulwater}}}{\delta^{18}\overline{\text{O}}_{\text{inf iltration}} - \delta^{18}\overline{\text{O}}_{\text{foulwater}}} \right) \times Q_{\text{wastewater}}(t)$$

**Eq. 2.3-3**

and

$$R_{\text{inf iltration}}(t) = \frac{Q_{\text{Infiltration}}(t)}{Q_{\text{wastewater}}(t)}$$

**Eq. 2.3-4**

where the  $\delta^{18}\text{O}_{\text{infiltration}}(t)$  and  $\delta^{18}\text{O}_{\text{foulwater}}(t)$  are considered constant during the experimental period and the spatial average values have been considered and  $R_{\text{infiltration}}(t)$  is the infiltration ratio [-].

Before applying this method for estimating the infiltration into a sewer system the following hypothesis have to be verified:

- the tracer must be conservative and into the sewer system the  $\delta^{18}\text{O}$  seem to respect that (De Benèdittis and Bertrand-Krajewski, 2004);
- the drinking water source must be unique in order to have a low temporal variability of the isotopic composition;
- the difference between  $\delta^{18}\text{O}_{\text{foulwater}}$  and  $\delta^{18}\text{O}_{\text{infiltration}}$  must be more than a certain percentage based on the expected infiltration ratio (De Benèdittis and Bertrand-Krajewski, 2004);
- the infiltration contributes must have a low spatial variability over the drainage area, otherwise the area to be investigated should be divided into sub-catchments of low spatial isotopic variability.

### ***2.3.2 Pollutograph method***

The second method developed within the APUSS project by Kracht and Gujer (2004) and applied in Rome on a sewer system consists on the separation hydrograph measuring a chemical tracer in wastewater diluted by the infiltration water and the wastewater flow rate at the outlet of

an urban sewer network. The chemical tracer measured during the experimental campaigns has been the Chemical Oxygen Demand (COD). The method bases on the following assumptions:

- the concentration of the chemical tracer has to be negligible into the infiltration source compared to the wastewater flow;
- the tracer has to be conservative in sewer during the transport.

Assuming the Eq. 2.3-1 and using as a natural tracer COD, a mass balance can be written:

$$COD_{wastewater}(t) \times Q_{wastewater}(t) = COD_{foulwater}(t) \times Q_{foulwater}(t) + COD_{infiltration}(t) \times Q_{infiltration}(t)$$

**Eq. 2.3-5**

where  $COD_{wastewater}(t)$  is the COD concentration of the wastewater after the mixing between the used drinking water and the infiltration;  $COD_{foulwater}(t)$  is the COD concentration of the foul water;  $COD_{infiltration}(t)$  is the COD concentration of the infiltration contributes. Contrary to the isotopic method, this method can assess the infiltration due to the water network leakages.

Rearranging the Eq. 2.3-1 and Eq. 2.3-5 assuming  $COD_{infiltration} = 0$ , the infiltration rate is:

$$Q_{infiltration}(t) = \left( \frac{COD_{foulwater} - COD_{wastewater}}{COD_{foulwater}} \right) \times Q_{wastewater}(t)$$

**Eq. 2.3-6**

and the infiltration ratio is:

$$R_{infiltration}(t) = \frac{Q_{infiltration}(t)}{Q_{wastewater}(t)}$$

**Eq. 2.3-7**

A submersible spectrometer probe (UV 100-400 nm and VIS 400-750 nm) was mounted inside the sewer pipe for continuously measuring COD and storing data every two minutes.

An example of an absorption spectra in the range UV-VIS are shown in Fig. 2.3.1 and the spectrometer (type spectro::lser, scan Mexxtechnik GmbH, Vienna) used during the experimental campaigns in Rome is shown in Fig. 2.3.2.

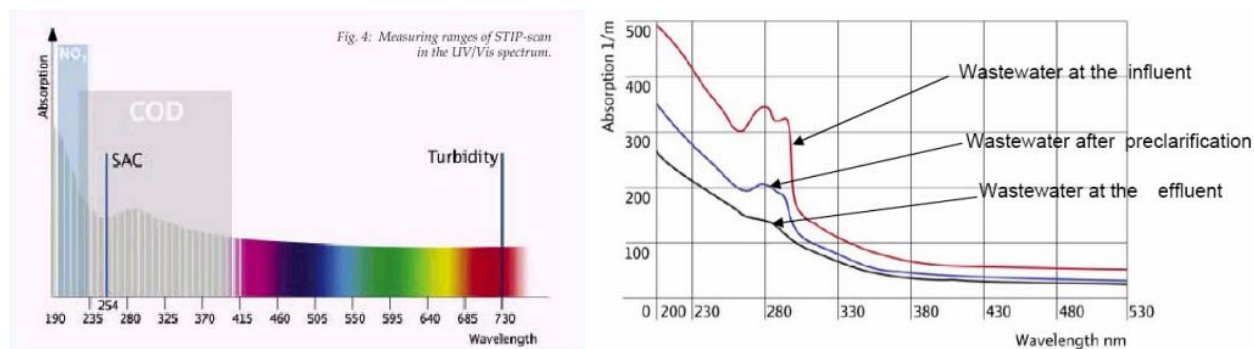


**Fig. 2.3.1: Absorption spectra in the range UV-VIS of wastewater.**



**Fig. 2.3.2: Spectrometer used during the experiments in Rome (trade: s::can). It is 506 mm high and its diameter is 44 mm.**

### 2.3.2.1 Isotopic method

This paragraph deals with the environmental stable isotopes. Particular emphasis is given to 18-oxygen in water used in catchment hydrology because the isotopic method applied for quantifying the infiltration is based on the principle that different parasitical water infiltrating into sewer systems could have different abundance of the stable isotope of water 18-oxygen and distinguishable on the basis of this. This paragraph develops in the following points:

- basic concepts of stable isotopes;
- physicochemical, biological and diffusive fractionation;
- hydrograph separation.

### *Environmental stable isotopes*

Isotopes are atoms of the same element that have the same numbers of protons and electrons but different numbers of neutrons. The difference in the number of neutrons between



the various isotopes of an element means that the various isotopes have similar charges but different masses.

The environmental isotopes are the naturally occurring isotopes of elements found in abundance in the environment: H, C, N, O and S. The stable isotopes of these elements serve as tracers of water, carbon, nutrient and solute cycling, as they are light elements then isotopes of an element can have large difference atomic weight that determines molecules with different weight react with different kinetic rates.

As three isotopes of hydrogen  $^1\text{H}$ ,  $^2\text{H}$ ,  $^3\text{H}$  and three ones of oxygen  $^{16}\text{O}$ ,  $^{17}\text{O}$ ,  $^{18}\text{O}$  exist, different water molecules exist whose just four are more abundant (Eq. 2.3-1). Water molecules with different weight have different rate during physical, chemical and biological reactions, as a consequence, there is isotopes partitioning or fractionation.

**Tab. 2.3-1: isotopic abundance of hydrogen, oxygen and water.**

$^1\text{H}$	99.984 %	$^{16}\text{O}$	99.760%
$^2\text{H}$	0.156%	$^{17}\text{O}$	0.039%
$^3\text{H}$	10-16%	$^{18}\text{O}$	0.204%
$\text{H}_2^{16}\text{O}$	$\text{H}^2\text{H}^{16}\text{O}$	$\text{H}_2^{17}\text{O}$	$\text{H}_2^{18}\text{O}$
997.450 p.p.m.	150 p.p.m.	420 p.p.m.	1980 p.p.m.

The interest in hydrogeology is the comparison among isotope abundances in different water analyzed in different laboratories. As systematic and random errors can affect the results in order to reduce these isotopic compositions is referred to a standard, in particular for oxygen it is the ocean water. Then oxygen is reported as “delta” ( $\delta$ ) values in parts per thousand (permil) enrichments or depletions relative to the Standard Mean Ocean Water (SMOW) defined by the International Atomic Energy Agency (IAEA).  $\delta$  values are calculated by:

$$\delta^{18}\text{O}_{\text{sample}} = \left[ \left( \frac{(^{18}\text{O}/^{16}\text{O})_{\text{sample}}}{(^{18}\text{O}/^{16}\text{O})_{\text{reference}}} \right) - 1 \right] \times 1000\text{‰ SMOW}$$

**Eq. 2.3-8**

where  $(^{18}\text{O}/^{16}\text{O})_{\text{sample}}$  is the true isotopic ratio in the sample and  $(^{18}\text{O}/^{16}\text{O})_{\text{reference}}$  is the true isotopic ratio in the ocean water measured by means of the same isotope ratio mass spectrometry.

As the fractionation does not impart huge variation in isotopes concentration then d-value are expressed as the parts per thousand. A positive  $\delta$  value means that the sample contains more

of the heavy isotope than the standard; a negative  $\delta$  value means that the sample contains less of the heavy isotope than the standard.

Typical one standard deviation analytical precisions for oxygen ranges between 0.10‰ and 0.20‰.

### ***Physical, chemical and biological fractionations***

Several books deal with the environmental isotopes, this paragraph mainly refers to Clark and Fritz (1997) and Kendall and McDonnell (1998), as well as recent scientific papers.

In this paragraph, the isotopic fractionation is discussed in order to understand theoretically which  $\delta^{18}\text{O}$  variation in drinking water could happen in a private house during the civil use. I have neglected the effects of industrial use because the method in Rome has been applied in residential area with few commercial activities.

Isotope fractionation occurs in any thermodynamic reaction due to differences in the rate of reaction of molecules with different weight. For elements of low atomic numbers, these mass differences are large enough for many physical, chemical, and biological processes or reactions to “fractionate” or change the relative proportions of various isotopes. Two different types of processes - equilibrium and kinetic isotope effects - cause isotope fractionation. As a consequence, of fractionation processes, waters and solutes often develop unique isotopic compositions (ratios of heavy to light isotopes) that may be indicative of their source or of the processes that formed them.

Fractionation divides in:

- physicochemical fractionation that happens during physicochemical reactions under equilibrium condition or no equilibrium (kinetic) condition;
- biological fractionation;
- diffusive fractionation.

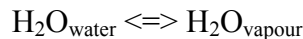
A private house can be considered as a system where different activities involve the water in different type of reactions and I have taken into account in the present dissertation just the following ones:

1. evaporation and condensation in a washing machine, in the heater and in a dishwasher;
2. evaporation in sewer pipes;

### 3. biological reaction due to organic matter discharged in sewer pipes;

then physicochemical and biological fractionations of water molecule could occur.

Firstly, let consider the fractionation during the evaporation and condensation of water molecules, called physicochemical fractionation. Under equilibrium conditions the redistribution of isotopes of an element among various species or compounds occur and the forward and backward reaction rates of any particular isotope are identical. This does not mean that the isotopic compositions of two compounds at equilibrium are identical, but only that the ratios of the different isotopes in each compound are constant. During equilibrium reactions, the heavier isotope generally becomes enriched (preferentially accumulates) in the species or compound with the higher energy state. During phase changes, the ratio of heavy to light isotopes in the molecules in the two phases changes, as well. For example, for water molecule a physical fractionation can be the partitioning of stable isotopes between  $^{16}\text{O}$  and  $^{18}\text{O}$  during evaporation and condensation:



**Eq. 2.3-9**

during that phenomenon the heavy isotopes ( $^{18}\text{O}$  and  $^2\text{H}$ ) have stronger bond and need more energy to evaporate than the lighter ones ( $^{16}\text{O}$  and  $^1\text{H}$ ) (Fig. 2.3.3). Then, the aqueous phase will enrich of heavy isotopes and the partitioning of stable isotopes between  $^{16}\text{O}$  and  $^{18}\text{O}$  can be expressed by use of the isotopic fractionation factor  $\alpha$  which is the ratio of the isotope ratios for the reactant and the product:

$$\alpha^{18}\text{O}_{\text{water-vapour}} = \frac{\left( \frac{^{18}\text{O}}{^{16}\text{O}} \right)_{\text{water}}}{\left( \frac{^{18}\text{O}}{^{16}\text{O}} \right)_{\text{vapour}}}$$

**Eq. 2.3-10**

$\alpha$  values tend to be very close to 1. Kinetic fractionation factors are typically described in terms of enrichment or discrimination factors.

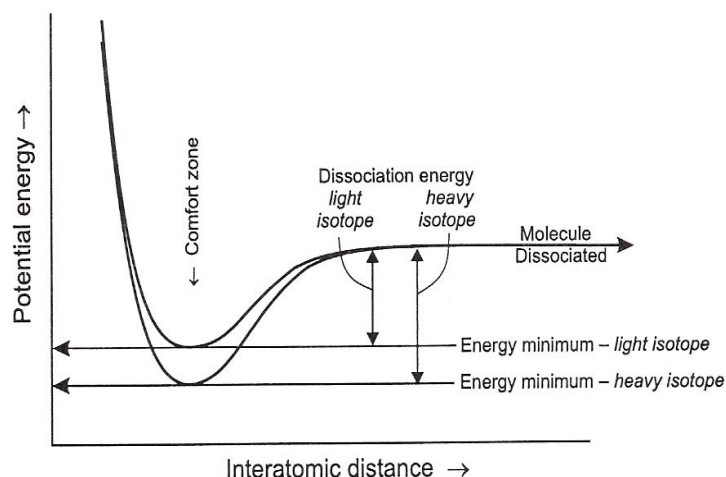


**Fig. 2.3.3: Relazione tra l'energia potenziale e la distanza inter-atomica per isotopi pesanti e leggeri di una molecola. L'energia di dissociazione differisce per i due isotopi, e influisce sulle velocità di reazione, quindi sul frazionamento isotopico (from Clark & Fritz, 1997).**

An useful equation that relates  $\delta$  values and fractionation factors for an isotope specie in two phases or reagents is:  $\alpha_{A-B} = (1000 + \delta_A) / (1000 + \delta_B)$ .

Moreover, the fractionation is strongly dependent on the temperature effect (Clark and Fritz, 1997) because the dissociation energy varies with temperature for a given isotopic species

$$Q = m\sigma^{3/2} \sum e^{-E/KT}$$

**Eq. 2.3-11**

where  $\sigma$  is a symmetry value;  $m$  is the mass;  $E$  is the energy state and the summation is taken over all energy states from the zero-point to the energy of the dissociated molecules [ $\text{J mole}^{-1}$ ];  $k$  is the Boltzman constant equal to  $1.380658 \cdot 10^{-23} \text{ JK}^{-1}$ ;  $T$  is the temperature [K]. At high temperatures  $\alpha$  is close to 1, but at environmental temperature it departs from 1 and the fractionation is consistent. The fractionation factor  $\alpha$  can be determined experimentally, anyway below  $\alpha$  vs. temperature is plotted for the most important environmental isotopes.

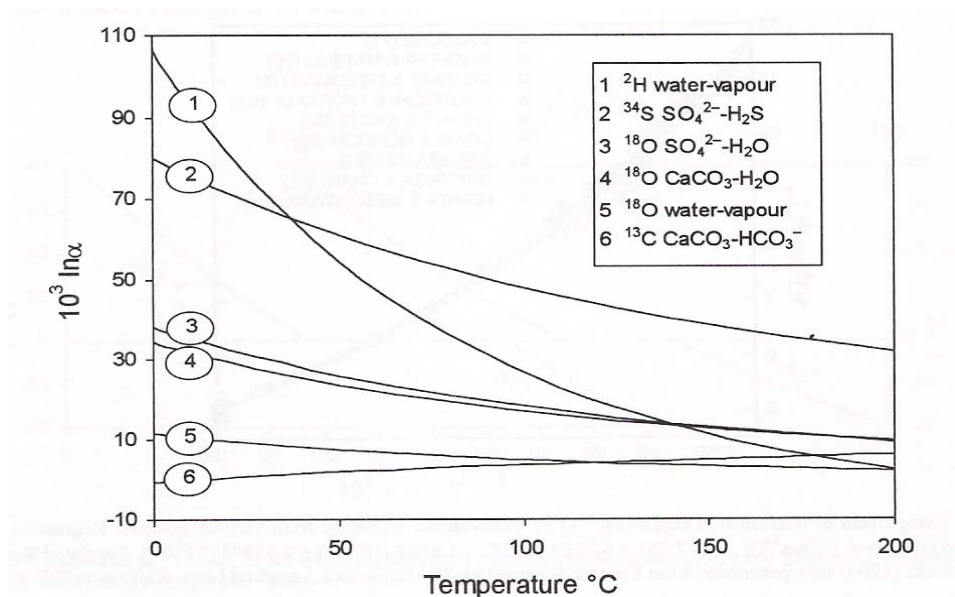


Fig. 2.3.4 Fractionation factors  $\alpha$  vs. temperature (from Clark & Fritz, 1997)

From the Fig. 2.3.4 it is evident that Deuterium is more sensitive to temperature variation than  $^{18}\text{O}$  because of difference in dissociation energy of  $\text{H}_2^{18}\text{O}$  and  $^2\text{HHO}$ . Consequently, during evaporation the difference in vapour pressure imparts disproportional enrichment in terms of  $^{18}\text{O}$  in the water phase. This difference accounts for  $^2\text{H}$  enrichment in water vapour, which is roughly 8 times greater than for  $^{18}\text{O}$ , under equilibrium condition (Clark & Fritz, 1997).

Physicochemical reactions under nonequilibrium (kinetic) condition in systems out of isotopic equilibrium where forward and backward reaction rates are not identical. The reactions may, in fact, be unidirectional if the reaction products become physically isolated from the reactants. Reaction rates depend on the ratios of the masses of the isotopes and their vibrational, translational and rotational energies; as a general rule, bonds between the lighter isotopes are broken more easily than the stronger bonds between the heavy isotopes. Hence, the lighter isotopes react more readily and become concentrated in the products, and the residual reactants become enriched in the heavy isotopes. For example, one of the most important parameter that affect the kinetic reactions during the evaporation and condensation is humidity and the enrichment follows a Rayleigh distillation. This is an exponential relation that describes the partitioning of isotopes between two reservoirs as one reservoir decreases in size. The equations can be used to describe an isotope fractionation process if: (1) material is continuously removed from a mixed system containing molecules of two or more isotopic species (e.g., water with  $^{18}\text{O}$  and  $^{16}\text{O}$ , or sulphate with  $^{34}\text{S}$  and  $^{32}\text{S}$ ), (2) the fractionation accompanying the removal process at any instance is described by the fractionation factor  $\alpha$ , and (3)  $\alpha$  does not change during the

process. Under these conditions, the evolution of the isotopic composition in the residual (reactant) material is described by:

$$\frac{R}{R^0} = \left( \frac{X_1}{X_{1^0}} \right)^{\alpha-1}$$

**Eq. 2.3-12**

where  $R$  is the ratio of the isotopes (e.g.,  $^{18}\text{O}/^{16}\text{O}$ ) in the reactant,  $R^0$  is the initial ratio,  $X_1$  is the concentration or amount of the more abundant (lighter) isotope (e.g.,  $^{16}\text{O}$ ), and  $X_{1^0}$  is the initial concentration. Because the concentration of  $X_{\text{light}} \gg X_{\text{heavy}}$ ,  $X_1$  is approximately equal to the amount of original material in the phase. Then, if  $f = X_1/X_{1^0}$  is the fraction of material remaining, then:

$$R = R^0 f^{(\alpha-1)}$$

**Eq. 2.3-13**

the term "Rayleigh fractionation" should only be used for chemically open systems where the isotopic species removed at every instant were in thermodynamic and isotopic equilibrium with those remaining in the system at the moment of removal (Kendall and McDonnell, 1998).

Finally, the diffusive fractionation happens when atoms or molecules diffuse through another medium, as air, soil, water or vacuum. Fractionation arises from the differences in the diffusive velocities between isotopes. For the water molecules, the diffusivity in air of  $\text{H}_2^{16}\text{O}$  is greater than  $^2\text{HH}^{16}\text{O}$  or  $\text{H}_2^{18}\text{O}$ .

For example, the biological processes, that happen in a wastewater stream, are generally unidirectional and are examples of kinetic isotope reactions. Organisms preferentially use the lighter isotopic species because of the lower energy "costs" associated with breaking the bonds in these molecules, resulting in significant fractionations between the substrate (heavier) and the biologically mediated product (lighter). Kinetic isotopic fractionations of biologically-mediated processes vary in magnitude, depending on reaction rates, concentrations of products and reactants, environmental conditions, and in the case of metabolic transformations species of the organism. The variability of the fractionations makes interpretation of isotopic data difficult, particularly for nitrogen and sulphur. The fractionations are very different from the equivalent equilibrium reaction and typically larger than this. The magnitude of the fractionation depends on the reaction pathway utilized (i.e. which is the rate-limiting step) and the relative energies of the bonds severed and formed by the reaction. In general, slower reaction steps show greater

isotopic fractionation than faster steps because the organism has time to be more selective (i.e., the organism saves internal energy by preferentially breaking light-isotope bonds). If the substrate concentration is large enough then the isotopic composition of the reservoir is insignificantly changed by the reaction. For unidirectional reactions the change in the isotope ratio of the substrate relative to the fraction of the unreacted substrate can be described by the Rayleigh equation:

$$R_s = R_s^0 f^{(\alpha-1)}$$

**Eq. 2.3-14**

where  $R_s$  and  $R_s^0$  are the ratios of the unreacted and initial substrate, respectively, and  $f$  is the fraction of unreacted substrate. Some important biological fractionations can happen during photosynthesis, oxidation of sulphide, ammonia volatilization, nitrification, denitrification and methanogenesis. The oxidation of sulphide could determine an enrichment of water of  $^{18}\text{O}$  of  $0\pm 2\text{‰}$  SMOW, although the oxygen contribution from water depends of the enzymes pathways (Toran and Harris, 1989). Regarding the oxidation of organic matter Clark and Fritz (1997) as well as Kendall and McDonnell (1998) deal with it in detail, but only the isotopic variation of carbon seems to occur.

When the processes above take place, it is important to distinguish where the isotopes exchange takes place :

- in closed systems in the case of the equilibrium fractionations "closed" means that the reactant and product remain in close contact, in their own closed (finite) system during the entire reaction, so that the two reservoirs are always in chemical and isotopic equilibrium. For the kinetic fractionations "closed" means there is a limited supply of reactant, which is undergoing irreversible, quantitative, conversion to product in an isolated system;
- in opened systems that in the case of the equilibrium fractionations "open" means that the product, once formed at equilibrium, escapes to outside the system and does not interact again with the residual substrate (and, consequently, is no longer in equilibrium with the substrate). For the kinetic fractionations, "open" means that the supply of substrate is infinite (which it cannot be in a closed system). The Rayleigh equation applies to an open system.

The condensation of water vapour to droplets in a cloud is a phenomenon as described in the first point above. There is continuous exchange between the isotopes in the vapour and water droplets and, from the isotopic method point of view, it could happen in a heater, a washing machine and a dishwasher. While the condensation and evaporation occurring within sewer pipes are phenomena as described in the second point.

The passage below is integrally extracted from Kendall and McDonnell (1998) Chapter 2.

*The isotope enrichment achieved can be very different in closed vs. open systems. For example, Fig. 2.3.5 shows the changes in the  $\delta^{18}\text{O}$  of water and vapor during evaporation (an open-system process) where the vapor is continuously removed (i.e. isolated from the water) with a constant fractionation factor  $\alpha_{L-V} = 1.010$  (i.e. the newly formed vapor is always 10‰ lighter than the residual water). As evaporation progresses the  $\delta^{18}\text{O}$  of the remaining water (solid line A), becomes heavier and heavier. The  $\delta^{18}\text{O}$  of the instantaneously formed vapor (solid line B) describes a curve parallel to that of the remaining water, but lower than it (for all values of  $f$ ) by the precise amount dictated by the fractionation factor for ambient temperature, in this case by 10‰. For higher temperatures, the  $\alpha$  value would be smaller and the curves closer together. The integrated curve, giving the isotopic composition of the accumulated vapour thus removed, is shown as solid line C. Mass balance considerations require that the isotope content of the total accumulated vapour approaches the initial water  $\delta^{18}\text{O}$  value as  $f \rightarrow 0$ ; hence, any process should be carried out to completion (with 100% yield) to avoid isotopic fractionation.*

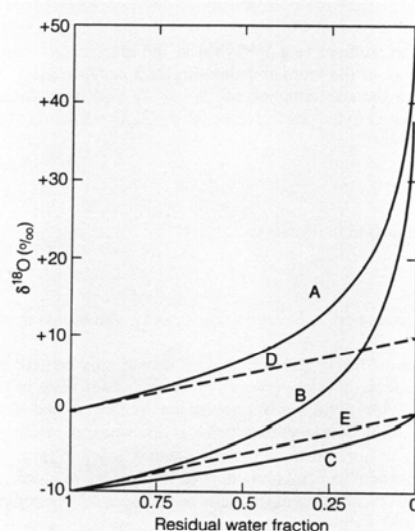


**Figure 2.3.** Isotopic change under open- and closed-system Rayleigh conditions for evaporation with a fractionation factor  $\alpha = 1.01$  for an initial liquid composition of  $\delta^{18}\text{O} = 0$ . The  $\delta^{18}\text{O}$  of the **remaining water** (solid line A), the **instantaneous vapor** being removed (solid line B), and the **accumulated vapor** being removed (solid line C) all increase during single-phase, open-system, evaporation under equilibrium conditions. The  $\delta^{18}\text{O}$  of water (dashed line D) and vapor (dashed line E) in a two-phase closed system also increase during evaporation, but much less than in an open system; for a closed system, the  $\delta$  values of the instantaneous and cumulative vapor are identical. Modified from Gat and Gofiantini (1981).

**Fig. 2.3.5** (from Kendall and McDonnell, 1998)



The dashed lines in Fig. 2.3.5 show the  $\delta^{18}\text{O}$  of vapor (E) and water (D) during equilibrium evaporation in a closed system (i.e. where the vapor and water are in contact for the entire phase change). Note that the  $\delta^{18}\text{O}$  of vapor in the open system where the vapor is continuously removed (line B) is always heavier than the  $\delta^{18}\text{O}$  of vapor in a closed system where the vapor (line E) and water (line D) remain in contact. In both cases, the evaporation takes place under equilibrium conditions with  $\alpha = 1.010$ , but the cumulative vapor in the closed system remains in equilibrium with the water during the entire phase change. As a rule, fractionations in a true "open-system" Rayleigh process create a much larger range in the isotopic compositions of the products and reactants than in closed systems. This is because of the lack of back reactions in open systems. Natural processes will produce fractionations between these two "ideal" cases.

Evaporation from an open-water surface fractionates the isotopes of hydrogen and oxygen in a manner which depends on a number of environmental parameters, the most important of which is the ambient humidity. This is illustrated for various relative humidities in Fig. 2.3.6. The higher the humidity, the smaller the change in  $\delta^{18}\text{O}$  and  $\delta\text{D}$  during evaporation. For example, at 95% humidity, the  $d$  values are constant for evaporation of the last 85% of the water. Evaporation results in lines with slopes  $< 8$  on a  $\delta^{18}\text{O}$  vs.  $\delta\text{D}$  plot (i.e. the data plot on lines below the MWL that intersect the MWL at the composition of the original water).

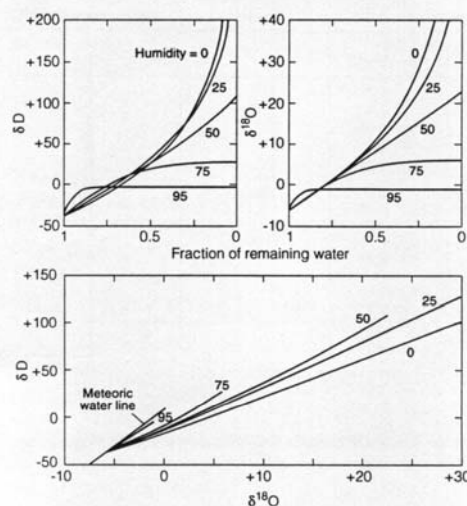


Figure 2.5. The effect of humidity on the  $\delta^{18}\text{O}$  and  $\delta\text{D}$  values of the residual water fraction during evaporation. Higher humidities result in less fractionation because of back exchange between the water and the vapor, and evaporation lines with higher slopes. Modified from Gat and Gofiantini (1981).

Fig. 2.3.6 (from Kendall and McDonnell, 1998)

*Evaporation at 0% humidity describes open-system evaporation. Note that the two upper diagrams on Fig. 2.3.6. are Rayleigh-type plots, similar to Fig. 2.3.5 but with larger changes in  $\delta^{18}\text{O}$  during open-system evaporation on Fig. 2.3.6. The  $d$  values on the curved fractionation lines on the upper diagrams plot along nearly straight lines on the lower  $\delta^{18}\text{O}$  vs.  $D$  plot. The "length" of the evaporation lines on the  $\delta^{18}\text{O}$  vs.  $\delta D$  plot reflect the range of values of water produced during total evaporation under different humidities. For example, the short line for 95% humidity indicates that the water changes little during the entire evaporation process.*

Consequence of the fractionation and Rayleigh processes of the water mass is the spatial isotopic distribution over country, continental as well as the altitude distribution over mountains and aquifers (see Fig. 2.3.7). The air mass follows a trajectory from its vapour source area (ocean) to higher altitudes and over continents, it cools and loses its water vapour along the way as precipitation, a process known as "rainout". Within the cloud there is both equilibrium fractionation that partitions  $^{18}\text{O}$  and  $^2\text{H}$  into rain and snow, than non-equilibrium fractionation modelled with Rayleigh equation that distils the heavy isotopes from the vapour. As a consequence the condensate that becomes rain or snow consists in heavy water molecules and the cloud that migrates over the lands consists in the lighter water molecules. Such complex phenomena can be predictable indeed, because it is sensitive to: seasons, altitude, latitude, continentally and paleoclimates. Craig (1961) defined a relationship between  $^{18}\text{O}$  and  $^2\text{H}$  in worldwide fresh surface water  $\delta^2\text{H} = 8\delta^{18}\text{O} + 10\text{‰}$  called the Global Meteoric Water Line (GMWL) or just the MWL, or even the Craig Line. The slope is 8 (actually, different data sets give slightly different values) because this is approximately the value produced by equilibrium Rayleigh condensation of rain at about 100% humidity. The value of 8 is also close to the ratio of the equilibrium fractionation factors for H and O isotopes at 25-30°C. At equilibrium, the  $d$  values of the rain and the vapor both plot along the MWL, but separated by the  $^{18}\text{O}$  and  $^2\text{H}$  enrichment values corresponding to the temperature of the cloud base where rainout occurred. The y-intercept value of 10 in the GMWL equation is called the deuterium excess (or  $\delta$ -excess, or  $\delta$  parameter) value for this equation. The term only applies to the calculated y-intercept for sets of meteoric data "fitted" to a slope of 8; typical  $d$ -excess values range from 0 to 20. The fact that the intercept of the GMWL is 10 instead of 0 means that the GMWL does not intersect  $d^{18}\text{O} = \delta D = 0$ , which is the composition of average ocean water (SMOW). The GMWL does not intersect the composition of the ocean, the source of most of the water vapor that produces rain, because of the 10‰ kinetic enrichment in D of vapor evaporating from the ocean at an average humidity of 85%.

In Italy, Longinelli and Selmo (2003) analyzed 77 stations over the country and for the precipitation found out the relationship:  $\delta^2\text{H} = 7.61\delta^{18}\text{O} + 9.21\text{‰}$ . One of the principal factor affecting the isotopic composition of precipitation in Italy is elevation and the mean vertical isotopic gradient measured is close to  $-0.2$  permil/100 m.

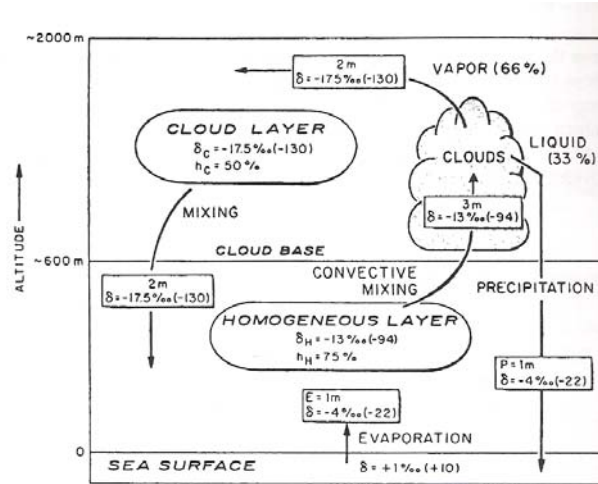


Fig. 2.3.7 scheme of the water cycle (from Clark & Fritz, 1997)

Anyway, the isotopic composition of the rain is not directly transfer to the groundwater but several variations in the isotopes content occur throughout the soil and into the aquifers. Often the isotopic composition of groundwater is not sensitive to the seasonal variation of precipitation but the physical characteristics of the unsaturated zone, the length of the flowpath and residence time are critical aspects on the groundwater isotopic composition. A critical depth exist below which the variability is less than the analytical precision of  $2\sigma$  (see Fig. 2.3.8).

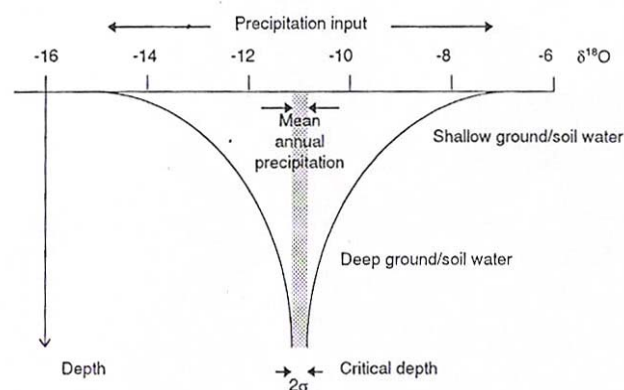


Fig. 2.3.8 schematic attenuation of seasonal isotope variations in recharge waters during infiltration through the unsaturated zone and movement within the saturated zone and the critical depth (from Clark & Fritz, 1997)

In several studies the comparison between the  $\delta^{18}\text{O}$  values of shallow groundwater shows the same composition of precipitation at regional scale, despite some temporal bias due to the time need to recharge. For example, higher the soil permeability, shorter the recharge time of an unconfined shallow aquifer (i.e. sand aquifer).

The isotopic method for assessing the infiltration is based on the hydrograph separation method where a source is the groundwater, then it is important to define a representative value of the isotopes abundance of 18-oxygen spatially and temporally in the catchments under investigation. Nevertheless the temporally variation it is not of interest in this case because the method is applied for 24 hour, whereas the spatial variability is of great interest. The spatial variability have to be estimated over the area to be investigated and in depth. In both cases it is possible to assume the variability not significant if it is around the analytical precision  $\pm 0.20\text{‰}$ . In subsurface environment the ratio between the isotopes is not perfectly conservative, it is possible that the oxygen ratio can change as a result of both isotopic fractionation and molecular exchange (Bishop, 1990). Molecular exchange occurs because of atom substitution between water and other oxygen rich molecules in subsurface environment.

### ***Hydrograph separation***

The hydrograph separation is a technique well described in literature that allows to quantifying, for example, different contributions to the recharge of a water body. The method is applied for quantifying the infiltration in an urban sewer system and it is explained in §[3.5]. In that case the water contributions to the wastewater stream are two: drinking water and groundwater, that is contribution can be distinguished into two classes identified by two different  $\delta^{18}\text{O}$  values. This means that if other sources with the same  $\delta^{18}\text{O}$  value of groundwater infiltrates into the sewer (e.g. springs) it is not possible to say how much water comes from springs and how much from groundwater. On the contrary if there are infiltration from water which  $\delta^{18}\text{O}$  value is unknown the infiltration calculated by the isotopic method explained in §[3.5] is wrong.

Consequently, a very good knowledge of the hydrogeology of the area where the sewer system have to be investigated is needed. Moreover if different water contribution to the infiltration can occur in that area the isotopic method in §[3.5] has to be upgraded to a multi-tracer hydrograph separation method. In such a method several conservative chemical, isotopic and parameter have to monitored in the area in order to distinguished all the water contributions.

Hydrograph separation model using stable isotopes started with studies by Dincer et al. (1970), Martinec (1975) and Fritz et al. (1976) and has been used mainly in humid temperate

regions and it has been applied for separate the pre-storm from the storm water during a precipitation. Rodhe (1987) suggests that the sensitivity of the two component mixing model

$$Q_t \times C_t = Q_s \times C_s + Q_p \times C_p$$

Eq. 2.3-15

where Q is the discharge and C the concentration of the tracer, t, s and p refer to total, storm and pre-storm water component.

The uncertainty in input variables can be calculated as

$$|\Delta X| = \frac{1}{C_p - C_s} \sqrt{\Delta C_t^2 + \Delta C_s^2 + X^2 (\Delta C_p^2 + \Delta C_s^2)}$$

Eq. 2.3-16

where X is the fraction of the pre-storm water and  $\Delta X$  is its uncertainty. In those application he estimated an precision of 10-15%.

Laudoche et al. (2001) applied the hydrograph separation using isotopic, chemical and hydrological approaches in France for distinguishing the prestormwater from the stormwater in the aquifer. Precipitation, soil solution, springwater and stream-waters were sampled and analysed for stable water isotopes ( $^{18}\text{O}$  and  $^2\text{H}$ ), major chemical parameters ( $\text{SO}_4^{2-}$ ,  $\text{NO}_3^{2-}$ ,  $\text{Cl}^-$ ,  $\text{Na}^+$ ,  $\text{K}^+$ ,  $\text{Ca}^{2+}$ ,  $\text{Mg}^{2+}$ ,  $\text{NH}_4^+$ ,  $\text{H}^+$ ,  $\text{H}_4\text{SiO}_4$ , alkalinity and conductivity), dissolved organic carbon (DOC) and trace elements (Al, Rb, Sr, Ba, Pb and U).  $^{18}\text{O}$ , Si, DOC, Ba and U were finally selected to assess the different contributing sources using mass balance equations and end-member mixing diagrams. The conclusion was that chemical and isotopic tracer can be applied but the results have to be interpreted carefully, because different phenomena involved these tracers and they bring interesting but sometimes different informations.

From the isotopic method point of view we are interested in:

1. criteria for understanding if the method is applicable in a certain city;
2. how to characterize the isotopic content of possible infiltration sources over an urban catchment whose sewer has to be investigated;
3. how to sample.

The introduction of the multi-tracer approach introduce solutes and water parameters that are more affected by spatial and temporal variation over a catchment. Such variability is due to chemical and physical phenomena that affects more the solute concentration or mass and parameter values than the water isotope abundances.

Lee and Krothe (2001) focused on identifying the unique signatures of the rain, soil, epikarstic, and phreatic waters using dissolved inorganic carbon DIC and  $\delta^{13}\text{C}_{\text{DIC}}$  as tracers. It also attempts to create the four-component mixing model that describes the water, solute, and solute isotopic fluxes. Special care has to be taken if isotopic solutes are considered because if water isotopic composition  $\delta\text{D}$  or  $\delta^{18}\text{O}$  is a signature of the water, and thus can be used in mixing calculations and as a tracer of water flux, isotopic composition of solutes is a signature of the solute and does not necessarily reflect the signature of the water flux. Therefore, solute isotopic content should not be used as a tracer for the water flux unless the concentration of the solute is considered.

Laudon and Slaymaker (1997) used as alternative hydrological tracer electrical conductivity (EC) and silica concentration and verified the reliability of these tracers against water stable isotopes. They observed that the hydrograph drawn by EC and silica not always were equal to drawn using  $\delta\text{D}$  or  $\delta^{18}\text{O}$  because they are more flowpath tracers as they react with encountered mineral material, whereas  $\delta\text{D}$  or  $\delta^{18}\text{O}$  are at last undergone at slower reactions that could change their abundance in water.

Lambs (2000) used EC as easy trace to be analyzed for interpreting the hydrogeology in two catchments Garonne (France) and Ganges (Himalaya). The aim was to discriminate snow and glacier melt and he compare the results using EC with those using  $\delta^{18}\text{O}$ .

The reason for using EC as a hydrological tracer to immediately give a glimpse on the field site of the percentage the two kinds of water. For the Garonne stable oxygen isotopes give more precise results than conductivity. In each case, the phreatic water has the lower coefficient of variation. The apparent high variation in river water is due in fact to a general decrease in conductivity throughout the study period. The correlation between the values of conductivity and oxygen-18 for the gravel bar have been taken at four time periods, with an increasing number of points, and a better correlation coefficient (from 0.859 for 9 points to 0.952 for 26 points).

For the Ganges both EC and oxygen-18 discriminated well the different fluxes.

He concluded that the use of EC was useful even though not always precise as oxygen-18 because allows to distinguished different fluxes that have the same isotopic composition but different origin that is evident only if another tracer is used. Finally, EC is measurable in the field by means of a portable instrument and can be useful for adjusting sampling frequency and then for saving money in laboratory analyses.

## 2.4 Reference

- Best, J. L., and Roy, A. G. (1991). Mixing-layer distortion at the confluence of channels of different depth. *Nature (London)*, 350, 411–413.
- Biron, P., Roy, A. G., and Best, J. L. (1996). The turbulent flow structure at concordant and discordant open channel confluences. *Exp. Fluids*, 21, 437–446.
- Bradbrook, K. F., Biron, P. M., Lane, S. N., Richards, K. S., and Roy, A. G. (1998). Investigation of controls on secondary circulation in a simple confluence geometry using a three-dimensional numerical model. *Hydrolog. Process.*, 12, 1371–1396.
- Bradbrook, K. F., Lane, S. N., and Richards, K. S. (2000). Numerical simulation of three-dimensional, time-averaged flow structure at river channel confluences. *Water Resour. Res.*, 36, 2731–2746.
- Bradbrook, K. F., Lane, S. N., Richards, K. S., Biron, P. M., and Roy, A. G. (2000). Large eddy simulation of periodic flow characteristics at river channel confluences. *J. Hydraul. Res.*, 38, 207–215.
- Bradbrook, K. F., Lane, S. N., Richards, K. S., Biron, P. M., and Roy, A. G. (2001). Role of bed discordance at asymmetrical river confluences. *J. Hydraul. Eng.*, 127, 351–368.
- Bishop, G.E. (1990). Episodic increases in stream acidity, catchment flow pathways and hydrograph separation. Ph.D. Thesis, Department of Geography, University of Cambridge, pp.246.
- Chau, K. W. (2000). Transverse mixing coefficient measurements in an open rectangular channel. *Advances in Environmental Research* 4 (2000) 287-294.
- Clark, I. D.; Fritz, P. (1997). *Environmental Isotopes in Hydrogeology*. CRC Press LLC, USA.
- Craig, H. (1961). Isotopic variations in meteoric waters. *Science* (133) 1702-1703.
- Dincer, T.; Payne, B. R.; Florkowski, T.; Martinec, J.; Tongogiorgi, E. (1970). Snowmelt runoff from measurements of tritium and oxygen-18. *Water Resource Research*, 6, 1, pp. 110-124.
- Fritz, P.; Cherry, J.A.; Weyer, R.U.; Sklash, M (1976). Storm runoff analyses using environmental isotopes and major ions. In: *Interpretation of environmental isotopes and hydrochemical data in groundwater hydrology*, Vienna International Atomic Energy Agency, pp. 111-130.

Giulianelli, M.; Mazza, M.; Prigiobbe, V.; Russo, F. (2003). Assessing exfiltration in an urban sewer by slug dosing of a chemical tracer (NaCl). NATO ARW on Enhancing Urban Environment, Rome, Italy, Nov. 5-9, 2003.

Laudouche, B.; Probst, A.; Viville, D.; Idir, S.; Baque, D.; Loubet, M.; Probst, J.-L.; Bariac, T. (2001). Hydrograph separation using isopiestic, chemical and hydrological approaches (Strengbach catchment, France). *Journal of Hydrology* 242, pp. 255-274.

Laudon, H.; Slaymaker, O. (1997). Hydrograph separation using stable isotopes, silica and electrical conductivity: an alpine example. *Journal of Hydrology* 201, pp. 82-101.

Lambs, L. (2000). Correlation of conductivity and stable isotope  $^{18}\text{O}$  for the assessment of water origin in river system. *Chemical Geology*, 164, pp. 161-170.

Lee, E. S.; Krothe, N. C. (2001). A four-component mixing model for water in a karst terrain in south-central Indiana, USA. Using solute concentration and stable isotopes as tracers. *Chemical Geology*, 179, pp. 129-143.

Marchi, E.; Rubatta, A. (2004). *Meccanica dei Fluidi*. Ed. UTET.

Martinec, J. (1975). Subsurface flow from snowmelt traced by tritium. *Water Resource Research* 6 (1) pp. 110-124.

Rieckermann, J.; Neumann, M.; Ort, C.; Huismann, J.L.; Gujer, W. (2004). Dispersion coefficient of sewers from tracer experiments. *Proceedings of the Int. Conference on Urban Drainage Modelling, Dresden 2004*, pp.417-426.

Rodhe, A. (1987). The origin of streamwater tracer by oxygen-18. Ph.D. Thesis, Uppsala University, UNGI Report Series A, No. 41, pp.260.

Singh, S. K. (2003). Treatment of stagnant zones in riverine advection-dispersion. *Journal of hydraulic engineering*, 129 (6), pp. 470-473. Biron, P. M.; Ramamurthy, A. S.; F. ASCE; and Han, S. (2004). Three -Dimensional Numerical Modeling of Mixing at River Confluences. *Journal of Hyd. Eng.* 130 (3), 243-253.

Prigiobbe, V.; Giulianelli, M. (2004). Design of tests for quantifying sewer leakages by QUEST-C method. *Conference on Urban Drainage Modelling, Dresden, 15th-17th September 2004*.

El-Hadi, N.; Harrington, A.; Hill, I.; Lau, Y.L. and Krishnappan, B.G. (1984). River mixing-a state of the art report. *Can. J. Civ. Engin.*, 11, 585-609.

Fisher, H.B. (1969). The effects of bends on dispersion in streams. *Wat. Resour. Res.*, 5, 496-506.

Kendall, C.; McDonnell, J. J. (1998). *Isotopes tracers in catchment hydrology*. Elsevier Science B. V. Netherlands.



Kracht, O.; Gresch, M.; de Benneditis, J.; Prigiobbe, V.; Gujer, W. (2003). Stable Isotopes of water as a natural tracers for the infiltration into urban sewer systems. Geophysical Research Abstracts, Vol. 5, 07852, European Geophysical Society 2003.

Kracht, O. (2003A). The stable isotope composition of water as a natural tracer for the quantification of extraneous infiltration into sewer system. Internal protocol of APUSS project.

Kracht, O. (2003B). Identification of the volume of extraneous infiltration from combined time series of discharge and pollutant load in the wastewater. Internal protocol of APUSS project.

Jobson, H. E. (1997). Predicting travel time and dispersion in rivers and streams. Journal of Hyd. Eng. 123 (11), 971-977

Jobson, H.E. and Sayre, W. W. (1970). Predicting concentration profiles in open channels, Am. Soc. Civ. Engin., 96 (HY10), 1983-1996.

Gaudet, J. M. & Roy, A. G. (1995). Effect of the bed morphology on flow mixing length at river confluences. Nature vol. 373, pp. 138-139.

Longinelli, A.; Selmo, E. (2003). Isotopic composition of precipitation in Italy: a first overall map. Journal of Hydrology 270, 75-88.

Nokes, R.I. (1986). Problems in turbulent dispersion, PhD Thesis, University of Canterbury, Christchurch.

Nokes, R. I. and Wood, I. R. (1988). Vertical and lateral turbulent dispersion: some experimental results, J. Fluid Mech., 187, 373-394.

Reichert, P. (1994). AQUASIM – A tool for simulation and data analysis of aquatic systems. Water Science and Technologies, 30, pp. 21-30.

Rieckermann, J.; Bareš, V.; Kracht, O.; Braun, D. and W. Gujer. (2003). Quantifying exfiltration with continuous dosing of artificial tracers. Pages 229-232 in Hydrosphere 2003, Brno, CZ.

Rieckermann, J.; Bareš, V.; Kracht, O.; Braun, D.; Prigiobbe, V, and Gujer. W. (2004). Assessing exfiltration from sewers with dynamic analysis of tracer experiments. 19th European Junior Scientist Workshop “Process data and integrated urban water modelling” France 11-14 March 2004.

Rutherford, J.C. (1994). River Mixing. John Wiley & Sons, Chichester.

Sayre, W.W. (1979). Shore-attached thermal plumes in rivers, in Shen, H.W. (ed.) Modelling in Rivers, Shen, Fort Collins, pp. 6.1-6.37.

Sayre, W.W. (1968). Dispersion of mass in open channel flow, PhD Thesis, Colorado state University, Fort Collins.

Taylor, G.I. (1921). Diffusion by continuous movements, *proc. London Math. Soc.*, Ser. 2, 20, 196-212.

Yotsukura, N. and Sayre, W.W. (1976). Transverse mixing in natural channels. *Wat. Resour. Res.*, 12, 695-704.

Gaudet, J. M. and Roy, A. G. (1995). Effect of bed morphology on flow mixing length at river confluences. *Nature (London)*, 373, 6510, 138–139.

De Serres, B., Roy, A. G., Biron, P. M., and Best, J. L. (1999). Three-dimensional structure of flow at a confluence of river channels with discordant beds. *Geomorphology*, 26, 313–335.

Webel, G. and Schatzmann, M. (1984). Transverse mixing in open channel flow. *J. Hydr. Engin.*, 110, 423-435.

Nokes, R.I. and Wood, I. R. (1988). Vertical and lateral turbulent dispersion: some experimental results, *J. Fluid Mech.*, 187, 373-349.

Toran, L. and Harris, R. F. (1989). Interpretation of sulphur and oxygen isotopes in biological and abiological sulphide oxidation. *Geochimica et Cosmochimica Acta* (53) 2341-2348.

# **CHAPTER 3**

## **Experimental Design and Field Application**

### **3.1 Introduction**

This chapter deals with both the experimental design based on uncertainty analysis for the application of the methods for assessing the infiltration and the exfiltration in urban sewers systems. Moreover, data from field experiments are discussed. The experimental design aimed to analyze the main uncertainty sources affecting each method and to estimate the error propagation in the results (infiltration and exfiltration ratio).

### **3.2 Experimental Design**

The objective of the experimental design is the optimization of an experiment in all its parts, that is: measurements, sampling, analyses, models to be used as reduction equations for calculating the result. Generally, the uncertainty analysis used during the experimental planning can be summarized into the following points (Coleman and Steele, 1999):

1. *planning of the experiments*: estimating the different ways for monitoring the phenomena. In this phase the uncertainty is not distinguished in systematic and random, but the all errors are considered as random, because the aim of this analysis is just for knowing how the errors can propagate through the models;
2. *design of the experiments*: choice of the equipments, architecture of the investigations, etc. In this phase a detailed uncertainty analysis has to be carried out, as matter of the fact, the sources of uncertainty are divided in random and systematic;
3. calibration of the equipments and assemble of the detectors;
4. first trials and possible variation of the hypothesis;
5. execution of the experiment: preliminary tests and final investigations;
6. data analysis and discussion.

For a brief introduction to the uncertainty analysis let consider the data reduction equation of a model:

$$r = r(x_1, \dots, x_n)$$

**Eq. 3.2-1**

where  $x_1, \dots, x_n$  are the model variables of the model affected by systematic and random errors.

The systematic errors are due to: calibration errors, data acquisition (e.g., installation or environmental bias), data reduction (e.g., substitution of the measured data with one from a fit curve) and conceptual errors (e.g., representatively of a point sampling over a cross section of the whole section property). They can't be reduced by increasing the number of measurements, but they have to be known from the technical informations or from the equipments and protocols used for measurements, sampling etc.

When the number of degrees of freedom is more than 9, the systematic uncertainty is:

$$B_r^2 = 2 \sum_{i=1}^{j-1} \sum_{k=i+1}^j \theta_i \theta_k B_{ik} + \sum_{i=1}^j \theta_i^2 B_i^2$$

**Eq. 3.2-2**

with:

$$\theta_i = \frac{\partial r}{\partial x_i}$$

**Eq. 3.2-3**

and

$$B^2 = \left( 2 \frac{\sum_{i=1}^N (x_i - x_{true})}{N-1} \right)^2$$

**Eq. 3.2-4**

and  $B_{ik}$  is the covariance of the systematic errors that can be estimated by:

$$B_{ik} = \sum_{\alpha=1}^L (B_i)_{\alpha} (B_k)_{\alpha}$$

**Eq. 3.2-5**

where L is the number of the independent sources of systematic errors which are common for the variables  $X_i$  and  $X_k$ .

The random errors are due to the experimental, and when the number of degrees of freedom is more than 9, the random uncertainty is:

$$P_r^2 = 2 \sum_{i=1}^{j-1} \sum_{k=i+1}^j \theta_i \theta_k P_{ik} + \sum_{i=1}^j \theta_i^2 P_i^2$$

**Eq. 3.2-6**

with:

$$P^2 = \left( 2 \frac{\sum_{i=1}^N (x_i - \mu)}{N-1} \right)^2$$

**Eq. 3.2-7**

where  $\mu$  is the mean value of the  $N > 10$  readings sampled from a Gaussian parent distribution and  $P_{ik}$  is the covariance of the random errors.

Furthermore, all the errors can be classified into three parts based on the level (or order) of the experiment where they occur:

1. Zeroth-order;
2. First-order;
3. Nth-order.

The Zeroth order errors consider the random and systematic errors due to instrumentation and measurements. For a sample to sample experiment, it is the uncertainty calculated when the repetition of the measurement of a single sample is done; while for a time-wise experiment, it is the uncertainty calculated as if the process were steady.

First order errors consider the random errors due to the variability of the investigated phenomena when the measurements are carried out by means of the same equipments, but the monitored sample changes. The sample could change because of the temporal variability (i.e. flow rate measurements by flowmeter) or spatial variability (i.e. permeability of soil measured over a large area). This order of error accounts of both the random errors due to the equipments itself and variability.

Nth order errors consider the propagation of the systematic and the random errors of the previous order through the model to the results. At this order, the errors are due to: the equipments' installations, interaction of the equipments and of the measurements with the surrounding environment and the error do not consider into the previous orders.

When the number of degrees of freedom is more than 9, the uncertainty that affect the equation Eq. 3.2-1 is:

$$U^2 = B^2 + P^2$$

**Eq. 3.2-8**

where B is the uncertainty that accounts of the systematic errors and can be reduced, for example, by improving the calibration; P is the uncertainty, which accounts of the random errors, sums up the first order errors and can be reduced, for example, by increasing the number of the measurements.

As explained above, the uncertainty analysis can be general or detailed (Coleman and Steele, 1999) depending on the scope of the analysis: general uncertainty analysis for planning and detailed uncertainty analysis for designing.

The detailed analysis is mainly used during the planning phase when, for example, we have not decided the instruments, yet, but we want to understand how the experiments can successfully give us the answer of interest. Moreover in the general uncertainty analysis we do not need to distinguish between systematic and random errors, the first ones can be as likely negative as positive at this stage, thus all the errors are considered random:  $U_{xi} = P_{xi}$  and  $B_{xi} = 0$  and the covariance terms are considered zero.

After a general uncertainty analysis, the detailed one is of interest because the equipments have been chosen and we need to know how the systematic and the random errors, which are considered separately, can propagate through the reduction equation (Eq. 3.2-1).

The Tab. 3.2-1 summarized how to use the uncertainty analysis during the all experimentation.

**Tab. 3.2-1: Uncertainty analysis in experimentation (modified from Coleman and Steele, 1999)**

Phase of Experiment	Type of Uncertainty Analysis	Uses of Uncertainty Analysis
Planning	General	Choose experiment to answer a question; preliminary design.
Design	Detailed	Choose instrumentation (zeroth-order estimates); detailed design (Nth-order estimates).
Construction	Detailed	Guide for decisions on changes, etc.
Debugging	Detailed	Verify and qualify operations: firsts-order and Nth-order comparisons.
Execution	Detailed	Balance checks and monitoring operation of apparatus; choice of test point runs.
Data Analysis	Detailed	Guide to choice of analysis techniques.
Reporting	Detailed	Systematic uncertainties, random uncertainties, and overall uncertainties reporting.

The general uncertainty analysis, as applied in this thesis experiment planning, consists of estimating the UMCs (Uncertainty Magnification Factors) and the UPCs (Uncertainty Percentage Factors) factors. The first factors indicate the influence of the uncertainty in that variable on the uncertainty in the result, and the second ones (Uncertainty Percentage Factors) give the percentage contribution of the uncertainty in that variable to the squared uncertainty in the result (Coleman & Steele, 1999). In practice, let us consider the observation equation:

$$f = f(X_i)$$

**Eq. 3.2-9**

where  $X_i$  is the vector of the measured variables. The UMFs and the UPCs for an equation Eq. 3.2-9 are defined as:

$$UMF_i = \frac{X_i}{f} \frac{\partial f}{\partial X_i}$$

**Eq. 3.2-10**

$$UPC_i = \frac{\left( \frac{\partial f}{\partial X_i} \right)^2 (U_{x_i})^2}{(U_f)^2} * 100$$

**Eq. 3.2-11**

where  $U_{x_i}$  is the uncertainty of the variable  $X_i$  and  $U_f$  is the uncertainty in the result of the observation equation calculated by error propagation equation for a linear model of random variables statistically independent.

The detailed uncertainty analysis, as applied in this thesis, considers the errors as random and systematic errors. Once defined them for each source of uncertainty, the uncertainty in the model results have to be calculated with error propagation techniques. In this thesis the uncertainty has been propagated throughout the model by applying the reduction equation (e.g., equation for estimating the infiltration ratio and the exfiltration ratio) several times to the variables' values sampled by Monte Carlo method from the assumed Gaussian probably density functions of variables. We decided to apply the MCS because of the several number of the variables and because the non-linearity of the used models.

The general uncertainty analysis has been applied for experimental planning of the field application of QUEST-C method (§[3.4]).

The detailed uncertainty analysis has been applied for experimental design of the field application of QUEST method (§[3.3]), of QUEST-C method (§[3.4]) and of isotopic method (§[3.5]).



### 3.3 QUEST

In this paragraph, the QUEST method for quantifying the exfiltration from an urban sewer pipe is discussed, and the uncertainty sources are analyzed. For the method's description see §[2.2.1]. It has been developed by Rieckermann & Gujer (2002) and it allows to estimate the exfiltration ratio by the given equation:

$$exf = \frac{Q_1 - Q_2}{Q_1}$$

**Eq. 3.3-1**

where  $Q_1$  is the flow rate at the beginning of the investigated reach [ $\text{m}^3 \text{s}^{-1}$ ];  $Q_2$  is the flow rate at the end of the investigated reach [ $\text{m}^3 \text{s}^{-1}$ ]. If the dosed indicator tracer is completely mixed, the Eq. 3.3-1 can be write as below:

$$exf = \frac{M_1 - M_3}{M_1}$$

**Eq. 3.3-2**

where  $M_1$  is the dosed mass of tracer for the indicator signal [kg];  $M_3$  is the tracer mass at the end of the investigated reach reduced of the losses due to the exfiltrations [kg],  $M_3$  can be calculated integrating the conductivity peak, if salt is used as a chemical tracer, measured at the end of the investigated reach:

$$M_3 = \int_{t=startIpeak}^{t=endIpeak} e \times Q(t) \times (C_{ind}(t) - C_{bl}(t)) dt$$

**Eq. 3.3-3**

where  $e$  is the calibration coefficient [ $\text{gr NaCl cm } \mu\text{S}^{-1}$ ];  $Q(t)$  is the flow rate during the indicator passage [ $\text{m}^3 \text{s}^{-1}$ ];  $C_{ind}(t)$  is the conductivity of wastewater stream during the indicator passage at the measuring manhole [ $\mu\text{S cm}^{-1}$ ];  $C_{bl}$  is the natural conductivity of the wastewater stream during the indicator passage, which has to be estimated by a linear or nonlinear regression [ $\mu\text{S cm}^{-1}$ ];  $t_{end(start)I_{peak}}$  is time of the end (beginning) of the indicator peak. The  $Q(t)$  can be estimated by an flowmeter or by a reference peaks. In the first case, for an uncertainty analysis we must consider the uncertainty affecting the flow measurements by means of flowmeter. In our case, an area velocity system SIGMA900 MAX has been used, and the errors are:

- random error for the velocity:  $\pm 2\%$  the measured velocity;

- random error for the level:  $\pm 0.00346$  [m];
- systematic error for the level:  $\pm 0.01156$  [m];
- errors for an incorrect installation;
- disturbances from solid matter in the wastewater stream like: toilet paper, plastic etc...

In the second case, the uncertainty affecting the flow rate value can be estimated as for the uncertainty affecting  $M_3$  and it is discussed below. A correlation between some flow rate values measured with the flowmeter and those calculated from the reference peaks is given in Fig. 3.3.1, the correlation coefficient is 0.45, this could be mean a low precision of either flowmeter either reference peak. Nevertheless, as the exfiltration ratio calculated using data from flow meter were unreliable we have decided to use for exfiltration ratio calculation the flow rate data estimated from reference peak integration.

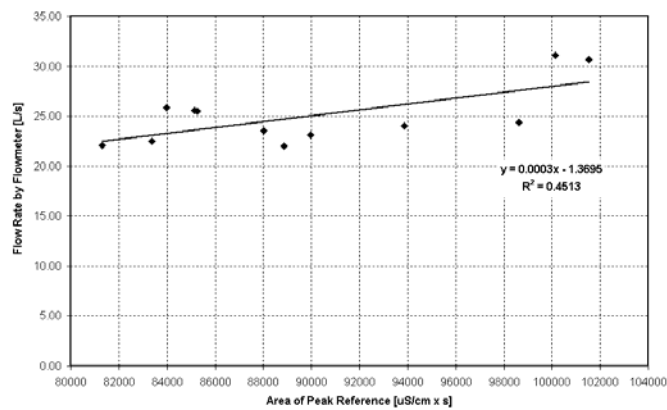


**Fig. 3.3.1: Correlation between the measured flow rate and the area of the reference peaks.**

Considering Eq. 3.3-3, the Eq. 3.3-2 becomes:

$$exf = 1 - \frac{\int_{t=startIpeak}^{t=endIpeak} e \times Q(t) \times (C_{Ind}(t) - C_{bl}(t)) dt}{M_1} * 100$$

**Eq. 3.3-4**

If the flow rate during the indicator passage is calculated from the reference peak integration (i.e., dilution method for flow rate estimation) the Eq. 3.3-4 becomes:

$$exf = 1 - \frac{M_2 \int_{t=startIpeak}^{t=endIpeak} e'(C_{Ind}(t) - C_{bl}(t))dt}{M_1 \int_{t=startRpeak}^{t=endRpeak} e(C_{Ref}(t) - C_{bl}(t))dt} * 100$$

**Eq. 3.3-5**

where  $M_2$  is the dosed mass of tracer for the reference signal [kg];  $e'$  is the calibration coefficient [gr NaCl cm  $\mu S^{-1}$ ];  $C_{ind}(t)$  is the conductivity of wastewater stream during the reference passage at the measuring manhole [ $\mu S$  cm $^{-1}$ ];  $C_{bl}$  is the natural conductivity of the wastewater stream during the reference passage which has to be estimated by a linear or nonlinear regression [ $\mu S$  cm $^{-1}$ ];  $t_{end(start)R_{peak}}$  is the time of the end (beginning) of the reference peak.

The Eq. 3.3-5 gives us a more accurate exfiltration ratio if:

- the same equipments are used for measuring the conductivity of both reference and indicator peaks;
- the values of the calibration coefficient are the same;
- the reference and indicator tracer solutions are prepared by the same equipments;
- the reference and the indicator peaks are as closer as possible to each other.

As the systematic errors affecting the numerator and the denominator are the same and then the propagated systematic errors into the results are minimized (Chrakroun et al., 1993).

The estimation of  $e$  serves for transforming the conductivity values in concentrations of NaCl.  $e$  has been estimated in laboratory adding known amounts of NaCl in a wastewater sample taken from the sewer to be investigated. In Fig. 3.3.2 an example of calibration curve is shown.

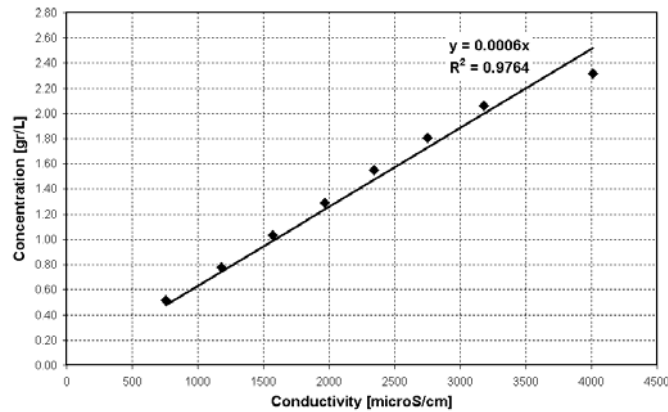


**Fig. 3.3.2: Calibration curve.** The conductivity values were corrected with the initial conductivity of the wastewater sample. The calculated calibration coefficient is 0.0006 [gr NaCl\*L $^{-1}$ / $\mu S$ \*cm $^{-1}$ ].

The  $e'$  and the  $e$  values are equal if the conductivities of the reference and the indicator peaks vary in the same interval over the calibration line.

Finally, the QUEST method can be applied in two different ways:

- not allowing the reference and the indicator conductivity peaks to overlap each other;
- allowing the overlapping.

In the first case, the advantage is that peaks are very distinguishable and the model is linear. The disadvantage is that the reference and the indicator peaks are not close to each other, then the flow value estimated from the reference peak could be quite unrepresentative of the flow during the passage of the indicator peak. The reduction of the distance between the peaks has to be carefully planned with preliminary investigations of the travel time.

In the second case the disadvantages are: the model is non-linear ( $C_{bl} = f(t)$ ,  $C_{ind} = f(M_1, t, C_{bl})$  and  $C_{ref} = f(M_2, t, C_{bl}, C_{ind})$ ) and reference and indicator peaks are to be distinguished using known peak formulae. The advantage is that the reference and the indicator peaks are very close to each other, and then the flow value estimated by the reference peak is more representative of the flow corresponding to the passage of the indicator peak than the previous case.

### ***3.3.1 Detailed uncertainty analysis***

Before the application of the QUEST method a detailed uncertainty analysis was carried out in order to plan accurately the experiments and for investigating if the tests were feasible with the proposed model by means of those equipments and in that experimental area.

The most important sources of error during the whole experimental activity were individuated and they are summarised in the Tab. 3.3-1. In particular the errors can be divided into the three orders as below:

1. the Zeroth order errors: the systematic and the random errors due to conductivity measurement of wastewater;
2. the First order errors: the random error due to the baseline variability and the flow variability that affects the tracer transport;
3. the Nth order errors: conductivity probe installation, tracer preparation and dosage, tracer adsorption and data reduction.

**Tab. 3.3-1: sources of uncertainty for each variable in equation Eq. 3.3-1. R: random error; S: systematic error.**

	Tracer Preparation			In the Field		Data Reduction		
	<i>Weighing of tracer</i>	<i>Dilution</i>	<i>Dosage</i> <i>e</i>	<i>Transport</i>	<i>Adsorption</i>	<i>Conductivity Measurements</i>	<i>Baseline fitting</i>	<i>Integration or Data Regression</i>
$M_1$	R		R					
$M_2$	R		R					
$C_{bl\_ref}$						R	R	
$C_{bl\_ind}$						R	R	
$C_{ref}$				S	R	R	R	R
$C_{Ind}$				S	R	R	R	R
$e$	R	R				R		S

The paragraphs below discuss the applied methodology for quantifying the uncertainty from every source shown in Tab. 3.3-1.

### 3.3.1.1 Preparation

Regarding to the preparation of the solution of NaCl to be dosed into the sewer pipe under investigation and for estimating the calibration values ( $e$  and  $e'$ ) in the equation Eq. 3.3-1, the random errors are principally due to:

- scale for weighting the solid tracer (i.e.: NaBr and CILi);
- graduated flask for the dilution of the solid tracer;
- human.

The used scale (trade Sartorius mod. BL1500) had an accuracy of  $\pm 0.1$  gr. The graduated flask had an accuracy of  $\pm 0.4$  mL at  $20^\circ\text{C}$ .

The error from the scale and human affect the mass of tracer dosed, because we don't care about the dilution, whereas every sources affect the calibration coefficient value. Nevertheless, if the conductivities of the indicator and the reference peak vary into a small range over the calibration line they are cross out in Eq. 3.3-5.

### 3.3.1.2 Field application

#### *Dosage*

The dosage of the tracer solutions were done injecting rapidly known mass of tracer (slug injection), then the error could be just human error due to not complete discharge of the tank containing the tracer solution. In particular, the injection was done by means of a funnel joint to a plastic tube long like the depth of the sewer invert level at the dosage manhole (Fig. 3.3.1).



Fig. 3.3.3: system used for dosing the tracer solution.

#### *Adsorption*

The tracer could be adsorbed onto the surface of:

- the suspended matter in the wastewater stream;
- the vegetation like as roots;
- solid deposits.

This losses, which are not proportional to the water leakages, could cause an overestimation of the exfiltration ratio. During the transport from the dosage manhole up to the sampling one, the tracer can be adsorbed on the solid matter in the sewer stream and on the biofilm that grows on the sewer wall. No estimations have been one.

#### *Transport*

The tracer transport is widely discussed in the chapter 2 from a theoretical point of view, while in this paragraph the reliability of the exfiltration ratio estimated over a sewer network is

discussed, and a mathematical approach for carrying out the experiments correctly in an urban sewer network, and an example of application has been published in the following paper:

Giulianelli, M.; Mazza, M.; Prigiobbe, V.; Russo, F. (2003). Assessing exfiltration in a urban sewer by slug dosing of chemical tracer (NaCl). Proceeding of a Workshop organized by NATO ARW on Enhancing Urban Environment, Rome, Italy, Nov. 5-9, 2003.

See annex 3.

### ***Conductivity measurements***

The errors during the measurements are of zeroth, first and Nth order. The zeroth order errors are due to the precision and accuracy of the equipments itself, the first order errors are due to the temporal variability of the measured parameters and, finally, the Nth order errors are due to the wrong installation. In order to minimize the Nth order errors, the conductivity probe (if NaCl is used as a tracer) has to be fixed after the vertical and transversal mixing have been completed.

During the experiments, the water depth changed between 5 - 12 cm, and the water width changed between 0.75 – 1.3 m in the investigated reach in Torraccia catchment. In Fig. 3.3.4, the relationship between the water depth and the water width is given. Nevertheless, as a rule of thumb for non-buoyant tracers a recommended mixing length in river would be  $(100 \div 300) d$  ( $d$  [m] is water width) (Rutherford, 1994) when the tracer is dosed in the mid-channel, and for the investigated reaches the minimum mixing lengths changed between 75 m and 130 m.

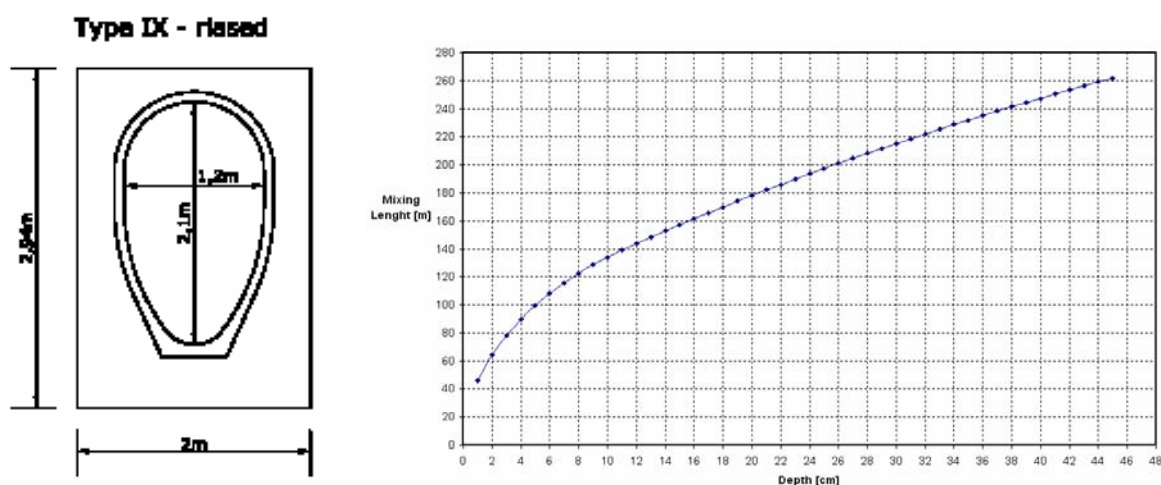


Fig. 3.3.4: Right: egg-shaped cross section of the investigated reach. Left: mixing length vs. water depth.

## ***Data reduction***

The errors due to the data reduction consist of baseline fitting and peak integration.

### **Baseline fitting**

The baseline fitting was approached with three different models: linear, squared and cubic. The linear one was the best fitting, because of the low variability of the natural conductivity of wastewater. One hundred data points have been chosen before and after each conductivity peak, because 100 has been estimated as the optimum for an accurate regression and acceptable time distance between the peaks. The routine for the baseline regression has been written in R-script and an example of baseline regression is given in the Fig. 3.3.5.

The used formula for estimating the standard error of the linear regression was by Montgomery and Peck (1992):

$$\sigma = \left[ \frac{\sum_{i=1}^N (Y_i - mX_i - c)^2}{N - 2} \right]^{1/2}$$

**Eq. 3.3-6**

where  $Y_i$  and  $X_i$  are the data pairs;  $m$  is the slope and  $c$  the intercept of the linear regression.

### **Peak integration**

The integration of the peaks has two main sources of uncertainty:

1. baseline trend under the peak;
2. location of the start and point of the peaks.

Start and of the end have been manually done located; in particular. Larger is the peak due to the dispersion, higher is the uncertainty in the definition of the start and the end point of the peak. For the reference peak, which has the shortest tail, the integration is less sensitive to the definition of the start and the end of the peak, instead for the indicator peak that is usually with longer tail the start and the end uncertainty could affect the peak integral. In the Fig. 3.3.7 the reference peaks are highlighted in green and the reference one in red.

## ***Error propagation for the detailed uncertainty analysis***

The error propagation for the detailed uncertainty analysis was carried out by a direct Monte Carlo Simulation (MCS). The Code develops as in Fig. 3.3.6, where NOP (Non



Overlapping Peak routine) is the routine where input data are uploaded and the parameters of the model are defined with normal distribution; Sysanal by Riechert (2001) does the MCS; Questnew by Rieckermann (2003) does the regression of the baseline and the separation of the peaks; Exfiltration calculates the exfiltration ratio. The routines written in R-script are included in this dissertation next.

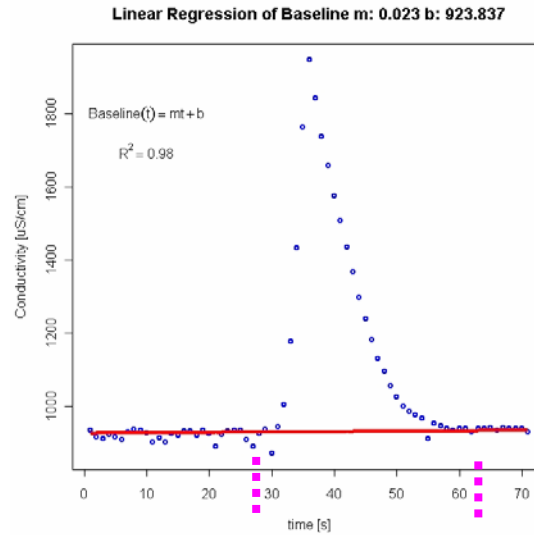


Fig. 3.3.5: Linear regression of the baseline for non-overlapping peak QUEST method (red line) and definition of the start and end of the peak (pink dot line).

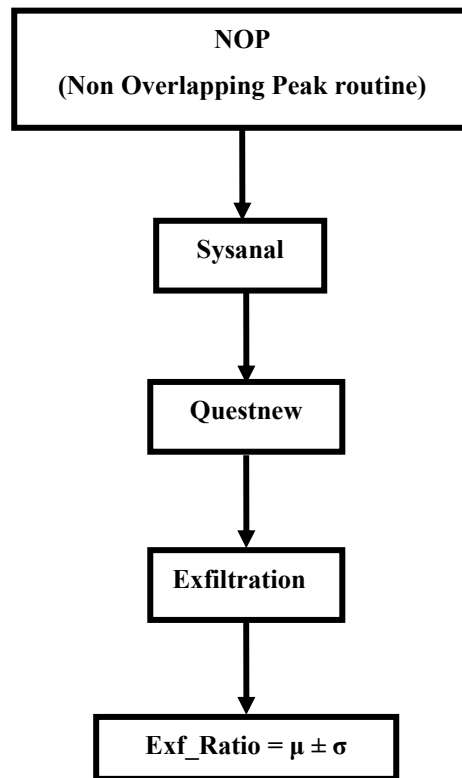


Fig. 3.3.6: Architecture of the routines for error propagation written in R-script environment.

### 3.3.2 Results of Detailed Uncertainty Analysis

Writing the Eq. 3.3-5 in a simpler way:

$$exf = 1 - \frac{M_2 * AreaPeak_1}{M_1 * AreaPeaks_2}$$

Eq. 3.3-7

where AreaPeak1 is the area under the Indicator peak;  $\overline{AreaPeaks_2}$  is the average area under the four References peaks (in green line in the Fig. 3.3.7) placed two immediately before and two immediately after the Indicator peak (in red line in the Fig. 3.3.7). Given the values of each source of uncertainty is in Tab. 3.3-2.

Among the experiments only five have been correctly carried out because:

1. the peaks were no-overlapped and close each other enough;
2. the mixing distance for the reference tracer dosed was correctly calculated;
3. the natural conductivity of wastewater during the experiment was not too high variable.

Five experiments were selected and the error propagation was carried out. The characteristics of the experiments and the calculated exfiltration are in the Tab. 3.3-3 and an example of the result representation is in Fig. 3.3.8.

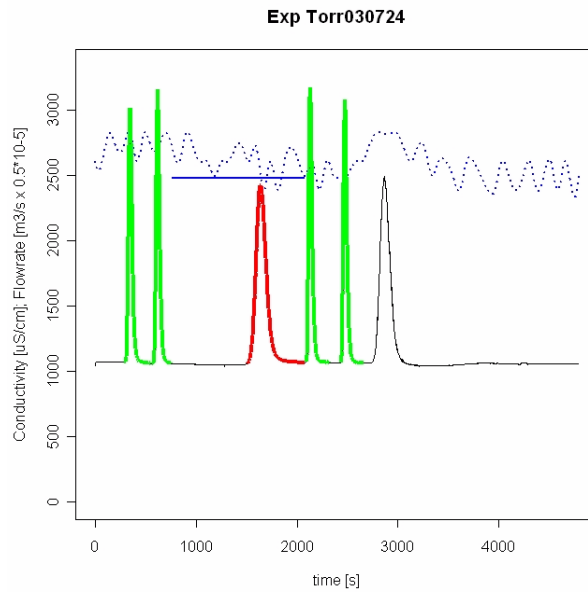


**Fig. 3.3.7: Conductivity peaks in green line the Reference ones and the Indicator one in red line.**

**Tab. 3.3-2: Values of the errors occurring during the QUEST method application.**

	Preparation			In the field		Data reduction		
	Weighing of tracer [gr]	Dilution [mL]	Dosage [gr]	Transport	Adsorption [gr]	Conductivity Measurements [%]	Baseline fitting	Peak fitting or regression
<b>M1</b>	±0.1	±0.4	0.0					
<b>M2</b>	±0.1	±0.4	0.0					
<b>Cbl_ref</b>						±0.5	S and R	
<b>Cbl_ind</b>						±0.5	S and R	
<b>Cref</b>				R	0.0	±0.5	S and R	From visual analysis
<b>CInd</b>				R	0.0	±0.5	S and R	From visual analysis
<b>e</b>	±0.1	±0.4				±0.5		R

**Tab. 3.3-3: Characteristic of the QUEST experiments.**

Experiment	Investigated length [m]	Duration [s]	Flowrate [L s <sup>-1</sup> ]	mean Exf. Ratio [%]	Coverage of the ground and backfilling
030710T	800	2000	10.63±0.50	7.11±0.02	Grass, concrete backfilling
030724T	800	2000	12.50±0.51	0.09±0.19	Idem
030730T	800	2000	12.48±0.45	5.94±0.41	Idem
040616T	400	4000	8.48±0.45	-1.73 ±4.69	Idem
040408I	1500	9000	22.59±0.45	1.66±0.11	Road, gravel backfilling

The exfiltration ratio calculated for the experiments called #T were carried out upon similar sewer pipes in terms of material, age, loads. Nevertheless, the exfiltration ratios change between -1.73 and 7.11 %, whereas the expected results were zero, then the method seem to be not accurate. Whereas the precision is less ten one, excepted for the experiment 040616T. On the contrary, the exfiltration calculated for the experiment 040408I confirms the expectation, because the investigated reach was submerged with groundwater and the expected result was zero.

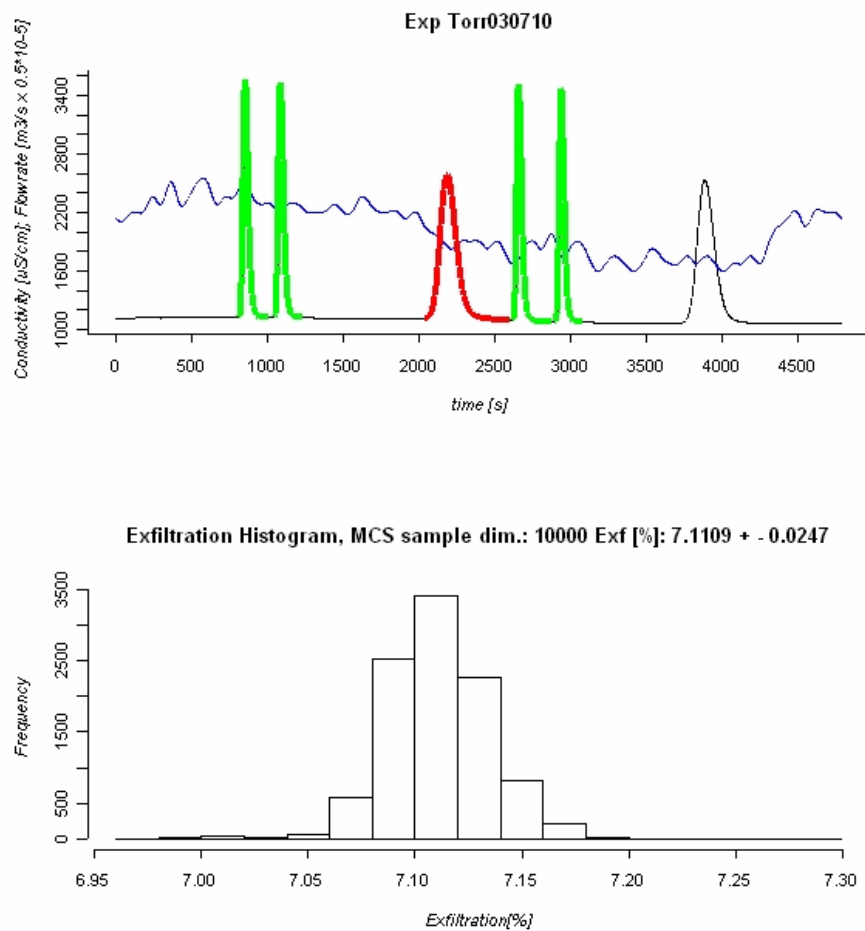


**Fig. 3.3.8: Conductivity and flow rate data of the experiment 030710T and the exfiltration histogram after the error propagation. Reference peaks (green lines), Indicator peaks (red lines), flowrate (blue lines); Exfiltration histogram for a sample size of 10,000.**

The routine use for the error propagation is enclosed below.

```
# INTEGRATION of Reference and Indicator peaks
```

```
#=====
```

```
# This routine calculates the area of peak after random sampling of parameter values.
```

```
# The parameters of model are the values affected by uncertainty, i.e.: conc, Q.meas,
```

```
# dosed mass, start and end of the peak and points for the baseline regression,
```

```
# (IDEA : it is distinguished the random error from the systematic error and the uncertainty takes in account both!!)
```

```
#Created    [031009]
```

```
#Last updated [031202]
```

```
#=====
```

```
# temporary experiment: 160604 Torraccia
```

```
rm(list=ls())
```

```
# set working directory
```

```
#=====
```

```
if(T)
```

```
{
```

```
setwd("C:\\Valentina_2004\\IRSA\\Exfiltration\\QUEST\\Exp2004\\Torraccia\\ExpTorr160604\\Data")
```

```

# set peakfit directory
# =====

source("C:/Valentina_2004/IRSA/Exfiltration/QUEST/Exp2003/R-Script/SimR_0903/libraries/sysanal_integrnop.r")
source("C:/Valentina_2004/IRSA/Exfiltration/QUEST/Exp2003/R-Script/SimR_0903/libraries/Questnew_v2.r")
source("C:/Valentina_2004/IRSA/Exfiltration/QUEST/Exp2003/R-Script/SimR_0903/libraries/Exfiltration.r")

# read data:
# =====

conc  <- read.csv("datacond.csv",header=TRUE,sep=";")
Q.meas <- read.csv("dataflow.csv",header=TRUE,sep=";")
}

# ===== INPUT PART =====

# time of the peak:
# =====

experiments <- matrix(c(0,1685))
time.ref.mean      <- c(415,630) # true values
time.ref.stdev     <- c(1,1)      # Random + Systematic uncertainty
time.ind.mean      <- c(730,1120) # true values
time.ind.stdev     <- c(1,1)

```

```

# regression time definition
# =====
time.regr.ref.bl.mean  <- c(10,10)          # true values
time.regr.ref.bl.stdev <- c(1,1)
time.regr.ind.bl.mean  <- c(10,10)          # true values
time.regr.ind.bl.stdev <- c(1,1)

# dosed mass definition -> Systematic Uncertainty
# =====
ref.ms.mean  <- c(650)          #true values [g NaCl]
ref.ms.stdev  <- c(0.002)        # balance uncertainty times cilinder one
n.ref <- length(ref.ms.mean)
ind.ms.mean  <- c(1300)          # [g NaCl]
ind.ms.stdev  <- c(0.002)
n.ind <- length(ind.ms.mean)

# parameter definition-> Systematic Uncertainty
# =====
e.mean  <- -0.0004              #Calibration parameter:  $y[\text{gr/L}] = 0.0006 * x[\text{umS/cm}]$ 
e.stdev <- -0.00002

```

```

# ===== END INPUT PART.
# Peak parameters sequence and Sampling
# =====

par.vector.mean <-c(e.mean,time.ref.mean,time.ind.mean,time.regr.ref.bl.mean,time.regr.ind.bl.mean,ref.ms.mean,ind.ms.mean)
names(par.vector.mean)<-
c("e.mean1",paste("time.ref.mean",1:length(c(time.ref.mean)),sep=""),paste("time.ind.mean",1:length(c(time.ind.mean)),sep=""),paste("time.regr.ref.bl.mean",1:length(c(time.regr.ref.bl.mean)),sep=""),
paste("time.regr.ind.bl.mean",1:length(c(time.regr.ind.bl.mean)),sep=""),paste("ref.ms.mean",1:length(c(ref.ms.mean)),sep=""),"ind.ms.mean1")
par.vector.stdev <-c(e.stdev,time.ref.stdev,time.ind.stdev,time.regr.ref.bl.stdev,time.regr.ind.bl.stdev,ref.ms.stdev,ind.ms.stdev)
names(par.vector.stdev)<-
c("e.stdev1",paste("time.ref.stdev",1:length(c(time.ref.stdev)),sep=""),paste("time.ind.stdev",1:length(c(time.ind.stdev)),sep=""),paste("time.regr.ref.bl.stdev",1:length(c(time.regr.ref.bl.stdev)),sep=""),
paste("time.regr.ind.bl.stdev",1:length(c(time.regr.ind.bl.stdev)),sep=""),paste("ref.ms.stdev",1:length(c(ref.ms.stdev)),sep=""),"ind.ms.stdev1")
samp.size <- 10000
corr <-diag(rep(1,length(c(par.vector.mean))))
dist <- "normal"
sensitivity <- "1" # switch to set on local (0) or global (1) sensitivity
{
if (sensitivity == "1")
{
vectors <- randsamp(samp.size,par.vector.mean,par.vector.stdev,corr,dist)
samp <- vectors$sample
# Monte Carlo Simulation

```



```

samp[,2:length(par.vector.mean)] <- round(vectors$sample[,2:length(par.vector.mean)],0)
}
else
{
  # fix by # the stand. dev. of parameter to process for sens. anal.
  #e.stdev1<-0;
  time.ref.stdev1<-0;
  time.ref.stdev2<-0;
  time.ref.stdev3<-0;
  time.ref.stdev4<-0;
  time.ref.stdev5<-0;
  time.ref.stdev6<-0;
  time.ref.stdev7<-0;
  time.ref.stdev8<-0;
  time.ind.stdev1<-0;
  time.ind.stdev2<-0;
  time.regr.ref.bl.stdev1<-0;
  time.regr.ref.bl.stdev2<-0;
  time.regr.ref.bl.stdev3<-0;
  time.regr.ref.bl.stdev4<-0;
  time.regr.ref.bl.stdev5<-0;
  time.regr.ref.bl.stdev6<-0;

```

```

time.regr.ref.bl.stdev7<-0;
time.regr.ref.bl.stdev8<-0;
time.regr.ind.bl.stdev1<-0;
time.regr.ind.bl.stdev2<-0;
ref.ms.stdev1<-0;
ref.ms.stdev2<-0;
ref.ms.stdev3<-0;
ref.ms.stdev4<-0;
ind.ms.stdev1<-0;
vectors    <-randsamp(samp.size,par.vector.mean,par.vector.stdev,corr,dist)
samp       <-vectors$sample
samp[,2:length(par.vector.mean)] <- round(vectors$sample[,2:length(par.vector.mean)],0)
      }

samp
}

# Composition of vector for exfiltration estimate
# =====
n.peak    <- length(c(time.ref.mean)/2)+length(c(time.ind.mean)/2)
exf.rate<-numeric(samp.size)
for ( f in 1:samp.size)
{
  par.vector.exf<-samp[f,] # here I should put out to reduce the time for the runs !!!!

```

```

e<-par.vector.exf[1]
time.ref<-par.vector.exf[(1+1):(length(c(time.ref.mean))+1)]
offset1<-length(c(time.ref.mean))+1
time.ind<-par.vector.exf[(1+offset1):(offset1+length(c(time.ind.mean)))]
offset2<-offset1+length(c(time.ind.mean))
time.regr.ref.bl<-par.vector.exf[(1+offset2):(offset2+length(c(time.regr.ref.bl.mean)))]
offset3<-offset2+length(c(time.regr.ref.bl.mean))
time.regr.ind.bl<-par.vector.exf[(offset3+1):(offset3+length(c(time.regr.ind.bl.mean)))]
offset4<-offset3+length(c(time.regr.ind.bl))
ref.ms<-par.vector.exf[(offset4+1):(offset4+length(c(ref.ms.mean)))]
offset5<-offset4+length(c(ref.ms.mean))
ind.ms<-par.vector.exf[(1+offset5):(offset5+length(c(ind.ms.mean)))]
# Model Definition and Exfiltration estimate
# =====
#type.flow\#base.shape
# first
#linear   Model 1
#mean     Model 2
#measured Model 3
#scaled
#K-mean   Model 4
#K-spline Model 5

```

```

# =====
base.shape    <-"first"
type.flow     <-"mean"  # how consider the flow for exf calculation
method        <-"mean"  #"mean", "spline", etc., this command is remarkable only for type.flow <-"forth"  # Exfiltration estimate
# =====

# read data:
# =====

Q.meas <- read.csv("dataflow.csv",header=TRUE,sep=";") #read flowrate data, they are measured every minute, so a generation of fictive data is
necessary in ordet to have a vector with the same lenght of concentration one

Q<-conc
x<-Q.meas[,1]
y<-Q.meas[,2]
Q.meas.spline<-spline(x,y,n=length(conc[,2]))
Q[,2]<-Q.meas.spline$y
names(Q)[2]<- "discharge"      #Interval of peak to fit
# =====

indicator <- 1 #which indicator pulse to analyse. This value is used to identify the colomn in "experiment" containing
               #the intervall to analyse (see row 100)


#masses of reference pulses
# =====

```

```

n.ref <- length(ref.ms)      #masses of indicator pulses
#=====

n.ind <-length(ind.ms)      #starting and ending times of reference pulses
#=====

dim(time.ref) <- c(2,length(time.ref)/2)

peak.ref    <-as.list(rep(0,n.ref))    #starting and ending times of indicator pulses
#=====

dim(time.ind)    <- c(2,length(time.ind)/2)    #create list of tracer masses
#=====


tracer.mass<-list(ref.ms=ref.ms,ind.ms=ind.ms)    #here there is a list consisting in two lines: the first of mass data with number equal to
Reference Pulse one

                                     #the second of mass data number of data equal to Reference Pulse one


#baseline separation of reference peaks
#=====


subdivision      <-100000      # maximum subdivision for the integration
ref.pulses       <-as.list(rep(0,n.ref)) #a list of numerical values is create to store the data of Ref. calculation
#kt.Q.meas       <-as.list(rep(0,n.ref))
#time.regr.ref.bl1<-time.regr.ref.bl
time.regr.ref.bl1<-matrix(time.regr.ref.bl,2,length(time.regr.ref.bl)/2)

```

```

for(i in 1:n.ref)
{
  mass          <- ref.ms[i]
  data          <- baseline.sep(conc,Q,round(time.ref[,i],0),round(time.regr.ref.bl1[,i],0),base.shape)
  data$C.pulse  <- as.numeric(data$C.pulse)
  Area          <- C.integrate(data$t.meas,data$C.pulse,subdivision)[1:2] #"[1:2]": pass only "value" and "abs. error" of numerical
integration
  Q.tracer      <- mass/(e*(Area$value))
  kt.Q.meas     <- corr.factor(mass,Area,time.ref[,i],Q,e)
  ref.pulses[[i]] <- list(mass=mass,data=data,Area=Area,Q.tracer=Q.tracer,k.t=kt.Q.meas$k.t,Q.meas=kt.Q.meas$Q.flowmeas.mean)
}

# Calculation of flow rate
#=====
Q.Ref      <-rep(0,n.ref)
k          <-numeric(n.ref)
t.kt       <-numeric(n.ref)
Q.kt       <-numeric(n.ref)
t.mean.Q   <-numeric(n.ref)

for (i in 1:n.ref)

```

```

{
  Q.Ref[i] <-ref.pulses[[i]]$Q.tracer
  k[i] <-ref.pulses[[i]]$k.t
  t.mean.Q[i] <-mean(time.ref[1,i]:time.ref[2,i])
  Q.kt[i] <-Q[t.mean.Q[i],2] #They are four values of flow measured in the middle of reference span
}
for (i in 1:n.ind)
{
  Flow<-
  regr.flow(Q.Ref,type.flow,conc,round(time.ind,0),n.ind,n.ref,Q,k,round(time.regr.ind.bl,0),method,e,Q.kt,t.mean.Q,time.ref)#,time.peak.ref)
  length.vector <- time.ind[2,i]-time.ind[1,i]+1+time.regr.ind.bl[1]+time.regr.ind.bl[2] #2*time.regr.ind.bl so C.pulse and Q.corrected have
the same length
  Q.corrected <- numeric(2*length.vector)
  dim(Q.corrected) <- c(length(Q.corrected)/2,2)
  start.Q <- time.ind[1,i]-time.regr.ind.bl[1]
  end.Q <- time.ind[2,i]+time.regr.ind.bl[2]
  Q.corrected[,1] <- start.Q:end.Q
}
flow$Q.regr
for (i in 1:length.vector)
{
  Q.corrected[i,2] <-flow$Q.regr[[i]]

```

```

}
#baseline separation of indicator peaks
#=====
ind.pulses      <- as.list(rep(0,n.ind)) #a list is create to store the data of Ind. calculation
  for(i in 1:n.ind)
  {
    names(ind.pulses)[i]  <- paste("ind.pulse",i, sep="")
    mass                  <- ind.ms[i]
    data                  <- baseline.sep(conc,Q,round(time.ind[,i],0),round(time.regr.ind.bl,0),base.shape)
    ind.pulses[[i]]      <- list(mass=mass,data=data)
  }
#compute exfiltration for each indicator pulse
#=====
  for(j in 1:n.ind)
  {
    start.C              <-time.ind[1,j]
    end.C                 <-time.ind[2,j]
    range                 <- 1:length(Q.corrected[,1])
    load.tointegrate      <-rep(0,length(range))
    load.tointegrate      <-ind.pulses[[j]]$data$C.pulse*Q.corrected[,2] # the problem is the different lenght of vector!!!
    Area                  <- sum (load.tointegrate)
    exfiltration          <- (1-(e*Area/ind.ms[j]))*100
  }

```



```

}
# Plot
# =====
range<-c(conc[1,1],conc[(length(conc[,2])-1),1])
Q.plot      <-Q[,2]
plot.sc.factor <-max(conc[range,2])/max(Q[range,2])
plot(conc,type="l",xlab="time                [s]",ylab="Conductivity                [microS/cm]                and                Flowrate
[L/s]",ylim=c(0,1.05*max(conc[range[1]:range[2],2])),main=paste("Peaks of Reference and Indicator Pulses and Flowrate"))
lines(Q.plot*plot.sc.factor*2.5,col="blue",lty=3,lwd=2)
lines(conc[time.ind[1,1]:time.ind[2,1],,],col="red",lwd=4)
lines(Q.corrected[,1],Q.corrected[,2]*plot.sc.factor*2.5,col="blue",lwd=2) #here flow rate from regression is plotted
for (i in 1:n.ref)
{
  lines(conc[time.ref[1,i]:time.ref[2,i],,],col="green",lwd=4)                #here reference peaks are coloured
}
# output of results
# =====
exf.rate[f]<-exfiltration
}
exf.rate # Uncertainty Analysis
# =====

```

```

E<- mean(exf.rate)
V<-var(exf.rate)
U<-2*V          # Uncertainty for sample > 10
print(paste("Exfiltration Mean :", round(E,2)," %",sep=""))
print(paste("Exfiltration Uncertainty :", round(U,2)," %",sep=""))
# plot
# ====
opar<-par()
  par(mfcol = c(2, 1),font.main=2,font.lab=3,cex=0.7,lab=c(8,10,20),mgp=c(3,1,0),mai=c(1,1,0.7,0.7),bty="l")
  plot(conc,type="l",xlab="time [s]",ylab="Conductivity [microS/cm] and Flowrate [L/s]",main=paste("Peaks of Reference and Indicator Pulses
and Flowrate"))
  lines(Q.plot*plot.sc.factor*2,col="blue",lty=3,lwd=2)
  lines(conc[time.ind[1,1]:time.ind[2,1],],col="red",lwd=4)
  lines(Q.corrected[,1],Q.corrected[,2]*plot.sc.factor*2.5,col="blue",lwd=2)    #here flow rate from regression is plotted
  for (i in 1:n.ref)
  {
    lines(conc[time.ref[1,i]:time.ref[2,i],],col="green",lwd=4)          #here reference peaks are coloured
  }
hist(exf.rate,xlab="exf [%]",ylab="frequencies",main=paste("Histogram of the frequencies of exfiltration ratio - sample dim.:",samp.size))
par(opar)
# end

```

### 3.4 QUEST-C

For the application of this method, a general uncertainty analysis was approached, it does not distinguish random and systematic errors and consider the covariance terms zero. The results are have been published in the following paper:

Prigiobbe, V.; Giulianelli, M. (2004). Experiment design of a novel method to assess exfiltration in sewer. Conference on Urban Drainage Modelling, Dresden, 15th-17th September 2004.

See annex 4.

Then, a detailed uncertainty analysis has been approached in collaboration with EAWAG and the results have been published in the following paper:

Rieckermann, J.; Bareš, V.; Braun, D.; Kracht, O.; Prigiobbe, V.; Gujer, W. (2004). Assessing exfiltration from sewers with dynamic analysis of tracer experiments. 19th European Junior Scientist Workshop “Process data and integrated urban water modelling” France 11-14 March 2004.

See annex 5.

### **3.5 ISOTOPIC METHOD**

For the application of this method a detailed uncertainty analysis was approached, and a distinction between random and systematic errors was done and the covariance terms were considered zero. The study and the results of the detailed uncertainty analysis have been presented in the following paper:

Prigiobbe, V.; Giulianelli, M. (2005). Application of a novel method for assessing the infiltration in an urban sewer system: case of study in APUSS project. Proposed for Water Science and Technologies.

See annex 6.

## 3.6 POLLUTOGRAPH METHOD

The equation for assessing the infiltration ratio by pollutograph method using the COD as a parameter of interest is:

$$R_{\text{inf}}(t) = \frac{Q_{\text{infiltration}}(t)}{Q_{\text{wastewater}}(t)} = \frac{COD_{\text{foul}}(t) - COD_{\text{ww}}(t)}{COD_{\text{ww}}(t)}$$

**Eq. 3.6-1**

where  $COD_{\text{ww}}(t)$  is measured by an in-line spectrometer probe (see Chapter 2),  $COD_{\text{foul}}(t)$  is a Fourier function of the time because of its diurnal and weekly periodicity:

$$COD_{\text{foul}}(t) = \sum_{i=1}^N a_i \sin(\omega_i t + \phi_i)$$

**Eq. 3.6-2**

where  $a_i$ ,  $\omega_i$  and  $\phi_i$  are amplitude, frequency and phase of the function, respectively;  $N$  is the number of the function useful for the  $COD_{\text{foul}}$  model. These parameters can be estimated mathematically with a non-linear regression model.

The experimental campaigns carried out for quantifying the infiltration using this method have been divided into three phases:

1. preliminary measurements campaigns for understanding the evident disturbance for the measurements;
2. calibration campaigns for determining the correlation between COD measured by the probe and that with standard laboratory procedures;
3. measurements of infiltration.

### 3.6.1 Preliminary campaigns

The probe was mounted in sewer at the outlet of the urban sewer network draining Infernetto area. It was fixed to the sewer walls with chains, which allow it to float over the water surface. The probe was protected against any accidental hits covering it with cylindrical shaped rubber (Fig. 3.6.1).

The preliminary campaigns were carried out from 24th March 2004 to 15th May 2004 and the COD concentrations measured is shown in Fig. 3.6.2. The COD measurements were very disturbed and a drift appears after two days from the cleaning, despite of the automatic cleaning before every measurements with compressed air. The disturbances were mainly due to turbulences because the probe was installed at the weir discharging the wastewater into a big tank of a pumping station, while the drift was due to a biofilm growing up on the windows crossed by the UV-VIS ray is emitted. Then the probe was moved upstream where the flow appeared less turbulent and the windows were cleaned with alcohol solution (10% in weight) every two days. After these precautions, the measurement trend improved a lot as in

Fig. 3.6.3.



Fig. 3.6.1: s::can covering.

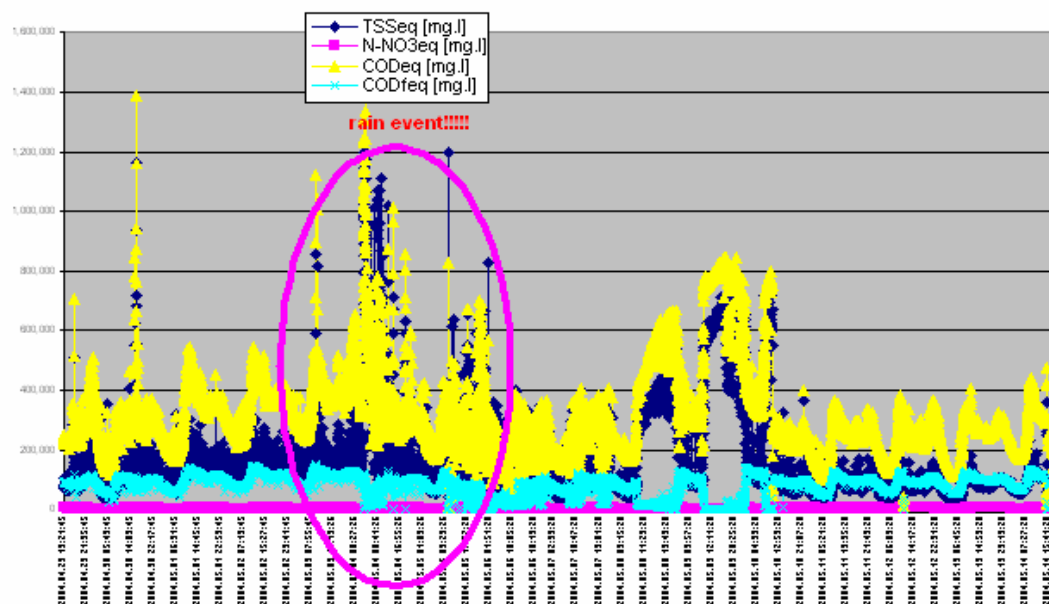


Fig. 3.6.2: Preliminary COD measurements.

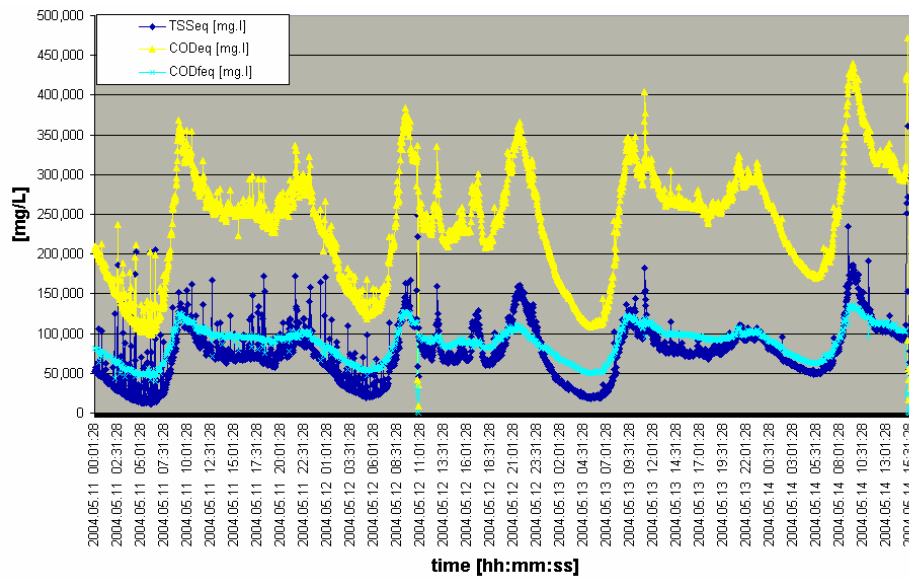


Fig. 3.6.3: COD measurements after changing sampling manhole and cleaning procedure.

### 3.6.2 Calibration and Infiltration Assessment

The calibration campaigns have been carried out on 10th October 2004 and on 20th November 2004, the data are shown in the Fig. 3.6.4. The reference COD in laboratory was measured using Merk Kit.

If data are fitted all together the calibration curve has a correlation coefficient 0.8815, whereas if the diurnal data (7:00am to 9:00pm) and nocturnal ones (10:00pm to 6:00am) are fitted separately the calibration curves have correlation coefficients 0.8013 and 0.9835, respectively (Fig. 3.6.5).

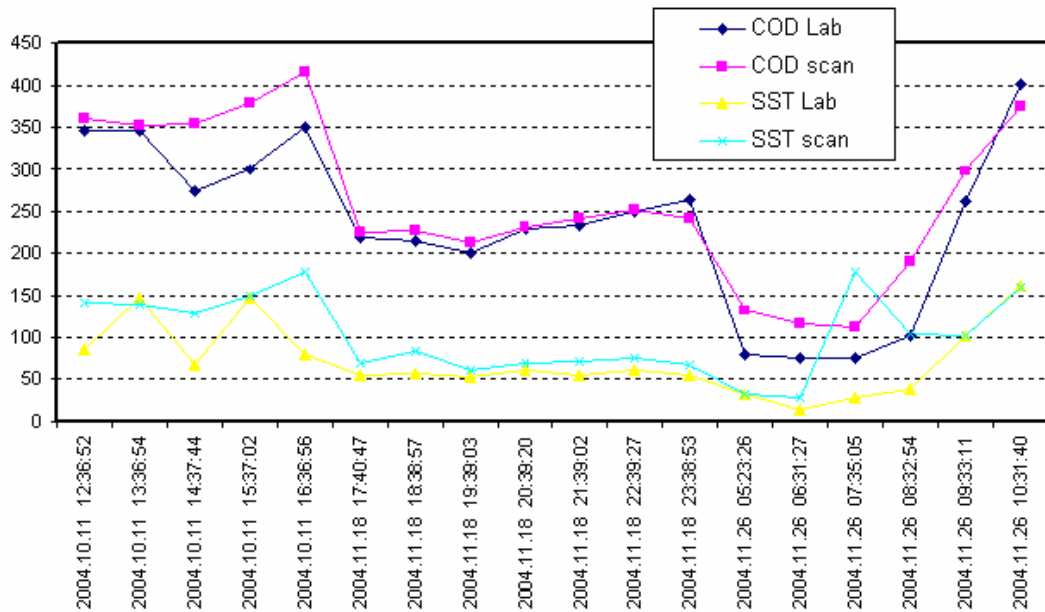


Fig. 3.6.4: COD time series for calibration of the spectrometer.

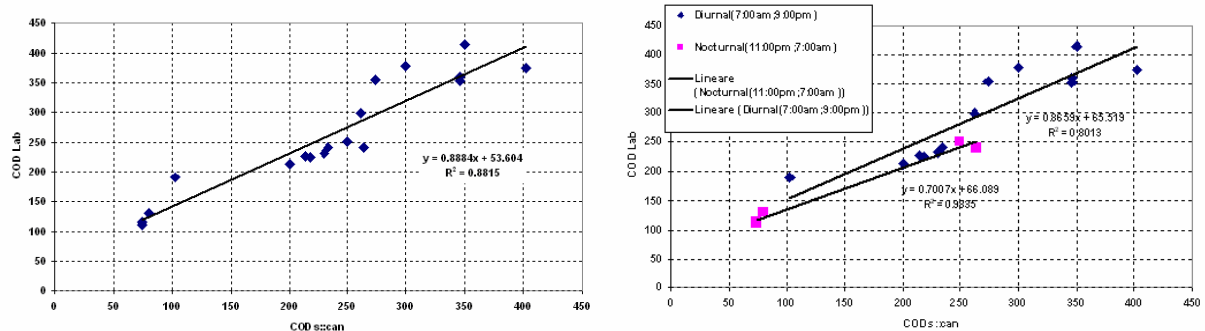


Fig. 3.6.5: COD from laboratory vs. COD from spectrometer and calibration curves.

The calibration curves can be summarized as followed:

Curve 1: all data fitted,  $COD_{lab} = 0.8884 COD_{spectr.} + 53.604$

Curve 2: diurnal data fitted,  $COD_{lab} = 0.8659 COD_{spectr.} + 65.519$

Curve 3: nocturnal data fitted,  $COD_{lab} = 0.7007 COD_{spectr.} + 66.089$

The COD data before calculating the infiltration ratio has been modified using the calibration curve 1 for both the diurnal and the nocturnal periods. The infiltration has been calculated using a routine written by Kracht (2004) in R-script that include a Monte Carlo simulation for the error propagation. The considered sources of errors concern the numerical parameter of the Fourier function (Eq. 3.6-2) used as a model for  $COD_{foul}(t)$ .

The infiltration ratio and rates are in Fig. 3.6.6.



Tab. 3.6-1 and the hydrograph separation estimated with this routine is displayed in the Fig. 3.6.6.

**Tab. 3.6-1 Infiltration ratio [-] and rate [L s<sup>-1</sup>] calculated after calibration of the measured COD**

	Min	1 <sup>st</sup> Quantile	Median	Mean	3 <sup>th</sup> Quantile	Max
<b>Infiltration ratio [-]</b>	0.3629	0.4842	0.5189	0.5227	0.5601	0.7198
<b>Infiltration rate [L s<sup>-1</sup>]</b>	58.62	78.21	83.81	84.42	90.46	116.26

data with calibration curve 1.

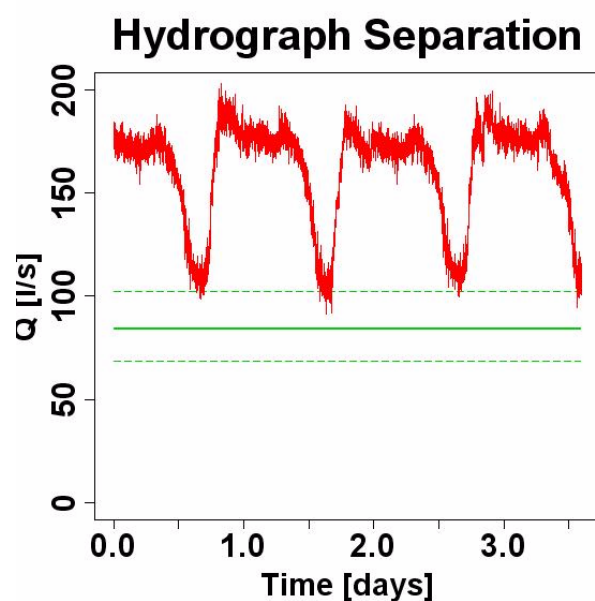


**Fig. 3.6.6 Hydrograph separation of the flows in Infernetto. In red the wastewater flow rate and in green the infiltration flow rate.**

### 3.7 References

Chakroun, W.; Taylor, R. P.; Steele, W. G.; Coleman, H. W. (1993). Bias Error Reduction Using Ratio to Baseline Experiments-Heat Transfer Case Study, *Journal of Thermophysics and Heat Transfer*, vol. 117, No. 4, Oct.-Dec. 1993, pp. 754-757.

Coleman, W. H., and Steele JR, W. G. (1999). *Experimentation and Uncertainty Analysis for Engineers- Second Edition*. John Wiley & Sons, INC., USA.

Montgomery, D.C., and Peck, E.A. (1992). *Introduction to linear regression analysis*. 2nd ed., Wiley, New York.

Oliphant, R. J. (1993). Identifying the long term research requirements of the water industry in the pipe technology area. UK: Foundation of water research FR 0406.

Reichert, P. (1994). AQUASIM – A tool for simulation and data analysis of aquatic systems. *Water Science and Technologies*, 30, pp. 21-30.

Rieckermann, J., and Gujer, W. (2002). Quantifying exfiltration from leaky sewers with artificial tracers. *Proceedings of the International Conference on "Sewer Operation and Maintenance 2002"*, Bradford, UK, 26-28 November 2002.

Rutherford, J.C. (1994). *River Mixing*. John Wiley & Sons, Chichester.

# Annex 1

Giulianelli, M.; Prigiobbe, V. (2004).  
Infiltrazione di acque di falda nelle fognature.  
L'ACQUA, 6, pp. 41-50.



Mario Giulianelli, Valentina Priglobbe\*

## INFILTRAZIONE DI ACQUE DI FALDA NELLE FOGNATURE URBANE

## INFILTRATION OF GROUNDWATER INTO URBAN SEWER SYSTEM

### Sommario

I fenomeni di infiltrazione delle acque parassite nelle reti di fognatura determinano in maniera diretta ed indiretta la contaminazione dell'ambiente idrico urbano superficiale, nonché problemi gestionali della rete di fognatura e degli impianti di depurazione. Il presente studio si sviluppa nell'ambito del progetto europeo APUSS (Assessing Infiltration and Exfiltration on the Performance of Urban Sewer Systems) il cui obiettivo è sviluppare nuovi metodi per quantificare le infiltrazioni e le esfiltrazioni nei sistemi fognari. L'IRSA-CNR, nell'ambito del progetto, deve validare in bacini urbani sperimentali i metodi di misura delle infiltrazioni ed esfiltrazioni messi a punto da altri partners del progetto.

Pur non essendo nuove le problematiche di infiltrazione ed esfiltrazione nelle infrastrutture di drenaggio urbano, il presente articolo introduce l'argomento secondo un approccio scientifico innovativo caratteristico del progetto APUSS che intende a mezzo di marcatori naturali valutare l'entità delle infiltrazioni e mediante traccianti chimici stimare le esfiltrazioni.

Nel presente articolo, dopo una generale trattazione dei principali fattori determinanti il deterioramento strutturale delle tubazioni fognarie, causa prima dei fenomeni in studio, vengono illustrati i primi risultati di alcune campagne di indagini di campo mirate all'individuazione della presenza di acque parassite (falda superficiale, sorgenti, perdite di acquedotto, ecc.).

Tali indagini consistettero nella caratterizzazione quali-quantitativa (COD, conducibilità, pH e portata) del refluo di una fognatura in un'area urbana sperimentale in condizioni di tempo asciutto. L'area in esame, denominata "Torraccia" è stata scelta per le sue caratteristiche ambientali e territoriali (urbanistica, geologia, idrogeologia, idrografia e pluviometria) ritenendola idonea allo studio che influenzano l'entità dei fenomeni in studio.

La scelta dell'area sperimentale in parola è stata determinata dalla disponibilità delle informazioni circa i principali parametri ambientali e territoriali (urbanistica, geologia, idrogeologia, idrografia e pluviometria) necessari alla caratterizzazione dell'area stessa nonché alla conduzione delle indagini di campo.

Le campagne sperimentali sono state condotte in diversi periodi stagionali al fine di evidenziare la variabilità stagionale le caratteristiche delle acque reflue in periodi di tempo asciutto da attribuire ad acque di infiltrazione di falda.

Parole chiave: Infiltrazioni, Fognature, Drenaggio urbano, Acque di falda.

### Summary

The Infiltrations of parasitical waters in the urban sewer system determine the contamination of the surface water body, as well as they cause some problems for the management of the sewer and the WWTPs.

The present study was carried out within the European Project APUSS (Assessing Infiltration and Exfiltration on the Performance of Urban Sewer Systems) that aims at developing new methods for quantifying the infiltrations and exfiltrations in urban sewer system. The objective of IRSA-CNR is to validate these methods applying them in the urban catchments.

Even if the problems concerning the not watertight are not new this paper brings up it following the scientific and the innovative approach that characterize the APUSS project. As a matter of the fact, the aims is to quantify the infiltrations by means of natural tracers and the exfiltrations by means of artificial chemical tracers in working sewer.

In this paper, after a brief introduction of the principal causes of the structural deterioration of the sewer pipes, which are the factor for the leakages and/or the infiltrations, the results of preliminary investigations for the application of a new method for infiltration quantification. In this preliminary study, the recording of discharge, COD, conductivity, pH during dry periods was carried out. The experiment was done in an urban catchment, called Torraccia, which was chosen because of its urbanity, geology, hydrogeology and hydrography as well as the infrastructures (sewer, street, etc.) that affect both the amount of infiltration and the experiment performances.

The experimental campaigns were carried out in different period of the year in order to highlight the season variability of the measured wastewater parameters thus to identify the more sensitive parameters to the infiltration.

Keywords: Infiltration, Sewer, Urban Drainage, Groundwater.

\* Mario Giulianelli, IRSA - CNR, Via Reno, 1 - 00198 Roma - Italia (m.giulianelli@irsa.rm.cnr.it); Valentina Priglobbe, Università degli Studi di Roma Tor Vergata - Roma - Italia (priglobbe@irsa.rm.cnr.it).

## 1. INTRODUZIONE

Il D.Lgs 152/99, che recepisce la direttiva europea sulle acque reflue 91/271, richiede che "La progettazione, la costruzione e la manutenzione delle reti fognarie si effettuano adottando le tecniche migliori che non comportino costi eccessivi, tenendo conto in particolare:

- a) del volume e delle caratteristiche delle acque reflue urbane;
- b) della prevenzione di eventuali fuoriuscite;
- c) della limitazione dell'inquinamento delle acque recipienti, dovuto a tracimazioni causate da piogge violente."

Il buon funzionamento di una rete di fognatura è di primaria importanza in una area urbana, infatti esso è critico e determinante sullo stato ecologico, economico e sociale tanto di una piccola quanto di una grande città. I fenomeni di infiltrazione ed exfiltrazione sono la conseguenza del cattivo stato di una fognatura, e più precisamente essi si manifestano quando la struttura fognaria perde la sua impermeabilità per effetto di fattori esterni e/o interni ad essa.

I principali fattori sono elencati secondo il seguente ordine di rilevanza:

- età della fognatura
- materiale di costruzione della fognatura
- dimensione delle tubazioni
- traffico stradale
- numero e tipo di connessioni delle abitazioni
- tipo di fognatura (mista o separata)
- regime delle portate transitorie
- livello della falda interessata dal tracciato fognario
- tipo di suolo circostante la tubazione
- profilo geometrico della rete
- presenza di sedimenti nella tubazione.

I sovraccarichi sul piano di calpestio possono generare crepe nelle pareti, collassi della tubazione; la consolidazione del terreno di posa può provocare cedimenti differenziali in diversi punti del tratto, l'età o la cattiva messa in opera dei manufatti può determinare difetti di tenuta delle giunzioni presenti tra tratti consecutivi, manufatti ed in corrispondenza degli allacci alle abitazioni. La perdita di tenuta può essere accertata mediante diversi metodi di indagine; usualmente essi sono eseguiti con ispezioni dirette laddove la grandezza dello specchio permette oppure mediante telecamere nei tratti di minore dimensione.

Se da un lato vi è il deterioramento strutturale che favorisce l'ingresso di acqua (Afflussi/Infiltrazioni, ovvero *Inflow/Infiltration*) e le perdite (Afflussi/Exfiltrazioni, ovvero *Inflow/Exfiltration*) dall'altro vi sono aspetti ambientali scatenanti il fenomeno che ne definiscono l'entità ed allo stesso tempo ne subiscono gli effetti. Un esempio, è la tipologia di ricopertura del piano campagna, essa è determinante per l'instaurarsi delle infiltrazioni, in quanto la sua permeabilità durante un evento meteorico influenza la penetrazione nel sottosuolo dell'acqua e quindi il verificarsi di afflussi diretti (*inflow*) in fognatura; inoltre, tale percolazione contribuisce alla ricarica della falda più superficiale che sommergendo la fognatura (Figura 1) determina le infiltrazioni (*Infiltration*).

L'obiettivo del progetto APUSS è definire dei metodi e dei modelli di valutazione delle infiltrazioni ed exfiltrazioni in modo da diagnosticare lo stato strutturale di una rete di fognatura e di individuare la miglior tecnica di intervento e di gestione dell'infrastruttura, definendo i tempi di manutenzione, riparazione e riabilitazione a fronte di costi contenuti.

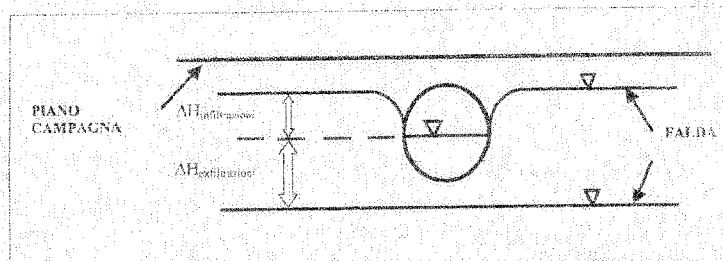


Figura 1 - Differenze di carico idraulico determinanti le infiltrazioni ( $\Delta H_{infiltrazioni}$ ) e le exfiltrazioni ( $\Delta H_{exfiltrazioni}$ ).

Nel presente articolo è trattato il problema dei fenomeni di infiltrazioni ed exfiltrazioni a partire dalle cause primarie responsabili dell'instaurarsi di essi: è presentato il progetto europeo con le sue finalità e sono riportati e discussi i risultati preliminari dell'attività sperimentale condotta nel bacino urbano nel Comune di Roma.

## 2. PRESENTAZIONE DEL PROGRAMMA DI RICERCA APUSS

### 2.1 Obiettivi

Il progetto di ricerca APUSS è finanziato dall'Unione Europea e rientra nel quinto programma quadro nell'ambito dell'obiettivo di implementare un sistema di gestione sostenibile delle aree urbane e della qualità delle acque. In particolare, il progetto ha lo scopo di sviluppare dei metodi e dei modelli per valutare le portate di infiltrazioni ed exfiltrazioni dagli specchi allo scopo di fornire agli operatori pubblici una strategia di intervento e di gestione delle reti di fognatura. Pertanto, il prodotto ultimo del progetto potrebbe costituire una parte di un piano di più ampio respiro concernente il monitoraggio di tutti quei fenomeni che interessano una rete di fognatura urbana.

L'IRSA ha il compito di applicare ed affinare sia i metodi e le tecniche basate su traccianti chimici, che validare il modello di gestione matematico di descrizione dei fenomeni di infiltrazione ed exfiltrazione.

### 2.2 Materiali e metodi

L'attività sperimentale ha avuto luogo in un bacino urbano delimitato all'interno del territorio comunale di Roma (latitudine  $41^{\circ}55'00''$ , longitudine  $0^{\circ}07'30''$ , altitudine media 40 m s.l.m.) di estensione 85 ha confinante a nord ed a nord-est con una grande arteria viaria della città di Roma (Grande Raccordo Anulare), ad ovest e a sud-ovest con la pianura alluvionale urbanizzata ed a nord-ovest con un corpo idrico superficiale di modeste dimensioni (fosso di S. Basilio).

L'assetto geostatigrafico può essere caratterizzato secondo le seguenti principali formazioni: 50-80 cm di coltre superficiale vegetale; 20 m di alluvioni pleistocenica sedimentaria di scarsa permeabilità costituita da argille brune e limi sabbiosi di origine fluvio-palustre in una limitata parte dell'area; 3-7 m di piroclastite litoidi, ovvero tufo lionato, la cui origine è legata al vulcanismo Sabatino e da quello dei Colli Albani, tufo grigio-variabile da semicoerente a litoidi al di sotto del quale vi è una serie vulcanica di termini pozzolanici.

Secondo i dati di letteratura la falda più superficiale è a 15-20 m sotto il piano campagna; il moto di filtrazione è dovuto alla fessurazione nella formazione del tufo lionato, per cui la permeabilità può variare da  $10^{-6}$  a  $10^{-4}$  cm/s.

L'area è dotata di fognatura mista (Figura 2) costituita da tubazioni di calcestruzzo prefabbricate ovoidali di dimensioni



100x120 cm, 150x180 cm e 120x210 cm. La rete fognaria è stata implementata in un programma denominato AquaBase utilizzato nell'ambito del progetto APUSS come database di scambio tra i membri.

L'altezza di pioggia media è di 74.5 mm, con minimo in luglio di valore medio 17.7 mm e massimo in novembre di valore medio di 136.3 mm.

In corrispondenza del pozzetto terminale della rete, indicato nella Figura 2 con una freccia, è stato eseguito il campionamento per la caratterizzazione e la misura di portata in condizioni di tempo asciutto (stabilito come 48-h dopo l'ultimo evento di pioggia).

Il campionamento è stato realizzato mediante campionatore automatico American Sigma 900MAX con pompa peristaltica di prelievo. Le misure di flusso sono state eseguite con sonda sommersa SIGMA dotata di sensore di livello e di velocità. Per la determinazione dei parametri chimico-fisici sono state impiegate sonde portatili WTW con sensori di conducibilità e pH. I campioni di acque reflue sono stati prelevati istantaneamente ogni ora ed analizzati in laboratorio per la determinazione, secondo le metodiche IRSA-CNR (IRSA, 1984), dei parametri COD e SST.

La scelta parametri di qualità è stata dettata dall'esigenza di determinarne sia i valori istantanei che la variabilità giornaliera e stagionale.

Nella seguente Tabella I è riportata una scheda tecnica che sintetizza gli aspetti costruttivi e territoriali più significativi per lo studio dei fenomeni di infiltrazioni ed exfiltrazioni.

letteratura. La Tabella II seguente riporta i metodi sia attualmente collaudati che in fase di sperimentazione (Wirahadikusumah et al., 1998).

Tuttavia, essendo il deterioramento il risultato di una concomitanza nel tempo di numerosi fenomeni (Tabella III), l'età della rete è l'aspetto a cui è necessario porre maggiore attenzione (Tafari & Selvakumar, 2002), e che può essere aggravato da una cattiva esecuzione dell'impianto fognario. Le fognature sono generalmente realizzate mediante escavazione di una trincea in cui sono collocate le tubazioni. La resistenza della tubazione alle sollecitazioni dinamiche e statiche verticali è fortemente influenzata dalle caratteristiche meccaniche del terreno di rifianco (coefficiente  $k_0$  di spinta a riposo) e dall'angolo d'appoggio della tubazione. Poiché  $k_0$  è funzione dell'angolo di attrito  $\phi'$  del terreno, a sua volta dipendente dal grado di addensamento, una buona messa in opera consiste in una accurata costipazione ( $k_0 \approx 1$ ) del materiale di rifianco (Di Natale et al., 2001).

La granulometria del materiale di rifianco della tubazione ha una forte influenza anche sulla portata delle exfiltrazioni. Durante il fenomeno di exfiltrazione si verifica sia una occlusione della sezione di perdita all'interno della tubazione fognaria ad opera dei solidi presenti nelle acque reflue che una colmatazione dei vuoti nel suolo circostante la tubazione per effetto sia della deposizione sui granelli del materiale solido trasportato dalle perdite che, probabilmente, delle trasformazioni chimiche e/o biologiche. Il processo di perdita da una tubazione fognaria si può esaurire in un'ora per un'acqua reflua avente una concentrazione di solidi sedimentabili variabile tra 2 e 13 ml/l e una

**TABELLA I - Aspetti territoriali ed infrastrutturali di Torraccia**

Parametro	Valore di riferimento
Numero di abitanti serviti	5 858
Dotazione idrica	475 L/(ab. g.)
Età della fognatura	10 anni circa
Materiale di costruzione delle tubazioni	Calcestruzzo
Dimensione delle tubazioni	100x150 cm, 120x180 cm e 120x210 cm
Traffico stradale	N.d.
Numero di allacci	87
Tipo di fognatura	Mista
Regime delle portate transitive in tempo asciutto	0,1-41 L/s
Livello della falda interessata dal tracciato fognario	9-20 m al di sotto del piano campagna
Tipo di suolo circostante la tubazione	Tufo lionato
Profilo geometrico della rete	Pendenza 0,5% e 0,9%

### 3. CAUSE PRIMARIE DI DETERIORAMENTO STRUTTURALE DELLE TUBAZIONI FOGNARIE

Per cause primarie si intendono tutti quei fattori riguardanti esclusivamente lo stato dell'infrastruttura e che favoriscono il fenomeno di infiltrazione ed exfiltrazione. Pertanto, è evidente che la conoscenza dello stato generale di una fognatura costituisce il primo obiettivo da raggiungere. Alla indagine conoscitiva segue la necessità di un idoneo intervento di riabilitazione del sistema.

Numerosi sono i metodi di indagine degli specchi fognari noti in

granulometria del materiale di riempimento variabile tra 0-3 mm e 2-40 mm (Rauch & Stegner, 1994).

In Tabella IV sono indicate le portate di infiltrazione in una tubazione collocata in diversi litotipi ed in presenza di un battente di falda positivo rispetto al livello idrico nella fognatura. Si osserva che all'aumentare della permeabilità del suolo, durante i periodi di pioggia, la portata delle infiltrazioni diminuisce, mentre generalmente durante l'anno è costante. Tuttavia, anche il tipo di ricopertura della superficie urbana gioca un ruolo determinante, in quanto se caratterizzato da una bassa permeabilità, la ricarica dell'aquifero urbano potrebbe essere insuffi-



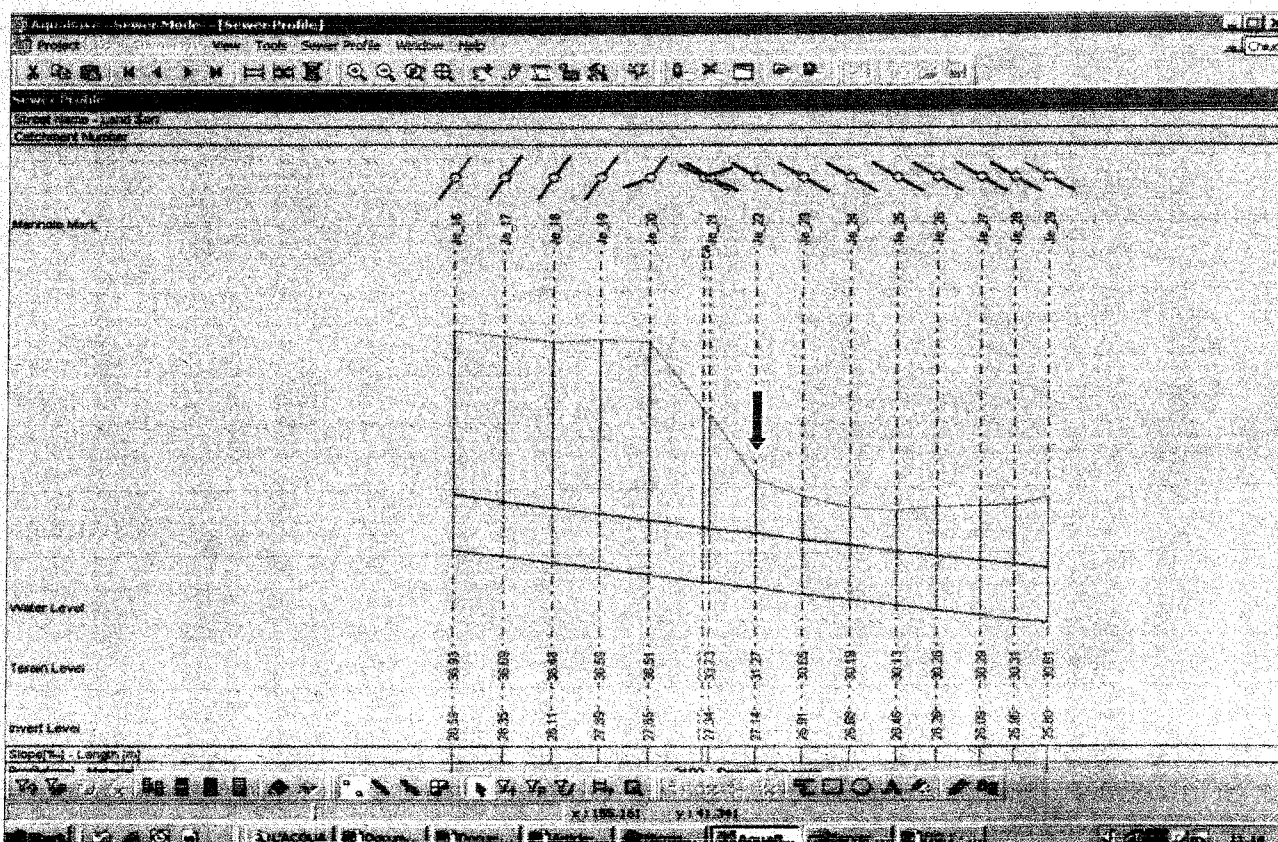
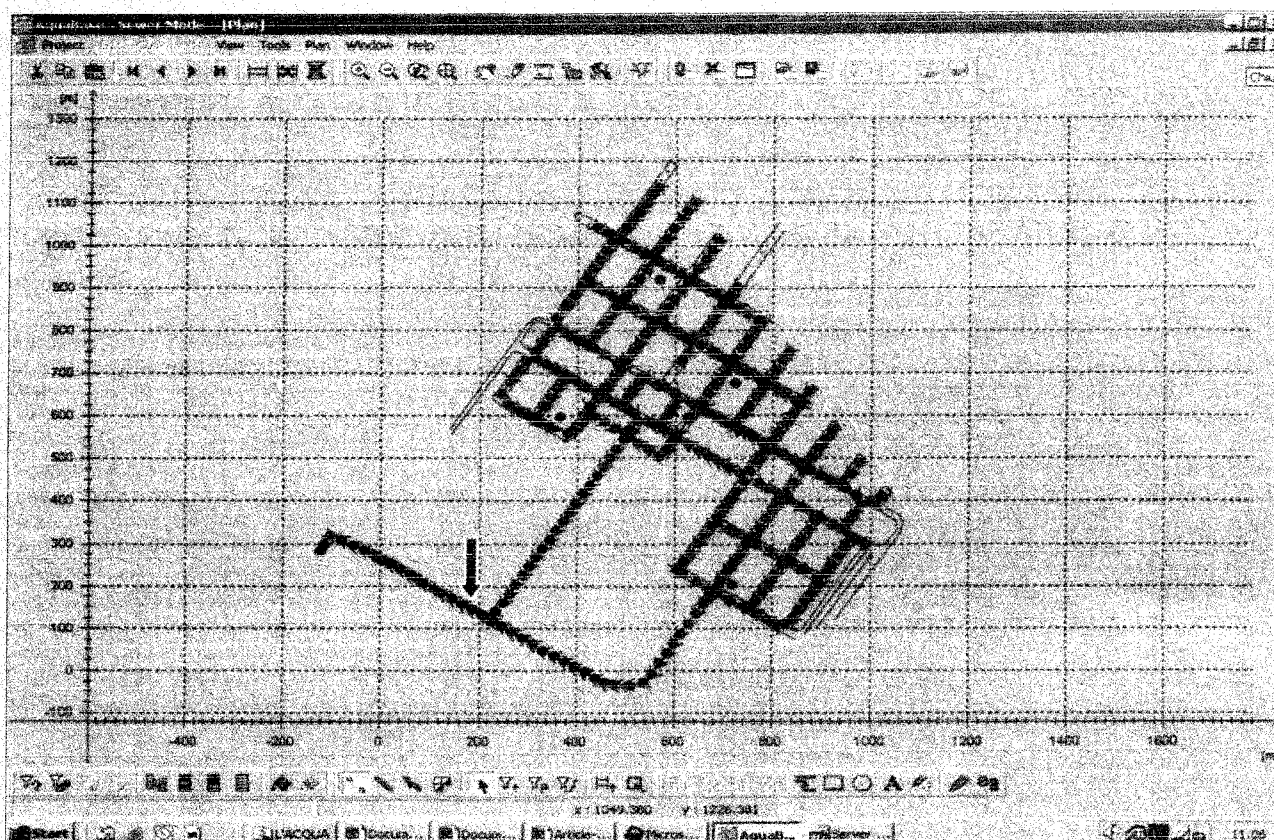


Figura 2 - Fognatura del bacino sperimentale implementata nel software AquaBase.  
a: mappa dell'intera rete; b: profilo longitudinale in prossimità della zona di misura.



TABELLA II - Tecniche indagine (Wirahadikusumah et al., 1998)

Tecniche	Vantaggi	Difficoltà nell'implementazione
Telecamera a circuito chiuso	<ul style="list-style-type: none"> <li>- Facile da usare e ben conosciuto</li> <li>- Nuovi sviluppi permettono la produzione di immagini di alta qualità e di sistemi di ispezione portatili</li> </ul>	<ul style="list-style-type: none"> <li>- Dipende dall'abilità e dall'esperienza dell'operatore</li> <li>- Dipende dalla qualità dell'immagine</li> <li>- Non fornisce informazioni sul materiale di riempimento circostante la tubazione</li> <li>- Incertezza nella rilevazione di alcuni difetti delle tubazioni</li> <li>- Difficile stimare la produzione di informazioni</li> </ul>
Sistema termografico ad infrarossi	<ul style="list-style-type: none"> <li>- Larga area di ispezione</li> <li>- permette l'ispezione nelle ore notturne</li> <li>- Rileva difetti sulle pareti delle tubazioni e fornisce informazioni sul materiale di riempimento circostante la tubazione</li> <li>- Alta produzione di informazioni</li> </ul>	<ul style="list-style-type: none"> <li>- Non fornisce informazioni sulla profondità delle crepe (difetti profondi sono difficili da rilevare)</li> <li>- L'interpretazione delle immagini dipende dalle condizioni ambientali e della superficie del suolo</li> <li>- Informazioni raccolte da un singolo tipo di sensore</li> </ul>
Metodo di misura ad ultrasuoni	<ul style="list-style-type: none"> <li>- Descrive la sezione trasversale della tubazione</li> <li>- Misura le inflessioni delle pareti delle tubazioni, la riduzione dello spessore per effetto della corrosione ed il volume di detriti</li> <li>- Alta produzione di informazioni</li> </ul>	<ul style="list-style-type: none"> <li>- Registra informazioni solo sulla parte della tubazione fuori dall'acqua o sotto l'acqua, ma non simultaneamente</li> <li>- Informazioni raccolte da un singolo tipo di sensore</li> </ul>
Radar di penetrazione del terreno	<ul style="list-style-type: none"> <li>- Fornisce il profilo delle sezioni trasversali in continuo</li> <li>- Identifica la profondità delle crepe</li> <li>- Alta produzione di informazioni</li> </ul>	<ul style="list-style-type: none"> <li>- L'interpretazione dei dati è difficile, richiede esperienza ed addestramento</li> </ul>
Sistemi avanzati (KARO, PIRAT, SSET)	<ul style="list-style-type: none"> <li>- Sistemi a multi sensori (quindi, forniscono più dati)</li> <li>- Fornisce in continuo il profilo delle pareti</li> <li>- Robotizzati</li> <li>- Sono previsti rapporti Costi/benefici più alti</li> </ul>	<ul style="list-style-type: none"> <li>- Sono disponibili ancora solo dei prototipi oppure sono ancora in fase di prova (sono richiesti ulteriori sviluppi per l'implementazione in campo)</li> <li>- Alti costi iniziali</li> </ul>

TABELLA III - Cause di danneggiamento della struttura fognaria (Jones, 1998; Davies et al., 2001)

<b>Abrasione e corrosione chimica</b>	La vulnerabilità dipende dal materiale della tubazione, le tubazioni in calcestruzzo sono più sensibili all'abrasione da parte dei solidi trasportati dal flusso e alla corrosione chimica causata dall'idrogeno solforato ( $H_2S$ ) rispetto a quelle in grès e in PVC. Inoltre, il pH delle acque e del suolo può rendere aggressivo l'ambiente interno ed esterno alla tubazione nei confronti del materiale di cui è costituita.
<b>Perdita di funzionalità delle guarnizioni di giunzione</b>	L'eccessiva pressione in corrispondenza della giunzione dovuta alla espansione del materiale di giunzione, può provocare una rottura della presa di giunzione (White, 1974). Pertanto, la dislocazione di un punto di giunzione o la perdita di funzionalità del sistema di impermeabilizzazione in corrispondenza di questa possono favorire le infiltrazioni (Figura 3.A) o le exfiltrazioni (Figura 3.B).
<b>Sovraccarichi o stress</b>	Il peso del terreno di ricopertura della tubazione, il passaggio delle automobili, i lavori su altre linee di servizio determinano sovraccarichi non sempre ammissibili per le tubazioni.
<b>Cattiva posa in opera della tubazione</b>	E' dovuta principalmente alla pessima qualità del terreno di riempimento dello scavo circostante la tubazione e può causare la frattura delle pareti della tubazione o l'allontanamento dei punti di giunzione.
<b>Livello della falda</b>	Il trasporto da parte delle acque di infiltrazione del terreno circostante all'interno della tubazione determina una perdita di resistenza meccanica alla compressione con possibili cedimenti differenziati lungo il tratto, nonché collassi.
<b>Radici</b>	La vegetazione arborea danneggia la struttura della tubazione e provoca l'apertura delle giunzioni.



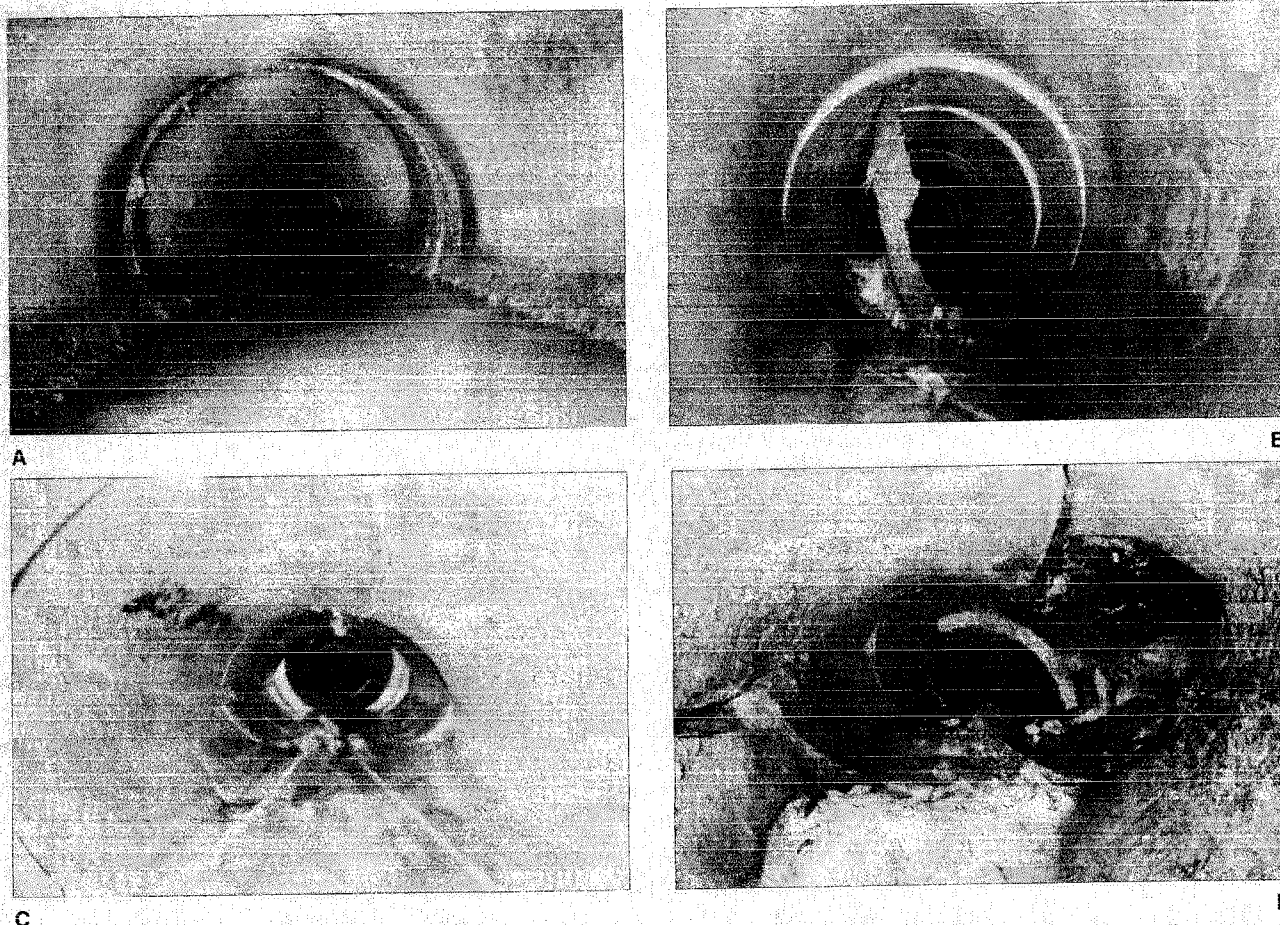


**Figura 3 -** Immagini eseguite mediante telecamera a circuito chiuso. A e B: danneggiamento della guarnizione di gomma; C e D: tubazione gravemente deteriorata e tubazione collassata (WRc Sewerage Rehabilitation Manual, 1983).

ciente ed il livello della falda potrebbe non variare dopo un evento di pioggia rimanendo al di sotto del piano di posa della fognatura. Superfici pavimentate rendono la quantità di acqua infiltrata trascurabile ed in questa circostanza prevalgono i fenomeni di exfiltrazioni. Di contro in presenza di superfici permeabili o semipermeabili costituite da ghiaia e sabbia si verifica una infiltrazione nel suolo di circa il 25-30% del totale di pioggia ed in questa situazione possono prevalere i fenomeni di infiltrazione.

#### 4. LE INFILTRAZIONI

L'interesse scientifico verso il problema delle infiltrazioni è determinato dal fatto che esse hanno un effetto negativo sul-

l'efficienza degli impianti di trattamento delle acque reflue. In particolari condizioni tale sovraccarico può raggiungere valori particolarmente elevati, determinando una indesiderata diluizione del carico inquinante addotto all'impianto, con un conseguente mal funzionamento del comparto biologico. Oltre a ciò, un aumento della portata nella rete comporta una maggiore quantità di acqua da sollevare in corrispondenza delle stazioni di pompaggio, nonché maggiore frequenza degli scarichi in corrispondenza degli scolmatori posti lungo la rete di fognatura con un conseguente notevole apporto di inquinanti al corpo ricettore (Diaz-Fierros, T. F. et al., 2002). Inoltre, le acque di infiltrazione erodono il materiale di rifianco trascinando, all'interno della tubazione, i granelli di terreno determinando quindi: la perdita di resistenza del terreno, la riduzione della sezione utile trasversale della fognatura e l'aumento di concen-

**TABELLA IV -** Valori delle portate di infiltrazione da utilizzare durante la progettazione di una tubazione fognaria (Murray, 1987)

Tipo di suolo circostante la tubazione	Posizione della falda rispetto alla fognatura	Portate presenti solo nei periodi piovosi Q (m <sup>3</sup> /(ha d))	Portate presenti tutto l'anno Q (m <sup>3</sup> /(ha d))	Totale
Argilla	sopra	28	1,1	29,1
Argilla sabbiosa	sopra	22	1,1	23,1
Sabbia argillosa	sopra	17	1,1	18,1
Rocce sciolte	sopra	*	1,1	*
Tutti	sopra	11	6,5	17,5

\*Variabile a seconda della componente predominante

trazione dei solidi nelle acque di fogna danneggiando gli impianti di sollevamento (giranti delle pompe centrifughe) lungo la rete o in corrispondenza degli impianti di trattamento.

Le acque parassite costituiscono per la loro qualità e quantità una componente non conforme al sistema fognario dimensionato: possono essere acque bianche o acque usate e sono posizionate nello spazio e nel tempo in differente modo. La seguente classificazione definisce quattro gruppi principali (Joannis et al., 1999):

- acque provenienti dalla falda superficiale circostante la tubazione (*Groundwater Infiltration, GWI*), esse sono propriamente definite infiltrazioni e sono fortemente dipendenti dalle condizioni stagionali e potendosi verificare durante tutto l'arco dell'anno costituiscono il contributo più dannoso. Esse possono avere luogo prevalentemente nei periodi di tempo asciutto in corrispondenza sia di giunzioni (tra tubazioni e tra tubazione e manufatti) che di fratture, crepe, etc. sulle pareti delle tubazioni;
- acque pluviali infiltratesi nel suolo e quindi drenate dalle tubazioni fognarie durante il tempo di pioggia (*Rainfall-Dependent Infiltration, RDI*) (Figura 4). Le principali vie di ingresso sono i chiusini stradali e i difetti strutturali lungo la rete. Ad esempio, per le fognature separate di tipo nero si può verificare il drenaggio delle perdite delle reti bianche, in corrispondenza dei piani interrati dove le due reti sono molto vicine;
- acque pluviali dovute a collegamenti illeciti con la rete fognaria (*Stormwater Inflow, SWI*), generalmente questa componente è evidenziata quando le fognature in oggetto sono separate di tipo nero (Figura 4);
- acque industriali addotte mediante collegamenti illeciti.

Alle prime tre classi appartengono le portate parassite di acque bianche (*parasitive clear water, ECP*), oggetto di studio nel progetto europeo A-PUSS che dipendono dalla lunghezza del tratto di fognatura, dall'estensione dell'area drenata, dalle caratteristiche della superficie di ricopertura e dalla densità abitativa. Questo ultimo parametro è molto importante, perché influenza fortemente il numero delle connessioni con le case e la lunghezza totale della rete.

Una ulteriore classificazione delle portate delle acque bianche parassite è possibile su scala temporale e spaziale, per chiarire meglio il termine generico afflussi/infiltrazioni contenente in sé due classi di acque parassite differenti nell'origine spaziale dei contributi, ovvero:

- gli afflussi diretti hanno luogo durante l'evento di pioggia e si esauriscono con esso, seguendo come andamento temporale quello dello ietogramma. Essi sono puntuali nello spazio e nel tempo, in particolare possono essere: i) quasi permanenti quando drenano acque di falda o di sorgente; ii) temporanee quando si presentano solo durante i periodi di tempo di pioggia. In questo secondo caso, in corrispondenza della sezione di consegna all'impianto di depurazione la portata si registra come un picco di breve durata (Figura 4);
- le infiltrazioni possono essere: i) permanenti o comunque variabili molto lentamente se hanno origine da una falda superficiale. Infatti, in tal caso esse hanno un andamento temporale pari a quello stagionale del livello della falda; ii) temporanee se hanno origine da un evento di pioggia.

Una rappresentazione dell'andamento temporale delle portate in tempo asciutto e in occasione di un evento di pioggia in una fognatura nera è riportata nella Figura 4; in essa sono evidenziati sia gli afflussi diretti (picco) verificatisi durante un evento di pioggia che le infiltrazioni che hanno avuto luogo nei giorni successivi all'evento stesso a causa della ricarica della falda superficiale.

I metodi di misura delle portate parassite, attualmente utilizzati e presenti in letteratura, si differenziano nella loro applicazione: in tempo di pioggia o in tempo asciutto. Nel primo caso essi si basano su un modello idrologico che valuta la quantità di portata pluviale drenata da una rete mista o bianca. Nel secondo caso i metodi prevedono anche l'apporto di acque parassite da parte di acque di falda, pertanto accanto al modello idrologico occorre applicare uno idrogeologico.

I modelli fino ora sviluppati si calibrano mediante misure pluviometriche, termometriche, idrometriche ed tensiometriche, necessarie per impostare il bilancio di massa sul sistema fognario. Tale bilancio porta alla stima degli apporti denominati sopra con gli acronimi: *GWI, SWI e RDI*.

Un modello è quello sviluppato da Belhadj et al. che valuta tutti e tre gli apporti suddetti (Belhadj et al., 1995), mentre i modelli MOUSE RDII (Mein et al., 1993), RORB (RORB Version 4.2) considerano la sola condizione di tempo di pioggia durante la quale si verificano gli apporti *RDI e SWI*.

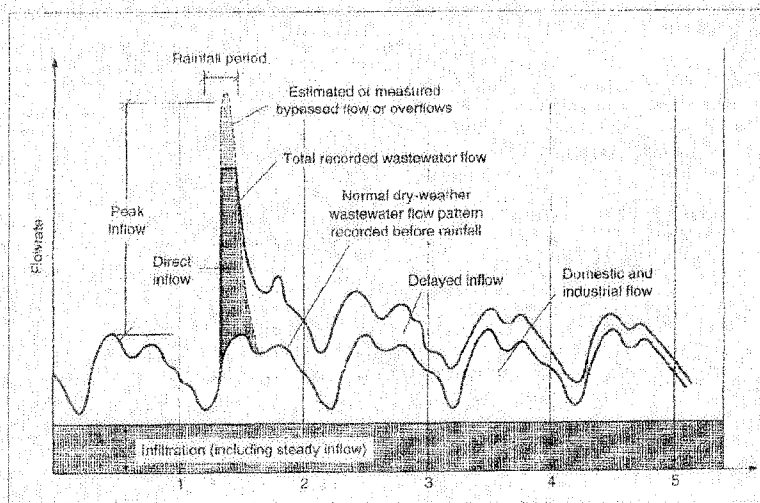


Figura 4 - Portate affluenti in una fognatura nera in condizioni meteorologiche variabili. La portata di acque parassite può variare nell'intervallo 0,2 e 28 m³/ha d, aumentando fino a 470 m³/ha d in occasione di pesanti eventi di pioggia (modificata da Tchobanoglous & Burton, 1991)

## 5. ATTIVITÀ SPERIMENTALE

Le campagne sperimentali condotte in questa prima fase del progetto hanno riguardato la caratterizzazione qualitativa e quantitativa delle acque di fognatura in corrispondenza della sezione di chiusura del bacino urbano di Terraccia (Tabella V). Le indagini hanno riguardato la misura in condizioni di tempo asciutto dei seguenti parametri: COD, conducibilità, pH e portata in diversi periodi stagionali e per una diversa durata del periodo di tempo asciutto precedente la campagna. L'obiettivo è stato quello di evidenziare la presenza di acque parassite mediante l'incremento di portata a seguito di infiltrazioni con conseguente alterazione dei valori dei suddetti parametri di qualità per effetto dell'ingresso parassite.

Durante i periodi di tempo asciutto, il livello della falda idrica più superficiale è 10-15 m circa di profondità dalla superficie

Tabella V - Campagne di misura

	3-4 Luglio 2002	29-30 Settembre 2002	7-8 Ottobre 2002	14-15 Ottobre 2002	12-13 Novembre 2003	8-9 Dicembre 2003	14-15 Gennaio 2004
Periodo di tempo asciutto precedente l'inizio delle misure	15 giorni	2 giorni	7 ore	3 giorni	4 giorni	7 giorni	10 giorni
Parametri misurati	Portata e COD	Portata, COD, conducibilità e pH	Portata, COD, conducibilità e pH	Portata, conducibilità e pH	Portata, COD, conducibilità e pH	Portata, COD, conducibilità e pH	Portata, COD, conducibilità e pH
Durata delle misure e del campionamento	24 ore	24 ore	24 ore	24 ore	24 ore	24 ore	24 ore

dell'area investigata, mantenendosi al di sotto del fondo della tubazione fognaria, per cui le infiltrazioni attese erano trascurabili.

I grafici a, b e c riportati in Figura 5 mostrano gli andamenti delle portate calcolate con il metodo area-velocity e gli andamenti di conducibilità, COD e pH valutati su campioni prelevati istantaneamente.

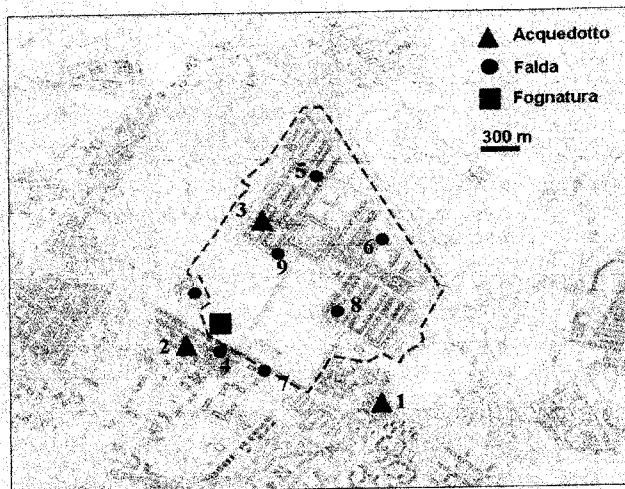
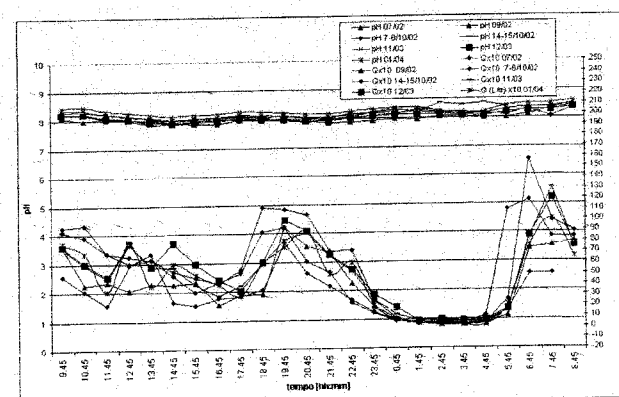
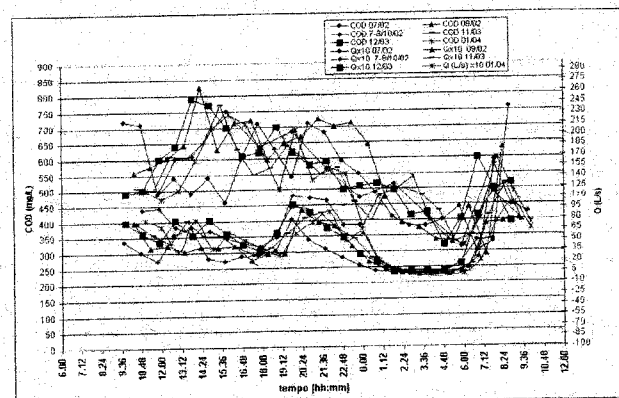
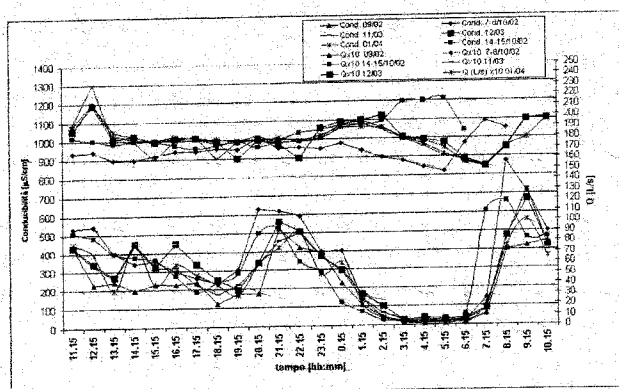


Figura 5 - Punti di campionamento nel sito sperimentale

Ai fini della determinazione dell'ingresso di acque di falda, i parametri da prendere in considerazione sono quelli sensibili alle variazioni di portata in fognatura: questa ultima può variare sia per effetto della variazione degli scarichi di acque usate che per il diverso apporto di acque di infiltrazione. La variazione spaziale della qualità del refluo dal momento dello scarico all'arrivo alla stazione di monitoraggio è considerata trascurabile viste le ridotte dimensioni dell'area in esame; mentre, la variazione temporale registrata nel punto di chiusura del bacino (Figura 5) è rappresentativa dell'intero bacino. Il parametro qualitativo più sensibile alla variazione della portata sarà quello preso in esame negli studi successivi.

Appare evidente, dai grafici in Figura 6, che il pH non varia al variare della portata transitante (var. 15,3 L/s), la conducibilità mostra una lieve oscillazione (var. 458  $\mu\text{S}/\text{cm}$ ), ed il COD varia sensibilmente (var. 711  $\text{mg}/\text{L}$ ). Gli andamenti giornalieri delle concentrazioni dei parametri presi in esame variano passando dalla stagione estiva a quella invernale. Tale variabilità oltre a contenere fattori di incertezza della misura e delle analisi di laboratorio da considerarsi pressappoco costanti passando da una campagna all'altra a causa della applicazione delle medesime metodologie, può essere attribuita a fattori esterni quali: usi dell'acqua da parte della popolazione residente nell'area investigata (fattori antropogenici), livello


Figura 6 - Idrogrammi (l/s) nella sezione di chiusura dell'area sperimentale di Torraccia ed orario della conducibilità ( $\mu\text{S}/\text{cm}$ ) (grafico a), del COD ( $\text{mg}/\text{L}$ ) (grafico b) e del pH (grafico c).



dell'acqua di falda (minime condizioni ambientali), etc. Per evidenziare la relazione presente tra la variazione degli andamenti quali-quantitativi esaminati e le mutate condizioni stagionali si è calcolata la deviazione standard dei parametri misurati durante le ore notturne in cui si instaura il minimo flusso. Durante questo intervallo giornaliero la popolazione del bacino investigato ha una influenza ridotta sull'andamento dell'idrogramma e, quindi, l'influenza stagionale (infiltrazioni dovute alla falda) è più evidente.

In Figura 7 si può osservare quanto segue. L'andamento della portata e del COD, è simile a causa della medesima sensibilità ai fattori ambientali (come il livello della falda) ed antropogenici (come utilizzo dell'acqua), passando dalle ore 0:45 a 3:45 l'andamento regolare decrescente della deviazione standard è attribuibile alla minore influenza della popolazione e non alle mutate condizioni della falda.

Si può concludere che il COD è un parametro indicativo del

l'utilizzo delle acque potabili in un'area urbana e che è sensibile quanto la portata di tempo asciutto. Pertanto esso può essere considerato come un tracciatore intrinseco del flusso da cui risalire all'apporto di acque parassite di acqua di falda.

La sua bassa variabilità stagionale mostra in questo caso una bassa variabilità di acque di infiltrazioni, il cui valore è da considerarsi trascurabile viste le buone condizioni strutturali della fognatura. Il livello della falda e la profondità delle tubazioni fognarie (Tabella VI).

## 6. CONCLUSIONI

Le acque di infiltrazione sono di grande interesse giacché gli impatti investono l'ambiente urbano a largo spettro: funzionalità della rete fognaria, impianti di depurazione, ambiente idrico superficiale e profondo. La stima delle portate di acque parassite e di perdita, per mezzo di metodi speditivi, permette di ottimizzare gli interventi di manutenzione delle reti fognarie e di sviluppare modelli matematici di integrazione ai già esistenti sistemi di calcolo del drenaggio urbano. Allo stato attuale della ricerca sono state caratterizzate quali-quantitativamente le acque di fognatura al fine di individuare i parametri sensibili alle variazioni del flusso in tempo asciutto. Dall'analisi dei dati è seguita risulta che il parametro più sensibile alla variazione di portata è il COD, tuttavia, nonostante una non possibile quantificazione delle acque di infiltrazione, dall'analisi dei dati risulta che le infiltrazioni sono pressoché nulle a conferma della caratterizzazione idrogeologica del bacino. Una campagna di approfondimento mediante sonde di misura dei parametri di conducibilità e COD in continuo è in corso di svolgimento, lo scopo è una caratterizzazione con maggior precisione ed accuratezza del refluo e quantificazione delle infiltrazioni.

Tabella VI - Caratteristiche qualitative dell'acqua di falda

Punti di campionamento	Livello della falda al di sotto del piano campagna [m]	Livello del fondo della fognatura al di sotto del piano campagna [m]
1	-	-
2	-	-
3	-	-
4	7.3	4 - 5
5	15.30	6 - 7
6	10.6	5 - 6
7	nd	-
8	12.70	9 - 10
9	11.20	5 - 7

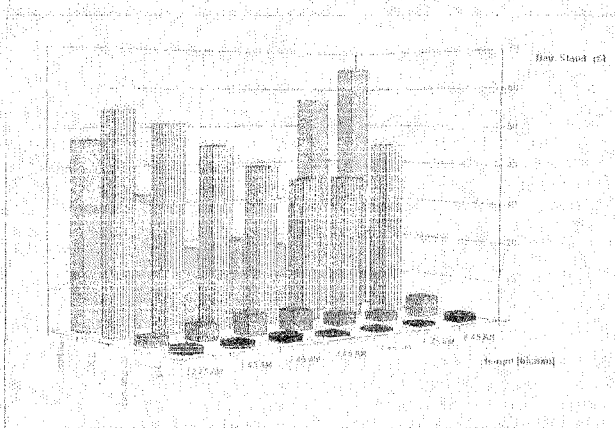


Figura 7 - Andamenti delle deviazioni standard percentuali di: portata, conducibilità, COD e pH durante il periodo di minimo flusso.

## RINGRAZIAMENTI

Gli autori desiderano ringraziare i tecnici dell'IRSA-CNR: Geom. Maurizio Ronda e P.L. Salvatore Tatti per il valido aiuto fornito durante lo svolgimento delle campagne sperimentali.

Il lavoro presentato rientra nell'ambito del progetto europeo di ricerca denominato APUSS (Assessing Infiltration and Exfiltration on the Performance of Urban Sewer Systems) i cui partners oltre all'IRSA-CNR sono: l'INSA di Lione (FR), l'EAWAG di Zurigo (CH), il Technical University di Dresda (DE), la Faculty of Civil Engineering dell'Università di Praga (CZ), la DHI Hydroinform (CZ), l'Hydroprojekt (CZ), la Middlesex University (UK), il LNEC (PT), l'Emschergergenossenschaft (DE) and IRSA-CNR (IT). Il progetto APUSS è finanziato Dalla Commissione Europea nell'ambito del 5° Programma Quadro - Key Action "Sustainable Management and Quality of Water" Contract n° EVK1-CT-2000-00072.

## BIBLIOGRAFIA

- Belhadj N., Joannis C., Raimbault G., "Modelling of rainfall induced infiltration into separate sewerage", *Wat. Sci. Tech.*, Vol.32, n. 1, 1995, pag. 161-168.
- Davies J. P., Clarke B. A., White J. T., Cunningham R. J., "Factors influencing the structural deterioration and collapse of rigid sewer pipes", *Urban Water*, n.3, 2001, pp. 73-89.
- Díaz-Fierros T. F., Puerta J., Suárez J., Díaz-Fierros V. E., "Contaminant loads of CSOs at the wastewater treatment plant of a city in NW Spain", *Urban Water*, n.4, 2002, pp. 291-299.
- Di Natale M., Fontana N., Greco R., "Influenza della compattazione del terreno di rifianco sul carico di rottura di tubazioni interrato", *L'Acqua*, n. 3, 2001, pp. 27-36.
- Istituto di Ricerca Sulle Acque "Metodi analitici per i fanghi" *IRSA-CNR*, Volume 2, Roma, 1984.
- Joannis C., Belhadj N., Raimbault G., "Rainfall induced infiltration into sewer systems", in *Proceedings of the sixth international conference on Urban Storm Drainage*, Ed. Jiri Marsalek & Harry C. Törnø, 1993.
- Jones M., "Sewer Leakage-- Detection and Cures", disponibile sul sito internet: <http://www.swopnet.com/eng/jones/leaksewer.html>, 1998.
- Mein R., Apostolidis N., "Application of a simple hydrologic model for sewer inflow/infiltration", in *Proceedings of Sixth International Conference on Urban Storm Drainage*, Jiri Marsalek and Harry C. Törnø, September 12-17 1993.
- Murray J. B., "Infiltration rates for separate sewage collection systems", *Water Science and Technology: Water Pollution Research and Control*, Rio de Janeiro, vol. 19, n. 3-4.
- Rauch W., Stegner T., "The colimation of leaks in sewer systems during dry weather flow", *Wat. Sci. Tech.*, Vol.30, n. 1, 1994, pp. 205-210.
- "RORB Version 4.2 Runoff Routing Program", Dept. of Civil Engineering of Monash University, Clayton, Australia, 1992, disponibile sul sito: <http://www.civil.eng.monash.edu.au/research/groups/water/RORB>.
- Tafiri A. N., Selvakumar A., "Wastewater collection system infrastructure research needs in the USA", *Urban Water*, n.4, 2002, pp. 21-29.
- Tchobanoglous B., Burton F. L., "Wastewater engineering: treatment, disposal and reuse", Metcalf & Eddy, third edition, McGraw-Hill, Inc, 1991.
- Wirahadikusumah R., Abraham D., Iseley T., Prasanth R., "Assessment technologies for sewer system rehabilitation", *Automation in construction*, vol. 7, 1998, pp. 259-270.
- WRC Sewerage Rehabilitation Manual, 1 Ed, 1983.

## Annex 2

Cardoso, A.; Prigiobbe, V.; Giulianelli, M.; Baer, E.; Coelho, S.T. (2005).  
Assessing the impact of infiltration and exfiltration in sewer systems using  
performance indicators: case studies of the APUSS project.  
10th International Conference on Urban Drainage, Copenhagen, Denmark,  
21-26 August 2005.

## **Assessing the impact of infiltration and exfiltration in sewer systems using performance indicators: case studies of the APUSS project**

A. Cardoso<sup>1\*</sup>, Prigiobbe, V.<sup>2</sup>, Giulianelli, M., Baer, E.<sup>3</sup>, , Coelho, S.T.<sup>1</sup>

<sup>1</sup> *LNEC, National Civil Engineering Laboratory of Portugal, Av. Do Brasil 101, 1700-066 Lisbon, Portugal*

<sup>2</sup> *Water Research Institute of the Italian National Research Council (IRSA-CNR), Via Reno, 1, 00198 Rome, Italy*

<sup>3</sup> *URGC Hydrologie Urbaine, INSA de Lyon, 34 avenue des Arts, 69621 Villeurbanne cedex, France*

### **Extended Abstract**

Sewer systems constitute a very significant patrimony in European cities. Their structural quality and functional efficiency are key parameters to guarantee the transfer of domestic and trade wastewater to treatment plants without infiltration nor exfiltration. Infiltration of groundwater is particularly detrimental to treatment plant efficiency, while exfiltration of wastewater can lead to groundwater contamination. The APUSS (Assessing infiltration and exfiltration on the Performance of Urban Sewer Systems) project, associating universities, SMEs and municipalities in 7 European countries, developed new methods and techniques to assess and quantify infiltration and exfiltration (I/E) in sewer systems. The methods were tested and validated in different catchments. Associated models and tools were established for application and end-user decision. The APUSS project is part of the European cluster CityNet dealing with Integrated Urban Water Management (Bertrand-Krajewski, 2002) and is funded by the European Commission under the FP5..

One of the objectives of the APUSS project was to provide end-users with integrated elements for decision support that account for I/E rates, impacts on wastewater treatment plant and on the economic value, and facilitate the comparison of different investment strategies to reduce infiltration and exfiltration. A set of performance indicators (PI) has been developed to assess the impact of I/E on sewer systems and has been applied to project case studies. This application was performed using the softwares AQUABASE and PItool/S, developed respectively by DHI/Hydroinform and LNEC.

The specific application considered herein is the sewer systems performance evaluation with regard to infiltration of clean water into foul sewers and exfiltration of sewage into the soil and groundwater. Experimental results obtained with the measurement methods developed in the APUSS project, systems' topology data and groundwater level are stored in AQUABASE that exports them in order to calculate the PI using the PITool/S.

This paper describes the establishment of performance indicators and their application to five project case studies, focusing on sewer systems characteristics, I/E measurements campaigns performed and computational applications.

The methodology for PI definition consists in the selection and development of three components for each aspect of performance analysed (Cardoso, 2003): the numerical value of

a sewer network property or state variable, which is expressive of the particular aspect being scrutinized (I/E); a classification of the PI values scoring them in relation to good or bad performance; an operator, which allows the performance values at element level to be aggregated across the system or parts of it to obtain an overall system performance figure. An example of a PI to assess the infiltration impact on the system performance is  $Q_{inf}/Q_{full}$  where  $Q_{inf}$  is the infiltration flow and  $Q_{full}$  is the pipe capacity.

There are five case studies, three are located in Rome, Italy, and two are located in Lyon, France. In Rome, the three experimental catchments (called Infernetto, Mostacciano and Torraccia) can be considered three different representative pictures of an urban area because geology, hydrogeology, sewer system and the town planning are quite spatial homogeneous. The developed methods within APUSS project for quantifying the I/E ratio were applied at catchment and pipe scale, respectively (Table 1).

**Table 1. Experimental catchments in Rome**

	Infernetto	Mostacciano	Torraccia
<b>Extension [ha]</b>	550	14	85
<b>Sewer</b>	dated 5-15 years, PVC and clay	dated 29 years, concrete	dated 10 years, concrete
<b>Soil</b>	silt-sand sediments, clay and gravel	alluvial and tuff	tuff
<b>Shallow Groundwater</b>	3-7 m under the ground	-	15-20 m under the ground
<b>Town Planning</b>	private houses and gardens	high buildings and yards	small buildings and yards
<b>Infiltration [-]</b>	0.49	-	0.15
<b>Exfiltration [-]</b>	-0.07*	-	-0.02**

Note: estimated in a representative pipe of (\*)1500 m and (\*\*) 500 m length.

In the French case studies, infiltration and exfiltration measurement campaigns have been carried out in 2 main catchments in Lyon: i) the Yzeron catchment (2800 ha) and ii) the Ecully catchment (230 ha). Infiltration and exfiltration rates have been measured using two of the methods developed within the APUSS project: the QUEST method based on NaCl mass balance for exfiltration and the oxygen isotopic method for infiltration. Several conventional methods for the estimation of infiltration have also been applied and compared to the APUSS method. Temporal variations at daily and seasonal scales and also spatial variations were analysed for infiltration. Regarding exfiltration, seasonal variations have been investigated.

Fig.1 shows an example of comparison of the PI referred to above applied to the experimental data available.

The use of PI allows a standardized and objective comparison of the performance of sewer systems having different characteristics, and the evolution of performance along the time. It constitutes a means to technically support the establishment of priorities for rehabilitation and/or construction investments concerning I/E impacts.

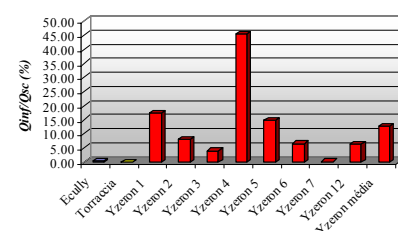


Fig.1 – PI application

## References

- Bertrand-Krajewski, J.L. (2002) - Assessing infiltration and exfiltration on the performance of urban sewer systems. Umweltbundesamt/Federal Environment Agency – Austria.
- Cardoso, A. (2003) Infiltration and exfiltration performance indicators. Sewer systems performance assessment methodology and formulation. APUSS Deliverable 9.1. LNEC. Draft document, diffusion restricted to APUSS partners and EU Commission.



## Annex 3

Giulianelli, M.; Mazza, M.; Prigiobbe, V.; Russo, F. (2003). Assessing exfiltration in a urban sewer by slug dosing of chemical tracer (NaCl). Proceeding of a Workshop organized by NATO ARW on Enhancing Urban Environment, Rome, Italy, Nov. 5-9, 2003.

## ASSESSING EXFILTRATION IN AN URBAN SEWER BY SLUG DOSING OF A CHEMICAL TRACER (NaCl)

V. PRIGIOBBE<sup>1, 2,\*</sup>, M. MAZZA<sup>2</sup>, F. RUSSO<sup>1, 3</sup>, M. GIULIANELLI<sup>1</sup>

<sup>1</sup> IRSA – National Research Council, Rome - Italy

<sup>2</sup> Università degli Studi di Roma "Tor Vergata", Rome - Italy

<sup>3</sup> Università degli Studi di Roma "La Sapienza", Rome - Italy

\* (email address: [prigiobbe@ing.uniroma2.it](mailto:prigiobbe@ing.uniroma2.it))

### Abstract

This paper presents the application of a chemical tracer (Sodium Chloride) dosed in the not watertight sewer pipes by slug pulses. The study is developed within the European Project APUSS. The method applied, called QUEST (QUantification of Exfiltration from Sewer with artificial Tracers), aims at quantifying the exfiltration ratio in working reaches in a more speedy, simple and cheap way than traditional ones, i.e. CCTV.

As in the dry weather the water depth in combined sewer is low, in comparison with the available height, the part affected by leakage (e.g. joints, cracks on the wall etc.) is quite small. Therefore, the exfiltration ratio could be so small that the estimations should be affected as less as possible by errors due to the measurements and the data analysis. At this aim, the data have been elaborated to recognize the most important sources of uncertainty and variability of processed data (e.g. background daily conductivity) on the proposed model.

In the paper, the results of application of non-overlapping QUEST method are presented. From the data analysis emerges that the exfiltration ratio estimates are reliable on the bases of the structural state of the tested pipes.

Keywords: exfiltration, artificial tracer, sewer and sewer rehabilitation.

### 1. Introduction

The water cycle in an urban area consists of both natural and artificial sources and water bodies (i.e.: superficial and deep). Regarding to the deep aquifers, several sources can recharge them, transporting high concentrations of organic and inorganic pollutants, too. Among these, there are the leakages from not watertight sewer pipes that could be a serious threat for groundwater quality because of large extension of urban drainage system. When the shallow unconfined and confined aquifers are connected, the transport in the subsoil of organic and inorganic compounds and pathogenic organisms might be serious. Thus the deep and confined water bodies used as drinking water supply could need advanced water treatment before the distribution. Several methods exist to evaluate the structural state of the sewer. Some of these consist in surveying directly the sewer pipes inside (i.e.: CCTV) and other ones in quantifying the exfiltration ratios by the detection of wastewater markers in the groundwater [1].

Instead, the QUEST method [2] is a direct way to assess the exfiltration from running

sewer network during the dry weather. It consists of a tracer mass balance on the investigated pipes. The solutions of tracer (NaCl) are dosed in two manholes of investigated reach, and at downstream the conductivity of sewerage is measured by means of in-line probes.

The sources of errors affecting the exfiltration ratio come from the experimental results and the data analysis. In particular, they are due to: flow rate, natural wastewater conductivity, shape of the tracer signals at the measuring point, transport of tracer and general disturbance in the sewer (e.g.: turbulence, solid matter).

So in order to minimize the errors (during the proper experiment and the data analysis), preliminary measurements of: flow rate, natural conductivity background and tracer transport should be carried out.

The paper presents the results of an application of QUEST method on an urban sewer network in a suburb area of Rome and highlights the importance of the preliminary tests of the sewer under investigation.

## **2. Material**

### **2.1 EXPERIMENTAL CATCHMENT**

The experiments were carried out on one part of sewer network in a suburb area in Rome, called Torraccia.

The sewer, dated thirteen years old, is an egg-shaped combined system build in concrete material. The investigated reaches are 4-9 m under the ground level and the total length was 724 meters long, with a slope of 0.9 %.

The tested sewer consists of two parts (red line in Fig. 1) the first is egg-shaped 120x180 cm, 483 m long whose 407 m tested; the second one is egg-shaped 120x210 cm, 241 m long whose 151 m tested.

As the tracer be fully mixed at the measuring cross section, a sufficient mixing length has to provide. For non-buoyant tracers, recommended mixing lengths for river are  $100-300 * d$  ( $d$  is channel width) [3] in the investigated reach it was close to 100 m about.

The geology of the catchment area is characterized by cracked tuff and pozzolan, while just around the reaches there is coarse gravel used as backfilling. Groundwater submerges the sewer only during the wet weather, while during the dry weather the water, infiltrated in the soil, is quickly drained towards a deeper aquifer for the high permeability of cracked tuff.

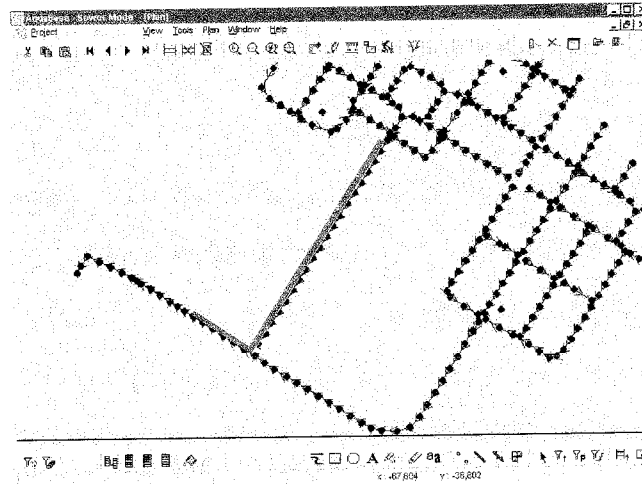


Fig. 1- Scheme of the tested sewer network implemented in AquaBase software developed by DHI within European Project APUSS. The red line indicates the investigated reaches ( $L = 724$  m).

Although the campaigns were carried out on a part of entire sewer system in the experimental catchment (red line in Fig. 1), the homogeneous characteristics of the area allow the extrapolation of the results to each pipe of sewer system of Torraccia.

## 2.2 EQUIPMENTS

The equipment consisted of one submerged probe (Sigma 900max) for the level and velocity measurements and three WTW conductivity probes (device LF 197 with sensor TetraCon 325). The conductivity data were recorded in a datalogger (GRANT SQ400) with a resolution of one second.

The chemical tracer was NaCl with purity 97%.

## 3. Method

The method QUEST [2] applied has been developed within European Project APUSS (Assessing Infiltration and Exfiltration on the Performance of Urban Sewer Systems). It consists of a slug dosage of a tracer solution at known concentration in two different manholes along the tested sewer pipe and the detection of tracer cloud at downstream (Fig. 2).

At the first manhole upstream of the investigated pipe the amount of tracer affected by exfiltration is dosed and at measuring manhole (Fig. 2) the conductivity is recorded. When the cloud of tracer arrives at this section a peak is detected, as it allows evaluating the residual mass of tracer it is called indicator peak.

At the second manhole the tracer slug dosage aims at estimating the flow rate and the conductivity peak measured at downstream is called reference peak.

Between the second manhole and the measuring one the exfiltration ratio is not assessed, because it affects both the indicator and the reference signals.

In the following Fig. 3 reference and indicator conductivity signals are shown together with the hydrograph.

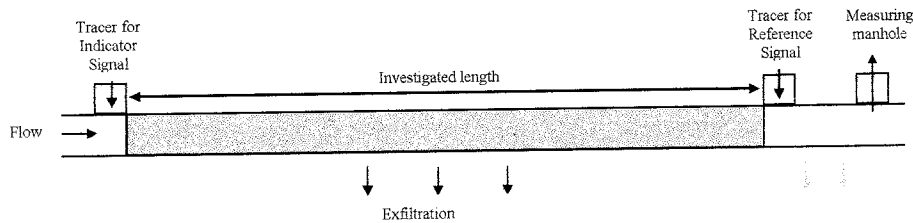


Fig. 2 - Conceptual scheme of the QUEST method (modified after [2]).

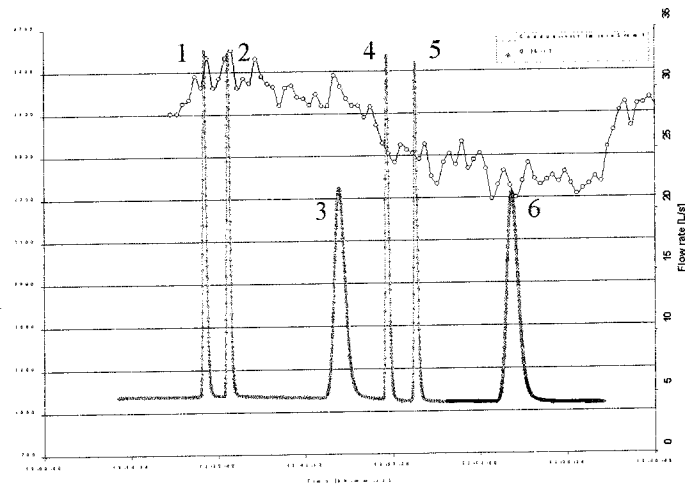


Fig. 3 - Graph of conductivity and flow rate vs. time. The peaks number 1, 2, 4 and 5 are the reference signals; the peaks number 3 and 6 are the indicator signals.

If the complete mixing occurs the exfiltration rate of tracer mass is equal to wastewater one, so the equation used for the calculation of exfiltration ratio is:

$$exf = 1 - \frac{M_{meas}}{M_{dosage}} \quad (1)$$

where  $M_{dosage}$  is the dosed NaCl amount [gr] and  $M_{meas}$  is evaluated by the following equation:

$$M_{meas} = \int_{span\_ind.} Q(t) * e * (C(t) - C_{baseline}(t)) dt \quad (2)$$

in the equation (2) *span ind.* indicates the time during which the conductivity peak of indicator signal passes through the measuring manhole;  $Q(t)$  is the flow rate during the indicator peak passage [L/s];  $C(t)$  is the indicator signal conductivity measured [ $\mu\text{S}/\text{cm}$ ];  $e$  is the conversion coefficient evaluated in the laboratory ( $e = 0.0006 \text{ gr} \cdot \text{cm}/\text{L} \cdot \mu\text{S}$ ) and  $C_{baseline}(t)$  is the background conductivity of wastewater during the indicator peak passage [ $\mu\text{S}/\text{cm}$ ].

#### 4. Experiment set up

The set up of the experiment concerned the dosage procedure, in particular: (i) where to dose the tracer for the indicator and reference signals along the investigated reaches; (ii) where to measure the conductivity; (iii) how much tracer to dose; (iv) if to overlap the reference and the indicator signals.

About the first and second points above, the manhole where to dose the tracer and where to measure the concentration don't only depend on the investigated part of the sewer, but also on the location of point inflows. Thus a system of continuity and tracer mass balance equations should be developed. For the our investigated sewer that system was written in order to define the location of the dosage points and the measuring one §[4.2]. A critical aspect is the model of the flow, so before solving the system different  $Q(t)$ -functions were studied §[4.1] and then used to evaluate the exfiltration ratio by (2). The results are discussed in §[5]. The model of the flow rate from which the exfiltration ratio evaluated were more reliable on the basis of the structure state of the pipes was used to solve the system in §[4.2].

The dosed amount of tracer has to be determined considering that the peak-baseline ratio has to be as high as possible, and meanwhile the precipitation of salt has to be avoided (360.00 gr/L at 20°C [4]).

Regards to the fourth point above, the analysis of baseline and discharge trend were carried out. The natural conductivity of wastewater and the flow rate were recorded on three days in order to define the period in the day when they were as steady as possible. In this period it is possible not to overlap the peaks, because the baseline can be modeled satisfactorily with a linear function and the unknown flow during the indicator passage can be obtained from the reference peaks measured just after and before the indicator one. An advantage of QUEST without overlapping is that the peak fitting is not to be used [2], but some pre-tests are to be carried out in order to determine the shape of the peak at the end of each investigated reach. The peak shape is necessary to evaluate the time interval between two subsequent dosages.

##### 4.1 FLOW RATE MODELS

The models used for the flow rate during the indicator passage are built using data from both reference peaks and in-line probe for discharge measurement. The models are:

1. mean value of flow rate measured by reference peaks (see Fig. 4 - a);
2. linear regression between the mean value of flow calculated from the two

reference peaks before the indicator peak and the two peaks after it (see Fig. 4 - b). The equation for the calculation of flow rate from the reference peak is:

$$Q_{ref} = \frac{M_{ref}}{\int_{span\_ref} (C(t) - C_{baseline}(t)) dt} \quad (3)$$

3. discharge measured by means of submerged probe (see Fig. 4 - c);
4. discharge measured by means of probe corrected by a factor  $\bar{K}$  (see Fig. 4 - d):

$$K_i = \frac{Q_{ref\_i}}{Q_{meas}(\Delta t_{Q_{ref\_i}})} \quad (4)$$

i = 1 : number of reference peaks

$$\bar{K} = \frac{\sum_{i=1}^{n\_ref} K_i}{n\_ref} \quad (5)$$

Each model above (called the Q(t) function) is used in equation (2) to estimate the exfiltration ratio. The first model and the second one are to be used when is not possible to measure by means of in-line probes. In particular, the first one is suitable when the flow is quite stable; instead the second one when the flow rate is quite variable. The third is to be used when the discharge is quite variable and it is possible to install flow-measuring devices. The fourth is applicable when it is possible install the flow-meter, but an accurate calibration of it is not possible.

#### 4.2 SYSTEM

The system of equations consists of three continuity equation, three mass balances and three exfiltration ratio equations. They were:

The equations written for our investigated sewer in Fig. 5 are:

$$Q_1 = Q_2 + Q_{12} = Q_2 + exf_{12} * Q_1 \quad (6)$$

$$Q_3 = Q_4 + Q_{34} = Q_4 + exf_{34} * Q_3 \quad (7)$$

$$Q_3 = Q_2 + Q_5 - Q_{23} = Q_2 + Q_5 - exf_{23} * (Q_3 + Q_5) \quad (8)$$

$$M_{ij} = M_j + exf_{ij} M_i \quad i = 1:3; j = 2:4 \quad (9)$$

$$exf_{ij} = \frac{M_{ij}}{M_i} \quad i = 1:3; j = 2:4 \quad (10)$$

where:  $Q_1$  = flow rate inlet [L/s];  $Q_2$  = flow rate measured at point 2 [L/s];  $Q_3$  = flow rate measured at point 3 [L/s];  $Q_5$  = flow rate inlet from the lateral inflow [L/s];  $Q_4$  = flow rate measured at point 4 [L/s];  $M_1$  = tracer mass dosed [gr];  $M_{2,3,4}$  = tracer mass measured [gr];  $Q_{12}$  = exfiltration rate from the first reach;  $Q_{23}$  = exfiltration rate from the node;  $Q_{34}$  = exfiltration rate from the second reach;  $exf_{12}$  = exfiltration ratio from

the first reach;  $\text{exf}_{23}$  = exfiltration ratio from the joint;  $\text{exf}_{34}$  = exfiltration ratio from the second reach.

The hypothesis of the model is assuming the complete mixing of tracer at 100 m about from the injection manhole thus from this point the loss of tracer is equal to the loss of wastewater.

As the grades of freedom are five, five values are to be determined by the experiments. The set up of the experiment (see Fig. 5) was: (1) measurement at point 2 in order to determine  $M_2$  and  $Q_2$  by dosing the tracer in point  $I_1$  and in point  $R_2$ ; (2) measurements in point 3 in order to determine  $M_3$  and  $Q_3$  by dosing the tracer in point  $I_1$  and in point  $R_2$ ; (3) measurements in point 4 in order to determine  $M_4$  by dosing the tracer in point  $I_1$ .

## 5. Results

The results concern three experimental campaigns carried out for the application of the QUEST method [2]. The dosed tracer masses were chosen in order to have the peaks of 2-3 times higher the average value of the baseline, while the concentration of tracer solution was 130 gr/L considering a limit concentration of 360 gr/L at 20°C into water [4]. In Table 1 the results of the three experiments evaluated using different models of the flow are shown. Because the exfiltration ratio calculated considering the mean values of  $Q$  by reference peaks are more reliable for the good state of the structure of the pipes, then the system of the equations §[4.2] was solved using this model of  $Q(t)$ -function. The exfiltration ratio for the part before the node and after it are shown in Table 2.



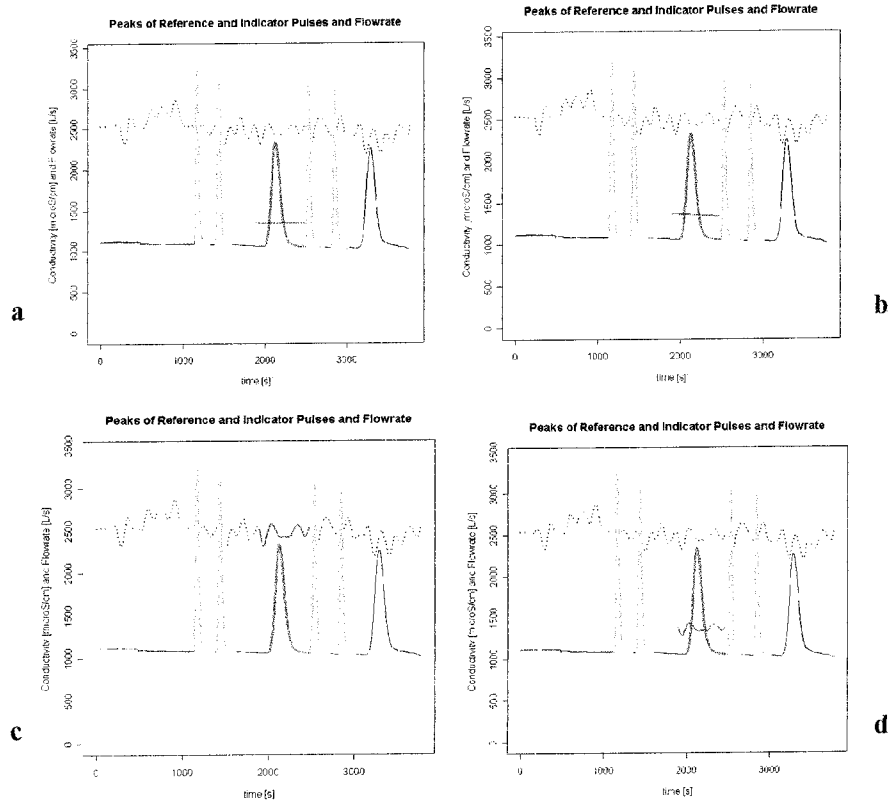


Fig. 4 - Conductivity [ $\mu\text{S}/\text{cm}$ ] and flow rate [ $\text{L}/\text{s} * 100$ ] vs. time [s]. The four pictures shown different ways to estimate  $Q(t)$  during the passage of the indicator peak. a: the flow rate is the average value of the measured one by means of reference pulses; b: the flow rate is determined by linear regression of average values measured by means of reference pulses; c: the flow rate is measured by means of the probe; d: the values of measured discharge during i-reference peak passage are scaled by means of average value of factor  $k$  (equations (4) and (5)).

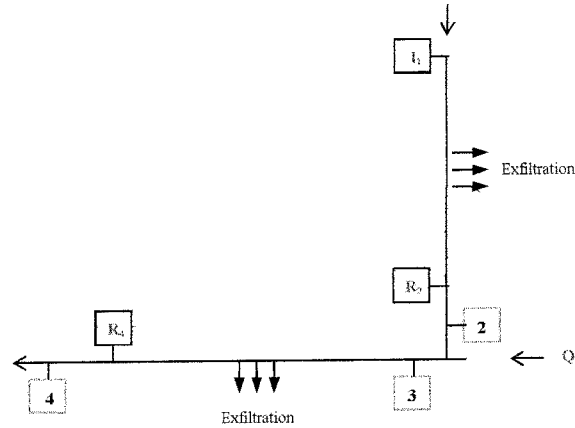


Fig. 5 - Scheme of investigated sewer network, the dosage and measuring manhole are indicated.  $I_1$  = tracer dosage for indicator signal;  $R_2$  = tracer dosage for reference signal; 2,3 and 4 = measuring points,  $Q_5$  = lateral inflow.

Table 1- Exfiltration ratio [%] evaluated for the entire tested system.

	Q mean	Q Linear	Q measured	Q modified by mean K-factor
Experiment 100703	7.08	6.17	-116.150	12.25
Experiment 240703	0.2	0.53	-81.220	5.83
Experiment 300703	3.9	8.62	-66.15	5.89
mean	3.73	5.11	-87.84	7.99
st.dev.	2.81	3.39	20.94	3.01

In Table 2, the results of the model A and B, respectively, are shown.

Table 2 - Exfiltration ratio [%] evaluated for the two tested reaches

	10th July 2003	24th July 2003	30th July 2003	Mean	st.dev.
First Reach	-0.123	-0.235	-0.211	-0.190	0.059
Second Reach	2.959	2.157	2.137	2.418	0.469

## 6. Discussion

In this paragraph the data shown in the Table 1 and 2 and the principal sources of uncertainty are discussed.

The results shown in Table 1 corresponds to the exfiltration ratio of the all investigated sewer, but calculated considering different  $Q(t)$ -functions. The values are very

changeable, but the high negative values are due to an overestimation of discharge due to systematic errors of the measurements. The results change into the same campaign because the equation (2) is very sensitive at the  $Q(t)$ -function, and into the same type of  $Q(t)$ -function because there are several factors that affect the exfiltration discharge. Some of these factors really change the leakage (e.g. the wastewater level, soil saturation, etc.) while some other ones are due to the sources of uncertainty, as below:

1. Peak shape
2. Peak distance
3. Natural conductivity of wastewater (baseline)
4.  $Q(t)$ -function during the passage of the indicator peak
5. Solid material in the flow (e.g. toilet paper, plastic, etc.) and turbulence
6. Tracer mixing

So particular care is to be taken to reduce the effect of these factors.

#### Peak shape and peak distance in time

In order to reduce the uncertainty in the definition of the start and the end of the peaks some pre-tests have to be carried out before the experiment on the investigated reach. Furthermore, from these pre-test the duration of the peak have to be determined in order to avoid the peak overlap and to decide the time for the tracer solution dosage during the experiment. The experiment duration has to be as short as possible because shorter is the experiment, smaller is the variability of natural conductivity and flow rate during a quasi-steady period of the day.

#### Background conductivity

The errors due to the variation of the natural conductivity can be reduced if the experiment is carried out when the conductivity is steady. So the experiment was carried out when the maximum variability was  $100 \mu\text{S}/\text{cm}$ .

In equation (2) the function  $C_{\text{baseline}}(t)$  is unknown under the peak and it has to be modeled. The model used was a first order polynomial using 200 data points equally distributed before and after the peak (see Table 3). Since the number of the regression points influences the distance between the peaks, we didn't consider more than 200 data points in order to reduce the duration of the experiment as much as possible.

Table 3 – Real\* and estimated\*\* area under an indicator peak overlapped at natural conductivity background and the error [%] between the real area and the estimated one.

	Area under the peak [ $\mu\text{S}\cdot\text{s}/\text{cm}$ ]	Relative Error [%]
<b>Real Area</b>	190936.000	0
<b>Number of regression points</b>		
<b>200</b>	192243.613	0.680
<b>100</b>	192915.689	1.026
<b>50</b>	193205.760	1.174

\* It is calculated by mathematical subtraction between the peak and the background conductivity.

\*\* It is calculated by mathematical subtraction between the peak and the modeled conductivity.

### **Q(t)-function during the passage of the indicator peak**

The variability of the discharge during the experiment and the availability of a suitable point of the installation and calibration of the flow-meter determine the Q(t)-function in (2).

The equation (2) is very sensitive to the Q(t)-function (see Table 1). If no discharge measurement are available, the flow rate can be measured by means of the reference signals and the overlapping QUEST method is advisable. Otherwise, to apply the non-overlapping QUEST method a measurement on three or four days has to be carried out in order to find the period when the flow is steady. The more changeable the flow is, the less reliable are the flow values calculated by reference peaks just before and after the indicator peak are.

The manhole used for the measuring station allows the installation of the flow-meter, but the calibration was not accurate. In the experiment on 30<sup>th</sup> and 24<sup>th</sup> July the maximum variability of the discharge was 5 L/s while during the experiment on 10<sup>th</sup> July it was 12 L/s. Thus for the experiments carried out on 30<sup>th</sup> and 24<sup>th</sup> July, the reliable exfiltration ratio are those calculated considering as the flow rate averaged on the four references peaks as linear §[4.1]. For the experiments carried out on 10<sup>th</sup> July the reliable values are for Q(t)-function scaled by a K-factor §[4.1].

### **Solid material in the flow and turbulence**

Solid materials and air intrusion the conductivity measurements. So during the experiments a metal net was enveloped around the conductivity probe and the measuring cross section was far from nodes or drops.

### **Tracer mixing**

In order that the exfiltration values of the QUEST [2] to be reliable, the loss of the tracer mass have to be equal to the loss of wastewater, thus the length of the investigated sewer has to be ensured for the complete mixing. To confirm a complete mixing was occurred over the cross section at the measuring point two probes were installed and the coefficient of variation was 0.98 %, minimum value suggested by [3].

The magnitude of the values of the model A in Table 2 were expected because: the tested sewer pipes are quite new, the ground is with traffic load equal to zero, the surrounding soil is tuff, the ratio depth WW and highness pipe is low (Table 1). The negative values of the exfiltration ratio in the first reach are due to the errors occurring during the measuring and data analysis and they don't indicate any addition, because there are not house connections along the investigated pipe that might discharge the salt accidentally.

## **7. Conclusions**

This paper shows some preliminary results of the application of a novel method to measure the exfiltrations in the urban sewer system called QUEST and developed by EAWAG within European APUSS project.

For an application in Rome at a sewer in good structure state, the authors proved that this method allows assessing exfiltration in a speedy and economic way. These results have provided reliable exfiltration ratios, on the basis of sewer structural state. Even if QUEST method cannot replace the use of common survey systems (like CCTV) for

the exact localization of the damages in the pipes.

The authors highlight the importance of some pre-test (peak shape study, conductivity and flow rate measurements) and of a characterization of sewer to be investigated in order to reduce the uncertainty in the results of the models proposed.

### Acknowledgment

*We thank Mr. Tatti and Mr. Ronda of Water Research Institute IRSA-CNR for their valid and expert help and their availability during the experimental campaigns.*

*We want to thank the APUSS team of EAWAG for his invaluable help during the whole period of experiments and data analysis.*

*This study has been carried out within the framework of the European research project APUSS (Assessing Infiltration and Exfiltration on the Performance of Urban Sewer Systems) which partners are INSA de LYON (FR), EAWAG (CH), Technical University of Dresden (DE), Faculty of Civil Engineering at University of Prague (CZ), DHI Hydroinform a.s. (CZ), Hydroprojekt a.s. (CZ), Middlesex University (UK), LNEC (PT), Emschergenossenschaft (DE) and IRSA-CNR (IT). APUSS is supported by the European Commission under the 5th Framework Programme and contributes to the implementation of the Key Action "Sustainable Management and Quality of Water" within the Energy, Environment and Sustainable Development Contract n° EVK1-CT-2000-00072.*

### 8. Reference

1. Barrett, M. H.; Hiscock, M. K.; Pedley, S.; Lerner, D.; Tellam, J.; French, M. "Marker species for identifying urban groundwater recharge sources: a review and case study in Nottingham" *Wat. Res.* Vol.33, n.14, pp 3083-3097, 1999.
2. Rieckermann, J. and Gujer, W. "Quantifying exfiltration from leaky sewers with artificial tracers" *Proceedings of the International Conference on "Sewer Operation and Maintenance 2002"*, Bradford, UK, 26-28 November 2002.
3. Rutherford J.C. "River Mixing" Wiley 1994.
4. Perry, Robert H.; Green, D. "Perry's chemical engineers' handbook" sixth edition: McGraw-Hill, 1984.

## Annex 4

Prigiobbe, V.; Giulianelli, M. (2004).  
Experiment design of a novel method to assess exfiltration in sewer.  
Conference on Urban Drainage Modelling, Dresden,  
15th-17th September 2004.

# Design of experiments for quantifying sewer leakages by QUEST-C method

V. Prigiobbe\*\*\* and M. Giulianelli\*

\* CNR – Water Research Institute, Via Reno 1, 00198 Rome, Italy.

(E-mail: [m.giulianelli@irsa.rm.cnr.it](mailto:m.giulianelli@irsa.rm.cnr.it))

\*\* Department of Civil Engineering, University of Rome “Tor Vergata”, Via del Politecnico 1, 00173 Rome, Italy. (E-mail: [prigiobbe@ing.uniroma2.it](mailto:prigiobbe@ing.uniroma2.it))

## Abstract

The structural state of sewer pipe is a crucial problem in urban areas because infiltrations and exfiltrations can occur and consequently contaminate the surface and deep water bodies, respectively. In this paper the application of a new method to quantify the sewer leakages (called exfiltrations) with tracers during dry weather is discussed.

This method, called QUEST-C (*Quantification of Exfiltration from Sewers with the help of Tracers-Continuous Dosing*) and developed by EAWAG (CH) within the European project APUSS, allows to estimate the exfiltrations by a mass balance of chemical tracers dosed continuously in a wastewater stream of operating sewers.

In the paper, we sum up our experience from a number of field experiments in order to discuss the application of the method in the field, critically: (i) planning of the experiments; (ii) the reliability of the obtained results; (iii) the overall applicability of the method in an urban area.

Finally, some findings with regard to the practical application and recommendations are presented for the future development of the method.

## Keywords

Artificial tracer; exfiltration; sewer; leakages; uncertainty

## INTRODUCTION

The quantification of the sewer leakages can be an useful tool for assessing the sewer performances, that is the structural state of the pipe. The not watertight pipes should be substituted with new ones because the wastewater leakages transport in the urban environment (e.g. subsoil and groundwater) organic and inorganic pollutants.

This paper deals with the application in Rome by IRSA (IT) of a novel method that has been developed within the European project APUSS (*Assessing Infiltration and Exfiltration on the Performance of Urban Sewer Systems*) by EAWAG (CH) for quantifying the exfiltration in the urban sewer systems.

An experimental design by a general uncertainty analysis was approached for individuating the most critical variables of the applied model (Rieckermann et al., 2003A). The final aim of this kind of analysis was to understand how to measure the variables of interest in order to achieve reliable results and optimize the technical and economical efforts. Then, three experiments were carried out in an urban sewer network in Rome, and the results are shown and discussed.

## STUDY AREAS

The experiments were carried out on three reaches of a sewer network in an urban area in Rome, called Torraccia. In this area the sewer, dated thirteen years, is an egg-shaped combined system build in concrete material. The investigated reaches are 4-9 m under the ground level with a slope of 0.9 %.

In Figure 1 the tested reaches are shown, in particular: the Reach 1 is 400 m long and egg-shaped 120x210 cm, the Reach 2 is 482 m long and egg-shaped 120x210 cm and the Reach 3 is 680 m long and egg-shaped 180x120 cm.

All the pipes are in subsoil characterized by cracked tuff and pozzolan. The groundwater submerges the sewer pipes only during the wet weather and it is quickly drained towards a deeper aquifer for the high permeability of cracked tuff.

The principal differences among the investigated reaches are: the flow rate, the number of house connection and nodes, the traffic load and the vegetation. A summarizing description of the tested reaches in terms of these characteristics is in Table 1.

**Table 1.** Different features of the investigated pipes.

	Reach 1	Reach 2	Reach 3
Average Flow rate [L/s]	28.20 ± 1.97	19.97 ± 2.04	9.50 ± 1.35
Water depth [cm]	13.35 ± 1.97	7.59 ± 1.97	7.49 ± 1.97
Number of HC	0	0	23
Number of nodes	0	0	7
Traffic	No	No	Yes
Vegetation	Grass	Grass	Eucalyptus

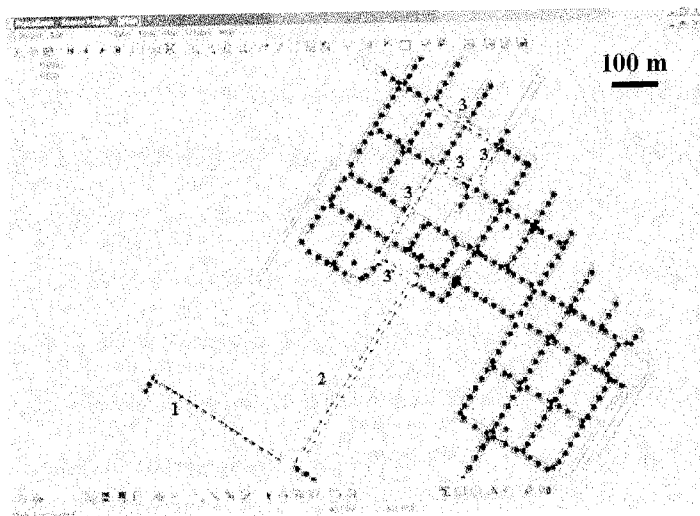


**Figure 1.** Scheme of the tested sewer network implemented in AquaBase software developed by Hydro Project and Hydro Inform (CZ) within European Project APUSS.

## METHOD QUEST-C

The method QUEST-C allows quantifying the exfiltration in urban sewer pipes (Rieckermann et al., 2003 A and B; Rieckermann et al., 2004). It consists of a continuous dosing of two different tracer solutions (LiCl and NaBr) at two different locations along a tested sewer. The LiCl solution has to be dosed for measuring the discharge at the beginning of investigated reach ( $Q_1$  in Figure 2), the NaBr solution has to be dosed for measuring the discharge at the end of investigated reach ( $Q_2$  in Figure 2). The wastewater samples taken at Manhole 3 are to be analyzed by means of IC in order to determine the  $Li^+$  and  $Br^-$ . The background concentration of  $Br^-$  is determined by sampling at Manhole 2.



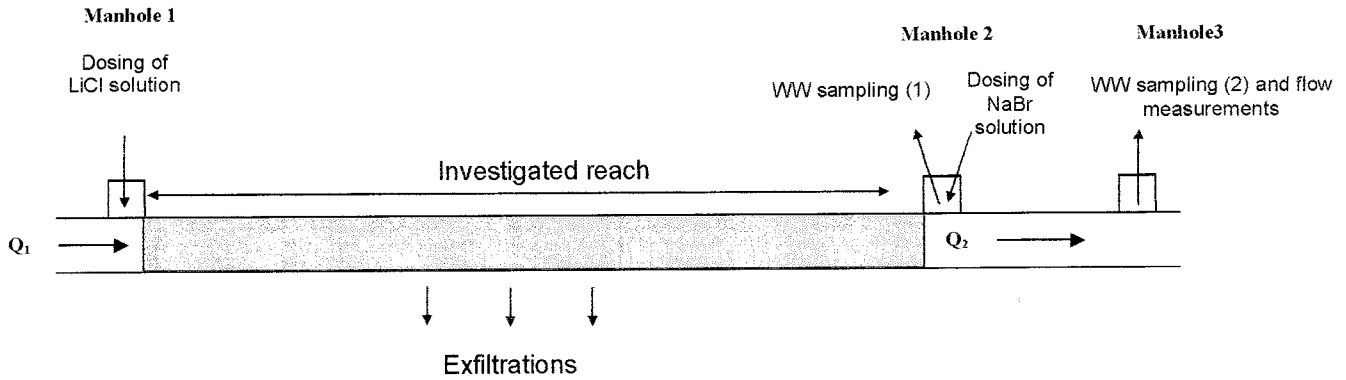


**Figure 2.** Scheme of tracer dosage and sampling of QUEST-C method (Modified from Rieckermann et al., 2003B)

The exfiltration ratio percentage is calculated by the following equation (1):

$$exf. = \left( \frac{Q_1 - Q_2}{Q_1} \right) * 100 \quad (1)$$

In particular, considering a steady flow the latter equation becomes:

$$exf. = \left( 1 - \frac{\frac{c_{solBr} * q_{solBr}}{C_{wwBr}}}{\frac{c_{solLi} * q_{solLi}}{C_{wwLi}}} \right) * 100 \quad (2)$$

where:  $c_{solBr(Li)}$  [mg/L] is the  $Br^-$  ( $Li^+$ ) concentration in the dosed solution;  $q_{solBr(Li)}$  [L/s] is the flowrate of the peristaltic pump dosing NaBr (LiCl) solution;  $C_{wwBr(Li)}$  [mg/L] is the concentration of  $Br^-$  ( $Li^+$ ) in the wastewater samples. The  $q_{solBr(Li)}$  is checked during the experiment in order to control the stability of the dosed tracer masses.

The equation (2) is applicable when the flow is quite steady during the trials, in this case Rieckermann et al. (2003B) estimated that the standard deviation of exfiltration ratio percentage changed between 2.4% - 2.6%, and Rieckermann et al. (2004) observed that it decreased at 0.5% as the flow rate variability was taken into account.

In the present paper the exfiltration ratio was calculated by the equation (2) because the flowmeter installation at the manhole 3 was not always possible, thus all the experiments were carried out in a period of the day chosen after measuring the flowrate for two days before.

### Measurements and analyses

The equipments used during the experiments are summarized in the Table 2 and differentiated on the grounds of the location of installation in Figure 2.

**Table 2.** Equipments used for the experimental campaigns

Manhole 1	Manhole 2	Manhole 3
Peristaltic dosing pump (Velp, mod. SO311)	Peristaltic dosing pump (Velp, mod. SO311)	Peristaltic sampling pump (Watson&Marlow, mod. SCIQ 323)
	Peristaltic sampling pump (Watson&Marlow, mod. SCIQ 323)	Flowmeter Area-velocity (SIGMA900 Max)*
		Each sample was filtered in the field by means of wathman filters with porosity 0.45 µm

\*The flow measurements need to check the flow variability.

The laboratory analyses for the determination of the  $\text{Li}^+$  and  $\text{Br}^-$  concentrations were carried out by means of Dionex Dx100 (anion column AS14 and cation column CS12).

The tracer concentrations in the dosed solution during the investigation were calculated by a mass balance on the basis of the solubility limits of NaBr and LiCl at 20°C in water, which are 905 gr/L and 832 gr/L, respectively. The dosage flow rates were calculated by a mass balance over the node knowing the average flow rate during the experiments from previous investigations (for two days about), the minimum detectable concentration by IC device and the solubility of NaBr and LiCl at 20°C in water.

### GENERAL UNCERTAINTY ANALYSIS FOR PLANNING THE QUEST-C EXPERIMENTS

Before the application of the QUEST-C method a general uncertainty analysis was carried out in order to plan accurately the experiments and for investigating if the tests were feasible with the proposed model (i.e. equation 2) by means of those equipments and in that experimental area.

Thus, for each variable in the equation 2, the UMCs (Uncertainty Magnification Factors) and the UPCs (Uncertainty Percentage Factors) were calculated. The first factors indicate the influence of the uncertainty in that variable on the uncertainty in the result, and the second ones (Uncertainty Percentage Factors) give the percentage contribution of the uncertainty in that variable to the squared uncertainty in the result (Coleman & Steele, 1999). In practice, let us consider the observation equation:

$$f = f(X_i) \quad (3)$$

where  $X_i$  is the vector of the measured variables. The UMFs and the UPCs for a equation (3) are defined as:

$$UMF_i = \frac{X_i}{f} \frac{\partial f}{\partial X_i} \quad (4)$$

$$UPC_i = \frac{\left( \frac{\partial f}{\partial X_i} \right)^2 (U_{X_i})^2}{(U_f)^2} * 100 \quad (5)$$

where  $U_{X_i}$  is the uncertainty of the variable  $X_i$  and  $U_f$  is the uncertainty in the result of the observation equation calculated by error propagation equation for a linear model of random variables statistically independent.

For our purpose the observation equation is the equation 2 and the UMF and UPC values were calculated for each variable after analyzing the sources of uncertainty that affect the QUEST-C method (Rieckermann et al., 2003B; Rieckermann et al., 2004) and the most important ones are summarised in the Table 3.

**Table 3.** Relevant sources of uncertainty for each variable in equation 2

	Preparation		Field application				Laboratory Analysis	
	Weight of chemical tracer	Dilution	Dosing of tracer solution	Adsorption on solid matter in sewer	Transport	Sampling	Storage of samples	Ion - Chromatograph
$C_{solLi}$	X	X	X					X
$C_{solBr}$	X	X	X					X
$Q_{solLi}$			X					
$Q_{solBr}$			X					
$C_{wwLi}$				X	X	X	X	X
$C_{wwBr}$				X	X	X	X	X

The paragraphs below discuss the applied methodology for quantifying the uncertainty from every source in Table 3. No difference between random and systematic uncertainties was taken in account at this stage, because we used the same equipments for measuring the similar variables in the numerator and in the denominator of equation 2 in order to minimize the systematic errors in the result. Generally spoken the ratio of two test results can have a lower systematic uncertainty than the systematic uncertainty in either of individual test results (Chakroun et al., 1993; Coleman & Steele, 1999).

### Preparation

The errors during the preparation of the chemical tracer solutions were principally due to:

- scale for weighting the solid tracer (i.e.: NaBr and CILi)
- graduated flask for the dilution of the solid tracer
- human

The scale (trade Sartorius mod. BL1500) had an accuracy of  $\pm 0.1$  gr. The graduated flask had an accuracy of  $\pm 0.4$  mL at  $20^\circ\text{C}$ . However, as the tracer solutions dosed during the experiment were analyzed by means of IC, the  $c_{solBr(Li)}$  parameters in Table 3 can only be affected by the uncertainty coming from the IC.

### Field application

#### Dosing of tracer solution

The dosage flow rates to be used during the tests were calculated on the grounds of the solubility of dosed tracers and the expected sewer discharge. The uncertainty during the tracer dosage could be due to:

- Instability on the dosing pump flow rate
- Stratification of the tracer in the bottle where it was stored

In order to estimate the errors coming from these two aspects, laboratory trials were carried out reproducing the field situation (e.g. the same pumps, the same tracer concentrations, the same bottles and the same pumping duration). Two calibrated bottles were put on two scales (trade OHAUS mod. GT4800) one with 50 grNaBr/L solution and another with 20 grLiCl/L one; the dosing pump flow rates were 50 mL/min and 12 mL/min, respectively. The level of the solution in the bottle and the weight were recorded for 70 minutes about.

No instability of the dosing pump flow rate and no tracer stratification were observed (Figure 3) at those concentrations for those tracers, at those pumping rates and duration. Anyway, the authors suggest recording the dosed tracer solution during the experiment in order to check the steady dosage that could be affected by possible pump inefficiency.

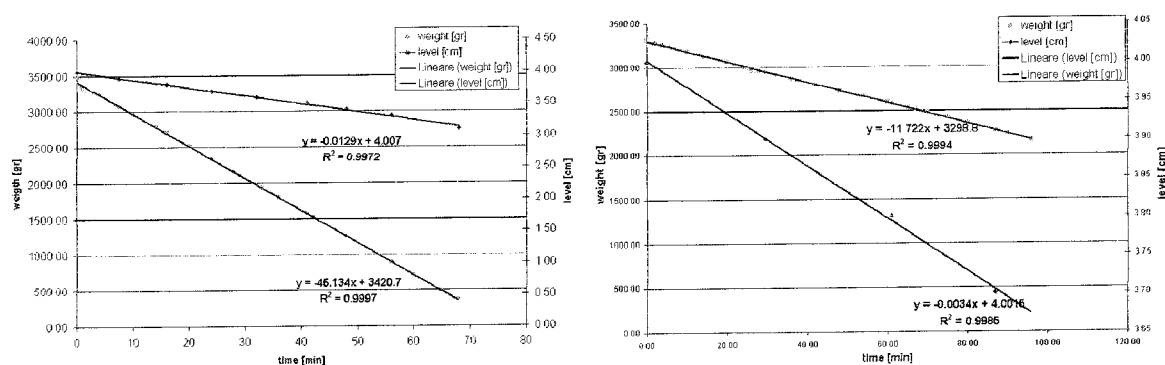


**Figure 3.** Weights and levels of tracer dosed solution in a tank vs. time, right graph for NaBr and left one for LiCl

### Adsorption

The tracer adsorption on the solid matter during the transport from the dosage manhole up to the sampling one in the sewer stream and on the biofilm that grows on the sewer wall was estimating in laboratory as by Ellis & Revitt (2003).

9.9 mgBr<sup>-</sup>/L were dosed into two beakers with 125 mL of raw wastewater in one of these biofilm (2.5 gr of biofilm taken from the wall of the investigated reach) was dispersed inside, too. The same test was separately carried out with 3.3 mgLi<sup>+</sup>/L. The duration of the trials was 120 min about. The results in Figure 4 show that the adsorption could be neglected in the beakers with WW for both chemical tracers, but the concentration decreases of 2 mg Br<sup>-</sup>/L in those ones with Br<sup>-</sup>, WW and dispersed biofilm.

The results show at these concentrations that the loss for adsorption onto bio-solids is 2 mgBr<sup>-</sup>/L, so it was advisable to reduce it, anyway as the maximum residential time of Br<sup>-</sup> in the tested sewer was estimated equal to 7 minutes about the adsorption on the solids could be considered negligible.

The adsorption during the storage period was not considered because the wastewater samples were immediately filtered in the field by means of filters with 0.45μm of porosity.

### Transport

The tracer transport can affect the exfiltration results because of the waves which might be due to sudden discharges in the urban catchment. The wave propagates faster than the average flow velocity (Henderson, 1966) and Huisman et al. (2000) showed experimentally that in sewer system the

hydraulic wave separated from the fluid. Thus if a wave is labelled with the tracer the celery causes the wave to travel faster than the dosed tracer solution that had labelled it and then the flowrate measured is uncorrected.

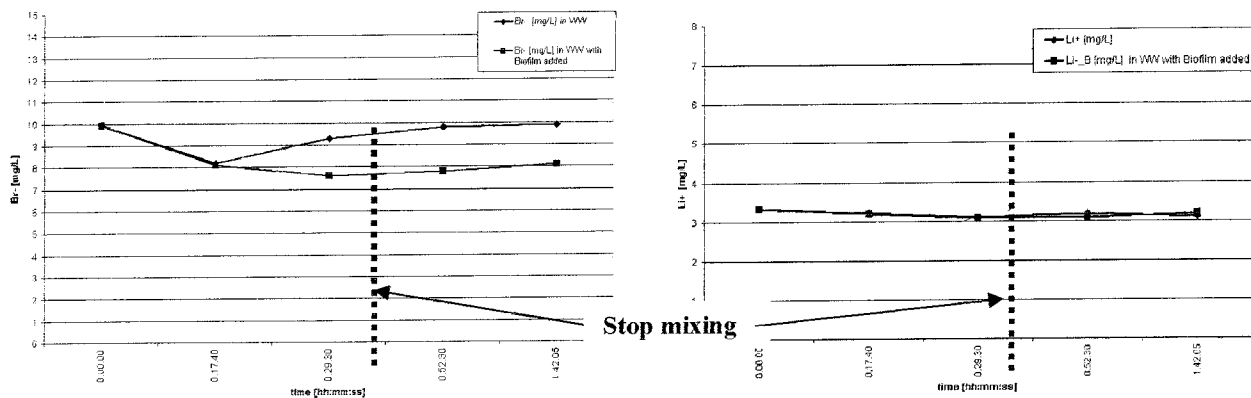


**Figure 4.** Tracer concentration vs. time; right graph for  $\text{Br}^-$  and left one for  $\text{Li}^+$

In Rieckermann et al. (2004) a dynamic analysis of the QUEST-C was approached in order to assess the error due to the transport in the resulting exfiltration ratio. From this analysis a systematic error of 0.2% and a standard deviation of 0.8% was computed. Thus, in order to reduce the uncertainty coming from the transport previous measurements of the flow rate should be carried out and the period when the discharges are quasi-steady would have to be chosen for investigations (Figure 5). Otherwise, the discharge values should be considered in computing the exfiltration ratio.

In order to quantify the error due to the transport only, one of the reach (i.e. Reach\_1 in Figure 1) was modelled with AQUASIM software (Reichert, 1994). The simulations consisted of virtual application of QUEST-C method, dosing 50 grLiCl/L and 20 grNaBr/L and flow rates 50 mL/min and 20 mL/min, respectively. The roughness coefficient ( $K_s = 55 \text{ m}^{1/3} \text{ s}^{-1}$ ) and the dispersion coefficient ( $D = 0.1 \text{ m}^2 \text{ s}^{-1}$ ) were calculated by parameter estimation tool in AQUASIM using concentration peaks of a slug dosage of NaCl tracer and measured discharge, the grid space for the calculation was 0.50 m (Di Giulio, 2003). At first in order to find out when investigating with low disturbance by flow variability the Reach 1 was tested with several 90 minute long flow trends, without any inflow/infiltration and exfiltration. The more accurate results were obtained with the flow pattern from 10.00 a.m. to 11.30 a.m.. The standard deviations of  $\text{Li}^+$  and  $\text{Br}^-$  concentrations during this period were used for UMP and UPC computations (Table 5).

Then, further simulations were carried out with this flow pattern, but exfiltrations of 0.5 L/s and 3.0 L/s and inflows of 5.0 L/s and 20 L/s were imposed and located along the investigated sewer as in Figure 5 (Table 4). The aim was to quantify the error in the exfiltration ratio when a dilution occurs for constant inflow/infiltration.

From the previous simulations on the Reach 1 and from the results in Table 4 the following observations can be argue:

- Lower flow variability and smaller losses, higher the accuracy of the results
- Higher constant inflow/infiltration, smaller the accuracy of the results. Consequently the method could be applied in the night on the urban sewer with sufficient water depth and whenever on the main sewer.
- The exfiltration ratio is very sensitive to the relative location of the exfiltration and inflow/infiltration because of the dilution of the stream labeled by the indicator tracer.

### Sampling

As the tracer has to be fully mixed at the measuring cross section, a sufficient mixing length has to be provided. For non-buoyant tracers a recommended mixing length in river is  $100-300 \cdot d$  ( $d$  is water width) (Rutherford, 1994). In particular, for the investigated reaches called 1, 2 and 3 in Figure 1 the minimum mixing lengths were 130 m, 75 m and 75 m, respectively.

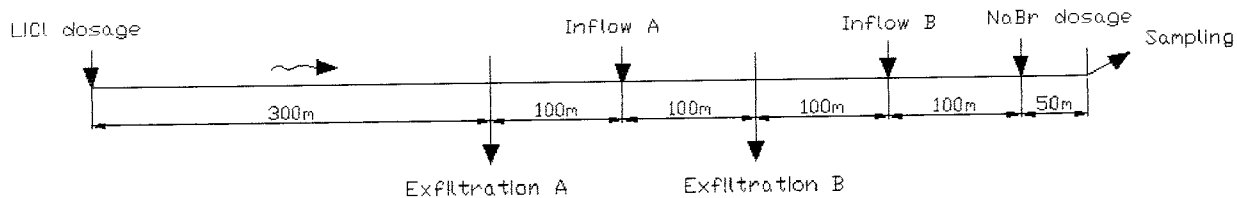


**Figure 5.** Simulated pipe scheme

**Table 4.** Summary and results of simulations with AQUASIM (Reichert, 1994)

	Sim 0	Sim 1	Sim 2	Sim 3
Inflow A [L/s]	5.00	5.0	5.0	5.0
Inflow B [L/s]	5.00	0.00	0.00	5.0
Exfiltration A [L/s]	0.00	0.5	0.00	0.5
Exfiltration B [L/s]	0.00	0.00	0.5	0.5
True Exf. Ratio [%]	0.00	2.16	2.16	4.33
Calculated Exf. Ratio [%]	0.65±1.17	2.65±1.15	2.58±1.16	4.65±1.17
	Sim 4	Sim 5	Sim 6	Sim 7
Inflow A [L/s]	20.00	20.0	20.0	20.0
Inflow B [L/s]	20.00	0.00	0.00	20.0
Exfiltration A [L/s]	0.00	3.0	0.00	3.0
Exfiltration B [L/s]	0.00	0.00	3.0	3.0
True Exf. Ratio [%]	0.00	12.98	12.98	25.97
Calculated Exf. Ratio [%]	0.57±1.16	7.23±1.06	12.73±1.24	18.87±1.51

### Laboratory analysis

#### Sample storage

Samples of WW and dosed tracer solution were taken during the field experiments and then stored for some hours until some days in the refrigerator at +4°C. The WW samples were filtered with two filters (1.2  $\mu\text{m}$  and 0.45  $\mu\text{m}$ ) just after sampling in the field. Thus the concentration variation during the storage because of dissolved solids was neglected.

#### IC analyses

The laboratory analyses consisted of determining the  $\text{Li}^+$  and  $\text{Br}^-$  concentrations in the WW samples and the dosed tracer solutions by means of IC. The values were measured with 8÷10 % uncertainty (APAT-IRSA/CNR, 2003).

## RESULTS AND DISCUSSION

In Table 5 below the values of each considered source of uncertainty are shown. A example of UMFs and UPCs are in Figure 6, they concern a previous investigation of the Reach 1. As a matter of the fact, they change as the absolute values of the model variables vary. UMFs assume the same value for every parameter (Figure 6) and they are more than 1, the influence of the uncertainty in the variable is increased as it propagates through the equation 2 into the exfiltration ratio (Coleman & Steele, 1999).

**Table 5.** Standard deviation of each source of uncertainty

Parameters	Preparation		Field application				Laboratory Analysis	
	Weight chemical tracer [gr]	Dilution [mL]	Dosing of tracer solution	Adsorption on solid matter in sewer [mg/L]	Transport [mg/L]	Sampling	Storage of samples	Ion – Chromatograph [%]
$c_{Li}$	0.1	0.4	0					10
$c_{Br}$	0.1	0.4	0					10
$q_{Li}$			0					
$q_{Br}$			0					
$C_{Li}$				0.0	0.108	0	0	10
$C_{Br}$				0.0-2.0	0.016	0	0	10

From the UPCs calculation we obtained two different results (Figure 6):

1.  $C_{Br}$  is the principal source of uncertainty on the exfiltration ratio when the adsorption of  $Br^-$  on the solid matter is considered equal to the estimated value (Figure 4), consequently the exfiltration by equation 2 could be underestimated. Thus, the distance between the Manhole 2 and 3 should be calculated just for an accurate tracer mixing;
2.  $C_{Li}$  is the principal source of uncertainty on the exfiltration ratio when the adsorption of  $Br^-$  on the solid matter is neglected. This means the errors affecting  $C_{Li}$  (e.g.: transport and IC analysis) have to be carefully reduced. In order to reduce the effect of the transport the exfiltration ratio should be evaluated by the average concentrations of the tracers.

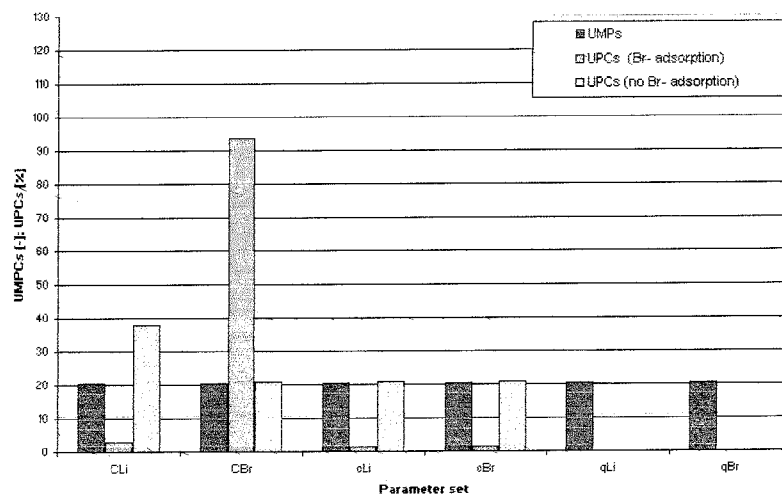


**Figure 6.** UMF and UPC values

In accordance to the discussion above three experiments were carried out in the Torraccia catchment to test the watertightness of the reaches in Figure 1 and in Table 6 the experiment settings and the

exfiltration ratio percentage computed by the average concentration of the tracers are summarized. In Figure 7 the trends of tracer concentrations and the flow rate are shown; each concentration value is referred to the  $\text{Li}^+$  and  $\text{Br}^-$  content in the sample taken for 10 minutes as from the indicated beginning. In Figure 7.A and C the flowrate was recorded at Manhole 3 while in the Figure 7B at Manhole 1.

**Table 6.** QUEST-C experiment setting and exfiltration ratio percentage in the investigated reaches

	Reach 1	Reach 2	Reach 3
cLi [gr/L]	18.04	20.10	24.22
cBr [gr/L]	50.35	58.86	50.98
qLi [mL/min]	62.61	45.43	28.44
qBr [mL/min]	62.91	36.32	23.75
<b>Exfiltration [%]</b>	<b>-8.69±0.62</b>	<b>-1.73 ± 4.69</b>	<b>20.80 ± 4.46</b>

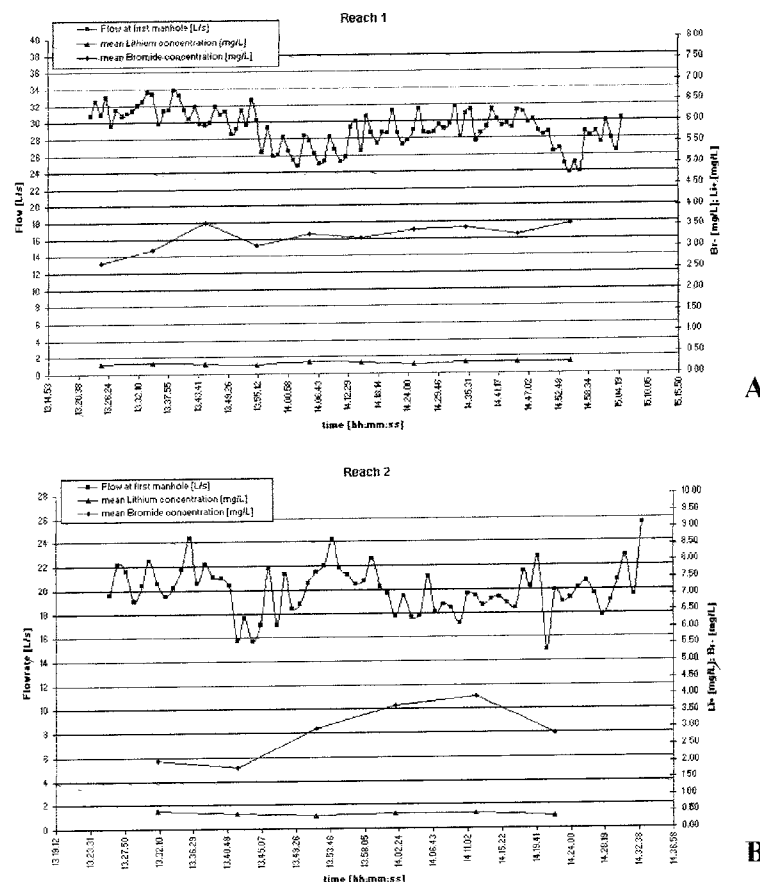


**Figure 7.** Tracer concentrations and flow rate vs. time. A. test on reach\_1; B. test on reach\_2; C. test on reach\_3.



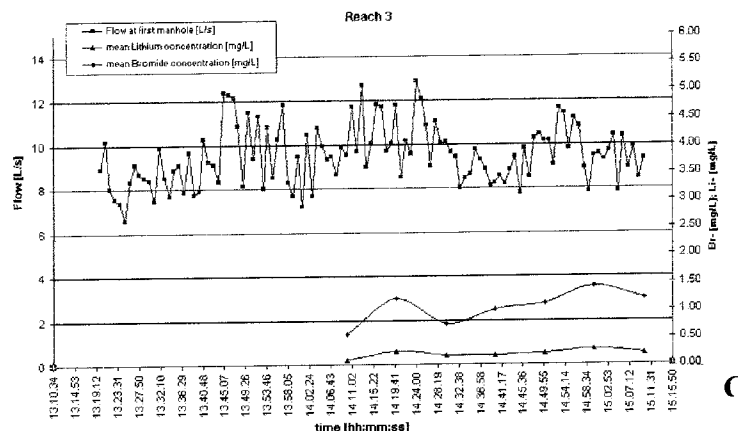


Figure 7. continues

The computed exfiltration ratios in Table 6 show two negative values. The negative exfiltration from the Reach 1 can very likely be due to some illicit Lithium discharges in the sewer during the experiment because of the strong deviation from zero that is more than the uncertainty estimated (Rieckermann et al., 2004).

Instead the negative absolute value of exfiltration ratio in Reach 2 is within the uncertainty value of the QUEST-C results, then we can assume that the exfiltration from this pipe was negligible during the investigation, as matter of the fact the expected value was zero because of the good structural state of sewer.

Finally, the high exfiltration ratio computed for the Reach 3 means that there are some important damages along the investigated pipes, but it is difficult to say if the calculated value is representative of the structural damages.

## CONCLUSION

In this paper a critical approach for the application a novel method called QUEST-C and developed in the European Project APUSS by EAWAG (CH) which allows to quantify the exfiltration in the urban sewer network is presented.

A general uncertainty analysis was carried out for individuating the most critical variables in the model applied was used. Specifically, the analysis was done using numerical data from a experiment carried out in a catchment in Rome in order to design the experiments to be done in this catchment, with the same equipments and tracers. Every considered source of uncertainty was studied individually and specifically for our experiment sets (e.g.: wastewater quality, sewer geometry, concentration of dosed tracer solution etc.), and then three experiments were done in accordance with the results of the general uncertainty analysis.

The experiments distinguished by the number of inflows along the investigated pipes, as a matter of the fact two reaches could be compared to a main sewer pipe and one to an urban sewer pipe.

The calculated exfiltration ratio percentage were for the two tests in accordance with the expected results because of the estimated structural state of the pipe.

Finally, the QUEST-C method allows assessing reliable leakage values for reaches like main sewer (e.g. low inflow compared to the main stream), but the results seem to be affected by small accuracy when many inflows are along the investigated reach as happens in urban area sewer or in sewers partly submerged by groundwater.

## Reference

- Asano T., Maeda M. and Takaki M. (1996). Wastewater reclamation and reuse in Japan: overview and implementation examples. *Wat. Sci. Tech.*, 34(11), 219-226.
- Chakroun, W.; Taylor, R. P.; Steele, W. G.; Coleman, H. W. (1993). Bias Error Reduction Using Ratio to Baseline Experiments-Heat Transfer Case Study, *Journal of Thermophysics and Heat Transfer*, vol. 117, No. 4, Oct.-Dec. 1993, pp. 754-757.
- Coleman, W. H.; Steele JR, W. G. (1999). *Experimentation and Uncertainty Analysis for Engineers*-Second Edition. John Wiley & Sons, INC., USA.
- Di Giulio, G. (2003). Quantificazione delle exfiltrazioni in fognature urbane mediante dosaggio in continuo di traccianti chimici. Thesis of graduation in Engineering for the Environment and the Territory, University of the Studies of Rome "Tor Vergata".
- Ellis, B; Revitt, M. (2003). Standard Protocols for Assessing the effect of the real sewer sediments and flow condition on the tracers. Deliverable 2.3 for the APUSS project by Urban Pollution Research Centre, Middlesex University.
- Henderson, F. (1966). *Open channel flow*. Macmillan, New York.
- Huisman, J.; Burckhardt, S.; Larsen, A.; Krebs, P. and Gujer, W. (2000) Propagation of waves and dissolved compounds in sewer. *J. of Environmental Engineering, ASCE*, 126 (1), 12-30.
- Istituto di Ricerca Sulle Acque (2003) Metodologie analitiche per il controllo della qualità delle acque. APAT e CNR/IRSA.
- Reichert, P. (1994). AQUASIM – A tool for simulation and data analysis of aquatic systems. . *Wat. Sci. Tech.*, 30: 21-30.
- Rieckermann, J. and Gujer, W. (2002) Quantifying exfiltration from leaky sewers with artificial tracers. *Proceedings of the International Conference on "Sewer Operation and Maintenance 2002"*, Bradford, UK, 26-28 November 2002.
- Rieckermann, J. and Bares, V. (2003-A). Documentation of a CONDOS experiment. Standard operation procedure. Deliverable 1.2. Exfiltration in APUSS project.
- Rieckermann, J.; Bareš, V.; Kracht, O.; Braun, D. and W. Gujer. (2003-B). Quantifying exfiltration with continuous dosing of artificial tracers. Pages 229-232 in *Hydrosphere 2003*, Brno, CZ.
- Rieckermann, J.; Bareš, V.; Kracht, O.; Braun, D.; Prigiobbe, V. and Gujer. W. (2004). Assessing exfiltration from sewers with dynamic analysis of tracer experiments. 19th European Junior Scientist Workshop "Process data and integrated urban water modelling" France 11-14 March 2004.
- Rutherford, J.C. (1994) *River Mixing*. John Wiley & Sons Ltd, London, U.K.

## Acknowledges

*This study has been carried out within the framework of the European research project APUSS (Assessing Infiltration and Exfiltration on the Performance of Urban Sewer Systems) which partners are INSA de LYON (FR), EAWAG (CH), Techn. Univ. of Dresden (DE), Faculty of Civil Eng. at Univ. of Prague (CZ), DHI Hydroinform a.s. (CZ), Hydroprojekt a.s. (CZ), Middlesex Univ. (UK), LNEC (PT), Emschergenossenschaft (DE) and IRSA-CNR (IT). APUSS is supported by the European Commission under the 5th Framework Programme and contributes to the implementation of the Key Action "Sustainable Management and Quality of Water" within the Energy, Environment and Sustainable Development Contract n° EVK1-CT-2000-00072. The project work of EAWAG is financially supported by the Swiss Federal Office for Education and Science (BBW).*

*Moreover, we want to thank the technicians Salvatore Tatti and Maurizio Ronda of IRSA-CNR, the ACEAATO2 S.p.A. and the student Agnese Ricci for the help during the experimental campaigns, the PhD Camilla Braguglia for the IC analyses.*

## Annex 5

Rieckermann, J.; Bareš, V.; Braun, D.; Kracht, O.; Prigiobbe, V.; Gujer, W. (2004).

Assessing exfiltration from sewers with dynamic analysis of tracer experiments.

19th European Junior Scientist Workshop “Process data and integrated urban water modelling” France 11-14 March 2004.

# Assessing Exfiltration from Sewers with Dynamic Analysis of Tracer Experiments

Jörg Rieckermann<sup>1</sup>, Vojtěch Bareš<sup>2</sup>, Daniel Braun<sup>3</sup>, Oliver Kracht<sup>1</sup>, Valentina Prigiobbe<sup>4</sup>, Willi Gujer<sup>1</sup>

## Abstract

Tracer methods are generally recognized as a possible tool to quantify exfiltration ratios, but the main criticism of these methods is the assumption of steady discharge and a missing uncertainty analysis. The authors present a novel approach for the dynamic analysis of a QUEST-C experiment that considers information on varying sewer flow. An assessment of uncertainty is developed that accounts for systematic and random errors in the measurements and the sampling scheme. It is shown that the precision of the exfiltration measurement with tracers can be significantly improved by the dynamic analysis.

## The quantification of exfiltration from sewers with tracers

Although urban sewer networks are built for longevity, damage occurs over time and the systems inevitably develop leaks. If such leaks are situated below the groundwater table, clean ground water may infiltrate sewer pipes; if the leak lies above the groundwater table, raw sewage may exfiltrate into the surrounding soil. As the quantity of exfiltration from sewers is an important variable in the assessment of these hazards, several attempts have been undertaken to develop measurement methods in the last decades.

Indirect methods try to deduct information on exfiltration from groundwater monitoring or a catchment-wide water balance. Direct measurements perform pressure testing on cracks or use tracer substances to identify leakage. Vollertsen et al. (2002) conclude:

*“The indirect methods for determination of the magnitude of the exfiltration are assessed to be based on such large a number of assumptions that they are considered non-conclusive. The direct determinations are based on measurement of very small differences in flow and are consequently difficult to perform with precision.”*

This indicates that the limiting factors for a successful application of the tracer methods are practical difficulties during the execution of the experiment. However, no detailed analysis of uncertainty of the computed exfiltration is reported in literature.

---

<sup>1</sup> Swiss Federal Institute of Aquatic Science and Technology (EAWAG) ) and Swiss Federal Institute of Technology (ETH) 8600 Dübendorf, Switzerland, e-mail: willi.gujer@eawag.ch

<sup>2</sup> Czech Technical University in Prague (CTU), Laboratory of Ecological Risks in Urban Drainage(LERMO), Thakurova 6, Prague 6, 166 29

<sup>3</sup> Swiss Federal Institute of Technology (ETH), 8093 Zürich, Switzerland

<sup>4</sup> Università degli Studi di Roma "Tor Vergata" Rome and IRSA CNR, Rome, Italy

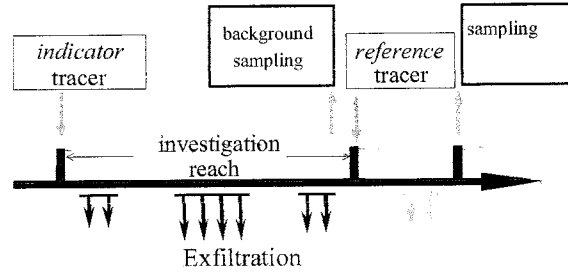


**Figure 1 Conceptual sketch of the QUEST-C method to quantify exfiltration**

In this paper, the QUEST-C tracer method is presented that aims at minimizing systematic and random errors by an optimal experimental and analytical setup. Results of a QUEST-C tracer experiment are presented and an assessment of uncertainty in the computed exfiltration is performed under the assumption of steady discharge. As this is a rather weak assumption, a novel approach for the analysis of QUEST-C experiments is presented that accounts for discharge variations.

### Exfiltration measurements with tracers

The basic principle of exfiltration measurements with tracers is to dose a well known amount of tracer to the sewer under investigation and to apply a mass balance on the investigation reach. Given conservative behavior of the substance, the tracer loss is directly related to the leakage in the reach. For practical applicability, the method must yield an accuracy of the computed tracer loss of a few percent, because exfiltration is supposed to be rather small. In order to obtain most accurate results, losses of the indicator tracer are mostly identified relative to a reference tracer which is not affected by exfiltration (Figure 1). Therefore, exfiltration from an experiment with an indicator tracer and a reference tracer (E) is expressed as a ratio relative to the labeled flow.

$$E = 1 - \frac{mass_{REF,in}}{mass_{IND,in}} \cdot \frac{mass_{IND,out}}{mass_{REF,out}} = 1 - \frac{\int c_{REF} \cdot q(t)_{REF} dt}{\int c_{IND} \cdot q(t)_{IND} dt} \cdot \frac{\int Q(t) \cdot C_{IND}(t) dt}{\int Q(t) \cdot C_{REF}(t) dt} \quad (1)$$

$c_{REF}$  and  $c_{IND}$  = tracer concentration of the dosing solution,  $q_{IND}$  and  $q_{REF}$  = dosing rates of the tracer solutions,  $C_{IND}$  and  $C_{REF}$  = tracer concentrations in the sample

Often, constant dosing pumps are used for a continuous dosing of the tracer solutions. This has the advantage that, if the discharge in the sewer is steady, the integrals in eq. (1) can be simplified because the constant discharge is crossed out and a single grab sample would be sufficient for exfiltration measurement.

Obviously, the computed exfiltration ratio is systematically wrong if the tracer concentrations are reduced or magnified in the sewer reach (e.g. adsorption or natural tracer background in the wastewater). Similarly, one has to account for a substantial random error if the analysis of the tracers in wastewater is not very precise. It might be for these reasons that early studies chose very specific tracer substances which are unlikely to be present in wastewater. (Ohlsen and Genders 1993) used radioactive

isotopes  $^{82}\text{Br}$  and Tritium, whereas Knudsen (1996) and Jensen and Madsen (1996) only report the use of “trace substances”. Most probably, fluorescent dyes like Naphthionate, Pyranine, Eosine, Sulforhodamine and Amidorhodamine G have been applied (Vollertsen et al. 2002).

The main criticism of these studies is that no assessment of uncertainty is documented. Especially, it is not clear if only the precision of the analytical procedure for tracer analysis is reported or if an extended analysis has been performed that also includes additional errors (e.g. pumping rates, sample dilution in the laboratory).

### **The QUEST-C method**

The QUEST-C method (Quantification of Exfiltration from Sewers with Tracers-Continuous dosing) was specifically developed with regard to an optimized management of uncertainty (Rieckermann et al. 2003). One key aspect of the method is that most systematic errors that occur in the field and in the laboratory are avoided by an optimal experimental procedure. Furthermore, it comprises a complete uncertainty analysis by linear error propagation. However, the data analysis is still based on the traditional assumption of constant discharge during the tracer experiment. As sewer flow is hardly ever steady, this is a critical assumption which will be investigated in this article.

#### Application study Rümlang, CH

A QUEST-C experiment was performed to quantify wastewater exfiltration in a trunk sewer at the village of Rümlang (CH). The diameter of the circular sewer is 0.9 m. The investigation reach was 643 m long, the total length of the section was 760 m. The average discharge during dry weather was  $24.4 \text{ l s}^{-1}$  with an average water depth of 0.11 m and a mean velocity of  $0.48 \text{ ms}^{-1}$ . The experiment was conducted from 11:00 – 13:30 which was identified as a period of almost steady flow from previous flow measurements. The investigation reach has no lateral inflows and is in very good structural conditions. The supposed watertightness makes it possible to check the computed result for bias.

#### Tracer substances

A  $15 \text{ g l}^{-1} \text{ Li}^{+}$  solution of Lithium Chloride was used as indicator tracer. The reference tracer was a  $25 \text{ g l}^{-1} \text{ Br}^{-}$  solution of Sodium Bromide. Important selection criteria for these tracers were a low background concentration in the wastewater matrix and the availability of an accurate analytical procedure. The natural background of Lithium in this sewer was negligible low. Bromide concentrations showed small fluctuations, which were corrected for by additional background sampling at the dosing point. All samples were analyzed by ion chromatography (IC) (Metrohm Compact IC). The IC showed a reproducibility of 1% of the measured value for  $\text{Li}^{+}$  and 0.5 % for  $\text{Br}^{-}$ . The results of laboratory batch tests suggest a conservative behavior of the tracers in wastewater and in the sample bottles. Lithium concentrations were not affected significantly after a storage period of two weeks. Non-filtrated samples showed 1.5% lower bromide concentrations; filtrated samples were not affected.

#### Equipment

Multi-channel peristaltic dosing pumps (ISMATEC BVK, ISMATEC MV-CA4) were used for the dosing of the tracer solutions. Both containers with tracer dosing solution

were placed on scales (OHAUS DP150) in order to record the pumping rates. Time-proportional composite sampling over 10 minutes was effectuated with further peristaltic pumps. The discharge during the experiment was measured with two flow meters based on the Doppler ultrasonic average velocity principle (SIGMA 950, American Sigma) which were installed at the end and the beginning of the sewer reach. The ratio  $\text{Br}^-/\text{Li}^+$  in the sample was measured together with a laboratory standard, which was prepared by mixing definite amounts of both tracer solutions on a precision scale in order to avoid systematic errors. The exfiltration ratio was calculated directly from the IC measurement readings, which are expressed as concentration equivalents ( $c_{eq}$ ). Together with the assumption of steady discharge, equation 1 is modified to:

$$E = 1 - \left( \frac{c_{eq,Br} w_{Li}}{c_{eq,Li} w_{Br}} \right) \cdot \frac{q_{Br}}{q_{Li}} \cdot \frac{C_{eq,Li}}{(C_{eq,Br-Br,back})} \quad (2)$$

$c_{eq,Br}$  and  $c_{eq,Li}$  = tracer concentration equivalents of laboratory standard,  $w_{Br}$  and  $w_{Li}$  = masses of tracer solutions in the laboratory standard,  $q_{Li}$  and  $q_{Br}$  = dosing rates of the tracer solutions,  $C_{eq,Li}$  and  $C_{eq,Br-Br,back}$  = tracer concentration equivalents in the sample

## Results

During the experiment two series of 10 samples were taken at the measuring point. The results of the first series, from which an average exfiltration ratio was calculated to -0.05 %, are presented in Figure 2. For series 2 we calculated -0.31 %. Considering all 20 samples of the two series, the estimated exfiltration ratio is -0.18 %. Because of the good structural condition of the sewer we expected the exfiltration to be zero which is in good accordance with the obtained results.

## Assessing uncertainty under the assumption of steady flow

The underlying concept of the QUEST-C method is to assess systematic errors where possible by redundant information. Random errors are calculated by Gaussian error

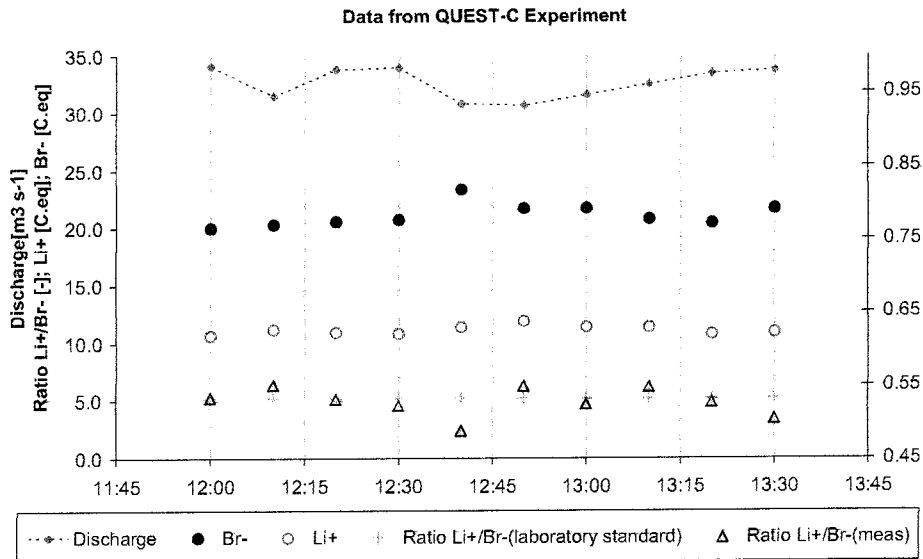


Figure 2 Concentration equivalents ( $\text{Li}^+$ ,  $\text{Br}^-$ ) and discharge from the QUEST-C experiment at Rümlang (sample series 1)

propagation on eq. (2) which hypothesizes steady flow. Details of the uncertainty analysis procedure are documented by Rieckermann et al. (2003), where the standard deviation in the computed exfiltration rate  $\sigma_E$  was computed to 2.4 % and 2.6 % for the two data sets. The largest error contributions were identified as those of the Bromide and Lithium concentration equivalents in the samples ( $C_{eq,Br}$  [69.7 %] and  $C_{eq,Li}$  [28.0 %]) and the concentration equivalents of the Lithium and Bromide standards ( $c_{eq,Lr}$  [0.9%] and  $c_{eq,Br}$  [0.01%]).

The Gaussian error propagation is a useful tool to identify the main error contributions, but the results are conditional on the assumption of steady discharge. When the variation of the tracer loads during the experiment is plotted (Figure 3), it can be noticed that the time-dependent fluctuations of the resulting exfiltration (black line) follow a certain pattern and are not random. As fluctuations in time cannot be accounted for in the steady state analysis, it is supposed that the computed error of 2% stems to some extent from the variability of the discharge over time. Consequently, the remaining stochastic uncertainty will be reduced if the model for exfiltration analysis properly considers the dynamics of the system.

### Dynamic analysis of the QUEST-C experiment: Including the discharge information

Although the tracer dosing rates were very constant during the experiment, variations in the ratio of tracer concentrations are observed (Figure 3). It must be noted that discharge fluctuations result in waves which travel at a higher speed than the main water body. Henderson (1966) estimates that kinematic waves travel with a speed of 5/3 of the mean velocity (assumptions: wide rectangular channel, constant friction coefficient). Generally spoken, this means that the two tracer substances that have been dosed to the same water element (which travels with a mean velocity) are diluted differently at the dosing point. Consequently, as very small error contributions in the order of a few percent are investigated, this effect blurs the precision of the computed exfiltration if eq.(2) is applied.

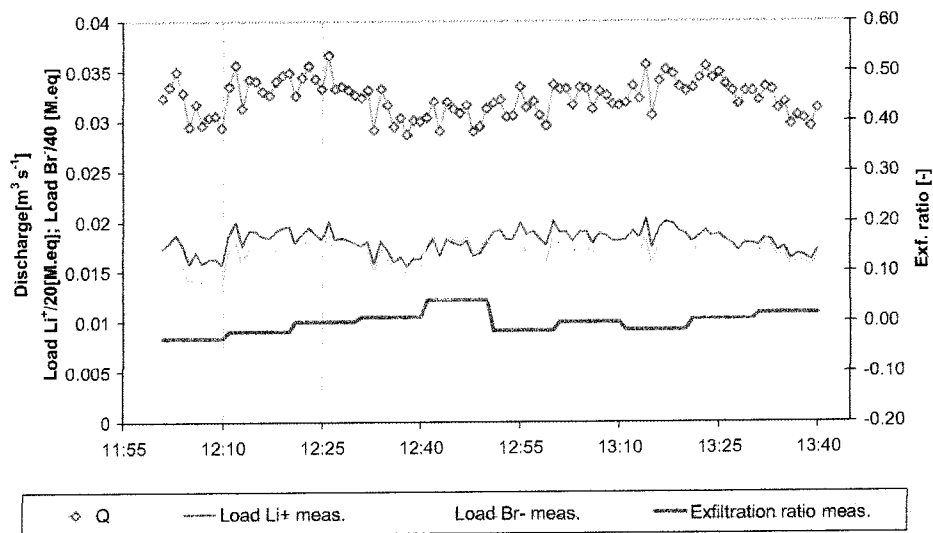


**Figure 3** Variation of the tracer loads during the experiment and the corresponding exfiltration ratio. The loads are computed from 10 min composite samples (series 1). They are presented in Mass equivalent units [ $M_{eq}$ ].



When information on the dynamic discharge is included in the QUEST-C method eq. (2) is modified to

$$E = 1 - \left( \frac{C_{eq,Br}}{C_{eq,Li}} \frac{w_{Li}}{w_{Br}} \right) \cdot \frac{q_{Br}}{q_{Li}} \cdot \frac{\int Q(t) \cdot C_{eq,Li}(t) dt}{\int Q(t) \cdot (C_{eq,Br-Br-back}) dt} \quad (3)$$

Applying eq.(3) is applied to data set 1, we compute an exfiltration of -0.12 %, which again is in accordance with our expectations. However, this intermediate result raises questions: what is the uncertainty in the computed exfiltration ratio and how can it be evaluated?

### Assessment of uncertainty for the dynamic analysis

We propose a Monte Carlo approach in which the uncertainty from the field and laboratory measurements (here: measurement error) and the uncertainty that results from the dynamic flow (here: transport error) are separated. It is assumed that the transport error is a) independent from the measurement error and b) additive to it.

Although from a conceptual point of view it should lead to more accurate exfiltration estimates, when further information is included in the data analysis, one must consider that additional errors are introduced, too. With regard to the discharge measurements we identified the following extra error contributions:

- **Errors in the flow measurements:** The devices used in this study compute the flow from Area-velocity measurements. Systematic errors in the level stem from an erroneous installation of the device and a false estimation of the sewer diameter. Random measurement errors affect the velocity readings and each water level measurement. As the sewer is circular the error contribution to the discharge is non-linear and is not cancelled out from eq. 3.
- **Errors in the tracer ratio in the samples from the starting point of sampling:** The starting point of sampling in the field always has an impact on the concentration ratio in the sample, because the varying discharge continuously causes fluctuations in the tracer concentrations. It depends on the experimental setup, the number of samples and the duration of sampling. Note: the longer the period of integration, the smaller is this error contribution.
- **Integration error by different time resolution of flow monitoring and sampling:** The tracer concentrations in the composite samples (10 min) have a different resolution than the flow data (1 min). For the computation of the load, a steady concentration over the sampling interval (Figure 5) is assumed. This also causes an error in the exfiltration ratio.

### Assessment of the measurement error

All error contributions for the individual model parameters have been summarized in Table 1. Almost all parameters of the error distributions are empirical estimates from the experimental data. Only  $w_{Li}$ ,  $w_{Br}$  and  $\nu$  were obtained from information of the manufacturer (scale and flow measurement device). The systematic and random error estimates on the water level ( $h_{syst}$ ,  $h_{rand}$ ) were assessed from practical experience. The systematic deviation of the diameter of the measuring cross-section  $d_{sewer}$  was

**Table 1 All error contributions for the model parameters of the exfiltration model (eq. (3)). All parameters were considered normal distributions with mean=0 and the specified standard deviations. (“n.c.”= not considered “—“ = not required)**

Parameter (p)	Unit	Description	$\sigma_{p, \text{systematic}}$	$\sigma_{p, \text{random}}$
h	[m]	water level measurement	$0.02/(3^{0.5})$	$0.006/(3^{0.5})$
$d_{\text{sewer}}$	[m]	sewer diameter	$0.015/(3^{0.5})$	--
$v$	$[m\ s^{-1}]$	velocity measurement	n.c.	$0.05\ v_{\text{meas}}$
$C_{eq, Li}$	[conc. eq.]	Standard concentration	--	0.032
$C_{eq, Br}$	[conc. eq.]	Standard concentration	--	0.069
$w_{Br}$	[g]	precision scale	--	2 E-04
$w_{Li}$	[g]	precision scale	--	2 E-04
$q_{Br}$	$[g\ s^{-1}]$	peristaltic dosing pump	n.c.	3 E-08
$q_{Li}$	$[g\ s^{-1}]$	peristaltic dosing pump	n.c.	9 E-08
$C_{eq, Li}$	[conc. eq.]	IC measurement, conc. equiv.	n.c.	$0.012\ C_{eq\ Li, meas}$
$C_{eq, Br}$	[conc. eq.]	IC measurement, conc. equiv.	n.c.	$0.005\ C_{eq\ Br, meas}$
$\Delta exf_{\text{transport}}$	[ - ]	transport error	assessed separately	

estimated from general assumptions on construction and the installation of the flow meter. In order to not over-predict error contributions from rectangular distributions, uncertainty estimates that reflect practical knowledge were considered to be normally distributed. After Evans et al. (2000) the standard deviation of a uniform distribution with  $[-a, +a]$  is transformed into the standard deviation of a normal distribution by

$$sd_{\text{rect}} = \frac{a}{\sqrt{3}} \quad (4)$$

2000 simulations of eq.(3) were performed for the Monte Carlo error propagation. The samples were drawn from the joint distribution of the model parameters without considering correlation of parameters or autocorrelation in time. First, the discharge was computed and the background subtraction was performed. Then, the discharge was multiplied with the corresponding tracer concentrations to compute the loads. Finally, the ratio of the integrated tracer loads and the input loads ratio are computed.

For the first series, the overall standard deviation in the estimated exfiltration due to the measurement error is computed to 0.5 % (Figure 4). The median of all simulation results is -0.1%. For the second series of samples we compute a standard deviation of 0.5% and a median of -0.3%.

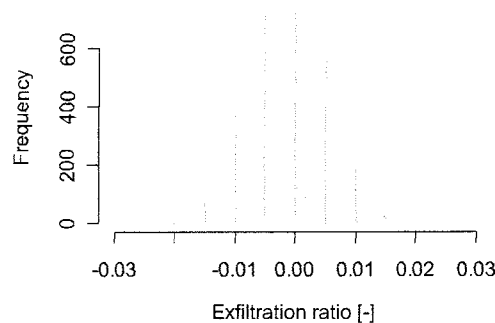


**Figure 4 Error contribution that results from the analytical procedure and the error of the flow measurement device (here: measurement error)**

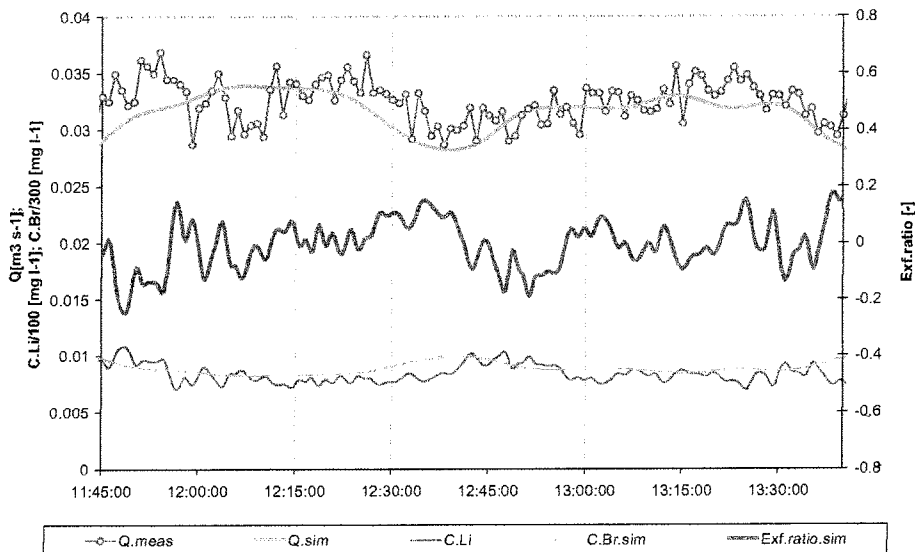


**Figure 5 Investigation of the transport error from hydrodynamic modeling**

#### Assessment of the transport error

As each reach has its transport characteristics (length, roughness, slope, etc.) a hydrodynamic model is needed to properly assess the error contribution of dynamic flow. A transport model of the Rümmlang sewer reach was implemented in AQUASIM (Reichert 1994) and calibrated by estimating the roughness coefficient ( $k_{st} = 80 \text{ m}^{1/3} \text{ s}^{-1}$ ) and the grid space ( $\Delta x = 0.25 \text{ m}$ ) from concentration and discharge data. A dispersion coefficient was not included in the model, because the grid size was chosen such that the numerical dispersion accounted for the real dispersion in the sewer system.

The Rümmlang experiment was modeled with the input data of discharge, pumping rates and the concentrations of the dosing solutions. The upper two graphs in Figure 5 show that the computed discharge is in good agreement with the data. It can also be seen, that Lithium and Bromide are affected differently by the dynamic flow pattern.

This indicates that in this specific constellation the magnitude of error by grab sampling can easily be in the order of 10%, whereas no preference for underestimation or overestimation of the exfiltration can be deduced. From this, it can be concluded that, even in periods with relatively low flow dynamics, grab sampling is worse than composite sampling.

In order to properly assess the dynamic error in the experimental results, a bootstrap resampling analysis was performed on the simulated discharge and tracer loads. From the composite samples it cannot be concluded whether the start of sampling in the Rümmlang experiment was a period of overestimation or underestimation of the exfiltration. Computing exfiltration from a large number of randomly-drawn time series of simulated loads and discharges allows for estimating the error contribution of dynamic transport and the starting point of sampling.

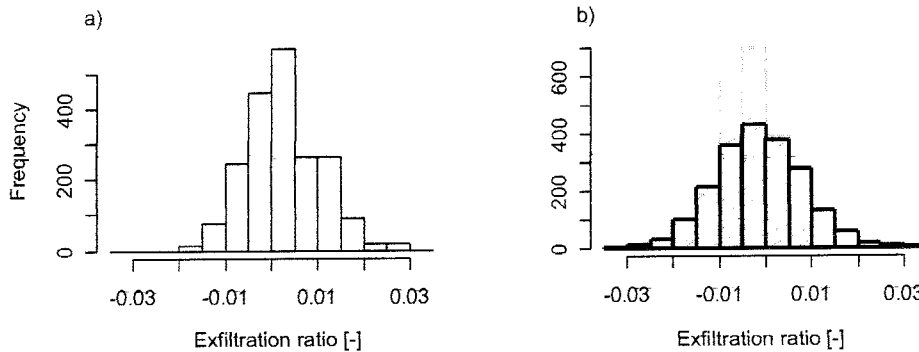


**Figure 6a: Estimated error contribution from the dynamic behavior of the system (here: transport error); 6b: Measurement uncertainty (grey) and combined uncertainty of both error contributions to the exfiltration ratio (black)**

For a more representative analysis, flow data from 6 subsequent days were used in the bootstrap procedure. In order to obtain reliable results, only the data in the time period of the experimental study were used for the data analysis. Eq. 3 was used to estimate the exfiltration from each data sample. From the computation of 1000 bootstrap simulations a median of 0.2% and a standard deviation of 0.8% was computed (Figure 6a).

#### Assessment of the combined uncertainty from measurements and dynamic transport

The combined uncertainty of the exfiltration ratio was computed under the assumption of additive errors (Figure 6b). From the samples of series 1 we estimate the exfiltration in the reach to 0 % (median) with an uncertainty of 1 % (expressed as one standard deviation). From sample series 2 we obtain the same values.

### **Discussion**

The dynamic analysis of this QUEST-C experiment at the sewer system of Rümmlang yielded a substantial lower uncertainty (1%) than the steady state analysis (2%). In general, this is a very promising result. However, it must be considered that the model uncertainty of eq. (3) has been assessed properly, but that minor effort has been put into the assessment of the uncertainty of the hydrodynamic computations. In order to assess the impact of the uncertain parameters ( $k_{st}$ ,  $\Delta x$ ), an error propagation on the results of the hydrodynamic model would be necessary. The model structure uncertainty is not fully accounted for by calibration; a cross validation of model results on further sewer data would increase the belief in the model results. The purpose of this paper is to indicate the emphasize and benefits of dynamic approaches to data analysis. Further analyses would have gone beyond the scope of this article.

For practical purposes it is considered beneficial to spend more resources in data acquisition and analysis when a high precision in exfiltration measurements is desired. Nevertheless, in this field study a special sewer reach with no connections was investigated. In cases with side-inflows, where upstream inflow measurement would be inconclusive, it may be possible to assess the inflows into the reach from the discharge data at the outlet of the system ("reverse modeling"). For the analysis of larger reaches or a whole sewer network it is therefore recommended that rather short reaches should be investigated. However, it must not be overlooked that the necessary mixing length must be provided. Rutherford (1994) recommends a length of  $300 \cdot d_{channel}$ .

## Conclusions

- In this paper, the authors showed that it is possible to accurately quantify exfiltration from sewers with the QUEST-C method. The discharge should be measured during each experiment and it is further recommended to include the information on the discharge in the analysis. Further, this study also highlights the importance of carefully choosing the optimal experimental time in order to avoid flow variations.
- On the one hand the uncertainty of computed exfiltration ratio is to a large extent dependent on the quality of the data (how careful is the experiment performed). On the other hand it depends on system intrinsic properties (baseline, flow, choice of tracer/measuring technique). For this reason, a general statement of the uncertainty of the methodology ((Ohlsen and Genders 1993), (Knudsen 1996), etc.) seems not reasonable. Ideally, an individual error assessment for each experiment according to the procedures discussed here should be performed and documented.
- It must be concluded that the choice of a very specific tracer does not necessarily improve the accuracy of the estimated exfiltration. It is also necessary to have an adequate model for data analysis.

## References

- Evans, M., N. Hastings, and B. Peacock. 2000. Statistical distributions, 3rd edition. John Wiley & Sons, New York.
- Henderson, F. M. 1966. Open Channel Flow.
- Jensen, A., and P. G. Madsen. 1996. Udsivning fra utætte kloakledninger. Stads og havneingeniøren:38-39.
- Knudsen, L., Andersen, U., Ørskov, P., Pedersen, C. M. 1996. Undgå forurening af drikkevandet. Stads og havneingeniøren:34-36.
- Ohlsen, B., and S. Genders. 1993. Udsivning fra kloakledninger. Stads- og havneingeniøren:5-58.
- Reichert, P. 1994. AQUASIM - A tool for simulation and data analysis of aquatic systems. Water Sci. Tech. **30**:21-30.
- Rieckermann, J., V. Bareš, O. Kracht, D. Braun, and W. Gujer. 2003. Quantifying exfiltration with continuous dosing of artificial tracers. Pages 229-232 in Hydrosphere 2003, Brno, CZ.
- Rutherford, J. C. 1994. River Mixing. Wiley.
- Vollertsen, J., K. Vorkamp, and T. Hvitved-Jacobsen. 2002. Udsivning af spildevand fra afløbssystemer. Miljøprojekt Nr. 685, Aalborg Universitet, Afdeling for Miljøteknik, Aalborg.

## Acknowledgements

The writers would like to thank the Swiss Federal Office for Education and Science (BBW) for financial support. This study has been carried out within the framework of the European research project APUSS (Assessing Infiltration and Exfiltration on the Performance of Urban Sewer Systems) which partners are INSA de LYON (FR), EAWAG (CH), Technical University of Dresden (DE), Faculty of Civil Engineering at University of Prague (CZ), DHI Hydroinform a.s. (CZ), Hydroprojekt a.s. (CZ), Middlesex University (UK), LNEC (PT), EmscherGenossenschaft (DE) and IRSA-CNR (IT). APUSS is supported by the European Commission under the 5th Framework Programme and contributes to the implementation of the Key Action "Sustainable Management and Quality of Water" within the Energy, Environment and Sustainable Development Contract n° EVK1-CT-2000-00072. The project APUSS is part of the CityNet, the network of European research projects on integrated urban water management.

## Annex 6

Prigiobbe, V.; Giulianelli, M. (2005).  
Application of a novel method for assessing the infiltration in an urban  
sewer system: case of study in APUSS project.  
Proposed for Water Science and Technologies.

# Application of a novel method for assessing the infiltration in an urban sewer system: case of study in APUSS project

Prigiobbe<sup>1,2</sup>, V. and Giulianelli<sup>1</sup>, M.

<sup>1</sup> Water Research Institute of the National Research Council (IRSA/CNR) Via Reno, 1 - 00198 - Rome – Italy  
([m.giulianelli@irsa.rm.cnr.it](mailto:m.giulianelli@irsa.rm.cnr.it))

<sup>2</sup> Civil Engineering Dept. of University of Rome “Tor Vergata” Via del Politecnico, 1 - 00173 - Rome – Italy  
([prigiobbe@ing.uniroma2.it](mailto:prigiobbe@ing.uniroma2.it))

## 1 Abstract

This paper presents the results of field applications of a novel method for quantifying the infiltration of parasitical water into sewer systems. The method bases on the hydrograph separation method with two components and uses as a conservative tracer  $\delta^{18}\text{O}$ . The two water components are groundwater (parasitical water) and drinking water (natural discharge into the investigated sewer systems). This method was applied at urban catchment scale for testing the effective water-tightness of two completely different sewer networks. An uncertainty analysis has done for experimental planning and an error propagation has been assessed by Monte Carlo simulations.

**Key words:**  $\delta^{18}\text{O}$ , infiltration, sewer system, hydrograph separation, uncertainty.

## 2 Introduction

Urban sewer systems are not watertight even if very high construction standards have been used applied for building them. The main causes of unwater-tightness have been studying in detail in the last years and can be grouped as follows (Gokhale and Graham, 2004):

- structural defects that include cracks, fractures, joint displacements, deformations and collapses;
- operational damages that include roots, siltation and blockage. The roots can cause structural damage as well as the opening of joints, while siltation can lead to blockage.

If the sewer pipes are not watertight, parasitical water (called infiltration) could enter into the system and/or leakages (called exfiltration) could be discharged into the surrounding environment. Both infiltration and exfiltration threat the natural water bodies (e.g., river, aquifer, ...) in an urban area.

This paper presents an application of a new method for quantifying the infiltration into urban sewer system during dry weather conditions. The method has been developed by Kracht (2003) within an European project called APUSS (Assessing Infiltration and Exfiltration on the Performance of Urban Sewer Systems). This method consists in the application on an urban area of the hydrograph separation method (Dincer et al., 1970, Martinec, 1975 and Fritz et al., 1976) with two components:

- Drinking water
- Groundwater

The resulting mixed water is the wastewater that flows into the sewer system.

The stable water isotope of oxygen  $\delta^{18}\text{O}$  is the conservative tracer used for distinguishing the sources and calculating the contribute from each one.

Anyway, for assessing the applicability of this method in an urban area accurate investigations have to be carried out beforehand.

Below, after a brief introduction of the method, the experimental design for the application of this method is described and the results of two field applications in Rome are finally discussed.

### 2.2 Method

The method applied in Rome for the quantification of the infiltration has been developed by Kracht (2003) is based on the separation of a wastewater hydrograph into two components using as a chemical tracer  $\delta^{18}\text{O}$ . The principle of this method is based on the contrast in the isotopic composition of the infiltration contributes and that of a given aqueduct. Given the total flow into a sewer as

$$Q_{\text{wastewater}}(t) = Q_{\text{foulwater}}(t) + Q_{\text{inf iltration}}(t) \quad (1)$$

where  $Q_{\text{wastewater}}(t)$  is the total flow measured at the outlet of an investigated urban sewer network [ $\text{m}^3 \text{s}^{-1}$ ];  $Q_{\text{foulwater}}(t)$  is the drinking water discharged into the sewer after the use [ $\text{m}^3 \text{s}^{-1}$ ];  $Q_{\text{infiltration}}(t)$  is the total contribute of infiltration to the sewer system under investigation [ $\text{m}^3 \text{s}^{-1}$ ]. Using as a natural tracer  $\delta^{18}\text{O}$  for tracing the two components, a mass balance can be written as

$$\delta^{18}\text{O}_{\text{wastewater}}(t) \times Q_{\text{wastewater}}(t) = \delta^{18}\text{O}_{\text{foulwater}}(t) \times Q_{\text{foulwater}}(t) + \delta^{18}\text{O}_{\text{infiltration}}(t) \times Q_{\text{infiltration}}(t) \quad (2)$$

where  $\delta^{18}\text{O}_{\text{wastewater}}(t)$  is the isotopic content of the wastewater after the mixing between the used drinking water and the infiltration [‰ vs. SMOW];  $\delta^{18}\text{O}_{\text{foulwater}}(t)$  is the isotopic content of the drinking water [‰ vs. SMOW];  $\delta^{18}\text{O}_{\text{infiltration}}(t)$  is the isotopic content of the infiltration contributes (e.g.: groundwater, springs, etc.) [‰ vs. SMOW]. Naturally, this method cannot assess the infiltration due to the water network leakages, because the contribution from the direct discharges or from the infiltration are not isotopically distinguishable.

By substitution for  $Q_{\text{foulwater}} = Q_{\text{wastewater}} - Q_{\text{infiltration}}$  and rearranging

$$Q_{\text{infiltration}}(t) = \left( \frac{\delta^{18}\text{O}_{\text{wastewater}}(t) - \delta^{18}\text{O}_{\text{foulwater}}}{\delta^{18}\text{O}_{\text{infiltration}} - \delta^{18}\text{O}_{\text{foulwater}}} \right) \times Q_{\text{wastewater}}(t) \quad (3)$$

and

$$R_{\text{infiltration}}(t) = \frac{Q_{\text{infiltration}}(t)}{Q_{\text{wastewater}}(t)} \quad (4)$$

where for  $\delta^{18}\text{O}_{\text{infiltration}}(t)$  and  $\delta^{18}\text{O}_{\text{foulwater}}(t)$  the spatial mean values have been considered and  $R_{\text{infiltration}}(t)$  is the infiltration ratio [-].

Before applying this method for estimating the infiltration going into a sewer system, the following hypotheses have to be verified:

- the tracer must be conservative during the water use and into the sewer system;
- the drinking water source must be unique;
- the difference between  $\delta^{18}\text{O}_{\text{foulwater}}$  and  $\delta^{18}\text{O}_{\text{infiltration}}$  must be more than a certain percentage based on the expected infiltration ratio (De Benèdittis and Bertrand-Krajewski, 2004);
- the infiltration contributes must have a low spatial variability over the drainage area otherwise the area must be divided into sub-catchments.

About the first point,  $\delta^{18}\text{O}$  content in each water component could change if fractionation and Raleigh distillation occur because of:

- Physical-chemical processes in open and closed systems (e.g., evaporation in washing machine or in sewer system);
- Redox reactions in open systems (e.g., organic matter oxidation in sewer system).

Concerning the physical-chemical processes as evaporation at the temperatures 10-25°C in sewer and 30-50°C in a washing machine, from the Figure 1 the fractionation coefficient ( $\alpha$ ) is around 1.01 (i.e., the formed vapour is always 10‰ lighter than the residual water), for that value of  $\alpha$  the Figure 1 shows the changes in the  $\delta^{18}\text{O}$  of water and vapour during evaporation in an open-system and in a closed-system. In both as evaporation progresses the  $\delta^{18}\text{O}$  of the remaining water becomes heavier and heavier, but the discrepancy between the vapour the remaining water fraction is more evident in closed system than in opened one.



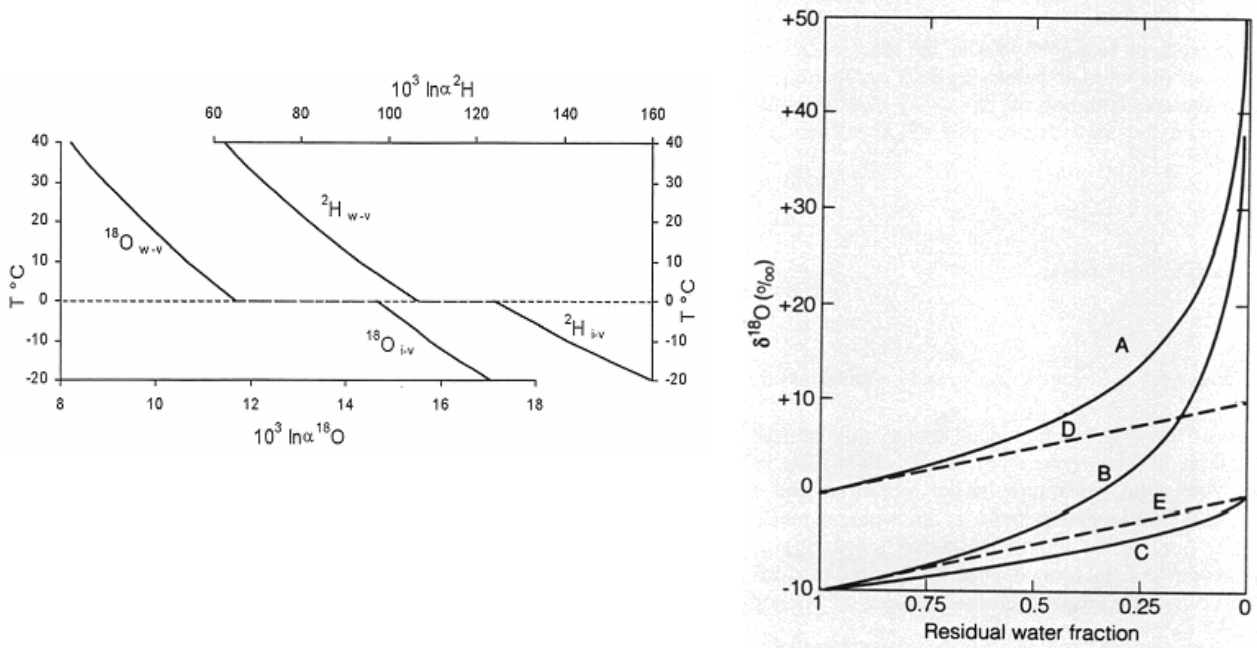


**Fig. 1** right: fractionation of  $^{18}\text{O}$  and  $^2\text{H}$  for water-vapour (from equations of Majoube, 1971) and ice-vapour (Majoube, 1971 and O'Neil, 1968) for temperature from  $-30 \div +50^\circ\text{C}$ . Left: isotopic change under opened- and closed-system Rayleigh conditions for evaporation with a fractionation factor  $\alpha = 1.01$  for an initial liquid composition of  $\delta^{18}\text{O}=0$ . The  $\delta^{18}\text{O}$  of the remaining water (solid line A), the instantaneous vapour being removed (solid line B), and the accumulated vapour being removed (solid line C) all increase during single-phase, open-system, evaporation under equilibrium conditions. The  $\delta^{18}\text{O}$  of water (dashed line D) and vapour (dashed line E) in a two-phase closed system also increase during evaporation, but much less than in an open system; for a closed system, the  $\delta$  values of the instantaneous and cumulative vapour are identical. Modified from Gat and Gonfiantini (1981) (Kendall and McDonnell, 1998).

Concerning the water  $\delta^{18}\text{O}$  exchange during redox reactions in wastewater no proper data are available in literature. In this work, these effects have been considered negligible and the water  $\delta^{18}\text{O}$  has been considered conservative. Nevertheless, an analysis of the variation of the  $\delta^{18}\text{O}$  in water during the civil water use and during redox reactions could be of interest.

The second point could be easily confirmed by interviews to the water authority. In this study, the sources of drinking water (called Peschiera springs) supplying the investigated areas are unique and placed about at 100 km from the city (Figure 2).

The third point can be confirmed only after field investigations, even though available former data can support such a hypothesis. In this work, we used data from Longinelli and Selmo (2003) that report rain  $\delta^{18}\text{O}$  in the area where Peschiera springs varying between  $-9\text{‰}$  and  $-8\text{‰}$ , and  $\delta^{18}\text{O}$  in the area where Rome is placed varying between  $-6\text{‰}$  and  $-5\text{‰}$ . As a consequence, we could reasonably have supposed the difference between  $\delta^{18}\text{O}_{\text{foulwater}}$  and  $\delta^{18}\text{O}_{\text{infiltration}}$  to be sensible.

The fourth point can be confirmed only after field investigations, even if available former data could support such a hypothesis, as well.

## 2.3 Laboratory analysis

The  $^{18}\text{O}/^{16}\text{O}$  ratio was measured following the Epstein-Mayeda technique (1953) based on the water- $\text{CO}_2$  equilibrium, the samples were prepared manually and then analyzed with the mass-spectrometer Finnigan MAT. The isotopic ratio in the water samples are expressed in terms of the mille difference ( $\delta\text{‰}$ ) with respect to the isotopic ratio of Standard mean Ocean Water (SMOW) defined by the International Atomic Energy Agency (IAEA).

$$\delta(\text{‰}) = \left[ \left( \frac{R_{\text{sample}}}{R_{\text{reference}}} \right) - 1 \right] \times 1000 \quad (5)$$

where R is the isotopic ratio  $^{18}\text{O}/^{16}\text{O}$ .

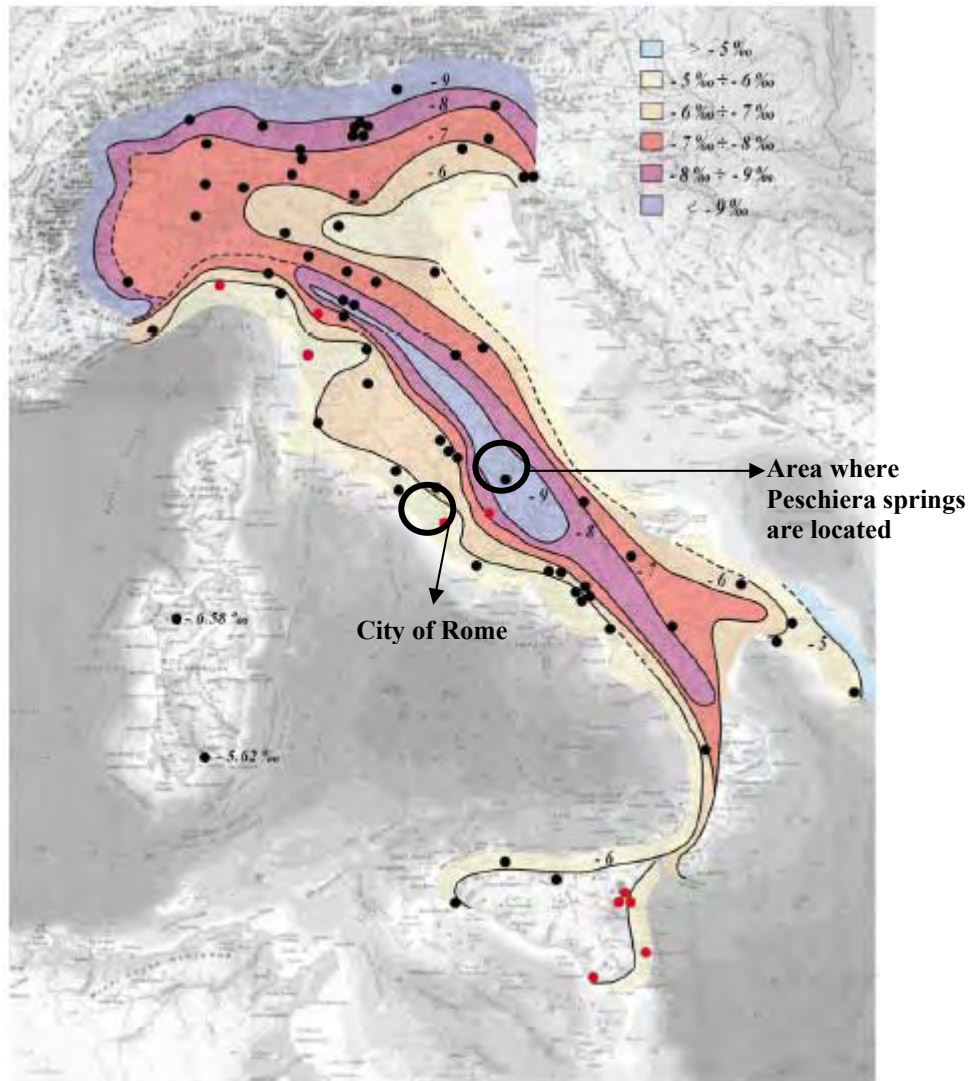


**Fig. 2** Contour lines reporting the overall variability of the mean oxygen isotopic composition of precipitation in Italy. Black dots refer to the collecting stations controlled and measured by the authors; red dots refer to the 10 stations controlled and measured by other colleagues (by Longinelli and Selmo, 2003).

## 2.4 Field measurements

Flow was measured by means of an area velocity flow meter based on the Doppler ultrasonic average velocity (model SIGMA 900MAX, American Sigma Inc., Medina, NY). The wastewater samples were taken by an automatic sampler equipped with the flow meter.

The conductivity was measured manually by means of the device model WTW 340 and the sensor model Tetracon 325.

## 2.5 Experimental Catchments

The investigated sewer systems are located in two urban catchments, called: Torraccia and Infernetto.

The experimental area called Torraccia is about 0.85 km<sup>2</sup>, whose 0.55 km<sup>2</sup> are residential and 0.30 km<sup>2</sup> are rural. It is located on a piroclastic plateau 40 m above the sea level. The first part consists of fine cinder and pumice and comes from Colli Albani and Monti Sabatini Vulcan with good and excellent technical characteristics and variable permeability due to clay lens that causes the formation of multi-layer groundwater, while below there is a clay bench 15 m thick alternated by silt-sand benches. At 30-32 m under the ground there is a confined aquifer in a calcareous sand bench. The urban area is characterized by residential building with yards. The sewer is egg-shaped combined system (1x1.2 m, 1.5x1.8 m and 1.5x2.1 m laid about at 4 – 9 m under the ground level) and it dates 14 years, the pipes' material is concrete. The whole sewer network (Figure 3) has been implemented in AquaBase software (DHI, 2004).

The experimental area called Infernetto is about 5.5 km<sup>2</sup> and it is characterized by residential houses with private gardens. The north-east part is located on the coastal deposits at 12-14 m above the sea level, the south-west part is located on alluvial of the external Tiber river delta at 2-3 m over the sea level. Thus major part of the subsoil is characterized by silt-sand sediments and the minor one by clay and gravel with poor technical characteristics. The shallow groundwater changes between 6-7 m and 3 m under the ground from north-east and south-west, while the altitude changes from 14 m over the sea level and 2 m over the sea level. The shallow groundwater in this area is part of a larger one that comes from north-east silt-sand deposits of Tirren sea. The sewer is circle-shape separated system (0.3 m, 0.6 m, 0.8 m and 1 m laid about at 2 – 6 m under the ground level) and it is dated 19 years about, the pipes' material is concrete (size 1.0 m), ceramic (sizes 0.6 m and 0.8 m) and PVC (size 0.3 m). The whole sewer network (Figure 3) has been implemented in AquaBase software.

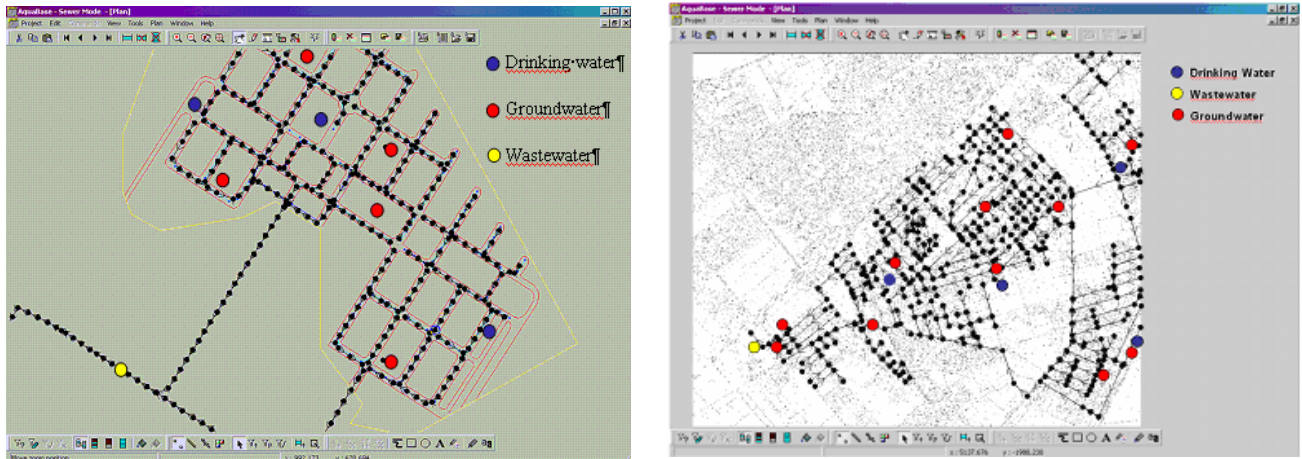


**Fig. 3** right: Sewer network in Torraccia catchment. Left: the sewer network in Infernetto catchment

The Infernetto and Torraccia areas have been chosen because, firstly, they respect the hypotheses given above, and, secondly, they are completely different as regards to: sewer system characteristics, geological and hydrogeological characteristics, and urbanization. We expected to find low values of infiltration in Torraccia and high values in Infernetto because in Torraccia the groundwater level was detected at 19 m about under the ground level, whereas in Infernetto at 6 m about under the ground level.

## 2.6 Sources of uncertainty

The errors can be classified into three parts on the basis of the level (or order) of the experiment when they occur:

- Zeroth-order
- First-order
- Nth-order

The Zeroth order errors consider the random and the systematic errors due to instrumentation and measurements. For a sample to sample experiment, it is the uncertainty calculated when the repetition of the measurement of a single sample is done, while for a time-wise experiment it is the uncertainty calculated as if the process were steady.

First order errors consider the random errors due to the variability of the investigated phenomena when the measurements are carried out by means of the same equipment, but the monitored sample changes. The sample could change because of the temporal variability (i.e., flow rate measurements by flowmeter) or spatial variability (i.e., permeability of soil measured over a large area). This order of error accounts of both the random errors due to the equipment itself and the variability of the phenomena.

Nth order errors consider the propagation of the systematic and the random errors of the previous order through the model up to the results. At this order the error are those do not consider into the previous orders, but those due to the equipments' installations, the interaction of both the equipments and the measurements with the surrounding environment.

The sources of uncertainty affecting the infiltration ratio calculated with the herein method can be divided into three parts:

### Zeroth order errors

- Human errors
- Errors due to the used instrumentations

- Measurement of the flowrate

#### First order errors

- Spatial variability of the infiltration contributes
- Temporal variability of the drinking water

#### Nth order errors

- Differences of  $\delta^{18}\text{O}$  between drinking water and infiltration contributes
- Conservation of the tracer
- Rappresentability of the wastewater samples
- Storage of the samples

Separately the sources of uncertainty are analysed below.

#### Zeroth order errors

The isotopic characterization of the samples has been done with the procedure suggested by Epstein and Mayeda (1953) with manual preparation of the sample and determination at the mass-spectrometer.

The errors could be due to both the low accuracy of the operator and the inefficiency of the equipments, the precision assessed by the laboratory is  $\pm 0.2\%$ .

If the used equation for assessing the infiltration were (3), the wastewater flow rate should be measured and the infiltration rate estimated would be affected by the error coming from this measurement. In this application, the flow meter is an area-velocity Doppler, and from technical sheets the level can be measured with an accuracy of  $\pm 0.01156$  m and precision  $\pm 0.00346$  m and the velocity  $\pm 2.0\%$  of the measured value.

#### First order error

An important hypothesis of this method is the spatial and temporal homogeneity of the two model components (i.e., drinking water and parasitical water).

The spatial variability over Infernetto and Torraccia catchments has been estimated for drinking water and infiltration contributes. Concerning the drinking water, as it is supplied from an unique and the same aqueduct, then the spatial variability is supposed to be low, that has been verified during the experiment period sampling drinking water all over the investigated area. In the Table 1 the isotopic composition of the groundwater, the conductivity and the depth of the water table in both the investigated areas are listed.

As regards the infiltration contributes, the spatial variability of the shallow groundwater has been calculated during the experiment period applying the following equation (Coleman and Steele, 1999):

$$P_{\text{Spat.Var.}} = \sqrt{P_{\text{First}}^2 - P_{\text{Zero}}^2} \quad (5)$$

where generally  $P_x$  is the random uncertainty equal to  $t \sigma_x$ ,  $t$  is the t-distribution taken equal 2 for sample size more then 10. In particular, in equation (5)  $P_{\text{Spat.Var.}}$  is random uncertainty due to the spatial variability of the isotopic composition of the groundwater over the whole investigated catchment;  $P_{\text{First}}$  is the random uncertainty of the groundwater samples;  $P_{\text{Zero}}$  is the random uncertainty estimated from the zero order errors. The  $P_{\text{Spat.Var.}}$  values were  $0.18\%$  for Infernetto and then standard deviation  $\pm 0.09\%$ , and not significant for Torraccia because the  $P_{\text{First}}$  was less then  $P_{\text{Zero}}$ .

The temporal variability over Infernetto and Torraccia catchments has been estimated for drinking water. At this aim, as conductivity has been individuated as an useful and a reliable parameter for distinguishing uncontaminated water and it is well correlated with  $\delta^{18}\text{O}$  (Lambs, 2000), the  $\delta^{18}\text{O}$  temporal variability for drinking water has been estimated from conductivity temporal variability of data recorded continuously with a time step of 1 seconds over four days. In Torraccia the temporal variability of conductivity has been estimated equal to  $635.59 \mu\text{S/cm} \pm 0.86 \mu\text{S/cm}$  and in Infernetto of  $609.60 \mu\text{S/cm} \pm 1.89 \mu\text{S/cm}$ . Figure 4 shows  $\delta^{18}\text{O}/\text{SMOW}$  vs. conductivity for the drinking water samples taken from Peschiera aqueduct in Torraccia and Infernetto areas, the correlation coefficient is  $R^2=0.99$ . It allows to estimate then the temporal variability of this  $\delta^{18}\text{O}$  has been estimated (by error propagation equation of linear models) equal to  $\pm 0.03\%$  and  $\pm 0.07\%$  in Torraccia and in Infernetto , respectively.

**Table 1** data of isotopic composition of groundwater, conductivity and depth of groundwater water table in the investigated areas.

	mean $\delta^{18}\text{O}/\text{SMOW}$	Cond. [ $\mu\text{S}/\text{cm}$ ]	Water table [m below the ground]
<b>Infernetto</b>			
GAR42	-5.88	1125	1,8-2
GAR67	-5.79	1426	-
GUB29E	-5.80	1154	6÷7
CAS23	-5.87	1187	7
BRE	-5.73	1145	11
ROM	-5.57	1130	-
GIO	-5.66	1034	6÷9
SOF	-5.79	1305	9
ROL	-5.51	1124	9
BOL	-5.47	1022	-
FORT	-5.63	1245	11÷12
GHI	-6.33	867	~8
mean	-5.75		
st.dev.	0.22		
<b>Torraccia</b>			
T1	-5.80	584	8.5
CHL	-5.57	641	12.24
ASQ	-5.44	734	13.97
SIR	-5.71	518	
mean	-5.63		
st.dev.	0.18		

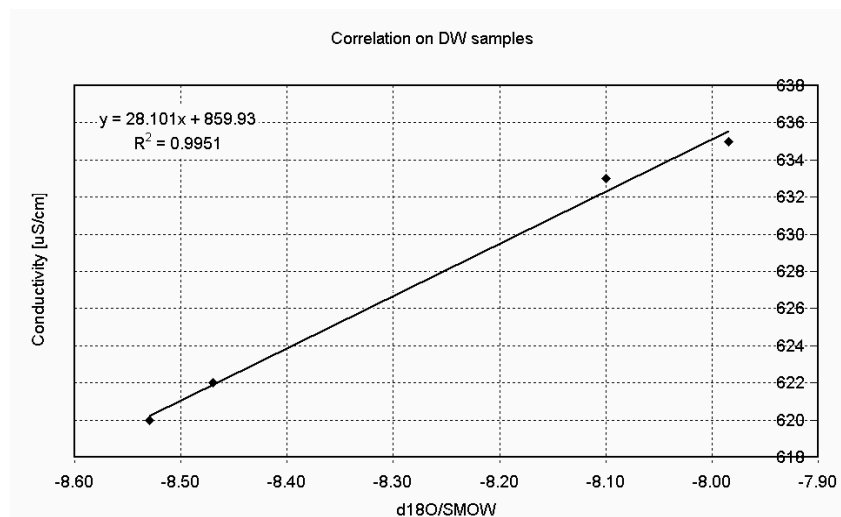


**Fig. 4** Correlation between  $\delta^{18}\text{O}$  and conductivity in drinking water from Peschiera aqueduct.

#### Nthorder error

*Differences of  $\delta^{18}\text{O}$  between drinking water and infiltration contributes*

The mixing model can be applied only when the different sources have sensible different isotopic compositions. De Benèdittis and Bertrand-Krajewski (2004) calculated the relationship between infiltration ratio uncertainty and the isotopic difference between the two sources (drinking water and groundwater) (see Figure 4).

In our case, the 18-oxygen differences between drinking water and groundwater are:

- 2.63‰ in Torraccia
- 2.36‰ in Infernetto

Then from the graph in Figure 5, the expected uncertainty in infiltration ratio calculated by equation (4) is around 5% for both areas.

Nevertheless, as a rule of thumb, we could assume that the method is applicable in those parts of Rome where: the shallow groundwater is recharged by local precipitation (unless  $\delta^{18}\text{O}$  variations within the unsaturated and saturated zones), and the drinking water is supplied by Pescara aqueduct, because the isotopic composition of the precipitations in Rome changes between -6‰ - -5‰, while that where the potable water comes from (about 100 km far from the city) changes between -9‰ - -8‰ Longinelli and Selmo (2003).

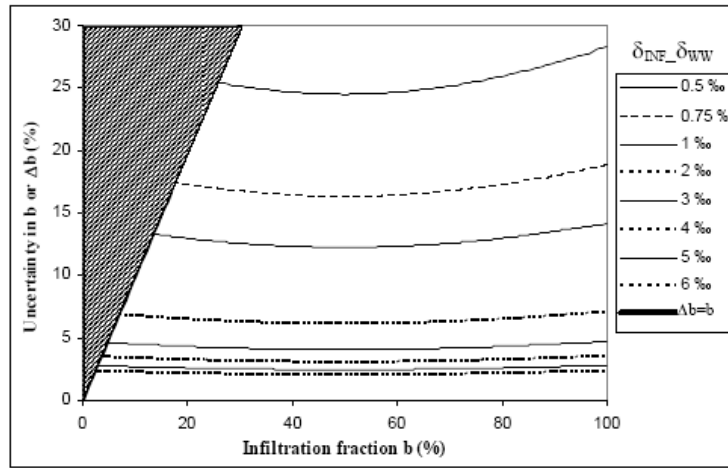


**Fig. 5** Uncertainty curves.  $\delta_{\text{INF}} - \delta_{\text{WW}}$  is 18-oxygen difference between parasitical water (e.g., groundwater) and drinking water (from De Benèdittis and Bertrand-Krajewski, 2004)

#### *Conservation of the tracer*

During the drinking water use,  $^{18}\text{O}$  variations could occur because of chemical-physical reactions.

One drinking water sample and one wastewater composite sample over four hours and immediately before the discharge into the sewer pipe were taken and then analyzed for 18-oxygen. The composition is shown in Table 2 and because the difference between the isotopic composition was less than the laboratory analysis error, we assumed the tracer to be conservative.

**Table 2**  $\delta^{18}\text{O}$  ‰ vs. SMOW in drinking water sample and composite wastewater sample stored at -4 °C.

Sample	$\delta^{18}\text{O}$ ‰ vs. SMOW
Drinking water	$-8.23 \pm 0.2$
Wastewater	$-8.49 \pm 0.2$

#### *Rappresentability of the wastewater samples*

The question to be answered is: How often must the sample be taken in order to be representative of the matrix of interest?

The sampling frequency should be set over the flow variability, higher the variability, higher sampling frequency. For instance, composite samples are advisable during the night period when the flat hydrograph is expected and grab samples could be taken during the morning and evening peaks, but a detailed investigation taking grab samples every hour by means of automatic samples is suggested.

#### *Storage of samples*



During the storage of wastewater samples,  $^{18}\text{O}$  variations could occur because of redox reactions. In order to reduce the organic matter to oxidise the wastewater samples were filtered by  $0.45\mu\text{m}$  filters, put in completely filled PVC bottles and then stored at low temperature. The conservation temperature values was determined after a simple trial: one wastewater sample was divided into two equal parts, the first one was analyzed after storing for 15 days in a refrigerator at  $4^\circ\text{C}$ , and the second group was stored for 15 days in a freezer at  $-4^\circ\text{C}$  and then analyzed. From the results in Table 3 temperature seems to be not relevant on the  $\delta^{18}\text{O}$  values.

**Table 3**  $\delta^{18}\text{O}$  ‰ vs. SMOW in wastewater samples, stored in completely filled PVC bottles at low temperature.

Conservation	$\delta^{18}\text{O}$ ‰ vs. SMOW
$4^\circ\text{C}$ for 15 days	$-8.08 \pm 0.2$
$-4^\circ\text{C}$ for 15 days	$-8.13 \pm 0.2$

### 3 Results and discussion

The experiment in Torraccia was on 15th March and it was carried out over 10 hours, from 11.00 a.m. to 8.00 p.m. Three drinking water samples were taken from different fountains and the isotopic average abundance was  $-8.14\text{‰}$ , this value has been considered as the 18-oxygen reference value for drinking water. Four groundwater samples were taken from piezometers spread all over the area evenly, the isotopic average abundance was  $-5.74\text{‰}$  this value has been considered as the 18-oxygen reference value for groundwater. At the outlet of the sewer system of Torraccia area five grab wastewater samples were taken from the sewer stream and the flow rate was measured, as well. The results are in Figure 6. In particular, Fig. 6 shows the results from laboratory analyses of the three water matrixes.

The  $\delta^{18}\text{O}$  abundance in wastewater is slightly higher than that in drinking water but strongly lower than that in groundwater water, that means the wastewater is a mix of the two sources, but the groundwater contributes are negligible in comparison to those due to the aqueduct. Then the infiltration rate must be low.

The experiment in Infernetto was on 8th April and it was carried out over 24 hours. Five drinking water samples were taken from different fountains and the isotopic average abundance was  $-8.11\text{‰}$ , this value has been considered as the 18-oxygen reference value for drinking water. Twelve groundwater samples were taken from the piezometers spread within the area evenly, the isotopic average abundance was  $-5.75\text{‰}$ , this value has been considered as the 18-oxygen reference value for groundwater water. At the outlet of the sewer system of Infernetto twenty-three wastewater samples were taken from the sewer stream and the flow rate was measured, as well. In the Figure 5 the results fom laboratory analyses of the three water matrixes are shown. The  $\delta^{18}\text{O}$  abundance in wastewater is higher than that in drinking water but lower than that in groundwater water that means, like Torraccia, that the wastewater is a mix of the two sources, but in this case the expected infiltration ratio is much more than in Torraccia area.

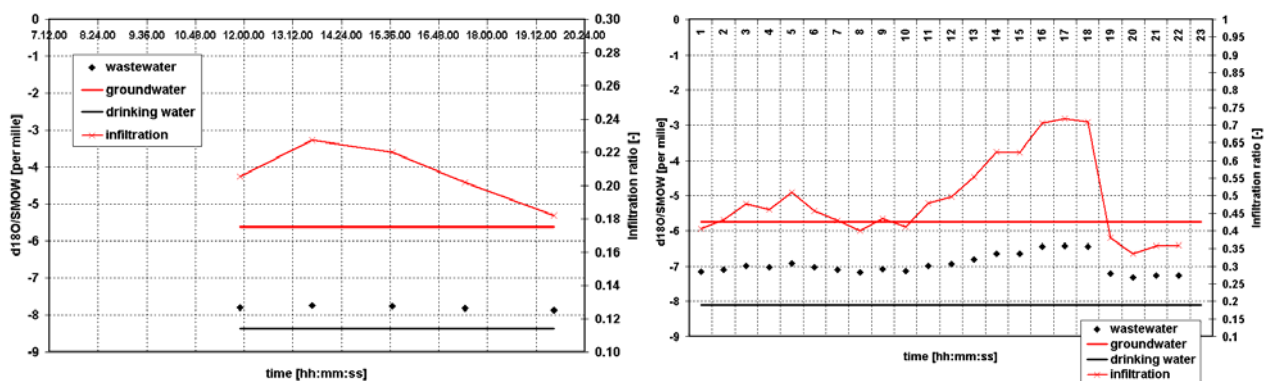


**Fig. 6** Left:  $\delta^{18}\text{O}$  in drinking water, groundwater and wastewater in Torraccia. Right:  $\delta^{18}\text{O}$  in drinking water, groundwater and wastewater in Infernetto.

The errors individuated have been quantified and distinguished in systematic and random (Table 4). The error values have been used for the error propagation analysis carried out on the data gathered during two experiments carried out in Torraccia and in Infernetto catchments with a random sampling routine based on the Monte Carlo method. The

statistical uncertainty affecting the infiltration ratio and infiltration rate estimated by the isotopic method has been calculated with a sample size equal to 10,000.

**Table 4** Errors affecting the infiltration ratio.

Error	Parameters	Random error	Systematic error	Estimation
Spatial variability of groundwater composition [‰]	$\delta^{18}\text{O}_{\text{GW}}$	I.: 0.09 T.: -	-	From field investigations
Temporal variability of drinking water composition [‰]	$\delta^{18}\text{O}_{\text{DW}}$	I.: 0.07 T.: 0.03	-	From conductivity measurements
Conservation of $\delta^{18}\text{O}$ during the water use [‰]	$\delta^{18}\text{O}_{\text{WW}}$	I.: - T.: -	-	From field investigations
Level measurement [m]	water depth	0.00346	0.01156	technical sheets
Velocity measurement [%]	flow velocity	2.0	-	technical sheets
$\delta^{18}\text{O}$ variation during the storage [‰]	$\delta^{18}\text{O}_{\text{WW}}$	I.: - T.: -	-	From field investigations
Laboratory analysis [‰]	$\delta^{18}\text{O}_{\text{GW,DW,WW}}$	0.20	-	From laboratory data

Note: I. indicates to Infernetto area; T. indicates to Torraccia area.

In Figure 7 are shows the infiltration rate vs. time with a Winshler-Box plot from the error propagation.

The daily average infiltration percentage in Torraccia catchment has been estimated of  $14.20\% \pm 1.80\%$  with precision  $\pm 21\%$ . The daily average infiltration percentage in Infernetto catchment has been estimated of  $49.90\% \pm 11.90\%$  with precision  $\pm 20\%$ . We can assume the precision of the method of 20%, and then the infiltration rate in Torraccia isn't significant. As a matter of the fact, in Torraccia the flow rate during the investigation varied more than the infiltration rate,  $\pm 1.67 \text{ L s}^{-1}$  and  $\pm 0.49 \text{ L s}^{-1}$ , respectively.

From Figure 8 it is possible to see that in Infernetto as the infiltration ratio strongly changes during the experiment. It increases during the nocturnal period and decreases during the diurnal period. The infiltration rate variability is negligible ( $\pm 7.82 \text{ L s}^{-1}$ ) in comparison to the wastewater flowrate variability ( $\pm 29.93 \text{ L s}^{-1}$ ). Although, we expected that during the night the infiltration rate increased, because of the water depth decreasing into the sewer pipes, but such a phenomena seems not to be taken place. On the contrary, the infiltration rate is quite steady all the day, whereas the infiltration is quite changeable ( $\pm 11.90\%$ ) and increases in the night when the drinking water consumptions decrease (Figure 9).



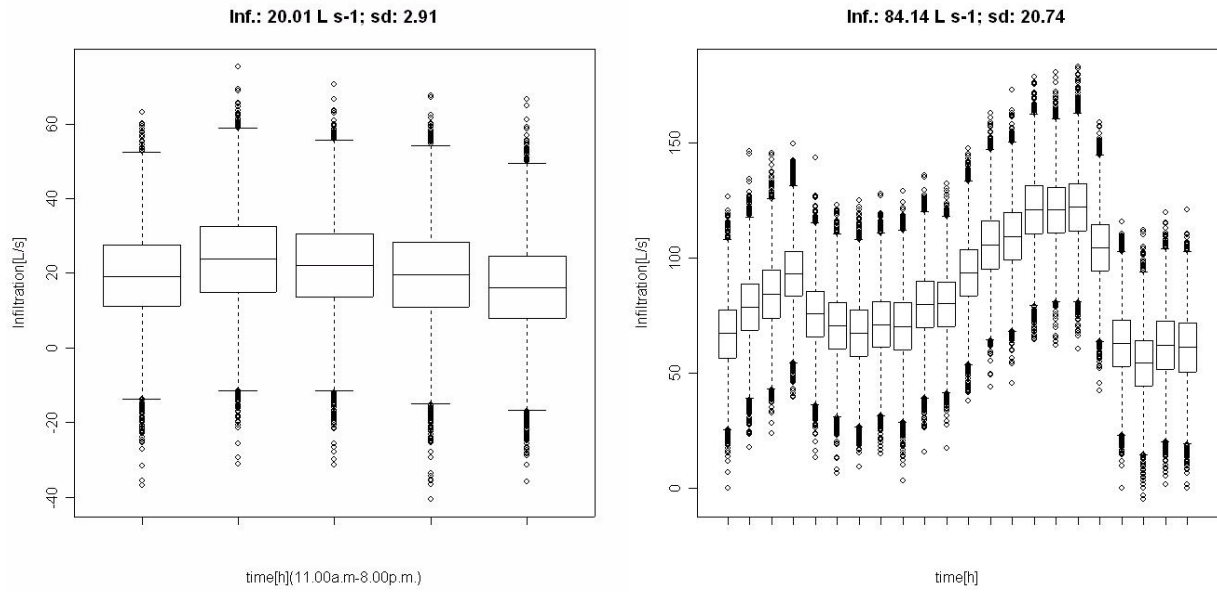


**Fig. 7** error propagation with Monte Carlo random sampling procedure. Sample size 10,000. Left: Torracchia. Right: Infernetto.

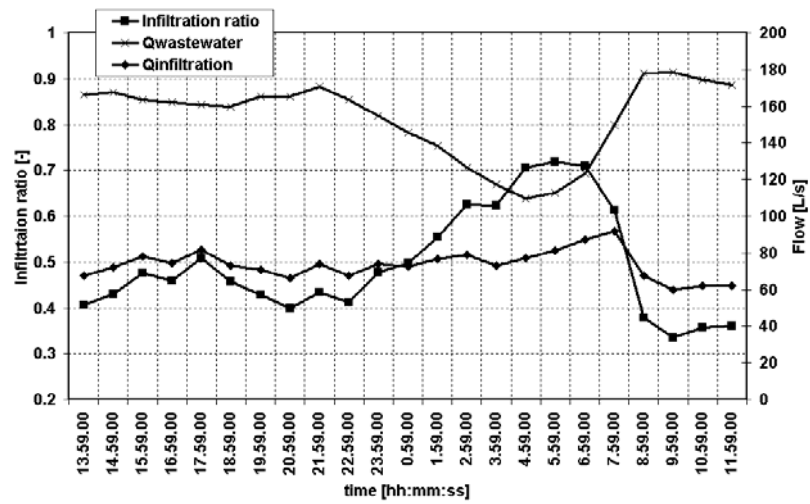


**Fig. 8** Infiltration ratio, infiltration rate and wastewater flow rate in Infernetto.

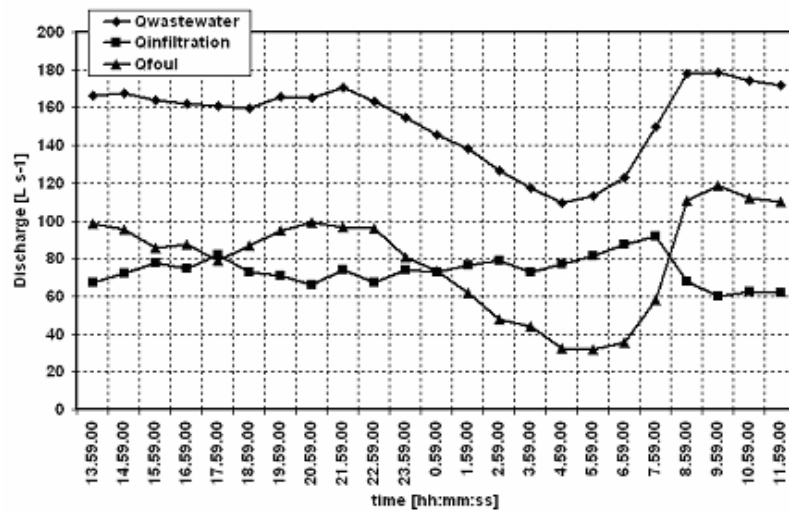


**Fig. 9** Hydrograph separation in Infernetto.

## 4 Conclusion

The paper describes an experimental experience for a field application of a new method, developed by Kracht (2003) within the European APUSS project, that allows quantifying the infiltrations in urban sewer networks. The experiments were carried out in two urban areas placed in Rome: Torraccia and Infernetto.

An experimental design by uncertainty analysis has been done, considering the following principal sources of error:

- laboratory analysis
- spatial variability of the infiltration contributes
- temporal variability of the drinking water
- differences of d18O between drinking water and infiltration contributes
- conservative tracer
- sampling
- storage of the samples
- measurement of the flowrate

and a precision of the method of 20% has been estimated.

The advantages of the method can be summarized as follows:

- the investigation is quite speedy, the field activity can be finished over four days (i.e., one for the preliminary investigation, one for the final experiment, one for laboratory analyses and one for data analyses)
- the investigation is quite cheap: three operators in the field and the equipments to be used (i.e., flowmeter, auto sampler and piezometer) are easy to install and manage;
- the method allows estimating the infiltration in an urban sewer network over a large area with sewer running;
- it is a reliable, speedy and cheap investigation for individuating which part of a sewer system should be investigated with direct diagnosis systems like CCTV.

The disadvantages can be summarized as follows:

- informations bout geology and hydrogeology of the area to be investigated must be available;
- the sewer network informations (e.g. material, age, location) must be available;
- wells for monitoring and sampling the shallow groundwater must be available.

## 5 References

- Dincer, T.; Payne, B. R.; Florkowski, T.; Martinec, J.; Tongogiorgi, E. (1970). Snowmelt runoff from measurements of tritium and oxygen-18. *Water Resource Research* 6 (1) pp. 110-124.
- Cingolani, T. (2004). Quantificazione delle infiltrazioni in fognatura mediante caratterizzazione isotopica. Thesis of graduation in Engineering for the Environment and the Territory, University of Rome "Tor Vergata".
- De Benedittis, J. ; Bertrand-Krajewski, J.-L. (2004). Measurement of infiltration rates in urban sewer systems: use of oxygen isotopes. WEM, Book.
- DHI (2004). Manual of AquaBase a database for sewer network developed within the European project APUSS. Prague, CR.
- Epstein and Mayeda (1953). Epstein, S., Mayeda, T., 1953. Variation of  $^{18}\text{O}$  content of water from natural sources. *Geochim. Cosmochim. Acta* 4, 213–224.
- Fritz, P.; Cherry, J.A.; Weyer, R.U.; Sklash, M (1976). Storm runoff analyses using environmental isotopes and major ions. In: *Interpretation of environmental isotopes and hydrochemical data in groundwater hydrology*, Vienna International Atomic Energy Agency, pp. 111-130.
- Gat, J.R. and Gonfiantini, R., (Eds 1981). *Stable Isotope Hydrology: Deuterium and Oxygen-18 in the Water Cycle*.
- Gokhale, S.; Graham, J. A. (2004). A new development in locating leaks in sanitary sewers. *Tunneling and Underground Space Technology* n.19, pp. 85-96.
- Kracht, O. (2003). Guideline: the stable isotopes composition of water as a natural tracer for the quantification of extraneous infiltration into sewer system. Internal APUSS protocol.
- Kendall, C.; McDonnell, J. J. (1998). *Isotopes tracers in catchment hydrology*. Elsevier Science B. V. Netherlands.
- Lamb, L. (2000). Correlation of conductivity and stable isotope  $^{18}\text{O}$  for the assessment of water origin in river system. *Chemical Geology*, 164, pp. 161-170.
- Longinelli, A.; Selmo, E. (2003). Isotopic composition of the precipitation in Italy: at first overall map. *Journal of Hydrology* (270) pp. 75-88.

- Majoube, M., 1971. Fractionnement en oxygène-18 et en deutérium entre l'eau et sa vapeur. Jour. Chem. Phys., 197, pp. 1423-1436.
- Martinec, J. (1975). Subsurface flow from snowmelt traced by tritium. Water Resource Research 6 (1) pp. 110-124.
- Clark, I. D.; Fritz, P. (1997). Environmental Isotopes in Hydrogeology. CRC Press LLC, USA.
- O'Neil, J.R., 1986. Theoretical and experimental aspects of isotopic fractionation. In: J.W. Valley, H.P. Taylor and J.R.

### **Acknowledgements**

*This study has been carried out within the framework of the European research project APUSS (Assessing Infiltration and Exfiltration on the Performance of Urban Sewer Systems) which partners are INSA de LYON (FR), EAWAG (CH), Techn.I Univ. of Dresden (DE), Faculty of Civil Eng. at Univ. of Prague (CZ), DHI Hydroinform a.s. (CZ), Hydroprojekt a.s. (CZ), Middlesex Univ. (UK), LNEC (PT), Emschergerossenschaft (DE) and IRSA-CNR (IT). APUSS is supported by the European Commission under the 5th Framework Programme and contributes to the implementation of the Key Action "Sustainable Management and Quality of Water" within the Energy, Environment and Sustainable Development Contract n° EVK1-CT-2000-00072. The project work of EAWAG is financially supported by the Swiss Federal Office for Education and Science (BBW).*

Moreover, we would like to thank the ACEA S.p.A. for his help during the installation of the equipments and Mr Mola of IGAC for his help during the isotopic analyses.

## *Annex 7*

FURTHER ENCLOSED ARTICLES

*16<sup>th</sup> European Junior Scientist Workshop*  
**“Real Time Control of Urban Drainage Systems”**  
*Milo, Etna Mountain, Italy*  
*7-10 November 2002*

**“GIS for infiltration and exfiltration management on urban  
drainage network in Rome”**

**Mario Giulianelli**

National Research Council – Water Research Institute, via Reno, 1 – 00194 Rome, Italy  
Email: m.giulianelli@irsa.rm.cnr.it

**Marco Paoluzzi**

University of L’Aquila – Architecture and Land Planning Department, Piazzale E. Pontieri, 1 – 67040  
Monteluco di Roio (AQ), Italy  
Email: paoluzzi@ing.univaq.it

**Valentina Prigiobbe**

University of Rome 2 – Civil Engineering Department, 00100 Roma, Italy  
Email: prigiobbe@uniroma2.it

**Abstract**

The structural integrity (efficiency) and the effectiveness of the drainage network is the main goal for Public Service supply to guarantee the Community’s health and wellness, conveying and draining rain waters, urban and industrial wastewaters.

Moreover, in order to guarantee the sewer system’s sustainability, it is of particular relevance checking the interaction between the environment where it operates, in different conditions; we have to concentrate on two topics:

- The sewer system’s sustainability: i.e. the conformity of the project to the required performances, the maintenance’s strategy and the operative duration of the system itself ;
- The environmental system impact: the way the processes of different drainage systems influence the flows of natural resources (goods and energy) and then how they influence the ecosystem and urban Community’s health.

The research task is providing to the public service management company a tool to handle parasitical waters, according to the next steps, described below:

- Quality and amount control and monitoring systems calibration;
- Parasitical waters management;
- G.I.S. development.

By overlaying several thematic maps it is possible to obtain a spatial distribution of any involved parameter; the following step is to link those parameters by a mathematical model that will give us the I/I and/or I/E flow rate for any sewer branch between two following manholes.

**Keywords:** GIS, urban drainage, parasitical waters, infiltration, exfiltration, EMS.

## **Introduction:**

At present, European freshwater resources, although plentiful and of good quality in some regions, are still under threat from a multitude of human impacts. This could reduce the amount and quality of the water available for human consumptions and other needed uses. Because of these problems, a better integrated water management is urgently needed to stop and reverse deterioration of water, taking into account the importance of the problems, their transboundary nature, their link with human activities in the catchments and their cross – media importance.

Taking into account that 65% of European population is living in urban environment, only occupying 1% of Europe's territory the threats to water resources become visible in towns, especially regarding freshwater supply and all the other "vital functions",.

As already said in the 1995 "Dobris Assessment" by European Environmental Commission, it comes out that European towns can count on sufficient amount of water resources in future, however there is a growing exploitation of the aquifers in surrounding territories and rising problems management of the collection and distribution resources.

An European town of a million inhabitants consumes daily 320,000 t of water, against a production of 300.000 t of wastewaters, with only 5% of the water needed for drinking water. Moreover losses in the distribution network that vary from 30% to 50% are reported.

Regarding the Italian case, the "Environment State Report – 2001" comes up to similar conclusions. The availability of water resources is enough to the needs of Italian urban systems and passes over the European average, however many towns, especially the southern ones, are affected by strong irregularity in the service. In total the Italian technical networks are affected by heavy losses percentage (23%), quickly growing in the last fifteen years (17% in 1987).

Then, managing water resources appears to be a key - node for the sustainability of the land transformation actions and anthropical settlement; water infrastructures planning, use and distribution is needed.

In effect it is a Directive already ratified by principles in the "Agenda 21" (Chapter 18) and in the "Dobris Assessment" (Chapter 10); the Italian laws (D.Lgs 152/99 and D.Lgs 258/00) provide in fact the "Water Protection Plan" (art. 44, D.Lgs 152/99) and the survey of the "water basin patterns and anthropical activity impact assessment" (art. 42) and of the "water bodies quality state" (art. 43).

With the "Galli law" (L. 36 by 15/01/1994) is needed that, also in Italy, the public service managers should be keen on enhancing their systems performances cutting down managing costs by keeping or improving the level of service to the customers. Two points are of importance to introduce an efficient and effective management :

- 1) Through an accurate analysis of their own performances, they should identify the areas where good management results are already achieved and those where the results have to be improved. This needs the identification of the customer satisfaction level more than traditional measures in terms of costs, products, etc.
- 2) It is needed to develop some to simplify the changes in work procedures in areas where the troubles are identified.

By the administrative level, the main new is the division between owner and manager with shared tasks and functions. In the new territory defined by regions, the local authorities should compulsory join to ensure a good management of services. The new organization of the service provides a “managing convention” to be signed by joined local authorities and by the operating manager. The main working tool is the definition, by joined local authorities, of a technical – financial plan (Piano d’Ambito) that should provide:

- assessment of plants and service state
  - service standards and financial investment to achieve them
  - financial plan time actuation table
  - minimal increase of productivity
- measuring the achieved service improvement by toll and fitting procedures

Then an EMS (environmental management system) had been developed to monitor and manage parasitical waters in sewer systems.

The employed tool is a GIS that manages the database of the patterns of the urban drainage network. The GIS helps to locate and highlight the patterns in relationships with the other elements of the system.

The GIS had been developed in the “APUSS” research project and was experimentally applied to quarters of Rome called “Torraccia” and “Mostacciano”. There an experimental basin of about 13 ha is directly owned by the IRSA – CNR, (National Council of Research – Water Research Institute) for its researches.

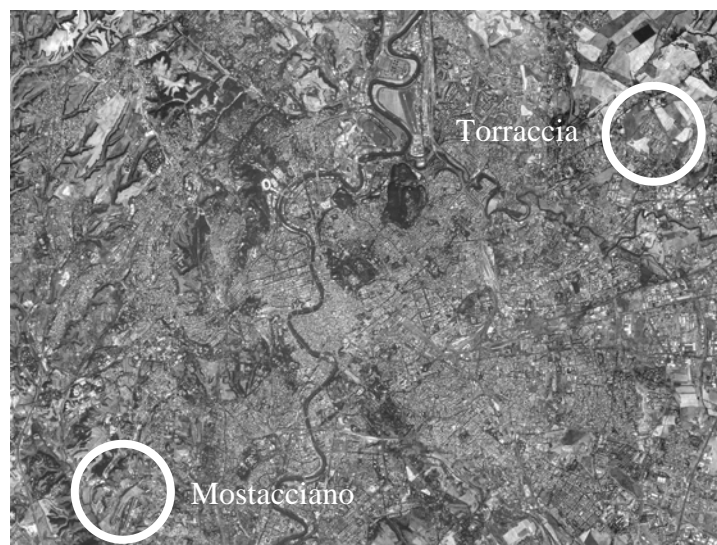


Fig. 1 – “Torraccia” and “Mostacciano” in Rome.

Early results and the analysis of the system in its components follow, starting from the mathematical model developed to statistically determine the flow of parasitical waters, the topologic system who defines the geometry of the network and finally the software that allows the system management by spatial queries.

## Mathematical Model:

The mathematical model, describes the possibility of the presence on the network of parasitical waters (infiltration and/or exfiltration). The model is still under development by the Technical University of Dresden (D) during the APUSS project.

Experimentally we noticed that the amount of parasitical waters in a network is affected by several factors such as human density, traffic flows, geology and of course geometry and use patterns of the pipes.

For the infiltration and exfiltration waters we came up to a function of this kind:

$$\left\{ \begin{array}{l} Q_{EXF} = ch^b - s \\ Q_{INF} = c(h_{falda} - h)^b - s \end{array} \right. \quad (1)$$

$Q_{EXF}$	exfiltration flow;
$Q_{INF}$	infiltration flow;
$c$	pipe conditions;
$s$	sediments / soil permeability;
$b$	function shape;
$h$	sewer water table;
$h_{falda}$	ground water table.

## Topology System:

It seems to be suitable to remember that the geometry of any GIS is based on three kinds of topology:

- Node: it represents punctual elements, in our case to this topology belong the manholes with whom are joined the elevation data (road and connection), type and dimension.



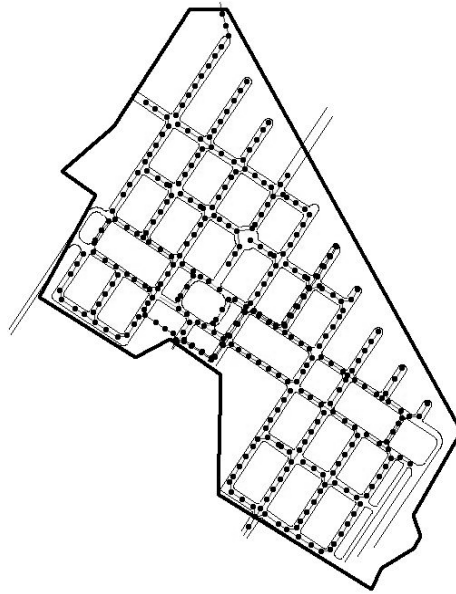


Fig. 2 - “Node” topology elements in “Torraccia”.

- **Network:** linear bidimensional elements; it describes the sewer network with joined data about flows, quality and geometry of pipes. As base element has been chosen the sewer between two following manholes, because this allows a good level of approximation and a better understanding of the system.

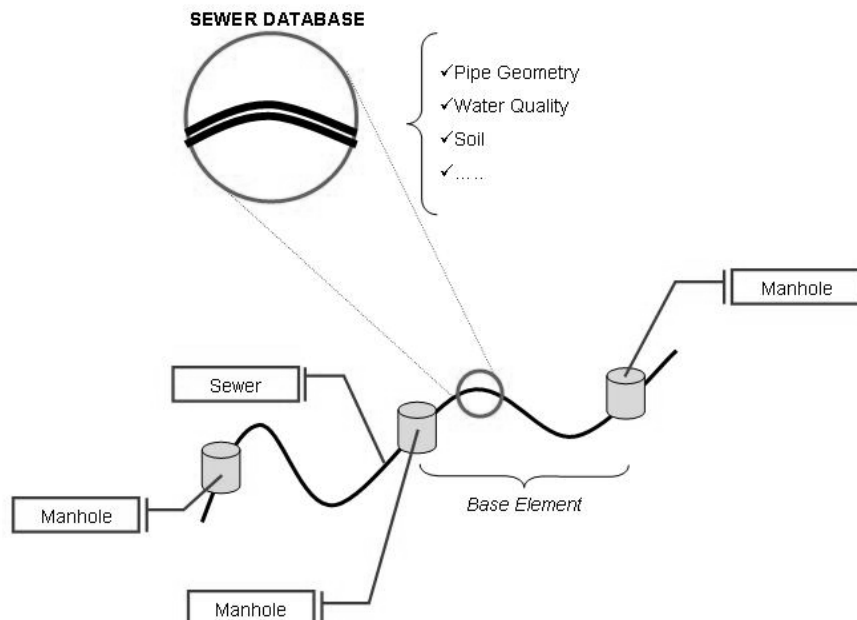


Fig. 3 – Urban drainage network modeling.

Data from every branch of the network are obtained by the analysis carried on by the DHI software “Aquabase”, starting from experimental data gathered in some sections.

To the network topology, in our system, belong also the soil contours and the groundwater table.

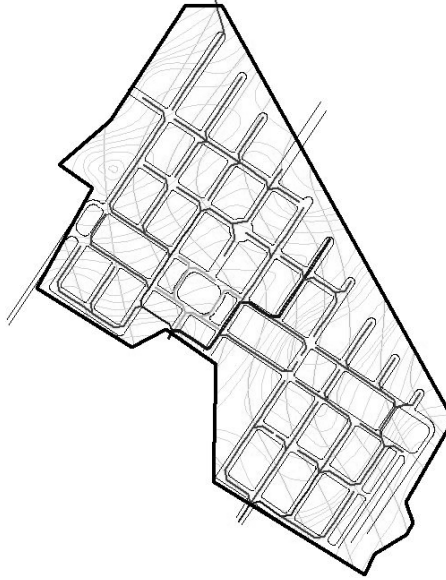


Fig. 4 – “Network” topology elements in “Torraccia”.

- Polygon: bidimensional elements to which it is possible to join a surface measure. To this category belong the themes about geology, density and road traffic.

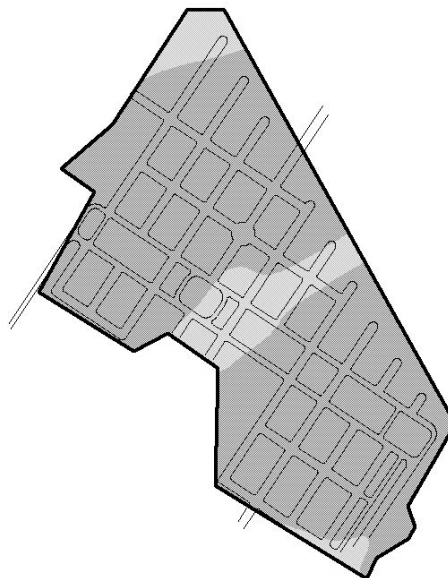


Fig. 5 - “Polygon” topology elements in “Torraccia”.

The previous topologies represent the spatial distribution of the parameters values of the function described in the above paragraph.

By topologic overlay (overlapping thematic maps) and database spatial join (database joining by common spatial characteristics) of the involved themes we came up to a new network topology where, per every branch of the sewer, are listed the values of all the parameters needed by the function  $Q_{I/E}$

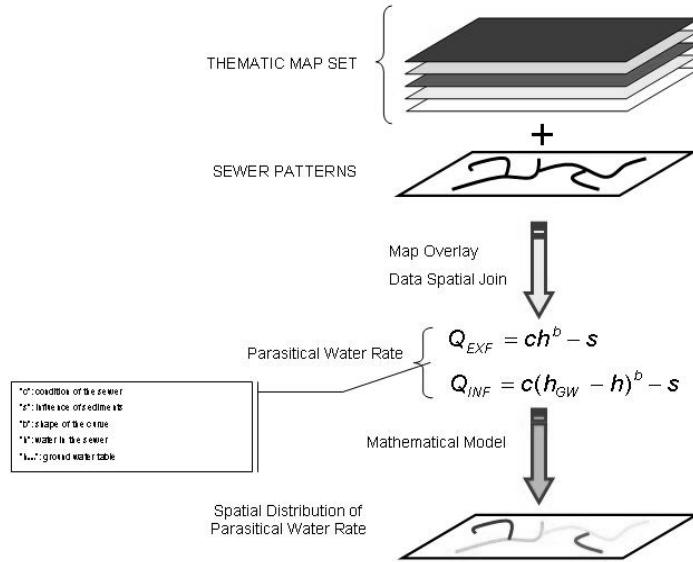


Fig. 6 – Implementation phases of the model in the geometry.

The next step is to carry on the function  $Q_{I/E}$  and loading the results in a new field of the database; then we have the spatial distribution of the values of  $Q_I$  and  $Q_E$ .

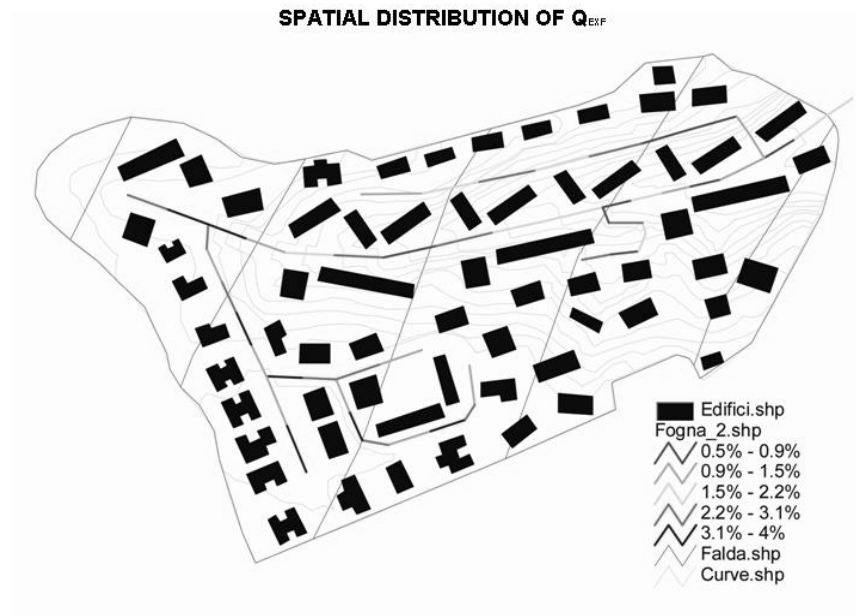


Fig. 7 – $Q_{EXF}$  spatial distribution in the “Mostacciano” network.

## Software:

To manage the acquired database as a whole, both spatial and alphanumeric, we needed a suitable software.

The best solution was the URBIS software by Theomedia, based on the ESRI standard data format (shapefile), fully adaptable to particular needs and mainly composed by open source components.

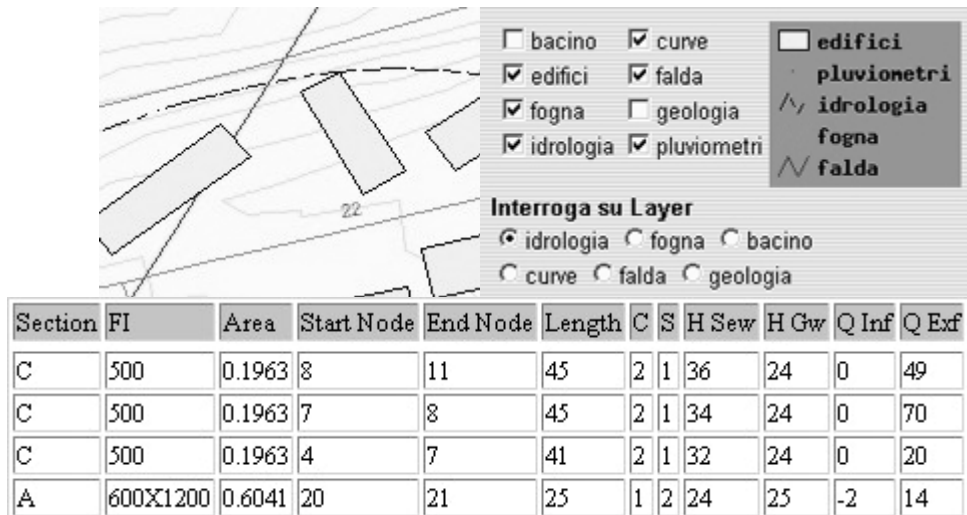


Fig. 8 – URBIS management software by Theomedia.

The system is composed by the following elements:

- MySQL: open source software to manage alphanumeric data. It has the task of database querying engine to run the queries.
- MapServer: open source software that deals with the vectorial topologies in ESRI shapefile format. It allows the spatial interrogation of the database in order to have every vector joined with a record of the database, allowing basic operations such as zoom, pan or more complex ones as spatial query or thematic overlay.
- Apache: open source software for web editing. It represents the graphic medium of the software that casts the outcome of the analysis on every web browser (MS Explorer, Netscape Navigator).
- URBIS: owned software of Theomedia that, using PHP language, links the three above programs.

## Conclusions:

Finally, adopting an EMS (such as the one defined by the ISO 14000 rules) to manage an urban drainage system, allows us to optimize the use, prevents pollution, improves the quality of the public service and the resources consumption is cut down; the main principle is that “you can’t manage what you don’t know”. All this about according to the rules on sustainable development of Agenda XXI – chp.18 “*protection of the quality and supply of freshwater resources: application of integrated approaches to the development, management and use of water resources*”.

## References:

- [1] **United Nations Division for Sustainable Development;**  
“*Agenda 21*”;  
Giugno 1992.
- [2] **EEA;**  
“*Europe’s environment – The Dobbris assessment*”;  
Agosto 1995.
- [3] **OECD;**  
“*Vers un developement durable – Indicateurs d’environnement*”;  
Febbraio 1998.
- [4] **L. 5 gennaio 1994, n. 36;**
- [5] **D. Lgs 11 maggio 1999, n. 152;**
- [6] **D. Lgs 18 agosto 2000, n. 258;**
- [7] **Ministero dell’Ambiente;**  
“*Relazione sullo stato dell’Ambiente*”;  
Gennaio 2001.
- [8] **IRSA - CNR;**  
“*Cartografia della vulnerabilità degli acquiferi: dagli studi conoscitivi all’applicazione normativa* ”;  
Atti della giornata di studio, Gennaio 1996.
- [9] **Openshaw, Roberts;**  
“*GeoComputation*”;  
Taylor & Francis, 2000.
- [10] **Longley, Goodchild, Maguire, Rhind;**  
“*GISs*”;  
ed. Wiley.
- [11] **Burrough, Mc Donnell;**  
“*Principles of Geographical Information Systems*”;  
ed. Oxford University Press.
- [12] **Goodchild, Steyaert, Bradley, Parks;**  
“*Geographical Information Systems and environmental modeling*”;  
ed. Wiley.
- [13] **Cinus, Moi, Murrau, Ponti, Raimondo;**  
“*Ingegneria di manutenzione applicata alle reti fognarie*”;  
L’Acqua 1/2001, ed. Ass. Idrotecnica Italiana.
- [14] **Benedini, Besson, Bosco, Carecchio, Priori, Zocchi;**  
“*Strumenti innovativi nell’industria idrica, il benchmarking a servizio del regolatore*”;  
L’Acqua 2/2001, ed. Ass. Idrotecnica Italiana.
- [15] **Bhaduri, Minner, Tatalovich, Harbor;**  
“*long term hydrologic impact of urbanization*”;  
Journal of Water Resources Planning and Management, 1/2001.
- [16] **Eschenbach, Magee, Zagona, Goranflo, Shane;**  
“*goal programming decision support system for multiobjective operation of reservoir systems*”;  
Journal of Water Resources Planning and Management, 2/2001.
- [17] **Bryan Ellis;**  
“*sewer infiltration / exfiltration and interactions with sewer flows and groundwater quality*”;  
UPRC, Middlesex University, London.
- [18] **Giulianelli, Benedini, Remedina;**  
“*indagine sperimentale sugli aspetti quantitative e qualitative delle acque di drenaggio urbano*”;  
IRSA – CNR, Rome 1997.
- [19] **Artina, Calenda, Calomino, Cao, La Loggia, Modica, Paoletti, Papiri, Rasulo, Veltri;**  
“*sistemi di fognatura – manuale di progettazione*”;  
ed. HOEPLI, Milan 1999.
- [20] **A.A.V.V.;**  
“*attuazione art. 141, comma 4 L. 388/2000 nel quadro degli obiettivi della L. 36/94*”;  
L’Acqua 6/2001, ed. Ass. Idrotecnica Italiana.
- [21] **<http://www.urbis.it>;**  
“*URBIS software website*”;
- [22] **<http://ewre-www.cv.ic.ac.uk>;**  
“*Environmental and Water Resource Engineering – Imperial College website*”;



## **STABLE ISOTOPES OF WATER AS A NATURAL TRACER FOR INFILTRATION INTO URBAN SEWER SYSTEMS**

O. Kracht (1), M. Gresch (1), J. de Bénédictis (2), V. Prigiobbe (3), W. Gujer (1)

(1) Swiss Federal Institute of Aquatic Science and Technology (EAWAG), Dübendorf (Switzerland), (2) Lyon National Institute of Applied Sciences (INSA), Lyon (France), (3) Water Research Institute of the Italian National Research Council (IRSA-CNR), Rome (Italy) (e-mail: oliver.kracht@eawag.ch)

An adequate understanding of the hydraulic interaction between leaky sewers and groundwater is essential for the sustainable management of both sewer systems and aquifers in urbanized areas. Undesirable infiltration of groundwater into sewers can contribute over 50% of the total discharge and is detrimental to treatment plant efficiency. On the other hand, in many European cities groundwater surface levels seem to be particularly controlled by the drainage effect of permeable sewer systems. However, nowadays methods for the quantification of these exchange processes are still subject to considerable uncertainties due to their underlying assumptions. The frequently used assumption that the night time minimum in the diurnal wastewater hydrograph is equal to the "parasitic discharge" has to be reconsidered to today's patterns of human life as well as to the long residence time of wastewater in the sewer networks of modern cities.

The suitability of stable water isotopes as a natural tracer to differentiate the origin of water in the sewer ("real" wastewater or infiltrating groundwater) is currently investigated in three different catchment areas. The studies are carried out within the framework of the European research project APUSS (Assessing Infiltration and Exfiltration on the Performance of Urban Sewer Systems):

1) The village of Rümlang (Zürich, Switzerland) is predominantly served with drinking water from the Lake Zürich. A large fraction of the lakes water is derived from precipitation in the Alps. This drinking water represents the intrinsic provenience of

the wastewater with an  $\delta^{18}\text{O}$  value around -11,5 per mill and  $\delta^2\text{H}$  value around -82 per mill vs. SMOW. In contrast, the local groundwater is originating from precipitation in a moderate altitude of about 450 m above sea level and shows comparatively enriched mean  $\delta^{18}\text{O}$  values of -9,7 per mill and  $\delta^2\text{H}$  values of -70 per mill with only small natural variations.

The isotopic separation between these endmembers is basically sufficient to estimate the ratio of infiltrating water in the sewer. Uncertainties yet derive from varying amounts of local groundwater in the water supply mains. These will be substituted by additionally purchased lake water in the next experimental stage.

2) The experimental site Toraccia (suburb of Rome, Italy) obtains drinking water from the Peschiera springs group that is situated in the central Apennines chain about 90 km north east of Rome. This spring water is transported to Rome by an aqueduct. A first campaign revealed an average mains water  $\delta^{18}\text{O}$  value of -8,4 per mill and  $\delta^2\text{H}$  value of -53 per mill. Potential sources of infiltration are occurrences of perched groundwater. These appear to be enriched compared to the drinking water about 2 to 3 per mill in the  $\delta^{18}\text{O}$  and 10 to 20 per mill in the  $\delta^2\text{H}$  value, but show disadvantageous strong variations.

3) Investigations in the urban area of Lyon (France) benefit from the isotopic differences between underground waters originating from the two rivers Rhone and Saone and their associated alluvial aquifers. The oxygen isotope composition of the Rhone water is roughly 3 per mill lighter than that of the river Saone, due to the large differences in the mean altitude and topographic situation of their catchment basins. Considerable amounts of mains water are extracted by production wells in the Rhone aquifer. In consequence a usable difference in the oxygen isotope composition between wastewater and local groundwater of about 1.5 per mill is available for application studies in certain parts of the city.

## Application of a method to assess parasitic infiltration into urban sewer systems by stable isotopes ( $\delta^{18}\text{O}$ )

PRIGIOBBE<sup>1,2</sup>, V.; SUCCHIARELLI<sup>3</sup>, C.; KRACHT<sup>4</sup>, O.; GIULIANELLI<sup>2</sup>, M.

<sup>1</sup> University of Rome "Tor Vergata", Civil Engineering Dept., Via del Politecnico 1, 00173 Roma (Italy)

<sup>2</sup> CNR – Water Research Institute, Via Reno 1, 00198 Roma (Italy) (e-mail: [m.giulianelli@irsa.rm.cnr.it](mailto:m.giulianelli@irsa.rm.cnr.it))

<sup>3</sup> Municipality of Rome, Territorial Policies and Planning Dept., Via del Turismo 30, 00144 Roma (Italy)

<sup>4</sup> Swiss Federal Institute of Aquatic Science and Technology (EAWAG), Überlandstrasse 133, 8600 Dübendorf (Switzerland)

### Abstract

Parasitic infiltrations (from groundwater, springs ...) into not watertight sewer pipes cause several problems (overflows along the sewer network and a threat for the receiving water, surplus consumption of energy at pumping stations and a reduced efficiency of the biological treatment processes).

We present the results of a practical implementation of a novel method to quantify the infiltration from groundwater into urban sewer systems during dry weather. This methodology was developed by EAWAG (CH) within the framework of the European research project APUSS. The approach is based on the isotopic characterization ( $\delta^{18}\text{O}$ ) of all types of water that are discharged by sewer pipes (foul water, infiltrating groundwater, spring water ...). It provides a speedy tool for a preliminary investigation on the extent of pipe damages in a catchment. Our experimental site Torraccia (a suburb of Rome) is one of places for the practical testing of this method by different APUSS project partners.

The area under investigation is a 55 ha large urban catchment, drained by a combined sewer system. Drinking water is supplied from a distance of about 100 km by the Peschiera aqueduct, fed by springs in a comparable high altitude in the Italian Apennine. This scenario supports the usability of the stable isotopes composition of water as a mixing tracer: The  $\delta^{18}\text{O}$  value of the drinking water can be expected to be lighter than that of the local groundwater, which is recharged from local precipitation in a moderate altitude.

Investigations in the catchment site Torraccia are of our special interest, as during dry weather the groundwater table is situated 10-15 meters below surface. This situation restricts the interaction between groundwater and sewer system: The infiltration of groundwater can be assumed to be zero. A comparison with the stable isotopes approach will therefore allow for estimating the accuracy of this method.

**Key words:** infiltration, sewer, isotopes, rehabilitation

---

*This study has been carried out within the framework of the European research project APUSS (Assessing Infiltration and Exfiltration on the Performance of Urban Sewer Systems) which partners are INSA de LYON (FR), EAWAG (CH), Techn.I Univ. of Dresden (DE), Faculty of Civil Eng. at Univ. of Prague (CZ), DHI Hydroinform a.s. (CZ), Hydroprojekt a.s. (CZ), Middlesex Univ. (UK), LNEC (PT), Emschergenossenschaft (DE) and IRSA-CNR (IT). APUSS is supported by the European Commission under the 5th Framework Programme and contributes to the implementation of the Key Action "Sustainable Management and Quality of Water" within the Energy, Environment and Sustainable Development Contract n° EVK1-CT-2000-00072. The project work of EAWAG is financially supported by the Swiss Federal Office for Education and Science (BBW).*



**VALUTAZIONE DELLO STATO STRUTTURALE DI RETI FOGNARIE URBANE  
MEDIANTE QUANTIFICAZIONE DELLE EXFILTRAZIONI ED INFILTRAZIONI  
Progetto Europeo APUSS**

**INTRODUZIONE**

Il controllo delle condizioni strutturali delle reti di fognatura urbane, in relazione allo loro efficiente tenuta per il drenaggio e il convogliamento delle acque di rifiuto agli impianti di depurazione, è in molti casi arduo e costoso e generalmente trascurato rispetto all'elevato impatto ambientale per il sottosuolo che queste infrastrutture presentano, a causa delle elevate concentrazioni di inquinanti dei flussi reflui, veicolati al loro interno. Le rotture strutturali e le connessioni difettose tra i giunti dei vari tratti delle tubazioni, sono la causa di: 1) perdite (o exfiltrazioni) di acque reflue dalla rete, 2) infiltrazioni al loro interno di acque sotterranee (o acque parassite). Nella gran parte dei casi, gli effetti di questi due processi si rendono manifesti solo in seguito ad una occulta evoluzione avanzata del dissesto:

- le exfiltrazioni producono un impatto ambientale con allagamenti, degradazione delle resistenze geomeccaniche dei terreni con cedimenti e movimenti franosi, e problematiche igienico-sanitarie con inquinamento di tipo organico ed inorganico delle acque sorgentizie, del suolo e dei corpi idrici sotterranei
- le infiltrazioni creano, incrementi anche elevati delle portate da convogliare e da sollevare in corrispondenza delle stazioni di pompaggio rispetto a quelle progettuali previste, ridotta capacità di depurazione degli impianti preposti, secondo la normativa vigente, per l'arrivo diluito dei liquami da trattare e afflussi terrigeni all'interno delle condotte con formazioni di cavità sotterranee che progrediscono esternamente con l'apertura di voragini stradali

Recentemente, nell'ambito di un progetto europeo denominato APUSS (*Assessing of infiltration and exfiltration on the Performance of the Urban Sewer System*)<sup>1</sup>, finalizzato a portare un contributo per risolvere questo tipo di problematiche, sono stati sviluppati e proposti da parte dell'istituto di ricerca svizzero EAWAG di Zurigo quattro nuove metodologie di indagine che riguardano la rilevazione e il controllo quantitativo di eventuali processi in atto, di infiltrazioni idriche all'interno della rete e/o di exfiltrazioni di liquami dalla fognatura. Le metodologie sono applicabili senza interrompere il deflusso ordinario dei liquami e da realizzarsi in condizioni di tempo asciutto.

Per la quantificazione delle infiltrazioni sono stati proposti i metodi: 1) della caratterizzazione isotopica e 2) della misura delle concentrazioni di marcatori caratteristici; mentre per la valutazione delle exfiltrazioni i metodi: 1) delle iniezioni discrete di masse note di un tracciante chimico o 2) del suo dosaggio in continuo.

Tali metodi sono in corso di applicazione, da parte dell'Istituto di Ricerca delle Acque del CNR, in due aree urbane sperimentali della città di Roma in collaborazione con l'Ufficio Pianificazione e Progettazione Generale del Dipartimento VI del Comune di Roma per il supporto cartografico e gli aspetti idrogeologici.

<sup>(A)</sup> Università di Roma "Tor Vergata", Dipartimento di Ingegneria Civile, Via del Politecnico, 1 – 00173 Roma; IRSA-CNR, Via Reno, 1 – 00198 Roma (e-mail: [prigiobbe@irsa.rm.cnr.it](mailto:prigiobbe@irsa.rm.cnr.it)).

<sup>(B)</sup> Comune di Roma, Dipartimento alle Politiche della Programmazione e Pianificazione del Territorio, Ufficio Pianificazione e Progettazione Generale, Via del Turismo, 30 – 00144, Roma (e-mail: [c.succhiarelli@comune.roma.it](mailto:c.succhiarelli@comune.roma.it)).

<sup>(C)</sup> Responsabile e coordinatore italiano del progetto APUSS, IRSA-CNR, Via Reno, 1 – 00198 – Roma (e-mail: [m.giulianelli@irsa.rm.cnr.it](mailto:m.giulianelli@irsa.rm.cnr.it)).

<sup>1</sup> Il progetto di ricerca APUSS è stato avviato nella sezione "Gestione Sostenibile e Qualità dell'acqua" nell'ambito del V Programma Quadro "Energia, Sviluppo Sostenibile e Ambiente" della Commissione Europea. Francia, Svizzera, Germania, Gran Bretagna, Repubblica Ceca, Portogallo e Italia sono le nazioni coinvolte, attraverso i rispettivi enti scientifici nazionali (partners del progetto) che condurranno singolarmente le ricerche su aree urbane sperimentali situate all'interno del proprio paese dove il relativo municipio fungerà da ente associato alla ricerca e destinatario finale dei risultati applicativi del progetto.

## LE AREE URBANE SPERIMENTALI

Le aree sperimentali sono state scelte in due territori urbani (fig. 1) interessati dagli insediamenti: 1) del Piano di Zona “Torraccia”, situato nel quadrante nord est di Roma e realizzato tra gli anni '80 e '90; 2) di Infernetto, situato nel quadrante sud ovest di Roma e caratterizzato da edilizia prevalentemente non pianificata.

Per l'individuazione delle due aree sperimentali sono state prese in considerazione determinate caratteristiche, in funzione dei metodi da applicare e dei modelli statistici per la programmazione della riabilitazione, costituite da:

1. area insediativa caratterizzata da una edilizia di tipologia omogenea;
2. caratteristiche geologiche ed idrogeologiche omogenee;
3. conoscenza di dettaglio della rete di fognatura (materiale, dimensioni, età, profondità, utilizzo);
4. possibilità di accesso alla fognatura per il campionamento e la misurazione dei parametri idraulici;
5. presenza di una falda idrica sotterranea poco profonda ed, almeno in un'area, interagente con la rete fognaria per la valutazione dei processi di infiltrazione;
6. possibilità di installazione dei piezometri per la caratterizzazione dei corpi idrici sotterranei, il monitoraggio chimico e idraulico delle oscillazioni del livello della falda idrica.

### *L'area sperimentale del Piano di Zona Torraccia*

L'area sperimentale presenta un'estensione di circa 85 ha, situata su un altipiano piroclastico avente un'altitudine media di 40 m s.l.m..

La costituzione geologica è costituita da depositi piroclastici dello spessore di circa 15-17 m, prevalentemente cineritici fini con livelli scoriacei e pomicei, provenienti dai complessi vulcanici dei Colli Albani e dei Monti Sabatini; presentano una permeabilità variabile per la presenza di livelli argillificati e sono sede di una circolazione idrica a falda libere sovrapposte che, in determinate aree possono interagire con la rete fognaria. Sottostanti sono presenti banchi argillosi con livelli torbosi per uno spessore complessivo di circa 15 m con intercalazione di un banco sabbioso limoso. Alla profondità di 30-32 m si rinviene un potente banco di ghiaie calcaree eterometriche sede di una falda idrica in pressione. L'area è dotata di una fognatura mista costituita da tubazioni prefabbricate ovoidali in calcestruzzo di dimensioni 100x120 cm, 150x180 cm e 150x210 cm.

### *L'area sperimentale di Infernetto*

L'area sperimentale insediativa ricade territorialmente su due ambiti morfologici distinti: 1) nella parte di nord-est, lo sviluppo urbano ha interessato i depositi costieri terrazzati con un'altitudine di 14-12 m s.l.m.; 2) nella parte di sud-ovest, poggia sui depositi alluvionali della piana deltizia esterna del Fiume Tevere a 2-3 m s.l.m..

Il sottosuolo è composto da sedimenti prevalentemente sabbiosi e limosi e subordinatamente da argille e ghiaie.

La circolazione idrica sotterranea è presente con una falda libera, ad una profondità del livello dal piano campagna, che diminuisce progressivamente, da circa 6 – 7 m a 3 m, man mano che la direzione del flusso idrico procede da nord-est a sud – ovest e l'altimetria dell'area passano da 14 m s.l.m a 2 m s.l.m., producendo nelle parti situate a quote minori una interazione con la rete fognaria. Il flusso idrico è alimentato da un bacino idrogeologico che si sviluppa nella parte di nord-est dell'area, costituito dai depositi sabbiosi e limosi degli antichi terrazzi costieri del mare Tirreno.

## METODOLOGIE PER LA QUANTIFICAZIONE DELLE INFILTRAZIONI

Per la quantificazione delle infiltrazioni in reti di fognatura di acque parassite sono stati sviluppati due metodologie:

1. la determinazione dell'abbondanza dell'isotopo stabile dell'ossigeno ( $^{18}\text{O}$ ) nell'acqua reflua della fognatura la cui variazione è influenzata dagli altri apporti isotopici dell'ossigeno ( $^{18}\text{O}$ ) dei vari flussi parassiti di infiltrazione, da

associare contemporaneamente alle misure di portata alla sezione di chiusura dell'area investigata e del livello della falda superficiale (Kracht *et al.*, 2003).

2. la misura della concentrazione di un marcatore naturale caratteristico presente nelle acque reflue (ad esempio COD), la cui variazione deve essere in funzione della quantità degli apporti idrici parassiti che affluiscono nella fognatura (Kracht *et al.*, 2002).

Le infiltrazioni calcolate si riferiscono alle acque parassite che interessano un'intera area urbana sottesa dalla sezione fognaria in cui si prelevano i campioni di acqua reflua. Qualora il valore stimato superasse la percentuale massima accettabile secondo gli standard definiti una ulteriore indagine di dettaglio mediante telecamera dovrebbe essere eseguita.

### **Metodo della caratterizzazione isotopica**

Il metodo sfrutta il tracciamento naturale di un'acqua, a seguito della modifica della sua composizione isotopica che i fenomeni fisici (variazioni di pressione e di temperatura, evaporazione, precipitazione, infiltrazione nel sottosuolo) e chimici che avvengono durante il ciclo idrologico del suo percorso. Pertanto, i flussi idrici provenienti da aree territoriali diverse possono avere una composizione isotopica che li caratterizza (acqua di pioggia, di sorgente, di falda, di torrente ecc.) e quindi permette di distinguere la presenza e l'origine degli apporti di acque parassite nella fognatura. Nella città di Roma le fonti di approvvigionamento distano parecchi chilometri provenendo da regioni in cui la composizione delle precipitazioni è variabile tra -9 ÷ -8 ‰, mentre l'abbondanza di 18-ossigeno nell'acqua di pioggia sul territorio romano è variabile tra -6 ÷ -5 ‰ (Longinelli e Selmo, 2003).

Il metodo, viene applicato determinando l'abbondanza dell'isotopo stabile dell'ossigeno ( $^{18}\text{O}$ ) nei diversi flussi idrici che, ipoteticamente nell'area della rete indagata, potrebbero interagire con infiltrazioni nelle canalizzazioni fognarie. L'abbondanza dell'isotopo stabile dell'ossigeno ( $^{18}\text{O}$ ) è data dalla applicazione della seguente relazione:

$$(\delta^{18}\text{O}) = \left[ \frac{\left( \frac{^{18}\text{O}}{^{16}\text{O}} \right)_{\text{campione}}}{\left( \frac{^{18}\text{O}}{^{16}\text{O}} \right)_{\text{riferimento}}} - 1 \right] * 1000 \quad [\text{‰}] \text{ VSMOW} \quad (1)$$

dove la concentrazione degli isotopi  $^{18}\text{O}$  è misurata in riferimento allo standard V-SMOW (Vienna Standard Mean Ocean Water) definita da International Atomic Energy Agency (IAEA).

Le ipotesi alla base della metodologia sono:

1. variazione trascurabile della composizione isotopica dell'acqua durante il trasporto in fognatura;
2. in assenza di infiltrazioni la composizione isotopica dell'acqua reflua è uguale a quella dell'acqua di acquedotto;

Il calcolo dell'infiltrazione media giornaliera di acque parassite nella rete fognaria è espressa mediante la seguente formula:

$$Inf.(t) = \frac{Q_I(t)}{Q_{mF}} = \frac{\delta^{18}\text{O}_F(t) - \delta^{18}\text{O}_{NI}(t)}{\delta^{18}\text{O}_{mI} - \delta^{18}\text{O}_{NI}(t)} * \frac{Q_F(t)}{Q_{mF}} \quad (2)$$

dove  $Q_I(t)$  è la portata di infiltrazione dovuta alle diverse sorgenti presenti nell'area investigata [L/s];  $Q_F(t)$  è la portata oraria delle acque reflue misurata in corrispondenza della sezione di chiusura della rete fognaria investigata e  $Q_{mF}$  è il suo valore medio giornaliero [L/s];  $\delta^{18}\text{O}_F(t)$  è l'abbondanza di 18-ossigeno rilevata nei campioni di acqua di fognatura [‰];  $\delta^{18}\text{O}_{NI}(t)$  è relativo all'acqua di fognatura in assenza di infiltrazioni ed assunta pari a quella dell'acquedotto [‰];  $\delta^{18}\text{O}_{mI}$  è il valore medio dell'abbondanza di 18-ossigeno dei vari flussi idrici di infiltrazione presenti nell'area [‰].

### **Metodo della misura delle concentrazioni di marcatori caratteristici**

Il metodo consiste nella determinazione delle infiltrazioni combinando le misure di portata dei flussi delle acque nere e di quelle di infiltrazione con i valori di concentrazione di un caratteristico marcatore naturale presente nelle acque di fognatura. Il principio alla base del metodo è che la concentrazione del marcatore tende a ridursi proporzionalmente alla quantità delle acque parassite che si infiltrano nella fognatura. A tale scopo il marcatore caratteristico deve avere una concentrazione: 1) trascurabile nelle acque di infiltrazione rispetto a quella presente nel refluo; 2) proporzionale alla portata transitante in fognatura senza diluizioni da parte delle attività umane stesse che contribuiscono agli scarichi in fognatura ed 3) essere conservativo durante il trasporto in fognatura.

Il COD è stato scelto come marcatore naturale caratteristico in quanto esso rispetta i punti sopra riportati, nonostante non sia conservativo per lunghi percorsi del refluo.

Il modello matematico per il calcolo delle infiltrazioni in una fognatura mista consiste innanzitutto nel dividere il flusso transitante in fognatura durante un periodo di tempo asciutto in due parti: acque reflue ed acque di infiltrazione, come mostrato nell'equazione (3):

$$Q_{\text{acque\_reflue}} = Q_{\text{acque\_usate}} + Q_{\text{acque\_parassite}} \quad (3)$$

dove  $Q_{\text{acque\_reflue}}$  è la portata totale transitante [L/s],  $Q_{\text{acque\_usate}}$  è la sola portata nera [L/s],  $Q_{\text{acque\_parassite}}$  è la portata infiltrata in tempo asciutto [L/s].

Impostando un bilancio di massa sull'intera area investigata, l'espressione per la determinazione del marcatore caratteristico è la seguente:

$$C_{\text{acque\_reflue}} = \frac{(Q_{\text{acque\_reflue}} - Q_{\text{acque\_parassite}}) * C_{\text{acque\_usate}} + Q_{\text{acque\_parassite}} * C_{\text{acque\_parassite}}}{Q_{\text{acque\_reflue}}} \quad (4)$$

dove  $C_{\text{acque\_reflue}}$  è la concentrazione rilevata nel flusso fognario a seguito delle infiltrazioni [mg/L],  $C_{\text{acque\_usate}}$  è la concentrazione dovuta alla sola portata nera [mg/L] e  $C_{\text{acque\_parassite}}$  è quella dovuta all'apporto di acque parassite [mg/L].

Se si sceglie di misurare la concentrazione delle sostanze per le quali l'acqua di falda a seguito dell'infiltrazione nella fognatura determina una diluizione,  $C_{\text{acque\_parassite}}$  deve essere prossima al valore zero. Pertanto, la (4) si può scrivere nel modo seguente:

$$C_{\text{acque\_reflue}} = \frac{(Q_{\text{acque\_reflue}} - Q_{\text{acque\_parassite}}) * C_{\text{acque\_usate}}}{Q_{\text{acque\_reflue}}} \quad (5)$$

I valori dei termini:  $C_{\text{acque\_usate}}$  e  $Q_{\text{acque\_parassite}}$  sono valutati matematicamente mediante la stima dei parametri. Assumendo per  $Q_{\text{acque\_parassite}}$  un valore costante in una scala temporale giornaliera,  $C_{\text{acque\_usate}}$  può essere rappresentato mediante una funzione periodica dato il tipico andamento delle portate fognarie.

La concentrazione del parametro di interesse dovrebbe essere misurato mediante una strumentazione on-line al fine di raccogliere una elevata mole di dati per il modello rappresentato dall'equ. (5). Il parametro scelto per le determinazioni è stato il COD.

Nel presente studio lo strumento che si sta impiegando per le misure è uno spettrometro on-line (s::can) (Fig. 2) che misura l'assorbanza dell'acqua nello spettro continuo del visibile (100-400 nm) e dell'ultravioletto (400-750 nm) da cui si può calcolare la concentrazione del COD (in particolare: COD disciolto, COD particolato e gli SST). Per il COD lo spettro di assorbimento è mostrato nella Fig. 3, mentre in Fig. 4 è mostrata l'andamento del COD misurato a valle dell'area sperimentale Infernetto.



Fig. 2 - Sonda utilizzata per le misurazioni (<http://www.s-can.at>)

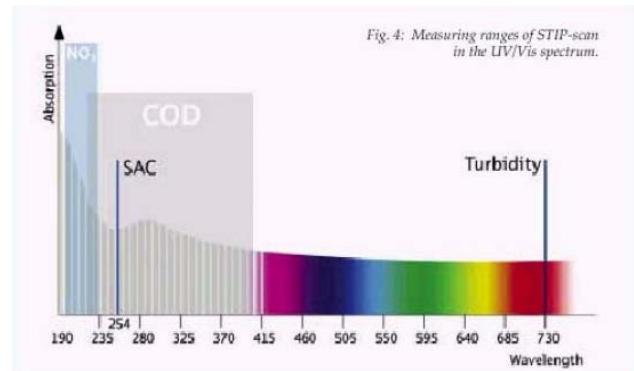


Fig. 3 - Spettro di assorbimento nell'intervallo UV/VIS di un campione di acqua reflue

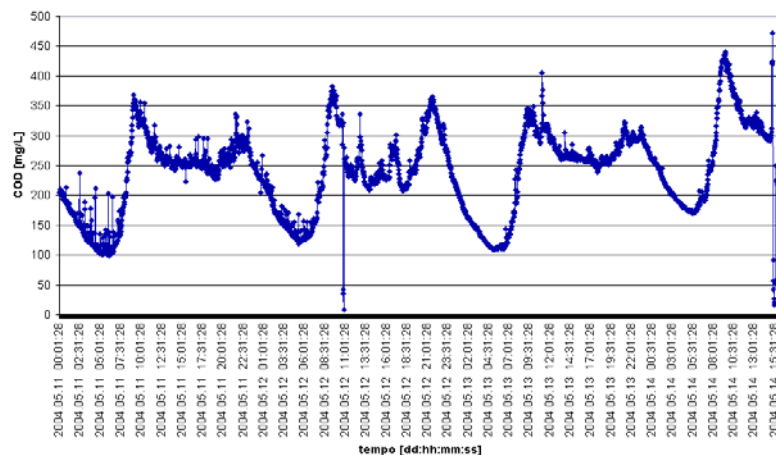


Fig. 4 – COD [mg/L] delle acque reflue misurato per tre giorni mediante spettrometro s::can nell'area Infernetto

Lo strumento deve essere calibrato al momento dell'installazione nel punto di interesse. La calibrazione consiste nel definire una relazione tra il valore di COD istantaneo misurato dallo spettrometro e quello determinato in laboratorio su campioni prelevati nello stesso punto di misura e contemporaneamente alla misura. La durata della calibrazione è di almeno 24 ore, giacché la matrice acquosa diurna è diversa da quella notturna.

## METODOLOGIE PER LA QUANTIFICAZIONE DELLE EXFILTRAZIONI

Per la quantificazione delle exfiltrazioni in reti di fognatura sono stati sviluppati due metodi costituiti da iniezioni: 1) discreto metodo QUEST (*QUantification of Exfiltration from Sewer with artificial Tracer*) e 2) in continuo, metodo QUEST-C (*QUantification of Exfiltration from Sewer with artificial Tracer Continuously dosed*), di quantità note di traccianti chimici conservativi in un flusso di acqua reflua (Rieckermann *et al.*, 2003 e 2004).

### Metodo delle iniezioni discrete di masse note di un tracciante chimico (metodo QUEST)

Il metodo consiste nel dosaggio di masse discrete note di una soluzione di tracciante in due differenti pozzetti lungo la tubazione sotto indagine e nella misura della concentrazione nel flusso a valle della stessa tubazione (Fig. 5). Il tracciante utilizzato durante gli esperimenti è stato NaCl la cui contrazione a valle del tratto esaminato è stata eseguita con una sonda di conducibilità viste le proprietà chimico-fisiche del tracciante utilizzato.

In fig. 5 è riportato uno schema che sintetizza i punti di dosaggio del tracciante e di misura. Nel pozzetto 1 si dosa la soluzione di tracciante che serve per rilevare l'acqua perduta a seguito delle exfiltrazioni, mentre al pozzetto 2 si dosa la

soluzione del medesimo tracciante al fine di misurare la portata residua nella tubazione investigata a seguito delle exfiltrazioni. Nel pozzetto 3 è misurata la concentrazione dei traccianti dosati nei pozzetti 1 e 2 e la portata.

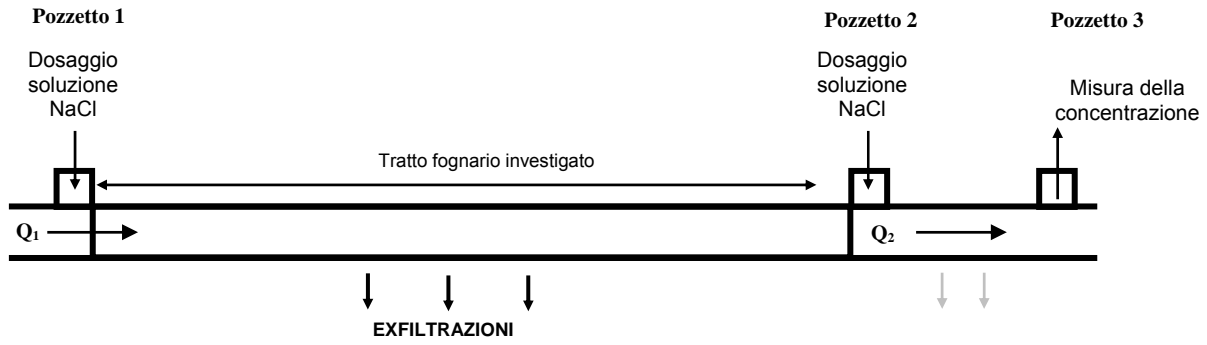


Fig. 5 – Schema del metodo QUEST (modificato da Rieckermann, 2003)

A seguito della completa miscelazione refluo-soluzione tracciante, la massa di tracciante perduta durante le exfiltrazioni è proporzionale alla portata di acqua exfiltrata. Quindi si può scrivere:

$$exf = 1 - \frac{M_m}{M_d} \quad (6)$$

dove  $exf$  è l'exfiltrazione [-];  $M_d$  è la massa di tracciante dosata al pozzetto 1 [gr] e  $M_m$  è la massa di tracciante residua misurata al pozzetto 3 [gr]. La massa residua di tracciante è calcolata dal seguente integrale:

$$M_m = \int_{\Delta t} Q(t) * e * (C(t) - C_{baseline}(t)) dt \quad (7)$$

dove  $C(t)$  è la conducibilità del refluo in corrispondenza del picco di concentrazione del tracciante a seguito del dosaggio [uS/cm] (Fig. 6);  $C_{baseline}(t)$  è la conducibilità naturale del refluo [uS/cm] (Fig. 6);  $e$  è il fattore di conversione da uS/cm a gr/L [gr/L/uS/cm];  $Q(t)$  è la portata durante il periodo di tempo di misura del picco di conducibilità [L/s] (Fig. 6). Quest'ultima se si mantiene costante durante l'esperimento è calcolata con la seguente equazione:

$$Q = \frac{M_d^I}{\int_{\Delta t} e * (C^I(t) - C_{baseline}^I(t)) dt} \quad (8)$$

dove  $M_d^I$  è la massa di tracciante dosata al pozzetto 2 [gr] e  $C^I(t)$  è la conducibilità del refluo in corrispondenza del picco di concentrazione del tracciante a seguito del dosaggio [uS/cm] (Fig. 6);

In caso contrario occorre considerare in (7) i valori di portata misurati con un idrometro (Giulianelli, Mazza, Prigobbe e Russo, 2003).

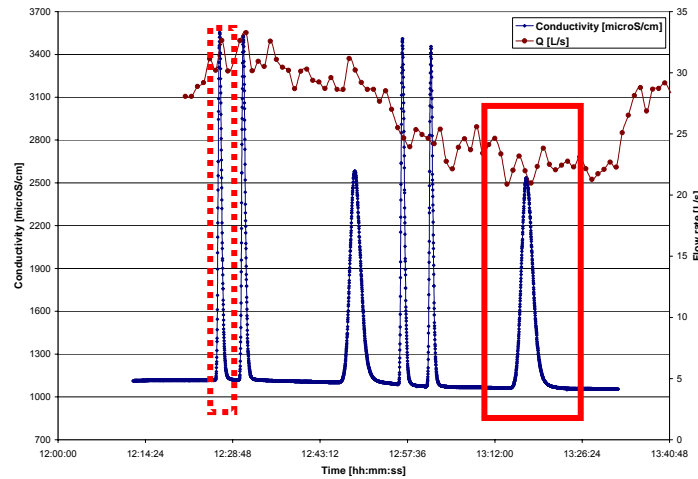


Fig. 6 – Andamento della conducibilità misurata al pozzetto 3 (Giulianelli, Mazza, Prigione e Russo, 2003). In linea continua la conducibilità dovuta al dosaggio nel pozzetto 1; in linea tratteggiata quella relativa al dosaggio nel pozzetto 2.

#### **Metodo del dosaggio in continuo di masse note di un tracciante chimico (metodo QUEST-C)**

Il metodo consiste nel dosaggio in continuo di due masse nell'unità di tempo note di traccianti in due differenti pozzetti lungo la tubazione sotto indagine e nella misura della contrazione nel flusso a valle della stessa tubazione (Fig. 7). I traccianti utilizzati durante gli esperimenti sono stati LiCl e NaBr.

In fig. 7 è di nuovo riportato uno schema che sintetizza i punti di dosaggio del tracciante e di misura. Nel pozzetto 1 si dosa una soluzione di tracciante LiCl che serve per rilevare l'acqua perduta a seguito delle exfiltrazioni, mentre al pozzetto 2 si dosa una soluzione di NaBr al fine di misurare la portata residua nella tubazione investigata a seguito delle exfiltrazioni. Nel pozzetto 3 è misurata la concentrazione dei traccianti dosati nei pozzetti 1 e 2 e la portata.

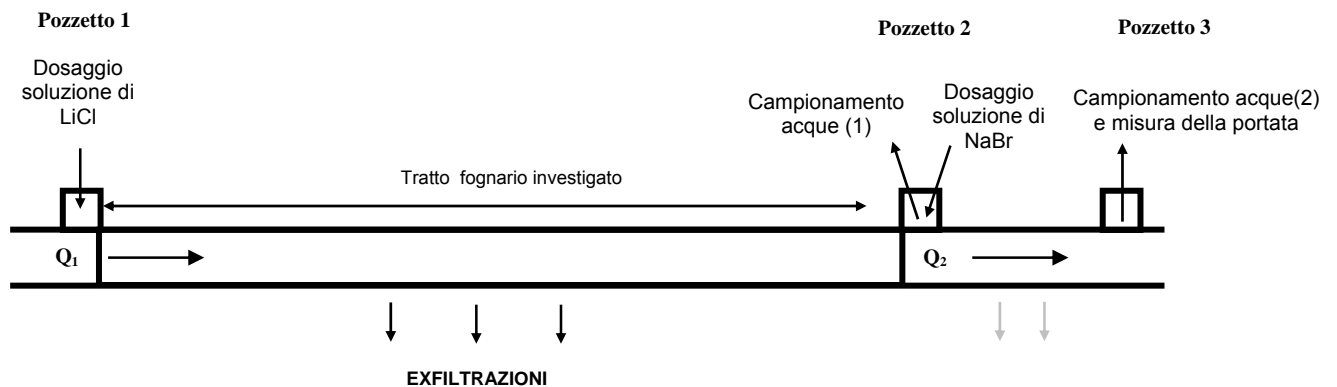


Fig. 7 - Schema di dosaggio dei traccianti chimici nel metodo QUEST-C (Modificato da Rieckermann et al., 2004)

Data la seguente espressione per le exfiltrazioni, ora espressa intermini della portata:

$$exf = 1 - \frac{Q_2}{Q_1} \quad (6)$$

exf è l'exfiltrazione [-];  $Q_1$  è la portata in ingresso al pozzetto 1 [L/s] e  $Q_2$  è la portata in uscita dal pozzetto 2 [L/s].

In condizioni quasi stazionarie di flusso, la portata può essere espressa mediante la seguente equazione:

$$Q = \frac{c_{sol} * q_{sol}}{C_{fogn}} \quad (7)$$

dove  $c_{sol}$  è la concentrazione del tracciante alimentata, costante durante il dosaggio [mg/L];  $q_{sol}$  è la portata di tracciante alimentata, costante durante il dosaggio [L/s] e  $C_{fogn}$  è la concentrazione del tracciante in fognatura misurata in laboratorio mediante Cromatografo Ionico [mg/L].

Quindi la (7) diventa:

$$exf. = \left( 1 - \frac{\frac{C_{sol\_Br} * q_{sol\_Br}}{C_{fogn\_Br}}}{\frac{C_{sol\_Li} * q_{sol\_Li}}{C_{fogn\_Li}}} \right) * 100 \quad (8)$$

dove i parametri presenti nell'espressione (7) sono ora resi specifici per ciascuna soluzione di tracciante dosata.

I campionamenti di acque avvengono in due punti: al pozzetto 2 per determinare la concentrazione naturale dello ione  $Br^-$  nelle acque reflue, ed al pozzetto 3 per determinare le concentrazioni degli ioni  $Li^+$  e  $Br^-$  dosate da cui calcolare le portate  $Q_1$  e  $Q_2$ .

Le misure di portata al pozzetto 3 sono necessarie per il controllo della variabilità del flusso durante l'esperimento; e qualora di verificassero delle repentine variazioni della portata i campioni prelevati in corrispondenza di esse devono essere scartati.

## ATTIVITA' SPERIMENTALE

Le attività operative del progetto che interessano le aree sperimentali sono state programmate e distinte in due fasi: 1) di monitoraggio, e 2) di applicazione delle metodologie. La fase di monitoraggio consente la caratterizzazione idrogeologica e della rete e la contestuale individuazione dei tratti fognari destinati all'applicazione delle metodologie descritte attraverso:

- posizionamento e installazione di piezometri per la definizione e il controllo del livello di falda e delle sue oscillazioni in relazione agli eventuali periodi di interazione con la rete fognaria;
- campionamento e analisi delle acque sotterranee per la determinazione del COD e 18-ossigeno;
- installazione di pluviometri per il controllo delle acque meteoriche al fine di individuare i periodi di tempo asciutto in cui applicare i metodi;
- campionamento delle acque reflue per la determinazione del COD e 18-ossigeno;
- misura della portata in fognatura nei punti di interesse della rete.

La fase di applicazione delle metodologie a sua volta distinta in tre sotto fasi: 1) analisi dei metodi e delle sorgenti di incertezza, 2) scelta delle apparecchiature idonee di misurazione e del periodo adatto per la conduzione delle sperimentazioni, 3) esecuzione delle campagne sperimentali ed analisi dei dati raccolti (Rieckermann et al., 2003; Rieckermann et al., 2004; Giulianelli, Mazza, Prigione e Russo, 2003; Prigione e Giulianelli, 2004).

## CONCLUSIONI

I metodi proposti riguardanti la quantificazione delle infiltrazioni ed exfiltrazioni in fognature operanti, presentano potenzialmente delle innovazioni quali economicità e velocità di applicazione; inoltre, non necessitano l'interruzione del flusso idrico nella fognatura investigata e fanno uso di traccianti naturali ed artificiali di facile utilizzo e determinazione con strumentazione da campo e da laboratorio già esistente sul mercato.



Allo stato attuale di avanzamento della ricerca le indagini sono condotte solo in tempo asciutto e l'accuratezza e la precisione del dato è in corso di analisi.

L'integrazione dei dati sperimentali provenienti dalle aree sperimentali delle città europee partecipanti al progetto consentirà lo sviluppo applicativo delle nuove metodologie ed il progetto APUSS fornirà agli enti gestori delle reti di fognatura i metodi speditivi di indagine costituiti da elaborati metodologici di indagine e software applicativi per:

- la conoscenza tecnica valutativa dell'efficienza della rete fognaria e degli effetti sull'ambiente idrogeologico;
- la localizzazione territoriale di exfiltrazioni ed infiltrazioni;
- la stima del grado di danneggiamento delle tubazioni per poter programmare gli interventi di riabilitazione in modo strategico.

## RINGRAZIAMENTI

*This study has been carried out within the framework of the European research project APUSS (Assessing Infiltration and Exfiltration on the Performance of Urban Sewer Systems) which partners are INSA de LYON (FR), EAWAG (CH), Techn.l Univ. of Dresden (DE), Faculty of Civil Eng. at Univ. of Prague (CZ), DHI Hydroinform a.s. (CZ), Hydroprojekt a.s. (CZ), Middlesex Univ. (UK), LNEC (PT), Emschergerossenschaft (DE) and IRSA-CNR (IT). APUSS is supported by the European Commission under the 5th Framework Programme and contributes to the implementation of the Key Action "Sustainable Management and Quality of Water" within the Energy, Environment and Sustainable Development Contract n° EVK1-CT-2000-00072. The project work of EAWAG is financially supported by the Swiss Federal Office for Education and Science (BBW).*

## BIBLIOGRAFIA

- GIULIANELLI, M.; MAZZA, M.; PRIGIOBBE, V.; RUSSO, F. (2003). *Assessing exfiltration in an urban sewer by slug dosing of a chemical tracer (NaCl)*. NATO ARW on Enhancing Urban Environment, Rome, Italy, NOV. 5-9, 2003.
- PRIGIOBBE, V.; GIULIANELLI, M. (2004). *Design of tests for quantifying sewer leakages by QUEST-C method*. Conference on Urban Drainage Modelling, Dresden, 15th-17th September 2004.
- KRACHT, O.; GRESCH, M.; DE BENEDITIS, J.; PRIGIOBBE, V.; GUJER, W. (2003). *Stable Isotopes of water as a natural tracers for the infiltration into urban sewer systems*. Geophysical Research Abstracts, Vol. 5, 07852, European Geophysical Society 2003.
- KRACHT, K. *The stable isotope composition of water as a natural tracer for the quantification of extraneous infiltration into sewer system* (2002). Report interno al progetto APUSS.
- LONGINELLI, A.; SELMO, E. (2003) *Isotopic composition of precipitation in Italy: a first overall map*. Journal of Hydrology 270, 75-88.
- RIECKERMANN, J.; BAREŠ, V.; KRACHT, O.; BRAUN, D. AND W. GUJER. (2003). *Quantifying exfiltration with continuous dosing of artificial tracers*. Pages 229-232 in Hydrosphere 2003, Brno, CZ.
- RIECKERMANN, J.; BAREŠ, V.; KRACHT, O.; BRAUN, D.; PRIGIOBBE, V. AND GUJER. W. (2004). *Assessing exfiltration from sewers with dynamic analysis of tracer experiments*. 19th European Junior Scientist Workshop "Process data and integrated urban water modelling" France 11-14 March 2004.

# Nuovi metodi per quantificare le infiltrazioni e delle exfiltrazioni nelle fognature urbane

MARIO GIULIANELLI<sup>1</sup>, VALENTINA PRIGIOBBE<sup>1,2</sup>, CLAUDIO SUCCHIARELLI<sup>3</sup>

<sup>1</sup> IRSA-CNR, Via Reno, 1 00198 Roma (e-mail: [m.giulianelli@irsa.rm.cnr.it](mailto:m.giulianelli@irsa.rm.cnr.it))

<sup>2</sup> Università di Roma "Tor Vergata", Dip. Ing. Civile, Via del Politecnico, 1 00173 Roma (e-mail: [prigiobbe@ing.uniroma2.it](mailto:prigiobbe@ing.uniroma2.it))

<sup>3</sup> Comune di Roma, Dipartimento alle Politiche della Programmazione e Pianificazione del Territorio Ufficio Pianificazione e Progettazione Generale, Via del Turismo, 30 00144 Roma (e-mail: [c.succhiarelli@comune.roma.it](mailto:c.succhiarelli@comune.roma.it))

## Abstract

La conoscenza dello stato strutturale delle reti di fognatura urbana è spesso ardua e costosa ed i danni alle tubazioni sono spesso evidenti solo a seguito di eventi eclatanti come collassi delle tubazioni, allagamenti delle strade, inquinamento della falda superficiale.

Nel presente articolo vengono presentati i risultati di una ricerca che si svolge nell'ambito di un progetto europeo denominato APUSS (*Assessing of infiltration and exfiltration on the Performance of the Urban Sewer Systems*) volto alla messa a punto di nuove metodologie per la quantificazione delle acque parassite (infiltrazioni) e delle perdite (exfiltrazioni).

Le infiltrazioni in parola provengono da sorgenti naturali, da falde e da corpi idrici superficiali interagenti con la rete di fognatura. Nel presente articolo l'entità delle infiltrazioni viene determinata, a scala di rete, mediante la caratterizzazione isotopica (isotopo stabile dell'ossigeno  $\delta^{18}\text{O}$ ) di ciascuna possibile sorgente di infiltrazione nonché del refluio fognario.

Le exfiltrazioni invece, valutate a scala di tratto fognario, vengono calcolate mediante impiego di traccianti chimici conservativi come LiCl e NaBr.

**Parole chiave:** infiltrazioni, exfiltrazioni, fognature, riabilitazione

## Introduzione

Lo studio riportato nel presente articolo è condotto dall'Istituto di Ricerca Sulle Acque del Consiglio Nazionale delle Ricerche (IRSA-CNR) nell'ambito del progetto europeo APUSS (*Assessing of infiltration and exfiltration on the Performance of Urban Sewer Systems*) nel quale sono coinvolti altri dieci gruppi di ricerca europei<sup>1</sup>.

L'IRSA il cui compito è quello di applicare e validare i nuovi metodi sviluppati nell'ambito di detto progetto per la quantificazione delle infiltrazioni e delle exfiltrazioni ha condotto, all'interno del Comune di Roma, numerose campagne sperimentali sui cui risultati si riferisce nel seguito.

Come noto, le infiltrazioni e le exfiltrazioni in una rete di fognatura possono avere luogo a seguito di una riduzione di tenuta idraulica tanto delle tubazioni quanto dei giunti (Figure 1 e 2) ed i loro effetti sono evidenziabili sia sul piano ambientale (inquinamento dei corpi idrici superficiali e profondi) che economico (maggiori portate da sollevare in corrispondenza delle stazioni di sollevamento, malfunzionamento degli impianti di depurazione, ecc.).

---

<sup>1</sup> This study has been carried out within the framework of the European research project APUSS (*Assessing Infiltration and Exfiltration on the Performance of Urban Sewer Systems*) which partners are INSA de LYON (FR), EAWAG (CH), Techn.I Univ. of Dresden (DE), Faculty of Civil Eng. at Univ. of Prague (CZ), DHI Hydroinform a.s. (CZ), Hydroprojekt a.s. (CZ), Middlesex Univ. (UK), LNEC (PT), Emschergenossenschaft (DE) and IRSA-CNR (IT). APUSS is supported by the European Commission under the 5th Framework Programme and contributes to the implementation of the Key Action "Sustainable Management and Quality of Water" within the Energy, Environment and Sustainable Development Contract n° EVK1-CT-2000-00072. The project work of EAWAG is financially supported by the Swiss Federal Office for Education and Science (BBW).

I metodi presentati in questo articolo sono innovativi sia perché permettono di valutare in sostanza lo stato strutturale di una fognatura senza che ne sia interrotto il funzionamento sia perché si basano sulla misura di traccianti chimici naturali ( $^{18}\text{O}$  per le infiltrazioni) (Kracht et al., 2003) ed artificiali (NaCl, LiCl, NaBr per le exfiltrazioni) (Rieckermann et al., 2003; Rieckermann et al., 2004) di facile determinazione, uso e, soprattutto, non inquinanti per l'ambiente.

Nella primo paragrafo di seguito sono introdotti brevemente i metodi applicati di quantificazione delle infiltrazioni e delle exfiltrazioni ed è descritta l'area dove sono state condotte le indagini. Nel secondo paragrafo vengono riportati e discussi i risultati ottenuti durante le campagne sperimentali. Infine, nel terzo paragrafo conclusivo vengono commentati i metodi applicati con particolare riguardo: alla applicabilità del metodo, ai relativi costi ed all'attendibilità del risultato.

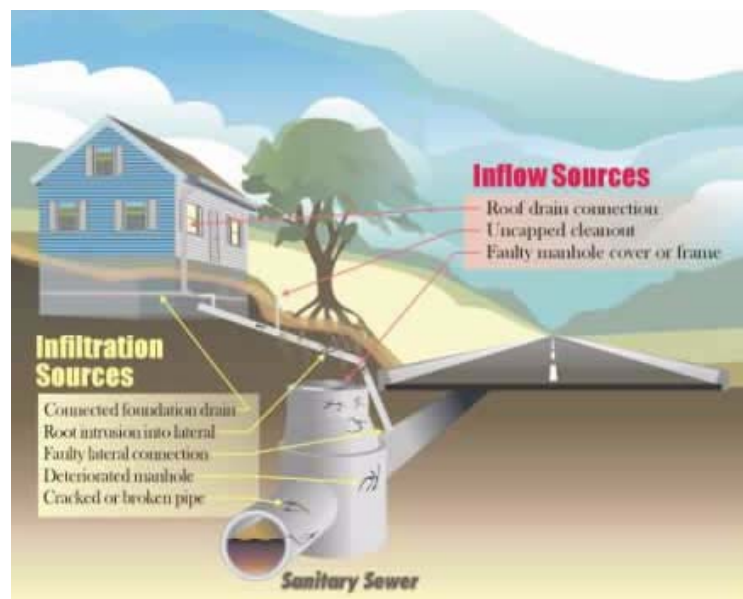


Figura 1. Sorgenti di infiltrazione in una fognatura urbana in tempo asciutto ([http://www.3riverswetweather.org/d\\_weather/d\\_inflow.stm](http://www.3riverswetweather.org/d_weather/d_inflow.stm))

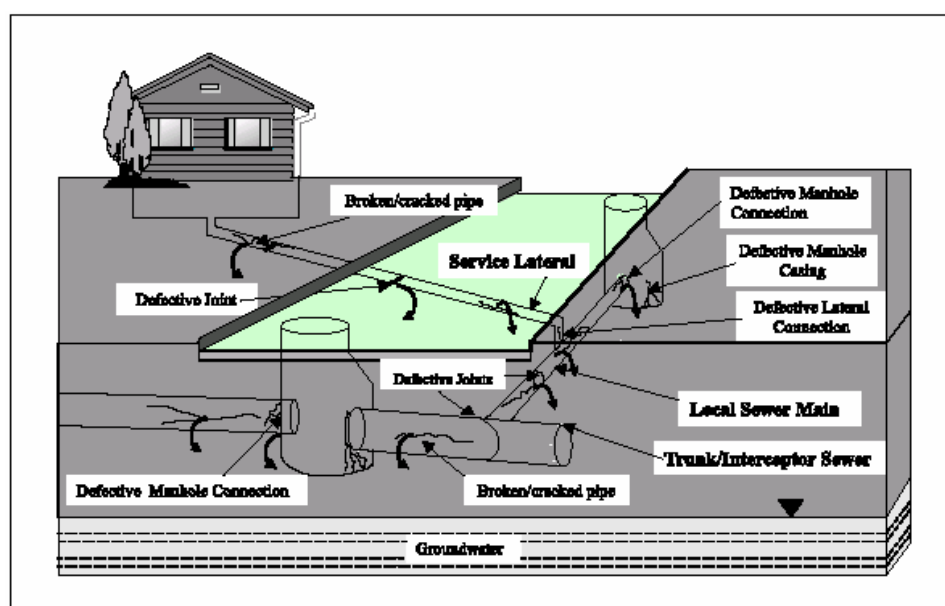


Figura 2. Sorgenti di exfiltrazione in una fognatura urbana in tempo asciutto (<http://www.epa.gov/ORD/NRMRL/Pubs/600R01034/600R01034.pdf>)

## Materiali e metodi

Prima dell'applicazione dei metodi è stata condotta una attenta ricerca di aree urbane in cui sperimentare le nuove metodologie. Lo scopo è stato quello di individuare zone in cui si avessero le seguenti caratteristiche ambientali ed infrastrutturali:

1. rete fognaria costruita nello stesso anno, con i medesimi materiali e con la stessa tipologia di manodopera
2. caratteristiche geologiche pressoché omogenee
3. buona conoscenza della idrogeologia
4. tipologie abitative omogenee
5. disponibilità delle informazioni sui carichi traffico
6. buon accesso alla fognatura

La necessità di individuare aree urbane di bassa eterogeneità scaturisce dal fatto che i tassi di infiltrazione ed exfiltrazione calcolati devono essere rappresentativi di una tipologia di area urbana. In particolare, i metodi applicati si distinguono non solo sulla base della tipologia delle misurazioni, ma anche per la scala a cui essi operano. Mentre il metodo dell'infiltrazioni si applica ad una intera rete fognaria e solo successivamente si può passare ad individuare quei tratti di rete maggiormente interessati dal fenomeno, quello delle exfiltrazioni va applicato ad un singolo tratto fognario e solo in un secondo tempo lo si può estrapolare all'intera rete.

### Quantificazione delle infiltrazioni

Il metodo per la quantificazione delle infiltrazioni (Kracht et al., 2003) consiste nella determinazione dell'isotopo stabile dell'ossigeno ( $^{18}\text{O}$ ) in tutti i contributi idrici di una rete di fognatura (acqua di acquedotto, di falda, di superficie, ecc.) e nell'acqua reflua stessa in una delimitata area urbana.

La quantità di tale isotopo è espresso dalla seguente relazione:

$$(\delta^{18}\text{O}) = \left[ \frac{\left( \frac{{}^{18}\text{O}}{{}^{16}\text{O}} \right)_{\text{campione}}}{\left( \frac{{}^{18}\text{O}}{{}^{16}\text{O}} \right)_{\text{riferimento}}} - 1 \right] * 1000 \text{ [‰]} \text{ VSMOW} \quad (1)$$

dove la concentrazione dell'isotopo  $^{18}\text{O}$  è misurata in riferimento allo standard V-SMOW (Vienna Standard Mean Ocean Water) definita da International Atomic Energy Agency (IAEA).

I valori isotopici dell'acqua risentono fortemente dei fenomeni fisici e chimici che la molecola d'acqua subisce durante il ciclo idrologico. Esistono interessanti correlazioni tra  $\delta^{18}\text{O}$  di un'acqua e la latitudine e l'altitudine da cui essa ha origine. Infatti, per effetto del frazionamento isotopico della molecola d'acqua a seguito delle variazioni di pressione e di temperatura a cui essa è sottoposta durante il suo percorso (evaporazione, precipitazione, infiltrazione nel sottosuolo) si determinano per acque di pioggia, di sorgente e di falda composizioni isotopiche caratteristiche su scale temporali e spaziali estese (Clark & Fritz, 1997). Pertanto, sorgenti di acqua provenienti da regioni differenti possono avere una composizione isotopica differente ed il metodo in oggetto sfrutta proprio il tracciamento naturale di un'acqua mediante  $\delta^{18}\text{O}$ .

Nella città di Roma le fonti di approvvigionamento distano parecchi decine di chilometri dal centro urbano; in particolare, esse si trovano in regioni in cui la composizione delle

precipitazioni è variabile tra -9÷-8‰, mentre  $\delta^{18}\text{O}$  nell'acqua di pioggia sul territorio romano, che ricarica la falda locale, è variabile tra -6÷-5‰ (Longinelli e Selmo, 2003). Questa differenziazione isotopica ha consentito di applicare il presente metodo potendo differenziare i principali contributi idrici alla rete di fognatura.

Le ipotesi alla base della metodologia sono:

1. variazione trascurabile della composizione isotopica dell'acqua durante il trasporto in fognatura
2. in assenza di infiltrazioni la composizione isotopica del refluo fognario è uguale a quella dell'acqua di acquedotto

Le misure in pratica consistono nella determinazione di  $\delta^{18}\text{O}$  nelle sorgenti d'acqua naturali ed artificiali (di falda, di superficie, di acquedotto) presenti nell'area di indagine e in quella di fogna, contemporaneamente alla misura di portata alla sezione di chiusura dell'area investigata e alla misura del livello della falda superficiale.

Il tasso di infiltrazione ( $Inf.(t)$ ) è espresso mediante la seguente formula:

$$Inf(t) = \frac{Q_I(t)}{Q_F(t)} = \frac{\delta^{18}\text{O}_F(t) - \delta^{18}\text{O}_{NI}(t)}{\delta^{18}\text{O}_I - \delta^{18}\text{O}_{NI}(t)} \quad (2)$$

dove  $Q_I(t)$  è la portata di infiltrazione [ $\text{m}^3/\text{s}$ ];  $Q_F(t)$  è la portata delle acque reflue misurata in corrispondenza della sezione di chiusura del bacino urbano investigato [ $\text{m}^3/\text{s}$ ];  $\delta^{18}\text{O}_F(t)$  è la quantità di ossigeno 18 nel refluo [‰];  $\delta^{18}\text{O}_{NI}(t)$  è la quantità di ossigeno 18 nell'acquedotto [‰];  $\delta^{18}\text{O}_I(t)$  è il valore medio dell'abbondanza di ossigeno 18 nelle sorgenti di infiltrazione presenti nell'area [‰].

Riguardo alla strumentazione utilizzata, la misura di portata in fognatura è stata eseguita mediante una sonda SIGMA900 MAX avente un misuratore di livello con sistema piezoresistivo ed uno di velocità con effetto doppler. Le analisi isotopiche sono state eseguite mediante la tecnica di equilibrio acqua- $\text{CO}_2$  suggerita da Epstein e Mayeda (1953) con preparazione manuale dei campioni e successiva determinazione allo spettrometro di massa (Finnigan MAT).

### **Quantificazione delle exfiltrazioni**

Il metodo messo a punto per la quantificazione delle exfiltrazioni da una rete di fognatura si basa sul dosaggio in continuo di due traccianti chimici ( $\text{LiCl}$  e  $\text{NaBr}$ ), ed è denominato QUEST-C (QUantification of Exfiltration from Sewer with artificial Tracer Continuously dosed) (Rieckermann et al., 2003; Rieckermann et al., 2004). Più in particolare,  $\text{LiCl}$  viene dosato al Pozzetto 1 e serve per misurare la portata all'inizio del tratto fognario in esame, mentre  $\text{NaBr}$  viene dosato al Pozzetto 2 e serve per misurare la portata alla fine del tratto investigato a seguito delle eventuali perdite (Figura 3). I prelievi di campioni di acque avvengono in due punti: al Pozzetto 2 (Figura 3) per determinare la concentrazione naturale dello ione  $\text{Br}^-$ , al Pozzetto 3 (Figura 3) per determinare le concentrazioni degli ioni  $\text{Li}^+$  e  $\text{Br}^-$  a seguito dei dosaggi ai Pozzetti 1 e 2 da cui si calcolano le portate  $Q_1$  e  $Q_2$ , con il metodo della diluizione.

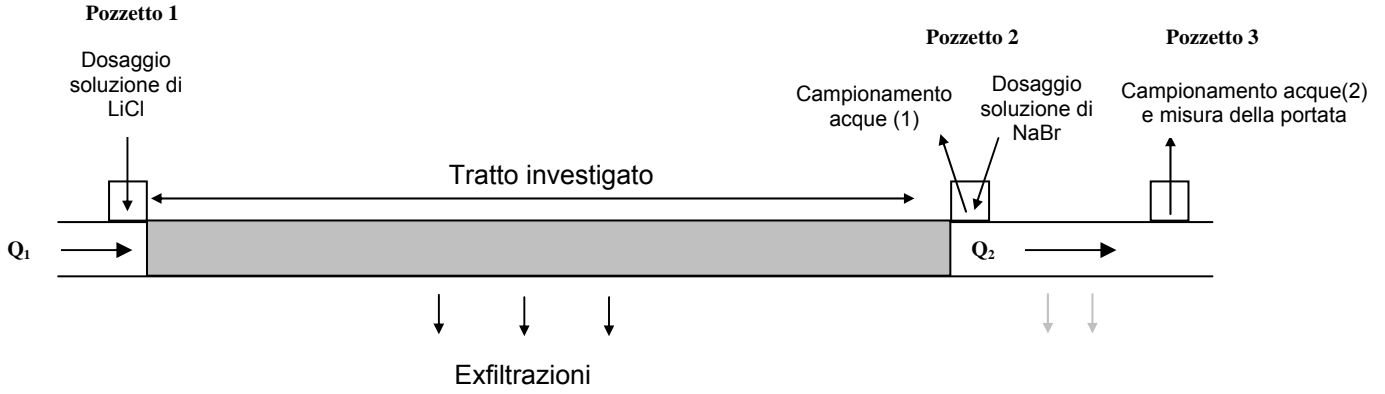


**Figura 3 - Schema di dosaggio dei traccianti chimici nel metodo QUEST-C (Modificato da Rieckermann et al., 2004)**

Le portate  $Q_1$  e  $Q_2$  in Figura 3 si ricavano a partire dalla seguente equazione di bilancio di massa:

$$\int_{t_0 - t_{viaggio}}^{t_1 - t_{viaggio}} c_{Li(Br)}(t) * q_{Li(Br)}(t) dt = \int_{t_0}^{t_1} C_{Li(Br)}(t) * Q_{1(2)}(t) dt \quad (3)$$

dove:  $t_0$  è il tempo di inizio del prelievo dei campioni ai pozzi (1) e (2) [s];  $t_1$  è il tempo di fine campionamento [s];  $t_{viaggio}$  è il tempo necessario per il trasporto della massa  $i$ -esima di tracciante dal punto dosaggio al punto di campionamento [s];  $c_{Li(Br)}(t)$  è la concentrazione di soluzione di tracciante dosata in continuo in fognatura [ $gr/sm^3$ ];  $q_{Li(Br)}(t)$  è la portata di dosaggio della soluzione [ $m^3/s$ ];  $C_{Li(Br)}(t)$  è la concentrazione del tracciante in fognatura a seguito della completa miscelazione [ $gr/sm^3$ ];  $Q_{1(2)}(t)$  è la portata in fognatura [ $m^3/s$ ].

I termini  $c_{Li(Br)}(t)$ ,  $q_{Li(Br)}(t)$ ,  $Q_{1(2)}(t)$  e  $C_{Li(Br)}(t)$  nell'equazione (3) sono considerati costanti durante l'intero periodo dell'esperimento (90 minuti circa) e pertanto l'equazione (3) diventa:

$$Q_{1(2)} = \frac{c_{Li(Br)} * q_{Li(Br)}}{C_{Li(Br)}} \quad (4)$$

Definendo il tasso di exfiltrazione con la seguente espressione:

$$exf. = \left( \frac{Q_1 - Q_2}{Q_1} \right) * 100 \quad (5)$$

e sostituendo l'equazione (4) per le portate  $Q_1$  e  $Q_2$  si ottiene:

$$exf. = \left( 1 - \frac{\frac{c_{Br} * q_{Br}}{C_{Br}}}{\frac{c_{Li} * q_{Li}}{C_{Li}}} \right) * 100 \quad (6)$$

I termini di concentrazione presenti nell'equazione (6) possono essere determinati mediante analisi cromatografiche.

## Area di indagine

L'area sperimentale presenta un'estensione di circa 85 ha, essa è situata su un altopiano piroclastico avente un'altitudine media di 40 m s.l.m..

La costituzione geologica è costituita da depositi piroclastici dello spessore di circa 15-17 m, prevalentemente cineritici fini con livelli scoriacei e pomicei, provenienti dai complessi vulcanici dei Colli Albani e dei Monti Sabatini. Essi presentano una permeabilità variabile per la presenza di livelli argillificati e sono sede di una circolazione idrica a falda libere sovrapposte che, in determinate aree possono interagire con la rete fognaria. Sottostanti sono presenti banchi argillosi con livelli torbosi per uno spessore complessivo di circa 15 m con intercalazione di un banco sabbioso limoso. Alla profondità di 30-32 m si rinviene un potente banco di ghiaie calcaree eterometriche sede di una falda idrica in pressione. L'area è dotata di una fognatura mista costituita da tubazioni prefabbricate ovoidali in calcestruzzo di dimensioni 100x120 cm, 150x180 cm e 150x210 cm posta a 4-9 m sotto il piano campagna con pendenza 0.9% ed età di 14 anni circa.

La fognatura è stata completamente implementata nel software AquaBase ideato nell'ambito del progetto APUSS dalla società DHI. Tale software consente essenzialmente allo stato attuale di gestire dati come le caratteristiche geometriche di una fognatura e le caratteristiche idrogeologiche. In Figura 4 è riportato uno schema della rete di Torraccia ed in rosso è evidenziata la parte investigata con il metodo QUEST-C di lunghezza complessiva 270 m, di cui in alto a destra è riportato il profilo geometrico.

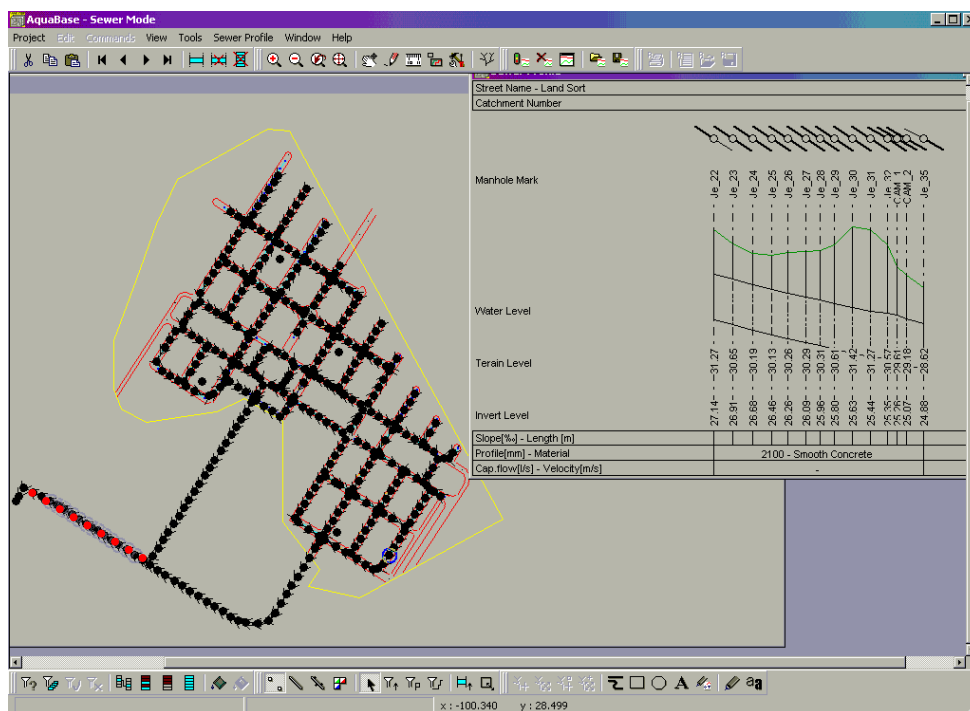


Figure 4 – Rete di fognatura di Torraccia implementata nel software AquaBase (HydroProject, DHI).

## Risultati e discussione

### Infiltrazioni

La pianificazione dell'attività sperimentale si è incentrata su una preliminare verifica di applicabilità del metodo ed una successiva definizione dei tempi di campionamento e misura delle matrici acquose e delle grandezze di interesse.

Al fine di verificare l'applicabilità del metodo si è verificato:

1. la sensibile differenza tra il contenuto di  $\delta^{18}\text{O}$  nell'acqua di falda superficiale e in quella di acquedotto;
2. la bassa variabilità spaziale di  $\delta^{18}\text{O}$  dell'acqua di falda superficiale;
3. la bassa variabilità temporale di  $\delta^{18}\text{O}$  nell'acqua di acquedotto.

tenendo conto che l'incertezza nella misura di  $\delta^{18}\text{O}$  è di 0,2‰.

Per la verifica dei punti 1 e 2 suddetti, sono stati prelevati sull'intero bacino di indagine campioni di acqua di acquedotto e di falda e sono stati caratterizzati isotopicamente.

Riguardo al punto 3, una volta accertato che la sorgente di acqua potabile nel quartiere Torraccia fosse unica (Sorgenti del Peschiera a 416 metri m.s.l. e a 80 Km da Roma) se ne è misurata la conducibilità per quattro giorni con una sonda WTW modello Cond 340i e sensore TetraCon® 325/S. Il valore medio è stato di 635,59  $\mu\text{S}/\text{cm}$  con deviazione standard di  $\pm 0,86$ . La scelta della misura di questo parametro scaturisce dal fatto che  $\delta^{18}\text{O}$  presenta in acque non contaminate una buona correlazione con alcuni parametri chimici come: salinità, conducibilità, durezza e ioni caratteristici del sottosuolo attraversato dall'acqua (Clark & Fritz, 1997; Lamb, 2003).

Una volta verificata l'applicabilità del metodo nel quartiere Torraccia è stato condotto l'esperimento della durata di 10 ore circa, durante le quali sono stati prelevati campioni di acqua di fognatura ogni due ore e campioni di acqua di falda e di acquedotto (Figura 5).

In Tabella 1 sono riportati i valori medi misurati nelle tre matrici acquose esaminate; i valori negativi indicano una composizione isotopica più leggera rispetto al riferimento VSMOW, caratteristica di acque di falda in regioni lontane dalla costa marittima ed ad alta quota.

Per il calcolo dei tassi di infiltrazione sono stati sostituiti nell'equazione (2) i valori medi di  $\delta^{18}\text{O}$  dell'acqua di falda e di acquedotto ed i valori misurati in ciascun campione prelevato di acque reflue (Figura 6).

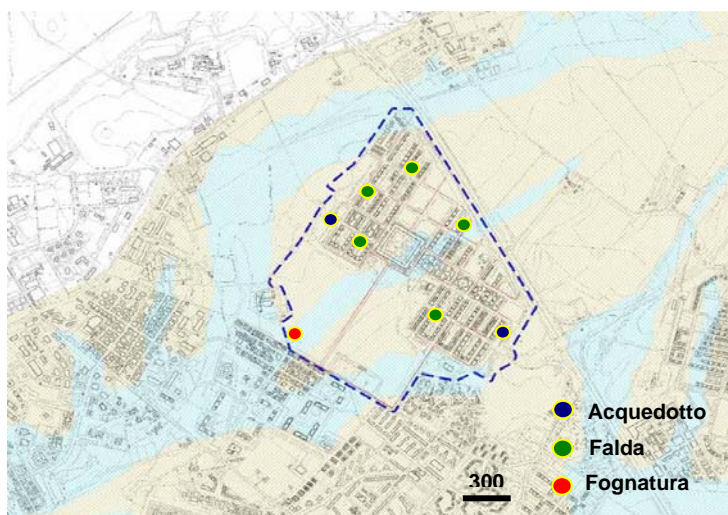


**Figura 5 - Punti di campionamento nel quartiere Torraccia**

**Tabella 1 -  $\delta^{18}\text{O}$  [‰] nelle tre matrici esaminate**

	Acquedotto	Falda	Fognatura
<b>valore medio [‰]</b>	<b>-8,43</b>	<b>-5,43</b>	<b>-7,75</b>
<b>dev. st.[‰]</b>	<b>0,01</b>	<b>0,27</b>	<b>0,10</b>

Il tasso di infiltrazione medio percentuale calcolato è di  $15,58\% \pm 1,28\%$  su una portata media in fognatura di  $28,17\text{m}^3/\text{s} \pm 1,66\text{m}^3/\text{s}$  (Figura 6).



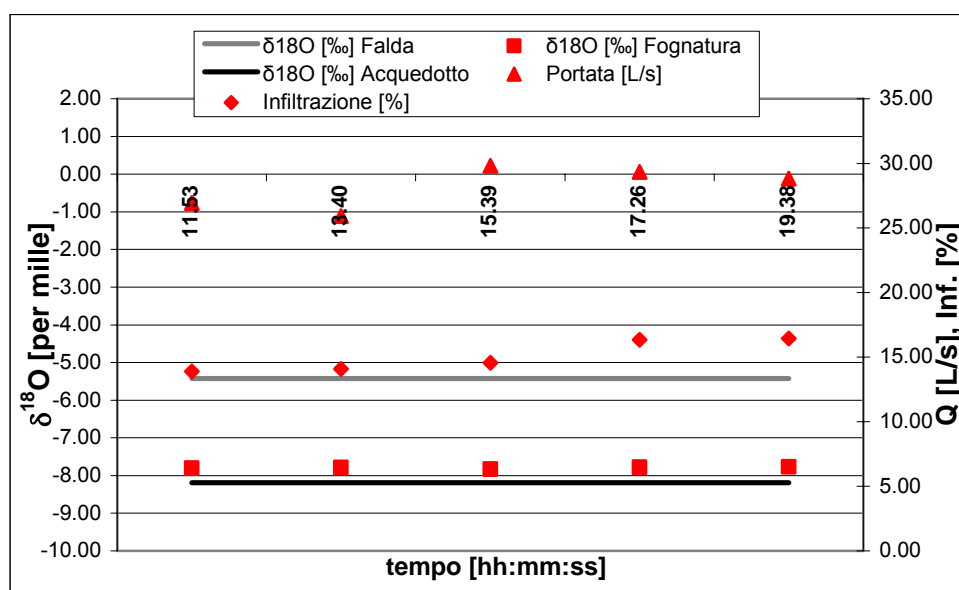


Figura 6 - Portata ed infiltrazione, calcolata con l'equazione (2), a valle dell'area investigata

## Exfiltrazioni

Il metodo QUEST-C è stato applicato su un tratto della fognatura nell'area urbana di Torracchia della lunghezza totale di 270 m di cui 220 m investigati e 50 m necessari per il completo mescolamento del tracciante<sup>2</sup> dosato al Pozzetto 2 in Figura 3. Il periodo della giornata di esecuzione dell'esperimento è stato scelto sulla base degli idrogrammi registrati; da essi si è evinto che il periodo ottimale era tra le ore 9.00÷12.00 e tra le 14.00÷16.00, perché in questi intervalli di tempo si è stimata la variabilità minima della portata<sup>3</sup>.

La strumentazione utilizzata in campo è riportata nella Tabella 2, ed è suddivisa per pozzetto di installazione. La misura di portata al Pozzetto 3 è esclusivamente eseguita per il controllo della variabilità del flusso durante l'esperimento.

Tabella 2- Strumentazione da campo

Pozzetto 1			Pozzetto 2			Pozzetto 3	
Pompa dosaggio	soluzione		Pompa dosaggio	soluzione		Pompa di campionamento (Watson&Marlow, mod.SCIQ 323)	
tracciante (Velp, mod. SO311)			tracciante (Velp, mod. SO311)			Misuratore di portata Area-velocity (SIGMA900 Max)	
Bilancia (EA Economy)			Bilancia (EA Economy)			Ciascun campione filtrato con filtri wathman di porosità 0.45 µm	
			Pompa di campionamento (Watson&Marlow, mod. SCIQ 323)				

La misura della concentrazione degli ioni nei campioni di acque reflue è stata condotta secondo i metodi di analisi delle acque IRSA (2004) e mediante IC Dionex Dx100, colonna ionica AS14 e colonna cationica CS12.

Il tasso di exfiltrazione è stato calcolato con l'equazione (6) in cui sono stati sostituiti sia i valori relativi alle soluzioni dosate di Br<sup>-</sup> e Li<sup>+</sup>, le cui concentrazioni sono state di 50 gr/L e

<sup>2</sup> Oltre una distanza di 100-300\*b [m], dove b è la larghezza del pelo libero (Ruthenford, 1994) si può assumere che la concentrazione del tracciante sul piano della sezione trasversale abbia gradiente nullo.

<sup>3</sup> La variazione di flusso comporta l'instaurarsi della propagazione dell'onda di variazione della portata e della concentrazione di tracciante a velocità diverse inficiando la prova (Huisman et al., 2000). Pertanto per ridurre l'effetto delle condizioni non stazionarie di portata in fognatura la prova deve essere condotta in periodi della giornata (di 90 min circa) in cui la portata si mantiene pressoché costante.

20 gr/L e le portate di 50 mL/min e 20 mL/min, rispettivamente, sia i valori medi di concentrazioni degli ioni  $\text{Br}^-$  e  $\text{Li}^+$  riscontrati nei campioni di fognatura.

Il tasso di exfiltrazione calcolato è risultato di  $2,1 \% \pm 1,0$ , in sostanziale accordo con l'attesa assenza di perdite, giacché il tratto esaminato ha come materiale di rifianco il calcestruzzo, ha un'età di 14 anni, non è soggetto a sollecitazioni dinamiche dovute al traffico automobilistico e non presenta alberature sovrastanti.

In Figura 7 sono riportate le concentrazioni degli ioni di interesse nei campioni di acqua prelevati e l'andamento della portata.

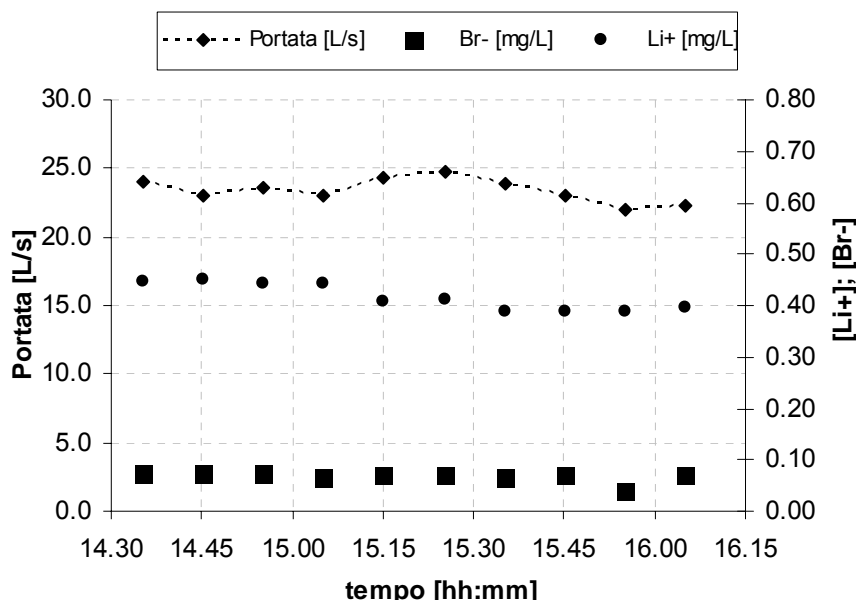


Figura 7- Portata e concentrazione degli ioni nei campioni di acqua di fognatura vs. tempo.

## Conclusione

In generale i criteri di valutazione della validità di un metodo consistono nel determinare:

- la facilità di esecuzione
- l'economicità della strumentazione e delle analisi necessarie
- la precisione ed accuratezza del risultato ottenuto

Il metodo per la valutazione delle infiltrazioni sopra esposto è risultato di agevole applicazione e sufficientemente speditivo una volta individuati i punti di prelievo di acqua di falda, di fognatura e di acquedotto. In eventuale assenza di piezometri nel territorio da investigare occorrerà però costruirli ad hoc a valle di una attenta indagine idrogeologica. In tale eventualità i costi totali si devono valutare non solo sulla base della strumentazione di campo necessaria (misuratore di portata con autocampionatore, 13.000 euro circa), ma a questi occorre aggiungere il costo per la realizzazione di un piezometro di profondità pari al piano di posa della tubazione fognaria più prossima (2000 euro circa), nonché il costo delle analisi di laboratorio (25 euro a campione) e la manodopera in campo di due persone per due giorni. Il tasso di infiltrazione calcolato risulta essere un valore preciso ed accurato in considerazione della deviazione standard e del livello della falda misurato durante l'esperimento condotto che è risultato essere tra 7-15 m dal piano campagna.

Il metodo delle exfiltrazioni QUEST-C risulta essere di facile applicazione, ma necessita di una accurata pianificazione della campagna sperimentale in termini di modalità di installazione delle stazioni di dosaggio e di misura e di sincronizzazione delle attività di dosaggio e campionamento. Riguardo ai costi totali il metodo richiede un investimento iniziale di circa 8000 euro per l'acquisto di tutta la strumentazione da campo come in

Tabella 1 a cui si deve aggiungere il costo delle analisi di laboratorio (25 euro a campione) e la manodopera in campo di tre persone per una giornata. Il tasso di exfiltrazione calcolato risulta essere un valore preciso ed accurato in considerazione della deviazione standard e del buono stato strutturale della tubazione esaminata.

## Riferimenti bibliografici

Clark, I. D., and Fritz, P. (1997). Environmental Isotopes in Hydrogeology. CRC Press; Boca Raton, 328 pp.

Epstein, S.; Mayeda, T. (1953) Variation of  $^{18}\text{O}$  content of water from natural sources. Geochim. Cosmochim. Acta 4, 213-224.

Huisman, J.; Burckhardt, S.; Larsen, A.; Krebs, P. and Gujer, W. (2000) Propagation of waves and dissolved compounds in sewer. J. of Environmental Engineering, ASCE, 126(1),12-30.

Istituto di Ricerca Sulle Acque (2003). Metodologie analitiche per il controllo della qualità delle acque. APAT e CNR/IRSA.

Kracht, O.; Gresch, M.; de Benneditis, J.; Prigiobbe, V.; Gujer, W. (2003). Stable Isotopes of water as a natural tracers for the infiltration into urban sewer systems. Geophysical Research Abstracts, Vol. 5, 07852, European Geophysical Society 2003.

Lambs, L. (2000). Correlation of conductivity and stable isotope  $^{18}\text{O}$  for the assessment of water origin in river system. Chemical Geology 164, 161-170.

Longinelli, A.; Selmo, E. (2003). Isotopic composition of precipitation in Italy: a first overall map. Journal of Hydrology 270, 75-88.

Rieckermann, J.; Bareš, V.; Kracht, O.; Braun, D. and W. Gujer. (2003). Quantifying exfiltration with continuous dosing of artificial tracers. Pages 229-232 in Hydrosphere 2003, Brno, CZ.

Rieckermann, J.; Bareš, V.; Kracht, O.; Braun, D.; Prigiobbe, V. and Gujer. W. (2004). Assessing exfiltration from sewers with dynamic analysis of tracer experiments. 19th European Junior Scientist Workshop "Process data and integrated urban water modelling" France 11-14 March 2004.

Ruthenford, J.C. (1994). River Mixing. John Wiley & Sons Ltd, London, U.K.

## Ringraziamenti

*Si vuole ringraziare il sig. Salvatore Tatti ed il geom. Maurizio Ronda dell'Istituto IRSA-CNR per il loro valente aiuto durante le campagne sperimentali, la dott.sa Camilla Braguglia per l'esecuzione delle analisi cromatografiche ed il dott. Luigi Dallai ed il dott. Marco Mola dell'Istituto IGAG del CNR l'esecuzione delle analisi isotopiche.*

## **Assessing the impact of infiltration and exfiltration in sewer systems using performance indicators: case studies of the APUSS project**

A. Cardoso<sup>1\*</sup>, Prigiobbe, V.<sup>2</sup>, Giulianelli, M., Baer, E.<sup>3</sup>, , Coelho, S.T.<sup>1</sup>

<sup>1</sup> *LNEC, National Civil Engineering Laboratory of Portugal, Av. Do Brasil 101, 1700-066 Lisbon, Portugal*

<sup>2</sup> *Water Research Institute of the Italian National Research Council (IRSA-CNR), Via Reno, 1, 00198 Rome, Italy*

<sup>3</sup> *URGC Hydrologie Urbaine, INSA de Lyon, 34 avenue des Arts, 69621 Villeurbanne cedex, France*

### **Extended Abstract**

Sewer systems constitute a very significant patrimony in European cities. Their structural quality and functional efficiency are key parameters to guarantee the transfer of domestic and trade wastewater to treatment plants without infiltration nor exfiltration. Infiltration of groundwater is particularly detrimental to treatment plant efficiency, while exfiltration of wastewater can lead to groundwater contamination. The APUSS (Assessing infiltration and exfiltration on the Performance of Urban Sewer Systems) project, associating universities, SMEs and municipalities in 7 European countries, developed new methods and techniques to assess and quantify infiltration and exfiltration (I/E) in sewer systems. The methods were tested and validated in different catchments. Associated models and tools were established for application and end-user decision. The APUSS project is part of the European cluster CityNet dealing with Integrated Urban Water Management (Bertrand-Krajewski, 2002) and is funded by the European Commission under the FP5..

One of the objectives of the APUSS project was to provide end-users with integrated elements for decision support that account for I/E rates, impacts on wastewater treatment plant and on the economic value, and facilitate the comparison of different investment strategies to reduce infiltration and exfiltration. A set of performance indicators (PI) has been developed to assess the impact of I/E on sewer systems and has been applied to project case studies. This application was performed using the softwares AQUABASE and PITool/S, developed respectively by DHI/Hydroinform and LNEC.

The specific application considered herein is the sewer systems performance evaluation with regard to infiltration of clean water into foul sewers and exfiltration of sewage into the soil and groundwater. Experimental results obtained with the measurement methods developed in the APUSS project, systems' topology data and groundwater level are stored in AQUABASE that exports them in order to calculate the PI using the PITool/S.

This paper describes the establishment of performance indicators and their application to five project case studies, focusing on sewer systems characteristics, I/E measurements campaigns performed and computational applications.

The methodology for PI definition consists in the selection and development of three components for each aspect of performance analysed (Cardoso, 2003): the numerical value of

a sewer network property or state variable, which is expressive of the particular aspect being scrutinized (I/E); a classification of the PI values scoring them in relation to good or bad performance; an operator, which allows the performance values at element level to be aggregated across the system or parts of it to obtain an overall system performance figure. An example of a PI to assess the infiltration impact on the system performance is  $Q_{inf}/Q_{full}$  where  $Q_{inf}$  is the infiltration flow and  $Q_{full}$  is the pipe capacity.

There are five case studies, three are located in Rome, Italy, and two are located in Lyon, France. In Rome, the three experimental catchments (called Infernetto, Mostacciano and Torraccia) can be considered three different representative pictures of an urban area because geology, hydrogeology, sewer system and the town planning are quite spatial homogeneous. The developed methods within APUSS project for quantifying the I/E ratio were applied at catchment and pipe scale, respectively (Table 1).

**Table 1. Experimental catchments in Rome**

	Infernetto	Mostacciano	Torraccia
<b>Extension [ha]</b>	550	14	85
<b>Sewer</b>	dated 5-15 years, PVC and clay	dated 29 years, concrete	dated 10 years, concrete
<b>Soil</b>	silt-sand sediments, clay and gravel	alluvial and tuff	tuff
<b>Shallow Groundwater</b>	3-7 m under the ground	-	15-20 m under the ground
<b>Town Planning</b>	private houses and gardens	high buildings and yards	small buildings and yards
<b>Infiltration [-]</b>	0.49	-	0.15
<b>Exfiltration [-]</b>	-0.07*	-	-0.02**

Note: estimated in a representative pipe of (\*)1500 m and (\*\*) 500 m length.

In the French case studies, infiltration and exfiltration measurement campaigns have been carried out in 2 main catchments in Lyon: i) the Yzeron catchment (2800 ha) and ii) the Ecully catchment (230 ha). Infiltration and exfiltration rates have been measured using two of the methods developed within the APUSS project: the QUEST method based on NaCl mass balance for exfiltration and the oxygen isotopic method for infiltration. Several conventional methods for the estimation of infiltration have also been applied and compared to the APUSS method. Temporal variations at daily and seasonal scales and also spatial variations were analysed for infiltration. Regarding exfiltration, seasonal variations have been investigated.

Fig.1 shows an example of comparison of the PI referred to above applied to the experimental data available.

The use of PI allows a standardized and objective comparison of the performance of sewer systems having different characteristics, and the evolution of performance along the time. It constitutes a means to technically support the establishment of priorities for rehabilitation and/or construction investments concerning I/E impacts.

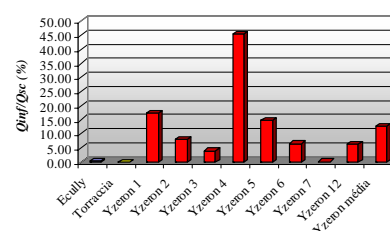


Fig.1 – PI application

## References

- Bertrand-Krajewski, J.L. (2002) - Assessing infiltration and exfiltration on the performance of urban sewer systems. Umweltbundesamt/Federal Environment Agency – Austria.
- Cardoso, A. (2003) Infiltration and exfiltration performance indicators. Sewer systems performance assessment methodology and formulation. APUSS Deliverable 9.1. LNEC. Draft document, diffusion restricted to APUSS partners and EU Commission.